



# UNIVERSITÀ DEGLI STUDI DI TORINO

DIPARTIMENTO DI SCIENZE CLINICHE E BIOLOGICHE

DOTTORATO DI RICERCA IN NEUROSCIENZE

CICLO XXXII

## **Role of Soluble Neuregulin1 in peripheral nerve regeneration and different tissue engineering strategies for long gap repair**

Thesis presented by: **Marwa El Soury**

Tutors: **Prof. Giovanna Gambarotta &**

**Prof. Isabelle Perroteau**

PhD coordinator: Prof. Marco Sassoè

Academic years: 2016-2020

Scientific disciplinary sectors: BIO/06 & BIO/13



## Acknowledgments

I would like to express my deepest thanks and gratitude for all the people who have been part of my life and helped me during the past years.

First of all, I would love to express my deepest acknowledgment and sincere appreciation for my dear tutor Prof. Giovanna Gambarotta, thank you for your assistance, support, guidance, fruitful advices and suggestions which have been of major importance for developing the work I am presenting here in my thesis. You have definitely helped me to think, grow and develop as a researcher. I have been lucky enough to be guided by her also during my master degree. Its almost 6 years since we have first met and you have always treated me as a mother more than being just a professor, you were so kind, inviting me for family dinners, caring and asking about my health whenever I was sick, giving me car lifts to the laboratory and much much more, Thank you Giò for everything you have done and still doing for me, really appreciate it.

Many thanks for Prof. Isabelle Perroteau for your valuable discussions, helpful advices and suggestions, Thanks for teaching me the proper way for criticizing and presenting data.

I would like to thank Prof. Stefano Geuna for hosting me in his laboratory during my master and PhD degree, he is such an inspiration and a great example of how a researcher should be.

To my dear Prof. Stefania Raimondo, it was a great pleasure working with you, thanks for your patience, your guidance and help whenever I needed.

Special thanks for Prof. Víctor Carriel for accepting to supervise me during my whole internship in the university of Granada. I am grateful for all the things you have taught me. It was my pleasure to work with you.

To my dear lab group in Italy: Benedetta, Federica F, Federica Z, Giacomo, Giulia, Luisa, Michela and Nicoletta. Thank you for being so friendly and welcoming, thanks for being my family in Italy and for helping me whenever I am in need, thanks for making these 4 years incredible.

To my dear Betta and Michela, I owe you a lot, you have been the first to teach and follow me in the lab, thanks for teaching me a lot of things, thanks for being always available for my help. Totally appreciate the time we have passed working together.

To all the master students I have been lucky to follow and work with during my PhD, to Alessia, Claudia, Ilaria and Isabella. It has been such a pleasure to work with you my dear girls.

To all the kind people I have met from the tissue engineering group, university of Granada and especially to my beloved friends from the lab: Aiora, Alberto, Ana, Carmen Miranda, Carmen

---

Morales, Cristina, Dani, David, Elisa, Fabiola, Fernando, Jesús, Maria Jesús, Marina, Olimpia and Óscar. Thanks for being immensely kind, friendly and welcoming. I am grateful to all the pleasant and delightful moments we shared together. Thanks for infinite laughs, happiness, and unforgettable memories. My stay in Granada was such an incredible experience thanks to you guys.

Special thanks to my dear friend Óscar who I have been lucky enough to have him as my lab partner during my stay in Granada. You are a great example of what a collaboration and a teamwork mean, all the worked presented in chapter 5 & 6 would not have been possible without you. Also, a special thanks for my dear friend Jesús. I have learned a lot from you guys, it was a real pleasure working with you and hope we can work again together in the future.

To my beloved Durand family: to my dear brother Dani, and his beautiful wife Mariana, and adorable kids Dani Jr and Camilla, thanks for lots of love and care, thanks for being a real family for me. Thanks Dani for always listening to my problems and always being there soothing and comforting me. Love you all and hope we can meet again soon.

To all my flatmates I had in Italy: Dalia, Mariana and Soha; and to all my flatmates I had in Spain: Carolina, Francesca, Lina and Paula, thanks for being a great company and a real family at home. Your love and support in difficult moments was of extreme importance for me. Love you more than you can imagine.

To my dear friends who became my special and beloved family in Italy, especially to Ahmed, Dalia, Hanaa, Hoda, Khaled, Kholoud, Mariana, Mohamed, Orayeb and Rossella; Thanks for being an important part in this journey, I have passed with you the most beautiful time I had in Torino, you will always be special for me, our memories would be carried forever in my heart. Love you my dear family.

To my dear friends in Spain Alba and Alicia, your friendship means a lot for me, thanks for all the beautiful memories and all the time I have spent with you and your families. It was a great blessing meeting you.

To all my professors in the university of Alexandria, especially to my dear Prof. Ismail Sabry and Prof. Essam Abd-Allah, I appreciate all the things I have learned from you during my bachelor degree, it has been the base for all what I have reached so far.

To my lifetime and true friends Dina & Moataz, you have taught me the true meaning of a real friendship and unconditional love. Unfortunately our destinies have made each one of us live in a different continent, but even though we are physically far, we are so close to each other and our souls are always together, thanks for always being there by my side, and for all your love and support.

To my greatest blessing in life, to my mum, dad, brother and grandma, no words could ever be enough to express my sincere love, appreciation, and gratitude. Thanks for always believing in me, thanks for all your trust and support in all my life choices. I would have never been able to achieve anything in my life without you by my side.

---

## List of Contents

<b>Abstract</b> .....	6
<b>Scientific problem &amp; Aim of research</b> .....	7
<b>PhD candidate contribution to the presented works</b> .....	9
<b>List of abbreviations</b> .....	10
<b>Chapter 1: Introduction</b> .....	11
<b>Chapter 2: Soluble neuregulin1 down-regulates myelination genes in Schwann cells</b> .....	62
<b>Chapter 3: Soluble neuregulin-1 (NRG1): a factor promoting peripheral nerve regeneration by affecting Schwann cell activity immediately after injury</b> .....	85
<b>Chapter 4: Fibroblasts colonizing nerve conduits express high levels of soluble Neuregulin1, a factor promoting Schwann cell dedifferentiation</b> .....	91
<b>Chapter 5: In vivo evaluation of chitosan conduits enriched with fibrin-collagen hydrogels +/- Adipose Derived Mesenchymal Stem Cells for Peripheral Nerve Repair</b> ....	122
<b>Chapter 6: Comparison of decellularization protocols to generate peripheral nerve grafts: a study on rat sciatic nerves.....</b>	143
<b>Chapter 7: General Discussion</b> .....	172

---

## ***Abstract***

### ***State of the art and purpose***

Peripheral nerve regeneration needs surgical action in case of severe injury. To repair nerve gaps, autografts are the gold standard but, as several drawbacks are present, tissue engineering techniques can be used to develop valid substitutes, like nerve conduits or decellularized nerve allografts.

Nevertheless, as hollow conduits are as efficient as autograft only in case of short gap repair, different strategies were developed to enrich conduits to promote long gap repair.

To this aim, it is important to understand the nature of the regeneration process, identifying cells and factors involved, such as Neuregulin1 (NRG1), a growth factor upregulated in response to nerve injury, playing a key role in nerve regeneration.

### ***Methods***

primary cell cultures, deep RNA sequencing, qRT-PCR, immunohistochemistry, TEM, SEM, western blots, functional analysis, *in vivo* nerve repair, morphometric analysis.

### ***Results & Additions to the current state of the art***

The regeneration analysis within a conduit after short gap repair showed that fibroblasts early colonizing the conduit express high levels of soluble NRG1 (known to be mainly released by Schwann cells following injury) and could play a key role in nerve regeneration within conduits. Indeed, we showed *in vitro* that NRG1 regulates the expression of genes involved in Schwann cell dedifferentiation, an important step for nerve regeneration.

For long gap repair two strategies were chosen: enrichment of chitosan conduits with hydrogel +/- Adipose Derived Mesenchymal Stem Cells (ADMSC) and a new decellularization protocol was tested.

In both hydrogel enriched chitosan conduits NRG1 was highly upregulated one week following repair. 15 weeks analysis showed that the sensory recovery was highly achieved just in ADMSC enriched conduits (analysis inside the conduit is still in progress).

The *in vitro* characterization of the newly tested decellularization protocol showed encouraging results and the prepared decellularized nerves are planned to be further tested *in vivo*.

## *Scientific problem and aim of work*

Peripheral nerves are highly susceptible to injuries. Spontaneous complete regeneration can occur in case of mild injuries, while severe nerve injuries with complete disruption in the nerve continuity are always in need of surgical intervention. Direct tensionless neurorrhaphy is the optimum solution in case of nerve transection without substance loss, while in case of nerve substance loss, there is a need to use a nerve substitute to fill the gap. There are various alternatives to repair short nerve gaps as the use of autografts, allografts and nerve conduits. Until now the autografts are the most efficient and is the surgeon's choice to repair critical nerve gaps. Nevertheless, there are some limitations accompanied with each repairing strategy, for example the autograft needs a second intervention to harvest the nerve graft, which results in donor site morbidity and possible neuroma formation, in addition to limited graft availability in terms of calibre and type. This has led to the use of allografts which are harvested from cadavers and have the advantage of supplying an illimited graft length of matching type and calibre, but its use should be accompanied by immunosuppression treatment, that could have a negative effect on patient.

Tissue engineering and regenerative medicine techniques have developed several artificial nerve conduits of natural or synthetic origins. Tubulisation technique has shown to be as efficient as autografts just in repairing short nerve gaps, while in critical nerve gaps tubulisation technique has poor regenerative outcome. The strategy of intraluminal fillers by hydrogels, cells or growth factors has aroused to enhance the conduit regeneration outcome in critical gaps.

Peripheral nerve injury induces morphological and molecular changes in the injured nerve environment. One of the main growth factors that have shown to play an important role in the peripheral nervous system during development and regeneration is Neuregulin1 (NRG1) whose different isoforms play different roles in peripheral nervous system: soluble NRG1 is expressed by Schwann cells immediately after injury and plays an important role in the process of Wallerian degeneration, a necessary step for nerve regeneration, while transmembrane NRG1 is expressed by axons and plays a key role in the myelination and remyelination processes during development and after nerve injury.

My PhD aims were focused on understanding the regeneration process into short and long nerve gaps.

Firstly, I was interested in studying the role played by soluble NRG1 in Schwann cells by comparing genes regulated *in vitro* after stimulation, with genes regulated *in vivo* after injury. For the study of short nerve gap regeneration, I focused on the regeneration process inside a hollow conduit used to repair a 10mm rat median nerve gap.

For the study of long nerve gap regeneration, I moved for one year to the Tissue Engineering Group under the supervision of prof Victor Carriel, in Granada University, where I focused in evaluating two different tissue engineering strategies:

1-enriching hollow chitosan conduits with a hybrid hydrogel composed of fibrin and collagen with or without Adipose Derived Mesenchymal Stem Cell (ADMSC) in repairing a 15mm rat sciatic nerve gap;

2- characterizing *in vitro* a new decellularization protocol to generate non immunogenic nerve allografts, that could be promising in repairing long nerve gaps.



## ***PhD candidate contribution to the presented work***

### ***Chapter 2: Soluble neuregulin1 down-regulates myelination genes in Schwann cells.***

Adult primary Schwann cell cultures preparation, cell stimulation, RNA extraction, all the primer design and real-time reactions, manuscript preparation.

### ***Chapter 3: Soluble neuregulin-1 (NRG1): a factor promoting peripheral nerve regeneration by affecting Schwann cell activity immediately after injury.***

Participation in preparation of the manuscript.

### ***Chapter 4: Fibroblasts colonizing nerve conduits express high levels of soluble Neuregulin1, a factor promoting Schwann cell dedifferentiation.***

Adult primary Schwann cells and Fibroblasts cultures preparation, participated in RNA and protein extraction, participated in real-time PCR reactions and western blot, manuscript draft preparation.

### ***Chapter 5: In vivo evaluation of chitosan conduits enriched with fibrin-collagen hydrogels +/- Adipose Derived Mesenchymal Stem Cells for Peripheral Nerve Repair***

Hydrogel preparation, *in vivo* animal surgeries, functional recovery assessment, animal sacrifice and sample collection (in equal contribution with García-García Ó.D), RNA and protein extraction, real-time PCR and western blotting analysis. Figures, data interpretation and initial manuscript preparation.

### ***Chapter 6: Comparison of decellularization protocols to generate peripheral nerve grafts: a study on rat sciatic nerves***

All laboratory analyses (in equal contribution with García-García Ó.D.); figures, data interpretation and manuscript preparation.

*List of abbreviations*

ADAM17	A Disintegrin And Metalloprotease 17
ADMSC	Adipose Derived Mesenchymal Stem Cells
AKT	Protein Kinase B
ANKRD27	Ankyrin repeat domain 27
ATF3	Activating Transcription Factor 3
BACE	$\beta$ -site of amyloid precursor protein cleaving enzyme
BDNF	Brain-derived neurotrophic factor
BMSC	Bone mesenchymal stem cell
CNS	Central nervous system
CNTF	Ciliary neurotrophic factor
CRD	Cystein-rich domain
CTR	Control group
DRG	Dorsal root ganglia
ECM	Extracellular matrix
EGF	Epidermal growth factor
FDA	Food and Drug Administration
GAG	Glycosaminoglycans
GDNF	Glial cell- derived neurotrophic factor
GGF2	Glial growth factor-2
ICD	Intracellular domain
JNK	c-Jun N-terminal kinase
MSC	Mesenchymal stem cell
NGF	Nerve growth factor
NRG1	Neuregulin1
NTF	N-terminus fragment
PEG	Polyethylene glycol
PGA	Polyglycolic acid
PHB	Poly-3-hydroxybutyrate
PI3K	Phosphatidylinositol-3-kinase
PLA	Polylactic acid
PLGA	Poly(lactic acid-co-glycolic acid)
PLLA	Poly-(l-lactic acid)
PNR	Peripheral nerve regeneration
PNS	Peripheral nervous system
SC	Schwann cell
TACE	Tumour necrosis factor- $\alpha$ converting enzyme
VEGF	Vascular endothelial growth factor

# *Chapter 1*

## *Introduction*

## List of Contents

1.Peripheral nerve general structure and anatomy .....	13
1.1 Stromal nerve component .....	15
1.2 Parenchymal nerve component.....	18
1.2.1 Nerve Fibres .....	18
1.2.2 Schwann Cells .....	19
1.3 Other peripheral nerve cells .....	22
1.4 Extracellular Matrix .....	23
2.Peripheral nerve degeneration and regeneration.....	25
3.Neuregulin: An important growth factor involved in peripheral nerve regeneration .....	29
4.Peripheral nerve injury and repair .....	37
4.1 Peripheral nerve injury classification .....	37
4.2 Peripheral nerve injury repairing strategies .....	39
4.2.1 Neurotmesis without nerve substance loss.....	39
4.2.2 Neurotmesis accompanied by nerve substance loss.....	41
4.2.2.1 Grafting technique .....	42
4.2.2.2 Tubulization technique.....	44
5.Tissue Engineering in peripheral nerve regeneration.....	45
5.1 Decellularized nerve allografts .....	45
5.2 Artificial nerve conduits .....	48
5.2.1 Natural-based nerve conduits .....	49
5.2.2 Synthetic nerve conduits.....	51
5.3 Intraluminal enrichment of nerves .....	52
6. References.....	57

## List of Figures

<b>Figure 1:</b> A representation of the complex structural organization of the nervous system.....	14
<b>Figure 2:</b> Stromal component of the peripheral nerve .....	17
<b>Figure 3 :</b> Myelinated axon anatomy, ultrastructure of myelinated and non-myelinated axons .....	19
<b>Figure 4:</b> Schwann cell developmental stages .....	20
<b>Figure 5:</b> The process of Radial sorting and fate decision of immature Schwann cells .....	21
<b>Figure 6:</b> Schematic representation of nerve Wallerian degeneration and regeneration.....	28
<b>Figure7:</b> Exons coding for the different Neuregulin1 isoforms .....	31
<b>Figure 8:</b> Proteolytic cleavage of Neuregulin1 .....	32
<b>Figure 9:</b> Different NRG-ErbB signalling pathways .....	34
<b>Figure 10 :</b> Sunderland peripheral nerve injury classification .....	39
<b>Figure 11:</b> Different surgical suturing techniques used in repairing peripheral nerves .....	41
<b>Figure 12:</b> Autografting repair techniques .....	43
<b>Figure13:</b> Artificial nerve conduits for peripheral nerve repair .....	45
<b>Figure14:</b> A graphical representation of an ideal decellularized nerve Allograft.....	48
<b>Figure15:</b> Intraluminal enrichment of hollow guiding nerve conduits .....	56

## 1-PERIPHERAL NERVE GENERAL STRUCTURE & ANATOMY

The nervous system is a highly complex system in our bodies, that is responsible in coordinating all the other body systems and responding to external environmental sensory information. This is achieved by transmitting signals to and from different body parts. The nervous system is divided into two interacting subsystems; the central and the peripheral nervous system (CNS and PNS respectively). The CNS includes the brain and the spinal cord, while all the remaining nervous structures comprise the PNS. Peripheral nerves are a set of complex networks of nerve fibres expanding throughout the body forming arborization that reaches all the tissues and organs conveying both sensory and motor stimuli from and to the CNS. PNS is further subdivided into somatic (voluntary movements control) and visceral or autonomic (involuntary) PNS, where the latter is further subdivided into sympathetic, parasympathetic and enteric nervous system (Figure 1).

Various classifications can be applied to nerve fibres: (1) Histologically, concerning the presence or absence of myelin sheath, nerves are classified as myelinated and non-myelinated nerve fibres (would be discussed in details later); (2) According to its emergence from the CNS, peripheral nerves can be categorized into either cranial or spinal nerves; cranial nerves (12 pairs) originating from the brainstem and innervating mostly the head, and spinal nerves (33 pairs) originating from the dorsal and ventral roots of the spinal cord, innervating all the body regions. Spinal nerves are further divided according to their origin into 8 cervical nerves, 12 thoracic nerves, 5 lumbar, 5 sacral and 3 coccygeal. (3) Depending on the direction of signal transmission and nerve function, nerves could be either afferent (sensory), efferent (motor) or mixed (sensory and motor). The afferent fibres convey sensory signals from PNS to CNS; in response to the received signal the efferent fibres deliver the motor signals from the CNS to PNS, controlling voluntary skeletal muscle movements (somatic fibres) or involuntary movements as in cardiac, smooth muscles and glandular secretion (visceral fibres). (4) According to Gasser and Erlanger's classification based on nerve diameter and conduction velocity, nerves are divided into A, B and C types. Group A is characterized by having large diameter and myelinated fibres and thus the highest conduction velocity of all body nerves. They comprise somatic afferent and efferent fibres. Group A is further subdivided into A alpha (afferent or efferent fibres), A beta (afferent or efferent fibres), A gamma (efferent fibres) and A delta (afferent fibres). Group B consisted of preganglionic autonomic fibres are myelinated

with a small diameter with a low conduction velocity. Group C are non-myelinated somatic afferent fibres and post ganglionic autonomic fibres having a small diameter and low conduction velocity. All nerves share the same morphology; similar to other body organs, peripheral nerves are anatomically composed of a stromal (connective tissue) component and parenchymal (main functional tissue) component.

## Nervous System

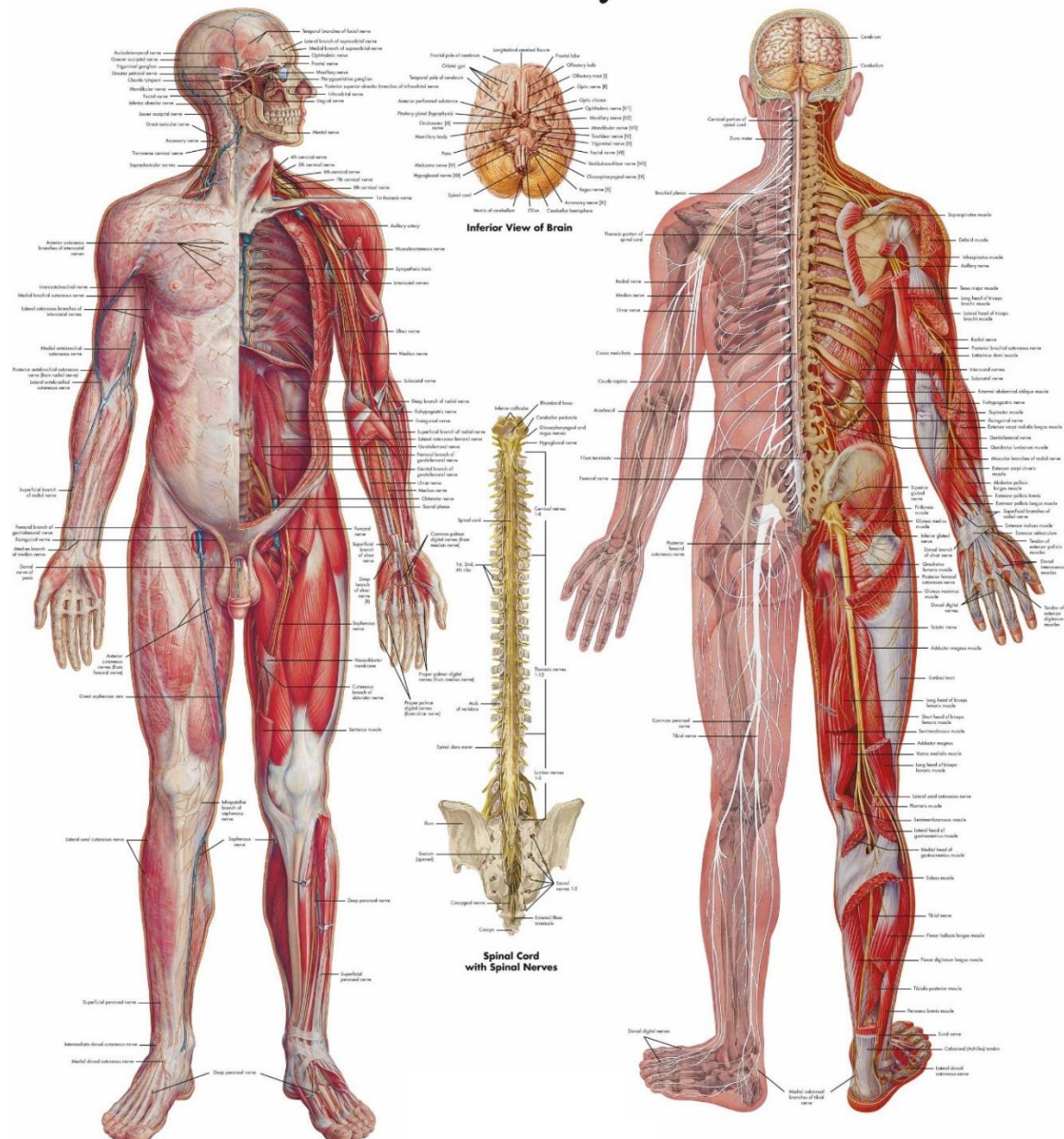


**Figure 1:** A representation of the complex structural organization of the nervous system. (3B scientific VR1620L [1001586].

### **1.1 Stromal nerve component (Connective tissue)**

Peripheral nerves are protected and supported by three layers of connective tissues which convey to nerves their resistance to mechanical stress caused by stretches associated with movements of the limbs and mechanical compressions from daily activities. The layers arranged from the outermost to the inner most are epineurium, perineurium and endoneurium (Figure 2) (Thomas, 1963).

The epineurium is a dense permeable connective tissue forming the outermost layer of the nerve associated connective tissue, it surrounds the nerve, defines its boundaries and supports its inner structure by holding together the internal fascicles. It includes fibroblasts (found scattered throughout the epineurium, having elongated processes and lacking a basement membrane), adipocytes, and mast cells (are distributed throughout connective tissue and are often located in the proximity of small blood). Epineurium merges with adipose tissue surrounding peripheral nerves, particularly in subcutaneous tissue. The amount of epineurial tissue varies along a nerve and is more abundant around joints. Large blood vessels are present, where they run parallel to fascicles and form numerous capillaries that penetrate to the other connective layers providing them with oxygen and nutrients (Thomas, 1963; Geuna et al., 2009)

The epineurium can be divided into 2 components, the interfascicular “internal” component, which is made of loose connective tissue that fills the space among the fascicles, and the circumferential “external” epineurium that forms the “skin” of the nerve, which is formed of a dense connective tissue (Geuna et al., 2009).

Epineurium contains three types of extracellular fibrillary structures of which the collagen fibres are the most prominent component. They are formed by the scattered fibroblasts that are mainly disposed longitudinally along the length of the nerve trunk; while some can be found as well in an oblique orientation. Elastin fibres that are more compact than collagen ones are mainly disposed longitudinally. Finally, fine filaments of microfibrils are present either in small bundles or intermixed with collagen fibres (Thomas, 1963; Geuna et al., 2009).

The perineurium is a multilayer dense connective tissue that encloses each nerve fascicle. It is composed of alternating concentric layers of flattened, squamous perineurial cells separated by layers of collagen fibres, fibroblasts are also present in between them. The number of perineurial cell layers depends on the size of the fascicle. As much as 8–16 concentric layers may be present around large nerve fascicles, but a single layer of perineurial cells surrounds small distal fascicles. Perineurial collagen fibrils are produced by perineurial cells. Compared



to epineurium, the perineurial collagen fibres are thinner and arranged longitudinally, just a few elastic fibres are scattered among them (Thomas, 1963; Geuna et al., 2009).

Adjacent perineurial cells within the same layer of perineurium are connected by tight and gap junctions. Cells of one layer are also connected to the successive layers by gap junctions. Tight junctions in the inner layers of the perineurium together with the tight junctions in endoneurial capillaries form the blood-nerve barrier structure. The perineurial cells are metabolically active, and probably play a role in maintaining electrolyte and glucose balance around the nerve cells (Geuna et al., 2009).

The inner endoneurial sheath located immediately outside the basement membrane of SCs consists of circular, longitudinal and oblique collagen fibres, while solely longitudinal collagen fibres are present in the external endoneurial sheath. The endoneurium is composed of loosely longitudinally arranged collagen fibres with a smaller diameter compared to the epineurium, but they are more condensed around the nerve fibres and capillaries, and subperineurially. The collagen is associated with microfibrils, but no elastin fibres are present. The endoneurium is a delicate connective tissue, enveloping individual nerve fibres within the fascicles. It surrounds Schwann cells and fills the space bounded externally by the perineurium. It is composed of fine loose collagen fibres that run parallel to the axons, few number of fibroblasts and macrophages can be found. The endoneurial collagen mostly originates from the Schwann cells, which are more prominent than fibroblasts. The collagen of the endoneurium is again orientated mainly in the length of the nerve trunk and is aggregated around the nerve fibres and blood vessels and also in a zone immediately internal to the perineurium. Elsewhere, the collagen is considerably less densely packed. The fibres are of smaller diameter than those of the epineurium. No elastin fibres are present in the endoneurium (Thomas, 1963; Geuna et al., 2009).

The collagen fibres surrounding SCs of large myelinated nerve fibres are organized into two layers. The inner layer is composed of collagen fibres of slightly smaller diameter than those of the outer layer. Fibres orientation is not uniform, they can be found in longitudinal, circular and oblique orientations. The outer layer consists solely of longitudinal collagen fibres that are more densely packed than in the inner layer. A similar sheath surrounds the Schwann cells containing small myelinated and non-myelinated axons but is less clearly organized into two layers (Thomas, 1963; Geuna et al., 2009).

In the endoneurium, collagen is loosely packed, but it is found more condensed around the nerve fibres and blood vessels, and subperineurially, leaving substantial extracellular fluid

spaces. Endoneurium contains fluid that flows in a proximo-distal direction along the nerve trunk while the basement membrane of cells defines the limits of the extracellular tissue space. Blood capillaries infiltrating within perineurium reaching the endoneurium provide the needed oxygen and substance supply to the internal axon-Schwann cell units (Thomas, 1963; Geuna et al., 2009).

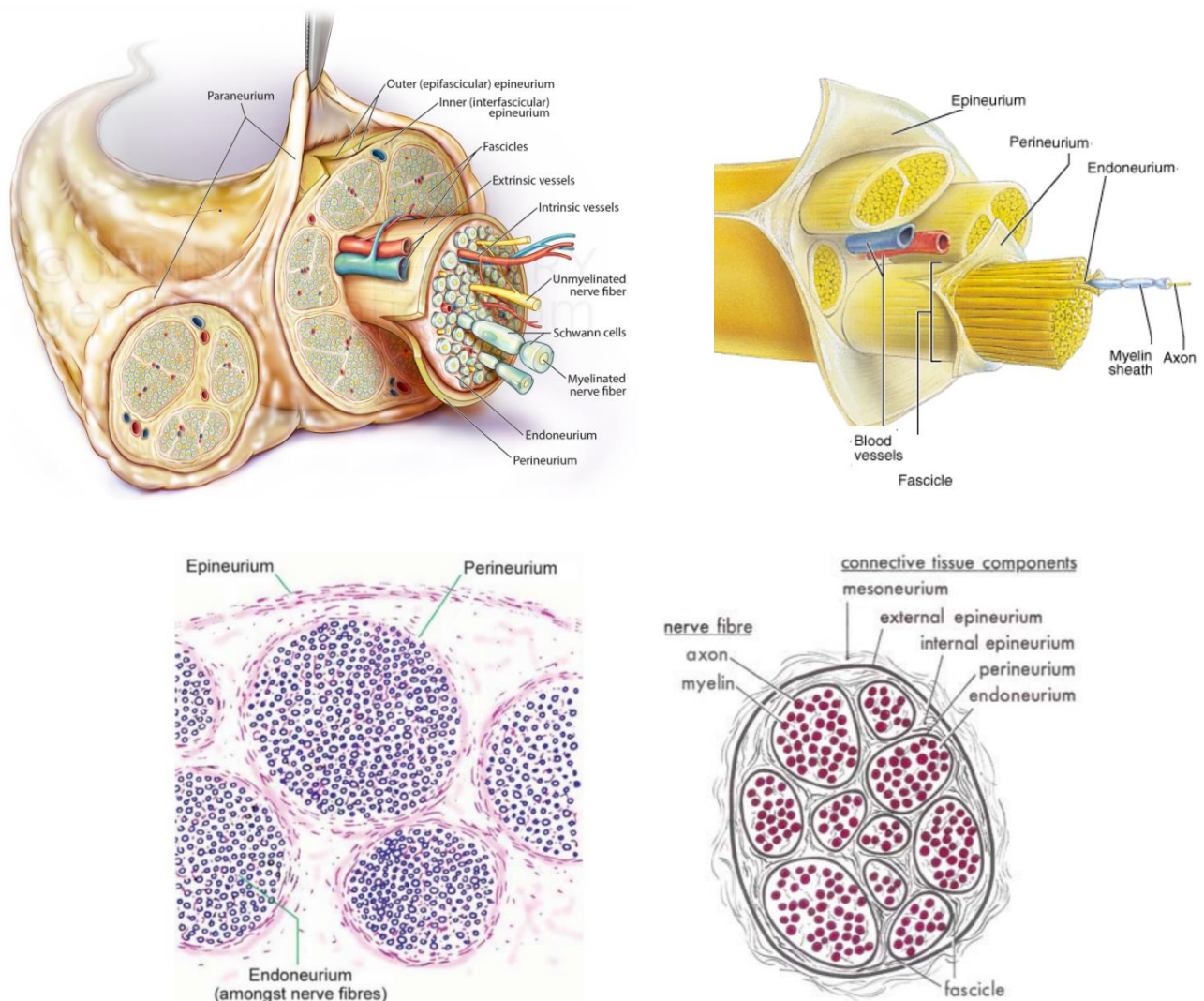


**Figure 2:** Stromal component of the peripheral nerve showing the 3 connective layers surrounding the nerve, collagen fibres stains weak pink with eosin in haematoxylin-eosin stain preparations (Pfister et al., 2011).

## 1.2 Parenchymal nerve component (nerve fibre and Schwann cells)

### 1.2.1 Nerve Fibre

Nerve fibre is the smallest functional building unit of peripheral nerves. The cell bodies (soma) of neurons are located in the ganglia. The soma of sensory neurons is found in the dorsal root ganglia or in the cranial ganglia and the bodies of neurons, part of the autonomic circuits, are housed inside the sympathetic and parasympathetic ganglia. On the contrary, the bodies of the motor neurons are located at the level of the CNS, in the ventral horn of the spinal cord or in the brainstem, while the axons of the peripheral neurons are part of the nerves.

As mentioned before, one of the main nerve classifications is based on the nerve/SC relationship that determines whether the nerve becomes myelinated or non-myelinated. The nerve and Schwann cells play together an independent role where one cell type is always dependent on the other. Briefly, during development immature Schwann cells adopt one of two fates either myelinating or non-myelinating dependent on the axonal signals they receive during the process of radial sorting; where large calibre axons of diameter more than  $1\mu\text{m}$  becomes myelinated. Axons of small diameters are gathered together and surrounded by a single membrane of Schwann cells (Remak cells or non-myelinating SCs) that serves for their protection; these axons are thus called non-myelinated axons (Jessen et al., 2015; Salzer, 2015).

Myelinated axons can be structurally identified into different regions; mainly the (1) Internode: which is the insulated axonal part that is wrapped by the Schwann cell cytoplasmic membrane (myelin). The internodal length varies directly with the fibre diameter ranging from  $150$  to  $1500\mu\text{m}$ . (2) Periaxonal space: a narrow space  $15\text{-}20\text{ nm}$  which separates the myelinated segment from its enclosed axon; (3) Nodes of Ranvier: the non-insulated axonal segment; (4) Paranodal regions are immediately adjacent to either sides of the node; they are the site of attachment between the axon and the myelin (5) Schmidt-Lanterman incisures (SLI) are oblique interruptions in the interparanodal myelin region where the myelin membrane compaction is lost (Figure 3).

One of the major biochemical characteristics that distinguishes myelin from other biological membranes is its high lipid-to-protein ratio: isolated myelin contains  $70\text{-}80\%$  lipids and  $20\text{-}30\%$  proteins. This relatively high lipid content and the particular characteristics of the lipids present in the sheath, provide the electrically insulating property required for the saltatory propagation of the nervous influx (Garbay et al., 2000).

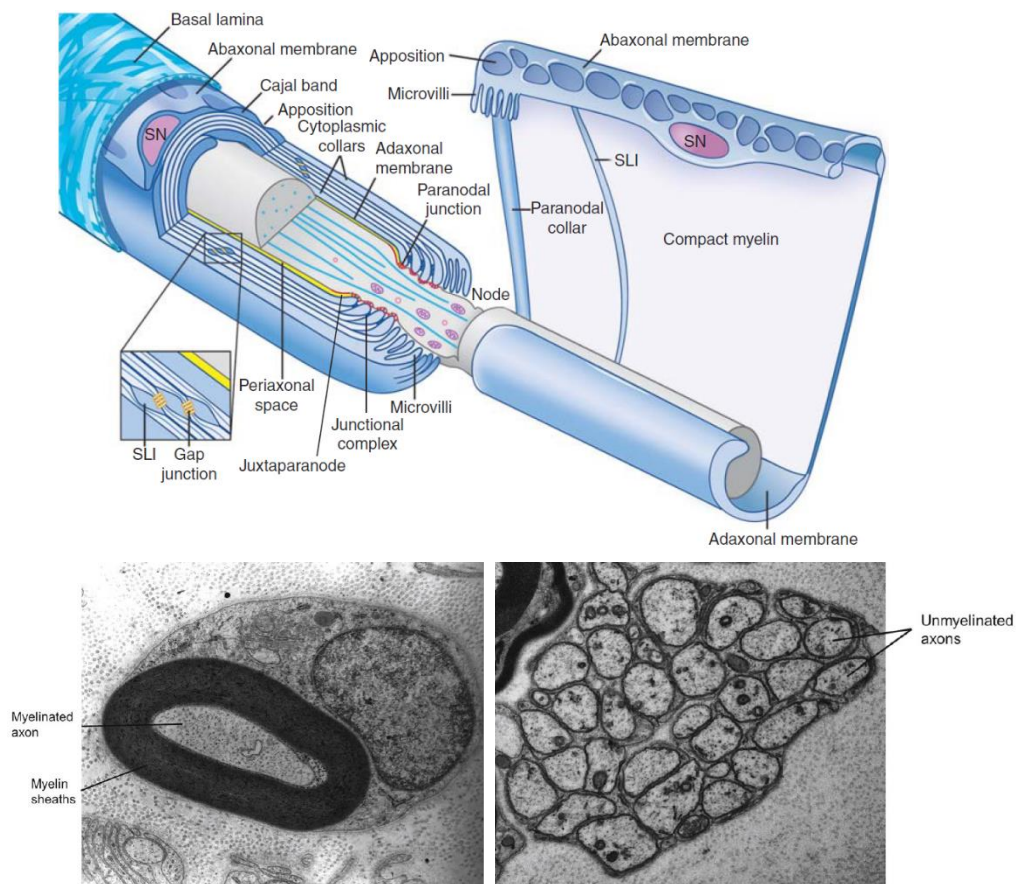


**Figure 3** : Myelinated axon anatomy, ultrastructure of myelinated and non-myelinated axons (Reina et al., 2015; Salzer, 2015).

### 1.2.2 Schwann Cells

Schwann cells (SCs) are the major glial cell type in the peripheral nervous system; differently from their central nervous system homologues, the oligodendrocytes, that ensheath multiple axons simultaneously, myelinating SCs only ensheath one large calibre axon, while non myelinating SCs simultaneously ensheath multiple small calibre axons. They play an important role in providing the nerve with metabolic as well as trophic support, nerve protection and survival and, most importantly, with the myelin sheath for the nerve saltatory conduction (Jessen & Mirsky, 2019; Jessen et al., 2015).

SCs are derived from neural crest cells (Figure 4); during development receive signals from the surrounding environment that guide their differentiation into Schwann cell precursors (SCPs) in early embryonic nerves (rat E14-15). SCPs are closely integrated with axons in newly

formed nerves and exclusively rely on axonal signals for their survival. The survival of both neurons and SCPs in the developing nerves is reciprocal. As much as neurons are dependent on SCPs for their survival, SCPs, themselves, require axon-derived factors for their survival. Further SCPs differentiate into immature Schwann cell (iSCs) (rat E17–18); in late embryonic and perinatal nerves, iSCs are no more dependent on axonal signals for their survival, as they become associated with basal lamina and connective tissue inside the nerve (Jessen & Mirsky, 2016; Jessen & Mirsky, 2019). Post-natally, iSCs adopt their final differentiation fate dependent on the axons they are going to ensheath. iSCs extend cellular processes inside the axonal bundles to select large calibre axons in a finely tuned multistep process termed radial sorting. This physiological process starts peri-natally and proceeds almost until the 10<sup>th</sup> postnatal day (P10) in the rodent peripheral nervous system (PNS).

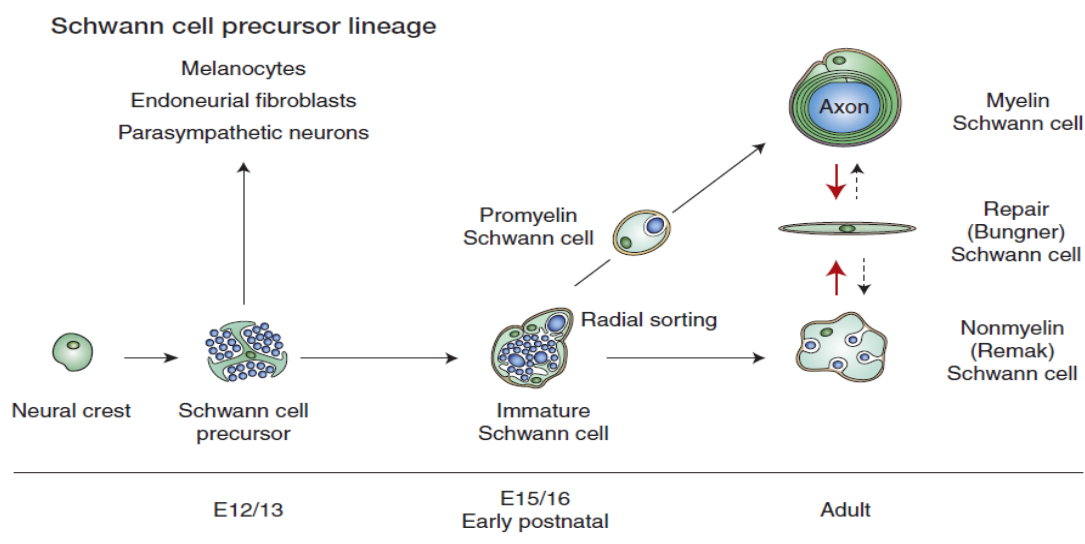


**Figure 4:** Schwann cell developmental stages (Jessen & Mirsky, 2015).

Axonal sorting requires multiple events: the formation of SC ‘families’ with multiple axons grouped in a common basal lamina, the matching of the number of axons and SCs, the insertion of SC processes around axons to recognize and segregate large ones, and the defasciculation of single axons with their own daughter SCs and basal lamina (Berti et al., 2011). The process results in individual pro-myelinating SC–axon units, promptly activating a molecular program to generate myelin sheaths (Figure 5).

According to the axonal diameter iSCs are associated with large calibre axons in the ratio of 1:1, they become pro-myelinating SCs that later differentiate into myelinating SCs.

Myelinating SCs wrap their plasma membranes several times around the axon forming the myelin sheath (myelinogenesis). The accumulation of new myelin lamellae occurs by the progression of the internal SC periaxonal cytoplasmic collar around the axon. Each myelin generating SC provides myelin sheath for only one segment of the axon. Thus, along the axonal length, several myelinating SCs form successive internode segments. The nodes of Ranvier are periodic interruptions that exist in between two successive internodes, where short portions of the axon are left uncovered by myelin. They are rich in voltage sensitive sodium channels that are directly responsible for the propagation of the action potential along the axon. Nodes of Ranvier are critical to the normal myelin functioning and serve for the saltatory conduction that ensure efficient and rapid propagation of action potential (Nave and Werner 2014; Salzer 2015).

Access to the entire myelinated nerve structure is ensured by narrow cytoplasmic channels that run spirally through the sheath (Schmidt Lanterman incisures), to the internal and external limits of the compact myelin (internal and external mesaxons), to the lateral edges of each myelin segment (the paranodal region and the nodes of Ranvier) and to the cell body. The compact region of each myelin segment located between two nodes of Ranvier, is called an internode (Salzer, 2015).

Small axons that are not myelinated are gathered together and are surrounded by a single layer of Schwann cell basal lamina; this type of SCs is called Remak or non-myelinating SC (Jessen et al., 2015).

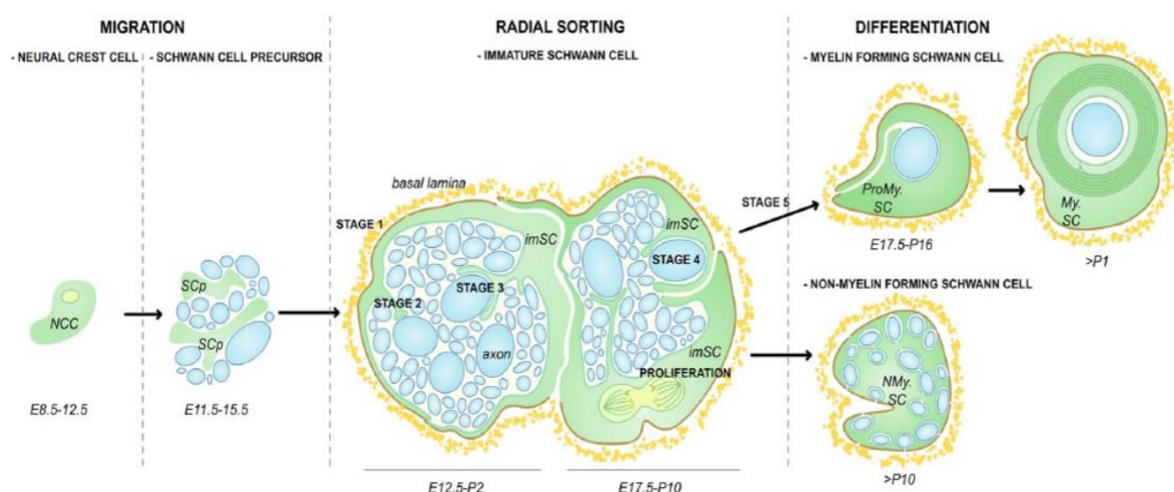


**Figure 5:** The process of Radial sorting and fate decision of immature Schwann cells (iSCs) (Feltri et al., 2015).

### 1.3 Other Peripheral nerve cells (fibroblasts and perineurial glia)

Fibroblasts share the same developmental origin with iSCs, as both are derived from SCPs (Joseph et al., 2004). SCPs adopt their fate during nerve development, the ones which remains in close contact with the nerve and receiving the nerve signals continue in the SC line; while those that loose the direct contact with nerves adopt the fibroblast fate (Woodhoo & Sommer, 2008). It was also observed that the appearance of iSCs and fibroblasts is linked temporarily with the disappearance of SCPs during the process of nerve development.

Fibroblasts are critical components of all nerve compartments, including endoneurium, perineurium, and epineurium. They were found to play various important roles in peripheral nerves. The first and most important is the collagen I secretion, that is one of the main ECM components in the peripheral nervous system. While previously it was thought that fibroblasts hamper the regeneration process by excess collagen secretion and scar formation, now it is known that they play an important role in nerve regeneration process: it was found that they play a role in the inflammatory response after nerve injury (Shamash et al., 2002); *in vitro* studies show that they release neuregulin1, a soluble pro-migratory factor that promotes SC migration (Dreesmann et al., 2009), which was also seen *in vivo* as a response to nerve injury (Fornasari et al., 2020). Moreover, they regulate SC sorting and directional collective migration and Büngner bands formation via ephrin-B/EphB2 signalling (Parrinello et al., 2010). This directional collective migration of SCs is essential to guide the axon regrowth across the wound. Perineurial cells are also derived from neural crest cells, they are the main cellular component of the perineurium, that is formed by multiple perineurial cells linked together via tight junctions, making this structure a component of the blood –nerve barrier, protecting the interior of the nerve from toxins, infection, and ionic flux.

Previously, perineurial cells were often mistaken and referred to as fibroblasts because of their similar flattened shape, but then they were distinguished because of the differences displayed by each cell population. Fibroblast has a compact nucleus and a large endoplasmic reticulum, whereas these features are lacking in perineurial cells. Additionally, perineurial cells have double basal lamina, whereas fibroblasts have a single basal lamina. Fibroblasts are almost always arranged in a large mass, whereas perineurial cells are joined carefully by tight junctions into a single sheet (Kucenas, 2015).

Studies have shown that perineurial glia is not only essential in motor axonal guidance and pathfinding, but also in motor nerve fasciculation. It has been shown that in the absence of

perineurial glia, SC migration along motor axons is delayed and SCs fail to myelinate motor axons (Kucenas et al., 2009; Binari et al., 2013)

#### **1.4 Extracellular Matrix (ECM)**

The nerve extracellular matrix is a three-dimensional structure found in between intercellular spaces. It is secreted by resident glial cells; it consists of water, carbohydrates, and various proteins, including collagens, proteoglycans, non-collagenous glycoproteins, and elastins, which play an important role in protecting, supporting, feeding and isolating neurons (Alovskaya et al., 2007; Gonzalez-Perez et al., 2013; Han et al., 2019). It is always in a dynamic state to respond to changes in the microenvironment, and has been shown to provide cues that affect cell migration, proliferation, and differentiation. In peripheral nerves, the extracellular matrix is found in the basal lamina of Schwann cells and in the endoneurium. The main structural components of the nerve ECM are collagen (type IV), laminin and fibronectin, where laminin is the main component of the basal laminal tubes (Alovskaya et al. 2007; Gonzalez-Perez et al., 2013; Han et al., 2019).

The ECM in peripheral nerves is divided into fibrillar (collagen, reticular and elastic) and non-fibrillar components (proteosaminoglycans and glycoproteins). These molecules are present in different proportions throughout the stromal layers of peripheral nerves, being important cues from a regenerative and biomechanical point of view. The fibril forming collagens type I and III build up the epineurium, while the network forming collagen type IV is localized in the basal lamina of blood vessels and peripheral nerve fibers. Collagen type V is described as a “minor” fibril forming collagen, but is abundant in peripheral nerves and might play a role in myelination. In addition, reticular fibers are mainly composed of collagen type III, but also contain collagen type V and several glycoproteins (Alovskaya et al., 2007; Gonzalez-Perez et al., 2013; Han et al., 2019).

Elastic fibers can be found in the perineurium. They are responsible for the visco-elastic properties of peripheral nerves and consist of about 90% of the protein elastin and for 10% of glycoproteins (Alovskaya et al., 2007; Gonzalez-Perez et al., 2013; Han et al., 2019).

The biggest group of non-fibrillar ECM components is represented by the proteosaminoglycans. They are composed of a core protein with several attached glycosaminoglycans (GAGs), which have either carboxylic or sulphated side chains.



Glycoproteins are represented by a heterogeneous group of ECM molecules (mainly composed of globular proteins associated with oligosaccharides) which play crucial roles in cell adhesion, migration and proliferation. In peripheral nerves, the most important glycoprotein from the structural, functional and regenerative point of view is laminin. This essential component of the nerve basal lamina promotes proliferation and migration of SCs during regeneration and guides newly formed axons. Fibronectin is another glycoprotein present in the basal lamina and in the connective tissue. It plays a similar role to laminin, supporting different cell functions during regeneration (Gonzalez-Perez et al., 2013; Han et al., 2019).

**Collagens** comprise three polypeptide chains (alpha chains) with characteristic triple helical collagenous and non-collagenous domains. In vertebrates, 27 types of collagen are present, based on their supramolecular assembly and other features, they are classified into 9 families. The fibrous collagen family includes abundant quantities of type I, type II, and type III, and lower quantities of type V and type XI. Type I, type III, and type V collagens are widely distributed in the body, while types II and XI are mainly confined to cartilage. The basal layer produced by Schwann cells mainly consists of type IV collagen, laminin and fibronectin (Gonzalez-Perez et al., 2013; G. H. Han et al., 2019).

**Proteoglycans** consist of a core protein covalently linked to a glycosaminoglycan side chain. Glycosaminoglycans are sulphated oligosaccharides that consist of dermatan sulphate, heparan sulphate/heparin, chondroitin sulphate or keratan sulphate repeating disaccharide units. They play a role in the hydration and permeability of the extracellular matrix, they also influence cellular activity via interactions with extracellular matrix components, growth factors, and cell surface receptors (Alovskaya et al., 2007; Gonzalez-Perez et al., 2013; Han et al., 2019).

**Laminin** is a key component of the basement membrane, plays different roles in cell migration, differentiation, and adhesion. Laminin is a heterotrimer of  $\alpha$ ,  $\beta$ , and  $\gamma$  chains. There are 18 different types that have been described so far (Durbeej, 2010).

**Fibronectin** represents another key component of the ECM and forms a fibrillary matrix similar to collagen to mediate cell-cell binding. Alternative mRNA splicing results in various fibronectin isoforms. 12 different isoforms have been described in mouse while 20 forms have been identified in humans (Gonzalez-Perez et al., 2013). In the nervous system, they are synthesized and secreted by Schwann cells and fibroblasts.

**Elastic fibres** consist of an elastin core surrounded by a microfiber network that together contributes to tissue elasticity and resilience. To generate elasticity, soluble precursor molecules are deposited in a preformed microfibril matrix and subsequently cross-linked to

form insoluble elastin polymers. Microfibrils are also present in some flexible tissues where elastin does not exist ( Han et al., 2019).

## 2.PERIPHERAL NERVE DEGENERATION & REGENERATION

While the central nervous system lacks the intrinsic capacity to regenerate following trauma, peripheral nervous system is characterised by its spontaneous regeneration. Nerve injury (independent on the injury type) provokes Wallerian degeneration a series of changes described over 150 years ago by August Waller 1850 (Waller, 1850) (Figure 6). Wallerian degeneration is accompanied by a set of morphological and biochemical alterations that prepare the nerve for subsequent regeneration. These changes occur in the distal stump at the level of axons and at the level of Schwann cells, the main glial cell type in the peripheral nervous system. These changes are vital for the process of axon regeneration and final target organ reinnervation. Following nerve injury as a result of the axonal continuity disruption, the synaptic transmission is lost and the target organ does not receive any nerve signal (Belanger et al., 2016).

Wallerian degeneration consists of a sequence of events resulting in axon and myelin fragmentation and subsequent debris elimination. Shortly after nerve transection morphologic changes begin to appear in the distal axon segment. Within hours, membranous organelles, glycogen (normally transported along the axon) and atypical swollen mitochondria begin to accumulate in paranodal regions and adjacent to the lesion site on both the proximal and distal sides of the injury site. Lysosomes as well begin to accumulate in the paranodal regions and adjacent to the lesion site by 2 h after injury. The accumulation of organelles in severed axon segments adjacent to the cut site is of a magnitude sufficient to enlarge the axon, thereby stretching and thinning the adjacent myelin sheath. Within 12 to 24 hours, axonal microtubules begin to become disorganized, indicating the beginning of dissolution of this portion of the axonal cytoskeleton. 1 to 2 days post-injury, calcium ions enter the axon segment via calcium-specific channels and activate calcium-dependent calpain proteases which degrade neurofilaments, microtubulins and other cytoskeletal components within the axon (Deumens et al., 2010) As these morphologic changes (named granular disintegration) progress, the normal axonal cytoskeleton, axolemma, and axonal organelles are degraded, converting the axoplasm into a watery fluid filled with amorphous and granular debris. At the time granular disintegration occurs, the myelin sheath surrounding the axon, is stretched but is still intact. It is worth mentioning that axonal degeneration direction depends mainly on the type of injury,

degeneration occurs in a distal-to-proximal direction following a cut injury, while axon degeneration proceeds in a proximal to-distal direction following a crush injury (Carroll and Worley 2016).

Both myelinating and non-myelinating SCs lose their contact with axons and trans-differentiate into a repair SC phenotype. The trans-differentiation process is accompanied by changes in gene expression. Myelination genes (P0 and MBP) together with node and internode related organizing genes (Connexin 32 and E-cadherin) are down-regulated, while regeneration associated genes (growth factors receptors, growth factors and adhesion molecules) are upregulated. The new repair SCs adopt new characteristics that differ from the normally present adult SCs (Jessen & Mirsky, 2016). In the early stages of Wallerian degeneration, repair Schwann cells mediate the initial breakdown of their own myelin sheath associated distal axon segments in a process called myelinophagy. Minutes following the nerve transection, widening of Schmidt–Lanterman incisures can be observed in Schwann cells immediately distal to the injury site; by 24–36 h after injury, this same alteration is evident in Schwann cells throughout the more distal portions of the nerve segment. As the Schmidt–Lanterman incisures open up, the cytoplasm of Schwann cells begins to swell and compress associated axons. 24 to 48 h after nerve transection, myelin destruction begins. Schwann cells start to fragment myelin sheath into myelin ovoids inside a special digestion chambers that are contained in special compartments in their cytoplasm. As Wallerian degeneration proceeds, digestion chambers are often found to also contain fragments of axoplasm. Degeneration in unmyelinated Schwann cells occurs in a similar fashion except, of course, that myelin ovoids are not seen (Carroll and Worley 2016). In subsequent days and weeks, myelin ovoids are further fragmented and cleared as macrophages begin to assist in the clearance of myelin and axonal debris. Resident macrophages normally present in the endoneurium (2–9% of endoneurial cell population) become activated during Wallerian degeneration, performing their activity together with the hematogenous macrophages that are recruited by Schwann cells into the degenerating distal nerve site. Macrophage infiltration is facilitated by the opening of the blood nerve barrier that is triggered by the release of histamine, serotonin, and other substances from resident mast cells. Their infiltration starts at 1 day, peaking at 4 days and markedly declining by 8 days post injury. Macrophage infiltration begins at the lesion site and proceeds in a proximal-to-distal direction, paralleling the breakdown of the myelin sheath. Macrophages can phagocytose myelin debris lying free in extracellular spaces (Carroll and Worley 2016).

After macrophages finish clearing myelin and axon debris from the distal nerve segment, they are eliminated from the nerve either by local apoptosis or by re-entering in the circulation. The process of myelin debris clearance is a prerequisite for subsequent axonal re-growth, as myelin remnants could inhibit axonal regeneration process.

Proximal to the injury site, the nerve cell body is deprived of essential trophic factors and consequently either undergoes programmed cell death (apoptosis) or a potentially reversible process called chromatolysis. Chromatolysis is characterized by a swelling in the cell body caused by the accumulating proteins that reflects increased production of proteins that will be required in the following regenerative phase. This switch in function of the cell body is evident through the granular appearance of the endoplasmic reticulum and the eccentric position adopted by the nucleus to accommodate the build-up of new proteins (Carroll and Worley 2016).

A regenerating bridge tissue is spontaneously formed to join the transected nerve stumps. Macrophages first enter the bridge region and start to secrete VEGF-A in response to hypoxia, that triggers vascularization (Cattin et al., 2015). These newly formed blood vessels form the guiding path for Schwann cells to cross the bridge and serve in directing regenerating axonal sprouts. The organized SC migration is directed by fibroblasts via ephrinB/EphB2 signalling that converts their normally repulsive behaviour into an adhesive one that is essential for their organization and migration in cords (Parrinello et al., 2010).

In the distal segment, SCs transdifferentiate into a repair phenotype. Four days after cutting of the sciatic nerve in the rat, proliferating repair SCs are aligned in columns forming “Bünger bands” in the basal lamina of the original nerve. They do not only act as a physical guide for axonal regrowth, but also secrete neurotrophic factors that support axon growth as ciliary neurotrophic factor (CNTF), brain-derived neurotrophic factor (BDNF), glial cell- derived neurotrophic factor (GDNF), and nerve growth factor (NGF). Furthermore, they produce neurite-promoting proteins such as fibronectin and laminin, which are incorporated into the extracellular matrix (ECM). Growth cones utilize these proteins for adhesion to the basal lamina of the endoneurium (Caillaud et al., 2018; Bolívar et al., 2020).

During nerve regeneration, neurons in the proximal nerve stump shift their gene expression from a transmitting to a growth mode. Genes that express cytoskeletal proteins, actin and tubulin, and GAP-43 which support axonal growth, are upregulated, while those associated with chemical transmission, as choline acetyltransferase and acetylcholinesterase, are

downregulated. Axonal growth cones are guided by SCs in the bridge region to reach the distal nerve portion (Caillaud et al., 2018).

The recovery can take from few weeks up to several months, depending on the re-establishment of the appropriate connection with the target organ. Following the successful direction of the regenerating axon to its target organ, a maturation process needs to occur. This process includes remyelination, axon enlargement, and finally, functional re-innervation.

Repair SC proliferation is then arrested, and they re-differentiate into myelinating SCs that remyelinate the newly regenerating axons. The newly formed myelin sheath is thinner with significantly shorter internodes. Following re-myelination, target innervation is restored, and signal transmission is recovered, the muscle fibre atrophy could be reversed as well. In the case of severe peripheral nerve injuries, usually fibrous scar tissue is formed, and complete regeneration is not achieved. Injured axons fail to regenerate with aberrant sprouting resulting in neuroma formation at the proximal nerve stump. Moreover, the failure of the regenerating axons to extend along the endoneurial tubes results in increased collagen fibrils deposition and shrinkage of endoneurial tubes and target organ (skeletal muscle fibre atrophy) (Deumens et al., 2010). Thus, a successful peripheral nerve regeneration after injury relies on both injured axons as well as non-neuronal cells, including SCs, endoneurial fibroblasts and macrophages. Together, these produce a supportive microenvironment allowing successful regrowth of the proximal nerve fibre ending (Caillaud et al., 2018).

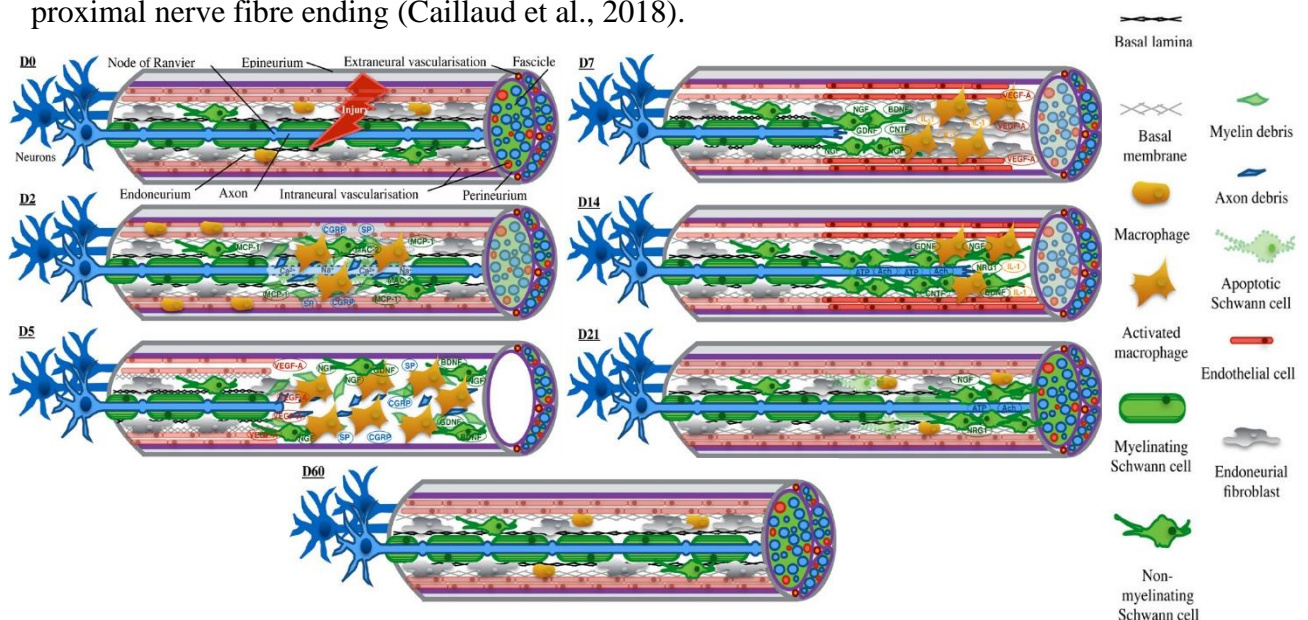


**Figure 6:** Schematic representation of nerve Wallerian degeneration and regeneration (Caillaud et al., 2018)

## 3-NEUREGULIN1: AN IMPORTANT GROWTH FACTOR INVOLVED IN PERIPHERAL NERVE REGENERATION

Growth factors are small diffusible proteins that are secreted in normal physiological conditions, playing an important role in the homeostatic maintenance of intact normal neurons. In response to injury, their expression changes. Both SCs and denervated organs secrete a wide set of growth factors that play a role in modulating axonal regrowth, elongation, adherence and attraction to target organ, as well as SC differentiation and re-myelination. The upregulation of these factors is fundamental in supporting axonal survival, growth and target reinnervation. At the end of the regeneration process their expression returns to normal basal levels(Li et al., 2020).

### **Neuregulins**

Neuregulins (NRG) are a large family of growth factors that are widely expressed in various tissues. They are encoded by four individual genes (NRG1–4) that contain a conserved epidermal growth factor (EGF) like domain of approximately 55 amino acids. The EGF like domain is essential for binding and activation of the tyrosine kinase receptors ErbB3 and ErbB4 (Talmage, 2008; Clark et al., 2012).

NRG1 is a complex gene containing more than 20 exons and several large introns, NRG1 encodes more than 30 protein isoforms that are generated by a combination of alternative mRNA splicing and the use of different transcription promoters (Figure 7) ( Mei & Xiong, 2008; Gambarotta et al., 2013).

### **Structural domains of Neuregulin1**

Most Neuregulin1 isoforms are originally synthesized as membrane anchored precursors called pro-NRG1 which are then processed and cleaved by metalloproteases (shedases). Pro-NRG1 are single pass transmembrane molecules that are composed from three main domains: the extracellular domain, the transmembrane domain and the intracellular domain.

**Pro-NRG1 extracellular domain:** it is the N-terminal side positioned outside the cell, where other sub-domains are present:

**Type specific N-terminal sequence:** specific for each type of the protein isoforms generating Nrg1 type I-VI.

Immunoglobulin (Ig) like domain: it is found mainly in type I and type II NRG1, and thus they are also known as Ig-NRG1.

Epidermal Growth Factor like domain (EGF): it is the core domain required for ErbB receptor binding and signalling; it is located in the membrane-proximal region of the extracellular domain. According to its C-terminal sequence,  $\alpha$  or  $\beta$  isoform are produced.

Glycosylation region: found in NRG1 type I, IV and V.

Kringle domains: consist of triple-looped, 3-disulfide bridges and are proposed to serve as protein-protein interaction sites, only found in Type II Nrg1.

Linker or stalk: it is the juxtamembrane region of the C-terminal side of the EGF-like domain which serves as the proteolytic cleavage site, according to which NRG1 isoforms are classified as 1, 2, 3 or 4. Linker 1 and 4 connect EGF-like  $\alpha$  or  $\beta$  with the TMc, linker 3 is found in isoforms lacking TMc, while the "2" isoforms are those that lack a linker and their EGF-like  $\alpha$  or  $\beta$  are directly connected to the TMc.

**Transmembrane domain (TMc):** transmembrane domain at the C-terminal of the EGF-like domain; Nrg1 isoforms that lack the TMc domain (isoforms with linker 3) are synthesized as soluble protein isoforms.

**Pro-NRG 1 intracellular domain:** it is the C-terminal cytoplasmic tail positioned inside the cell.

-Carboxy-terminal region: c1, c2 and c3 shared by all TMc containing NRG1, if they are only present and not followed by a carboxy tail a "c" form is generated.

-Carboxy tail: according to the carboxy-terminal region, can be either a, b or c forms, in the nervous system the "a" tail prevails.

-Cysteine rich domain (CRD): found in Type III NRG1 isoforms; due to the fact that CRD contains a Transmembrane domain (TMn), this makes NRG1 type III isoforms anchored to the membrane by an additional TM domain; therefore, both the N-terminal and the C-terminal are present in the intracellular cytoplasmic part of the cell.

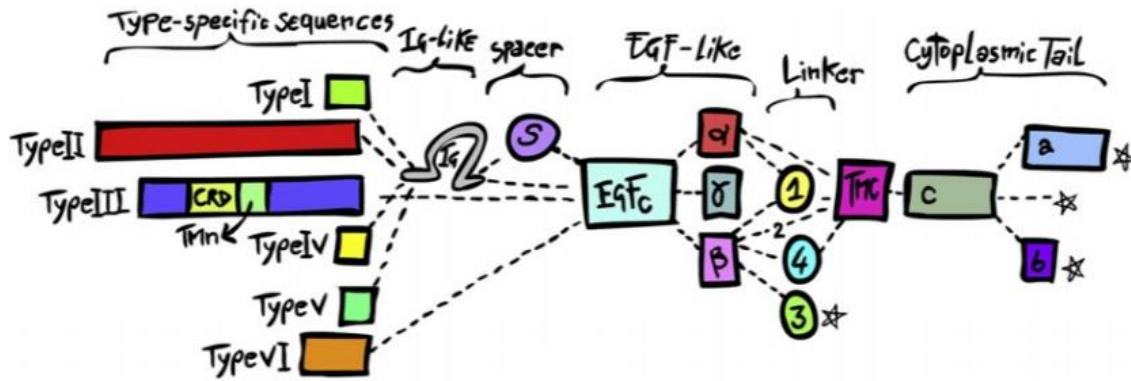


**Figure7:** Exons coding for the different Neuregulin1 isoforms. (Gambarotta et al., 2013)

Each of the protein types has a distinct amino terminal region, while all subtypes of Nrg1 proteins present an EGF-like domain required for receptor binding and signalling. Depending on the presence of either an Ig-like or a cysteine-rich domain (CRD) in their amino terminal (N-terminal) sequences, Nrg1 variants can be categorized into six types (Mei & Xiong, 2008), but the most studied isoform subtypes are types I-III.

NRG1 was known before under different names referring to their biological functions. The common identity of these factors was revealed through cDNA sequencing (Falls et al., 1993; Marchionni et al., 1993) since it was found that they were alternatively spliced products of a single gene that produces different isoforms, thus they were all named neuregulins (NRGs). The name Neuregulin1 was originally introduced by Mark Marchionni (Marchionni et al., 1993).

Nrg1 type I, also known as acetylcholine receptor inducing activity (ARIA), heregulin (HRG) and neu differentiation Factor (NDF), and Nrg1 type II, also known as glial growth factor (GGF), are collectively called Ig-NRGs, while Nrg1 type III, also known as sensory and motor neuron derived factor (SMDF), are called CRD-NRG1.

Most NRG1 isoforms are synthesized as a non-active membrane anchored precursor that need to be further processed and cleaved (Figure 8). The cleavage is catalysed by three type I transmembrane proteases: tumour necrosis factor- $\alpha$  converting enzyme (TACE, also known as ADAM17),  $\beta$ -site of amyloid precursor protein cleaving enzyme (BACE, also known as memapsin 2) and meltrin beta (also known as ADAM19).

Ig-NRGs are synthesized as a single pass transmembrane proprotein with the EGF-like domain facing the extracellular side, subsequently one proteolytic cleavage at the juxtamembrane



region that lies on the carboxy-terminal side of the EGF-like domain is enough to release mature diffusible NRG1 (N-terminal fragment, NRG1-NTF) that acts as a paracrine signal (Falls, 2003; Mei & Xiong, 2008). The process of releasing a bioactive ectodomain fragment is also called "ectodomain shedding".

By contrast, Type III NRG1 isoforms transverse the plasma membrane twice due to the presence of a characteristic hydrophobic CRD that serves as a second transmembrane domain; after proteolytic cleavage Type III NRG1 does not shed and remains attached to the membrane creating a transmembrane N-terminal fragment (NRG1-NTFm) that acts as a juxtacrine signal to cells with direct contact (Falls, 2003; Mei & Xiong, 2008). For all NRG1 isoforms possessing a transmembrane domain (TMC), the NRG1-C-terminal fragment (NRG1-CTF) is still anchored to the membrane after the first cleavage event, then another proteolytic cleavage takes place by  $\gamma$ -Secretase, with the release of the NRG intracellular domain (NRG-ICD) that can play a role in transcriptional activities (Bao et al., 2000).

Some NRG1 isoforms (type I/II, beta3) are synthesized without a transmembrane domain and are thus directly released into the extracellular space (Falls, 2003; Mei & Xiong, 2008)

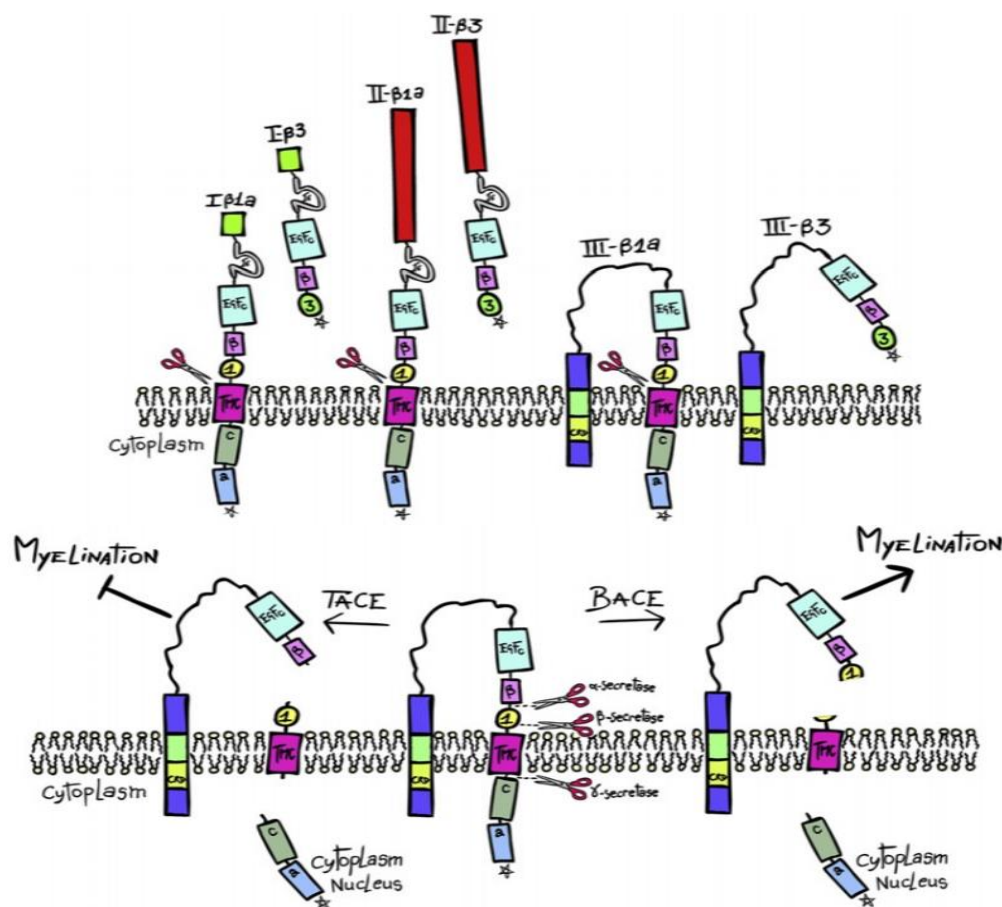


**Figure 8:** Proteolytic cleavage of Neuregulin1 (Gambarotta et al., 2013).

### **Signalling pathways mediated by NRG1-ErbB**

NRG1-ErbB signalling is one of the most complex signalling pathways that mediate different functions along different developmental stages (from embryogenesis to postnatal and adult stages) and different biological systems (cardiac development, myofibril formation and central and peripheral nervous system).

Three different signalling manner can be noticed: canonical forward signalling, non-canonical forward signalling and backward signalling (Figure 9a) (Mei & Nave, 2014; Mei & Xiong, 2008).

#### **Canonical forward signalling**

This is considered the main signalling manner, where ligand binding to the receptor induces the receptor dimerization and consequently receptor activation, the internal tyrosine kinase domain acquires the active asymmetric conformation leading to auto/trans phosphorylation of several tyrosine residues on the carboxy tail; then, these phosphorylated tyrosine residues recruit many effector molecules that transmit signals to different transducers.

Rich network of signalling pathways are activated, including the Raf-MEK-ERK and the PI3K-Akt-S6K signalling pathways (Figure 9b), and other downstream kinases may also be activated including Src, Shc, c-Abl, JNK, CDK 5, Fyn, Pyk2 (Mei & Nave, 2014).

Which ligand binds to which receptor and what partner the receptor dimerizes with, affects which sites in the receptor become phosphorylated. Depending on which tyrosine residues of the two receptors in the dimer are phosphorylated, particular phospho-tyrosine binding proteins will interact with the receptors, leading to a wide range of cellular responses.

One of the main regulatory and tuning mechanisms for this signalling pathway is the ligand-induced receptor endocytosis: once the ligand-receptor complex is internalized into the endosome, two fates can be determined, either the endosome fuses with a lysosome resulting in degradation of both the receptor and the cognate growth factor and subsequent signal termination (Waterman & Yarden, 2001) or it can be recycled back and used again at the cell surface.

#### **Non-canonical forward signalling**

This mechanism of signalling occurs mainly with juxtamembrane-a ErbB4 isoforms (JMa-CYT1 and JMa-CYT2) that can be proteolytically cleaved by TACE. NRG1 binds to ErbB4 receptor existing in a monomer state, which induces TACE to cleave the ErbB4 transmembrane

protein releasing the ErbB4 extracellular domain (Ecto-ErbB4) that contains the NRG1 binding site, while the remaining ErbB4 carboxy-terminal fragment (ErbB4-CTF) is left membrane anchored.

Furthermore a second cleavage of the ErbB4-CTF is mediated by  $\gamma$ -secretase, with release of the ErbB4 intracellular domain (ErbB4-ICD) into the cytoplasm; then, ErbB4-ICD can translocate into the nucleus where it can participate in transcriptional regulation processes (Mei & Xiong, 2008)

### Backward signalling

The roles normally played by NRG1 and ErbBs in NRG1-ErbB signalling, where NRG1 is the ligand that activates the tyrosine phosphorylation of their ErbB receptor are now reversed. The transmembrane nature of pro-NRG1 and Type III NRG1 allow them to act as a putative receptor to ErbB4 molecule which now will take the ligand role (Mei & Xiong, 2008).

Transmembrane ErbB4 or the soluble diffusible Ecto-ErbB4 bind to and activate pro-NRG1 or Type III NRG1, pro-NRG1 cytoplasmic tail interacts with non-receptor protein kinase LIM kinase 1 initiating a backward intracellular signalling.

The second back signalling mechanism is mediated by the NRG1-ICD that is released from the NRG1-CTF by  $\gamma$ -secretase and translocated to the nucleus participating in transcription regulation mechanisms (Mei & Xiong, 2008).

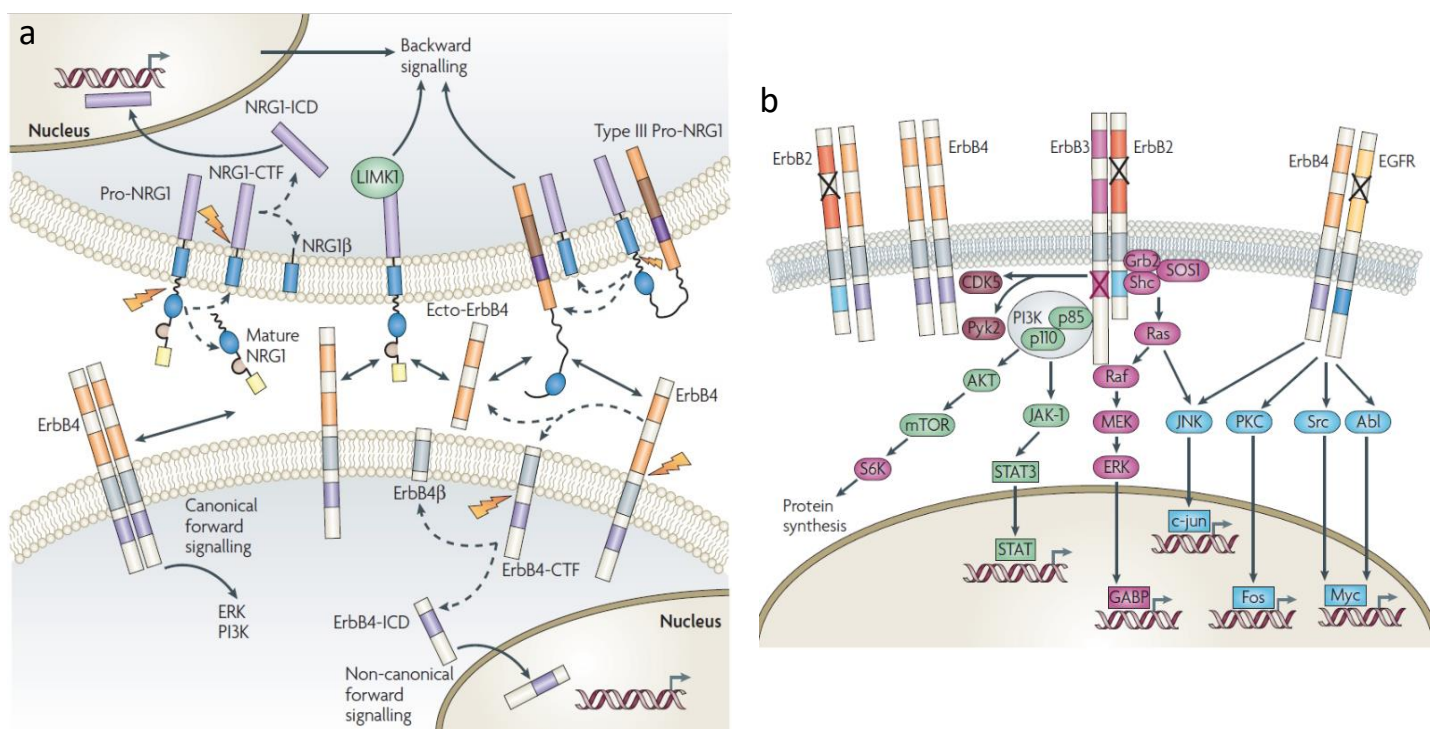


**Figure 9:** Different NRG1-ErbB signalling pathways; a) showing the canonical, non-canonical forward signalling and backward signalling, b) the activated pathways following canonical NRG1-ErbB signalling pathways (Mei & Xiong, 2008)

### **The role of NRG1-ErbB signalling in the nervous system**

NRG1s-ErbBs belong to a very complex system that plays major roles in many biological systems throughout different life stages starting from embryogenesis and development till postnatal and adult stages (Mei & Xiong, 2008).

The role played by the NRG1-ErbB signalling in the nervous system (both central and peripheral) is of special interest. In the CNS ErbB4 is expressed by migrating neuronal progenitors during development and in the adult life, while the heterodimer ErbB2-ErbB3 is the main NRG1 receptor playing a key role in the peripheral nervous system (Fricker & Bennett, 2011; Mei & Xiong, 2008).

### **Myelination during PNS development**

Axon myelination is essential for the saltatory conduction and rapid propagation of nerve impulses and is mediated by glial cells (oligodendrocytes in the CNS and Schwann cells in the PNS). NRG1-ErbB signalling plays an essential role in Schwann cell development and peripheral myelination. The ErbB2/3 heterodimer is the main NRG1 receptor in PNS, expressed by SCs, and transmembrane NRG1 is the main isoform expressed by axons.

NRG1 signalling is greatly associated with Schwann cell development, differentiation and survival as it controls Schwann cells at every stage of the lineage. Schwann cells pass through three main developmental stages: neural crest stem cells, Schwann cell precursors, immature Schwann cells and mature myelinating or non-myelinating SCs (Figure 4).

*In vitro* studies showed that NRG1 induces neural crest cells to determine the Schwann cell fate, stimulates Schwann cell proliferation, promotes the survival of Schwann cell precursors and immature Schwann cells, induces Schwann cell migration and there is evidence that NRG1 accelerates the production of SCs from SCPs (Jessen & Mirsky, 2005).

It was first thought that the axon diameter determines the fate of SCs, thus SCs surrounding axons with a diameter of 1  $\mu\text{m}$  or greater become myelinating SCs, while those surrounding axons of small diameter become non-myelinating SCs. A study by Taveggia and her colleagues on the role of NRG1 in myelination suggests that the level of axonal transmembrane NRG1,

rather than axon diameter, is the key instructive signal for myelination that determines the binary choice of SC phenotypes, with a threshold level triggering myelination (Taveggia et al., 2005).

The thickness of the myelin sheath depends on axonal size which could be determined through the total amount of transmembrane NRG1 present on the axonal surface. Thus, the transmembrane NRG1 signal acts as a biochemical measure of axonal size, and determines the amount of myelin synthesis that matches the axon size and yields optimal nerve conduction (Michailov et al., 2004). Overexpression of transmembrane NRG1 is associated with hypermyelination of peripheral nerve axons, while low levels of transmembrane NRG1 are associated with hypo-myelination.

### **Axon re-myelination following nerve injury**

Functional recovery after a peripheral nerve injury requires multiple reparative responses, where repair SCs and macrophages accumulate to rapidly remove myelin and degenerated axon debris, axons start to regenerate followed by remyelination and reinnervation of the target. Remyelination of regenerating axons is essential for the restoration of saltatory conduction after a nerve injury.

NRG1 or ErbB ablation when the myelination process is completed showed no effect, suggesting they are not required for the maintenance of myelin sheath integrity (Atanasoski et al., 2006).

Otherwise, transmembrane NRG1 shows an important role in axonal myelination during development, whereas regenerating axons lacking transmembrane NRG1 show a slower rate of regeneration with impaired remyelination (Michailov et al., 2004).

Ablation of soluble NRG1 showed no effect on myelination during development, while it plays an important role in remyelination following nerve injury. Peripheral nerve regeneration in animals lacking soluble NRG1 in SCs was severely impaired, while soluble NRG1 overexpression in motor neurons and dorsal root ganglia neurons improves remyelination after injury (Stassart et al., 2013). Immediately following nerve injury, Schwann cells produce high amounts of soluble NRG1 (Ronchi et al., 2016), that acts as an autocrine signal for SC survival and macrophage migration (Gambarotta et al., 2013).

Different NRG1 isoforms play different roles after peripheral nerve injury: soluble NRG1 plays a key role during the early phases following nerve injury corresponding to Wallerian degeneration and SC trans-differentiation, while transmembrane NRG1 plays a key role during

later phases corresponding to SC re-differentiation and to the remyelination process (Gambarotta et al., 2013).

## 4. PERIPHERAL NERVE INJURY & REPAIR

### 4.1 Peripheral nerve injury classification

There are different factors determining and governing the nerve regeneration outcome following a nerve injury including: the patient's age, the injury site and severity, the time window within the repair is performed (Carriel et al., 2014). In 1943, Seddon classified peripheral nerve injuries into three grades of severity: neuropraxia, axonotmesis and neurotmesis (Seddon, 1943).

**Neuropraxia:** it is the mildest form of nerve injury, where a local damage in axon and myelin occurs without affecting the continuity of axon or endoneurium sheath. The term “praxis” means “to do, to perform” and refers to a block in the conduction activity of nerve impulses, where nerve fibres are unable to transmit an action potential (Seddon, 1943; Burnett and Zager 2004).

This type of injury does not require surgical intervention, since the axonal continuity is preserved, and axonal Wallerian degeneration does not happen. Neuropraxia can result from exposure to an extreme stimulus of cold, heat, irradiation or electrical shock, also could result from mechanical stress as compression, concussion or traction. Recovery is rapid, spontaneous and complete; depending on the axonal damage degree, conduction block can be recovered within hours, days, weeks or up to a few months.

**Axonotmesis:** The term “tmesis” means “to cut”, it is used to describe lesions that are characterized by the complete interruption of axonal continuity with the preservation of the fascicular connective tissue. The axon and its myelin sheath are damaged, their continuity is lost, but without any alteration in the surrounding connective tissue (endoneurium, perineurium and epineurium). Axonal damage can occur due to nerve crush, pinch or prolonged pressure. The axonal portion downstream the injury site undergoes Wallerian degeneration, while the axonal portion upstream can spontaneously regrow into the intact endoneurial tubes. Nerve impulse transmission is compromised, the recovery is always spontaneous and does not need a surgical intervention. The time required for nerve recovery depends on the distance between

the lesion site and the target organ, as well as the degree of injury itself (Seddon, 1943; Burnett and Zager 2004).

**Neurotmesis:** it is the most severe injury type; it is characterized by a complete disruption of the entire nerve (nerve continuity is totally lost) accompanied by a severe damage of the connective tissue. Wallerian degeneration occurs in the distal nerve stump while proximal nerve stump undergoes retrograde degeneration. While the previous types of injury spontaneously regenerate, in neurotmesis spontaneous regeneration and functional recovery is rare and does not easily occur; however, successful regeneration might be achieved by surgical intervention (Seddon, 1943; Burnett and Zager 2004).

In 1951, a more detailed and accurate nerve injury classification, was made by Sunderland, injuries were categorized in grades with Latin numerical order, with ascending severity level (Grade I, II, III, IV, V). Grade I corresponds to Neuropraxia, grade II is equivalent to Axonotmesis, the late three grades (III, IV, V) correspond to Neurotmesis (Sunderland, 1951), which was divided in three categories with increasing level of severity (Figure 10).

*Grade III* is characterized by axonal and endoneurium damage with intact epineurium and perineurium.

In *grade IV* the axon, endoneurium and perineurium are completely destroyed and disconnected, while the epineurium is still intact.

In *grade V* the nerve and its connective tissues are completely transected, axonal continuity is absent, and the nerve is physically separated into a proximal and distal stump.

Later in 1989, Mackinnon and Dellon introduced an additional grade to Sunderland's classification, *grade VI*, which is a combination of different injury grades (Mackinnon, 1989).

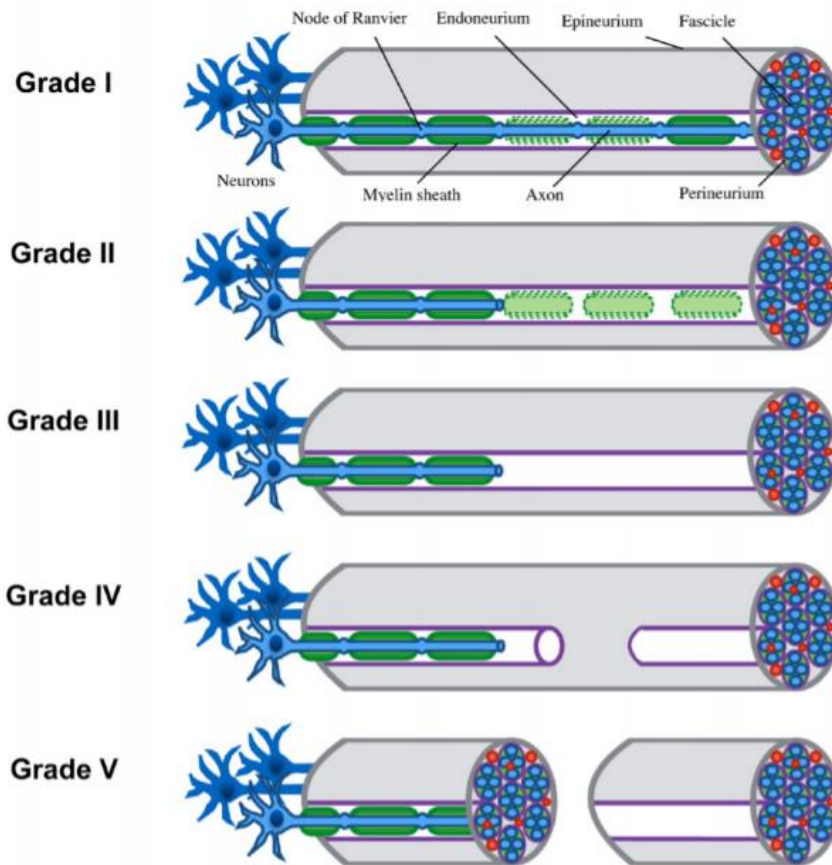


Figure 10 : Sunderland's peripheral nerve injury classification (Caillaud et al. , 2018)

## 4.2 Peripheral nerve injury repairing strategies

Nerve repair aims to restore the nerve functionality and the target organ reinnervation. In neurotmesis injuries, where the two nerve stumps are completely separated, surgical intervention is required to re-join the transected nerve. Depending on neurotmesis severity (with or without substance loss) and on nerve gap length, different surgical techniques are performed (Matsuyama et al., 2000).

### 4.2.1 Neurotmesis without nerve substance loss

**Direct repair** is preferred when the gap between the two nerve stumps is absent or short (5mm or less) and the two ends can be sutured with minimal tension. Nerve stumps should be



precisely aligned in order to obtain a successful and optimal nerve regeneration outcome. It is noticed that better regeneration outcome is always achieved when the nerve is purely motor or purely sensory, and lower regeneration outcomes are obtained with mixed nerves (Grinsell & Keating, 2014; Siemionow & Brzezicki, 2009)

Direct repair includes different surgical techniques: “end-to-end” repair, epineural sleeve repair and “end-to-side” repair.

**End-to-end repair** technique includes epineural repair, group-fascicular repair and fascicular repair (Siemionow & Brzezicki, 2009). Epineural repair is used to repair a sharp nerve injury with good fascicle alignment. Blood vessel within the epineurium (*vasa nervorum*) guide surgeons to achieve a correct fascicle positioning and precise aligning of the nerve stumps. 4-8 single sutures are passed through the internal and the external epineurium of the proximal and distal nerve stumps, Fibrin glue can substitute standard nylon sutures (Figure 11a).

Grouped fascicular repair is especially used in coaptating mixed nerve as the different groups of fascicles can be easily identified and matched. 2-3 sutures are placed into the interfascicular epineurium connecting groups of fascicles (Figure 11b)(Siemionow & Brzezicki, 2009).

Fascicular repair is not widely used anymore being a highly demanding technique that does not yield satisfactory level of regeneration. This technique requires the dissection of the interfascicular epineurium and the separation of different fascicles. 2-3 sutures per fascicle are placed within the perineurium augmenting the formation of scar tissue (Matsuyama et al., 2000; Siemionow & Brzezicki, 2009).

Although grouped fascicular and fascicular repair provides a better orientation and alignment of fascicles and a reduced possibility of misdirection of regenerating axons, yet their use is limited by the increased amount of needed sutures that increase the intraneural scar formation that disrupt the intraneural blood flow. Functional outcome of these suturing techniques is not superior to traditional epineural repair (Siemionow & Brzezicki, 2009).

**Epineural sleeve repair** has showed a faster functional recovery compared to traditional epineural end-to-end repair. In this technique the epineurium of the distal stump is rolled back by 2mm and the nerve segment underneath is resected, then the created epineural sleeve is pulled over to cover the nerve of the proximal nerve stump and fixed over by the help of two sutures (Figure 11c). The epineural sleeve provides a biological chamber that conserve all the axoplasmic fluid leakage from transected nerve stumps, providing a neuro permissive

environment for growing axons, indeed higher number of regenerating nerve fibres reach target organs and less neuroma formation was observed (Siemionow & Brzezicki, 2009).

**The end to side repair:** this technique is used when the proximal nerve stump of the damaged nerve is unavailable or when a significant nerve gap exists. The distal nerve stump of the injured nerve is coapted to the side of a healthy nerve. Collateral sprouting from the healthy nerve reinnervate the target organ of the dissected nerve, the donor nerve function remains normal without any compromise. This technique is widely used in brachial plexus injuries or facial nerve reconstruction (Matsuyama et al., 2000; Siemionow & Brzezicki, 2009).

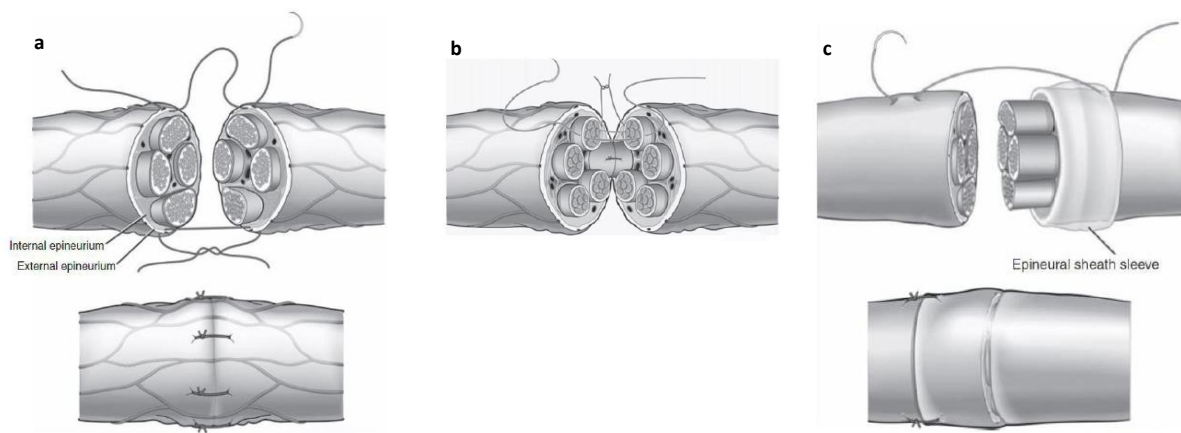


**Figure 11:** Different surgical suturing techniques used in repairing peripheral nerves not accompanied by substance loss. a: Epineural repair, b: grouped fascicle repair, c: epineural sleeve repair (Siemionow & Brzezicki, 2009).

#### 4.2.2 Neurotmesis accompanied by nerve substance loss

In case of critical nerve gaps accompanied by substance loss, - impossible to bridge without tension - a nerve grafting technique is required (Grinsell & Keating, 2014). Repairing a nerve under tension is highly uncommendable since nerve blood supply is disrupted.

A scaffold is required to substitute the missing nervous tissue, bridging the two nerve sides. Different strategies have been used to join the nerve gap and reconnect the nerve stumps, among which the use of grafts (nerve autograft or allograft and non-nerve grafts) or the tubulization technique, using conduits of different origin (natural or synthetic). (Carriel et al., 2014; Fornasari et al., 2020).

### 4.2.2.1 Grafting techniques

A graft is a piece of living tissue that is transplanted surgically. For repairing critical nerve gaps, surgeons use grafts of different sources. Nerve grafts can be adopted from the patient (autografts) or from a cadaver donor (allografts). Other biological grafts used for nerve reconstruction are blood vessels, skeletal muscles and tendons (biological conduits).

#### Nerve Autograft

Autografts are sensory donor nerves that are sacrificed from the patient and are usually used to replace an injured motor nerve (Siemionow & Brzezicki, 2009). Surgeons often choose to sacrifice a sensory cutaneous nerve and to lose the sensibility of the related region in favour of the recovery of motor nerve and its accompanied mechanical function. The currently used donor nerves include sural nerve, lateral antebrachial cutaneous nerve (LACN), anterior division of the medial antebrachial cutaneous nerve (MACN), dorsal cutaneous branch of the ulnar nerve (DCBUN) and superficial sensory branch of the radial nerve (SSN) (Matsuyama et al., 2000) (Table1).

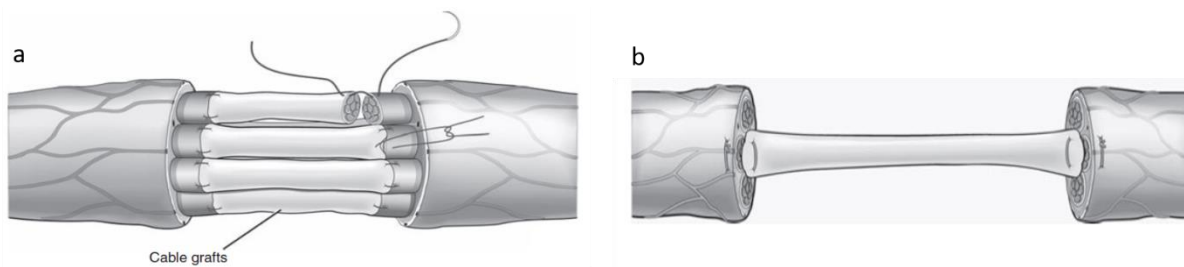
EXAMPLES OF DONOR NERVES AVAILABLE FOR AUTOGRAFTING			
Donor nerve		Available length (cm)	Hypesthesia
Medial antebrachial cutaneous nerve	MACN	10–12 (above elbow) 8–10 (below elbow)	Medial forearm
Lateral antebrachial cutaneous nerve	LACN	10–12	Lateral forearm
Superficial sensory branch of the radial nerve	SSR	20–30	Radial dorsal hand
Dorsal cutaneous branch of the ulnar nerve	DCBUN	4–6	Ulnar dorsal hand
Sural nerve		30–50	Lateral foot

Table 1: Available donor nerves for autografting (Siemionow & Brzezicki, 2009)

From all the above-mentioned sensory nerves, the sural nerve is commonly used providing a graft length ranging from 20 cm long if harvested alone, and up to 50 cm if harvested with the medial sural cutaneous nerve.

Autografts provide mechanical support and a growth permissive environment for nerve regeneration since they contain Schwann cells, basal laminae, neurotrophic factors and adhesion molecules (Lundborg, 2000). Two methods of nerve autografting can be applied either as a grouped cable graft repair or as a single fascicle nerve repair (Figure 12). The cable graft technique provides a maximum coverage of the cross-sectional area of the damaged nerve, where graft segments are interposed to the corresponding groups of fascicles both proximally

and distally generating a direct regeneration pathway (Grinsell & Keating, 2014). The single fascicle repair technique has the advantage of expanding the availability of autograft materials. On rat sciatic nerve model, it has been shown that a repair with a single fascicle that covers 25-59% of the injured nerve cross-sectional area resulted in a faster regeneration and a better functional outcome. Autografts are suitable for repairing short (3cm) and long (more than 3 cm) nerve gaps (Griffin et al., 2013).



**Figure 12:** Autografting repair techniques: a:cable grafting technique, b:single fascicle nerve repair (Siemionow & Brzezicki, 2009).

Despite being the “gold standard” in repairing all types of nerve gaps (short and long gaps), autografting technique demonstrates some disadvantages and limitations. For graft harvesting the patient must undergo a further operation, increasing the intervention time. The scarification of a healthy functional sensory nerve causes donor site morbidity, pain, scarring, neuroma formation and sensory loss in the site of nerve harvest (Moran, 2009). Moreover, the autografts have limited amount of available graft material with restricted lengths, different nerve calibre, supplying an unmatched nerve type (sensory to repair a motor nerve). These limitations have raised the need to search for other valid alternatives that can replace autografts in repairing nerve gaps (Carriel et al., 2014).

### **Nerve Allografts**

In nerve allograft the donor nerve derives from a cadaver. Allografts have the advantage of providing unlimited availability of nerves with matching calibre, length and type (sensory, motor and mixed nerves). Moreover, allograft allows to overcome autograft limitations and disadvantages. Unfortunately, allograft implantation must be accompanied by immunosuppressant treatment in order to prevent adverse immune reaction, inflammation and subsequent graft rejection. Immunosuppressant treatment can compromise patient quality of life, thus for reducing nerve immunogenicity, various protocols have been tested to get a

decellularized nerve graft. Decellularization is one of the tissue engineering and regenerative medicine techniques used nowadays, where the allograft is pre-treated in several ways to remove resident cells and their superficial antigens and to conserve the extracellular matrix (ECM), thus rendering the allograft nonimmunogenic. The only commercially available and FDA approved nerve allograft is the Avance® Nerve Grafts (AxoGen® Inc., Alachua, FL, USA) (Isaacs & Browne, 2014; Lovati et al., 2018).

### **Autogenous biological grafts (Biological Conduits)**

Autogenous biological grafts have the advantage of being supplied and harvested from the patient himself, thus taking advantage of their immunological compatibility. Blood vessels (veins and arteries) and skeletal muscles have received special attention thanks for their natural topography and oriented structures they could act as axon guiding channels (Geuna et al., 2014).

Vein grafts were chosen for their large availability and reduced side effects to their withdrawal. They have shown comparable results with autografts in short digital nerve repair. Since veins tend to collapse in larger nerve defects leading to nerve compression and unsuccessful recovery, the enrichment of the venous tubes with internal fillers such as skeletal muscle fibres were used to overcome this problem (muscle in vein conduit) (Geuna et al., 2003).

#### **4.2.2.2 Tubulization technique**

Due to the aforementioned limitations accompanied by autograft nerve transplantation, tubulization technique (Figure 13) has evolved as a valid alternative to substitute autografting technique. Mainly a tubular structure is used to connect the separated two nerve stumps together. It provides many advantages, since it supplies a suitable environment for regenerating nerves, moreover it limits excessive fibroblast infiltration and prevents fibrosis formation. Furthermore, it physically supports and guides regenerating axons aided by different neurotrophic factors enclosed inside the conduit.

Different artificial nerve conduits of various origins (biological or synthetic) are present nowadays, some of them are FDA approved and are successfully used in clinical practice. Unfortunately, conduits efficacy is just limited in repairing relatively short gaps ( $\leq 3$  cm) (Carriel et al., 2014). Further intraluminal enrichment of the hollow nerve conduits is recommended for improving conduit performance in repairing critical nerve gaps ( $\geq 3$  cm).

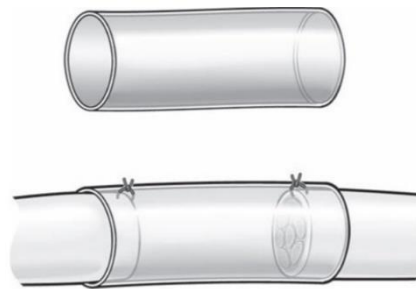


**Figure13:** Artificial nerve conduits for peripheral nerve repair (Siemionow & Brzezicki, 2009).

## 5. TISSUE ENGINEERING IN PERIPHERAL NERVE REGENERATION

Tissue engineering is a subfield of regenerative medicine that was evolved with the field of biomaterial development. It refers to the practice of combining scaffolds, cells, and biologically active molecules with the aim to assemble functional constructs as biological substitutes that restore, maintain, or improve damaged tissues or whole organs, or to promote endogenous regeneration. The approach was initially conceived to address the gap between the growing number of patients waiting for organ transplantation and the limited number of available donated organs (Furth et al., 2014).

Numerous nerve substitutes have been developed including: decellularized nerve allograft and artificial nerve conduits of natural or synthetic origins.

### 5.1. Decellularized nerve allografts

Decellularized nerve allografts, also known as acellular nerve grafts (ANG) are nerve allografts subjected to a decellularization pre-treatment (Figure 14). The decellularization technique aims at eliminating the immunogenic activity in allografts. The adverse immune reaction is provoked by the presence of the major histocompatibility complex (MHC) in tissues, that could lead to immunological rejection of the inserted allograft. In peripheral nerves, the components containing the MHC mainly include Schwann cells, the myelin sheath, and axons. The antigenicity of other structures, such as the basal lamina and extracellular matrix proteins is very weak. Decellularization techniques targets intracellular components and the antigenic epitopes related to the cell membranes (Crapo et al., 2011).

Generally, the choice of the decellularization method can vary from one tissue to another based on many factors including the tissue cellularity, density, lipid content and thickness (Gupta & Mishra, 2017). Unfortunately, each cell removal agent and method will result in an unavoidable alteration in the ECM composition and causes some degree of ultrastructure disruption. Minimization of these undesirable effects rather than complete avoidance is the objective of decellularization. Decellularization techniques can be divided into physical, chemical and biological methods (Gilbert et al., 2006).

**Physical methods** include physical treatments as changes in temperatures, freeze and thawing cycles, agitation and sonication. These physical changes facilitate cell membrane disruption and promote cell lysis. Freeze and thawing act by rupturing the cell membranes by forming ice crystals. Freeze-thaw cycles can cause cell lysis, while they allow to maintain mechanical integrity as well as ECM components such as collagen and GAGs. Agitation is usually used to wash away cellular and nuclear residuals.

Physical methods are often used in conjunction with chemical or enzymatic methods because alone they are ineffective at clearing genetic material from a scaffold after cell lysis. Excessive physical decellularization methods can disrupt the natural ECM ultrastructure and alter mechanical properties (Buckenmeyer et al., 2020).

**Chemical methods** include acid and base treatments, hypotonic and hypertonic solutions, detergents classified by their charge distribution (ionic, non-ionic and zwitterions), alcohols and chemical solvents (Gilpin & Yang, 2017).

Acids and bases catalyse the hydrolytic degradation of biomolecules, cytoplasmic components and nucleic acids; however, this could have adverse effects on GAG content. Peracetic acid is a common disinfection agent that acts as well like a decellularization agent by removing residual nucleic acids with minimal effect on the ECM composition and structure. Bases such as sodium hydroxide are extensively aggressive on the tissue, decreasing ECM mechanical properties more significantly than other chemical and enzymatic agents (Gilpin & Yang, 2017). Hypertonic solutions dissociate DNA from proteins, and hypotonic solutions can readily cause cell lysis by a simple osmotic effect, with minimal changes in the matrix molecules and architecture. Ionic, non-ionic and zwitterionic detergents can solubilize cell membranes and dissociate the DNA from proteins, and thus effectively remove cellular material from tissue; but they may also disrupt and dissociate proteins in the ECM. The removal of ECM proteins

and DNA by detergents is directly proportional with exposure time (Gilpin & Yang, 2017). The use of alcohols facilitates delipidation and causes tissue dehydration, leading to cell lysis (Crapo et al., 2011).

Ionic detergents include sodium dodecyl sulphate (SDS), sodium deoxycholate (SDC) and Triton X200. SDS is more effective than other detergents in removing cell residues and nuclei from dense tissues and organs but has the drawback of ultrastructure and ECM disruption. The addition of SDS to a decellularization protocol can make the difference between complete and incomplete cell nuclei removal. Non-ionic detergents as TritonX-100 effectively remove cell residues from thick tissues, with concomitant ECM protein loss accompanied by a decreased adverse immune response *in vivo*. The zwitterionic detergents (sulfobetaine-10, “SB-10”, sulfobetaine-16 “SB-16” and 3-[(3-cholamidopropyl) dimethylammonio]-1-propanesulfonate “CHAPS”) have the properties of both ionic and non-ionic detergents, they are the most effective for cell removal from thin tissues and may be ineffective for decellularization of thick tissues. A comparison among the detergents used in peripheral nerve decellularization showed a better preservation of ultrastructure by non-ionic and zwitterionic detergents but a better cell removal by using ionic detergents (Crapo et al., 2011).

Organic solvents as tributyl phosphate have recently been added to decellularization reagents and show mild effects on ECM (Deeken et al., 2011).

Combining multiple detergents increases ECM protein loss, but also allows for a more complete detergent removal from ECM after decellularization (Crapo et al., 2011).

**Biological methods** include enzymatic decellularization agents, which are categorized by the specific structures that they target (nucleases, collagenases, and proteases) and non-enzymatic decellularization agents (chelating). These enzymes can provide high specificity for the removal of cell residues or undesirable ECM constituents, but it is possible that enzyme residues may impair a future recellularization or cause an immune response (Crapo et al., 2011). Nucleases, specifically DNases and RNases, are used to aid in the removal of nucleic acids where the detergent combination would not reach the threshold for acceptable levels of residual DNA content.

Usually, different methods are combined together to achieve a better decellularization outcome. The optimization of the combined used detergents and their concentrations is a critical process that is required to obtain an ECM scaffold with minimized matrix disruption, adequate antigen removal, and limited cytotoxicity. Further removal of undesirable biological components, such



as DNA and other cellular components, can be improved by the inclusion of enzymatic treatment (Buckenmeyer et al., 2020).

In general, most of the recent literature reaffirms that detergent-based decellularization technique remains as one of the most efficient and used methods to remove the cellular component from a wide range of tissues, including peripheral nerves (Mendibil et al., 2020). Several protocols have been proposed for peripheral nerve decellularization. The methods described by Sondell (Sondell et al., 1998) and Hudson (Hudson et al., 2004) are the most widely studied. Currently, only one FDA approved and commercially available decellularized nerve allograft is available: Avance® nerve grafts (AxoGen® Inc., Alachua, FL, USA) (Lovati et al., 2018; Philips et al., 2018).

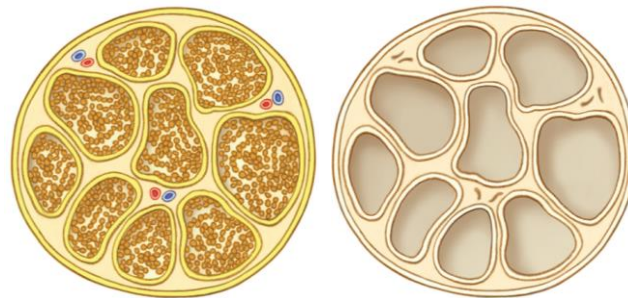


**Figure 14:** A graphical representation of an ideal decellularized nerve allograft. The basal lamina and extracellular matrix components are preserved while the cells and myelin are removed (Hundepool et al., 2017).

## 5.2 Artificial Nerve Conduits

An ideal nerve conduit that would promote a successful nerve regeneration should satisfy some essential characteristics. The first and most important feature is the biocompatibility, that the ability of a biomaterial to support cell growth and appropriate cell behaviour. The conduit material should not be toxic, it should integrate with the body without provoking any haemolysis, irritation, inflammation or rejection.

The conduit material should possess good permeability, pores on the scaffold wall should ensure the diffusion and free exchange of nutrients and oxygen between the regenerating axon inside the tube and the surrounding external environment, and at the same time pores should be of an appropriate size able to prevent unwanted cell infiltration (Fornasari et al., 2020).

Good biomechanical properties with an equilibrium between hardness and malleability are recommended. Indeed, a nerve conduit should be rigid enough to resist collapse under physiological conditions, thus protecting the nerve and preventing its compression. At the same time, it should retain some flexibility and malleability that are required to ease its microsurgical handling. The biomechanical properties of nerve guides depend on the nature of the material used for the scaffold preparation and the conduit dimensions (the wall thickness, the lumen diameter) (Isaacs & Browne, 2014).

Biodegradability and reabsorption of the conduit eliminates the need of a second surgery for conduit removal as in the case of silicone and polyethylene conduits. An ideal conduit should be intact for all the time needed by the regenerating axons to regrow across the gap and reconnect the target organ followed by gradual degradation and absorption with minimal foreign body reaction (Houshyar et al., 2019).

According to the material source, nerve conduits can be mainly classified into two categories: of natural or synthetic origins.

### **5.2.1 Natural-based nerve conduits**

Molecules of biological origin used in manufacturing nerve conduits have the advantage of being biocompatible, thus supporting cell survival, adhesion, migration and proliferation. Moreover, they ensure conduit degradation along time by the host enzymatic secretions without producing any cytotoxic degradation products. Thus, a conduit from a natural material eliminates the need of a second injury to remove it from host (Carriel et al., 2014).

The most used ECM proteins for conduit preparation are collagen, fibronectin and laminin, they provide a great support for regenerating axons (Gonzalez-Perez et al., 2013).

#### Collagen and other ECM components:

Collagen fibres are the main, most abundant and highly conserved ECM component among mammalian species, representing up to 70% of body's dry weight. It is one of the widely used biomaterials in tissue engineering both in hard and soft tissue reconstruction. Collagen type I and IV are greatly expressed in the three layers of nerve connective tissue (endo, peri and epineurium), specially playing an important role in peripheral nerve regeneration by promoting Schwann cell migration and proliferation (Geuna et al., 2009; Gonzalez-Perez et al., 2013). Type I collagen based nerve conduits are the most biocompatible nerve guide used nowadays

in clinical practice, with comparable outcomes to autograft in repairing nerve defects up to 2 cm (Carriel et al., 2014).

Five commercially available collagen type I based conduits are FDA approved: NeuraGen<sup>®</sup> and NeuraWrap<sup>®</sup> (Integra Life sciences Cor, USA), NeuroFlex<sup>®</sup>, NeuroMatrix<sup>®</sup> and NeuroMed<sup>®</sup> (Collagen Matrix Inc., USA). Among these conduits NeuraGen<sup>®</sup> has the most encouraging clinical data in sensory and motor recovery (Kehoe et al., 2012).

Fibronectin is present in the interstitial matrices and greatly influences cell migration and axonal growth; fibronectin scaffolds have proved to improve peripheral nerve regeneration as it promotes Schwann cell survival and proliferation. Thus, a great number of viable Schwann cells are maintained in fibronectin scaffolds (Deumens et al., 2010).

Laminin is the first ECM protein expressed during embryogenesis, and it has a positive effect in promoting neurite outgrowth and guiding developing neuritis during the nerve regeneration process. Laminin scaffolds were used to bridge 8mm long sciatic rat nerve gap with desirable regeneration outcomes (Kauppila et al., 1993).

#### Gelatine:

Gelatine is a natural biodegradable polymer derived from collagen thermal denaturation. It is biocompatible, possesses a good plasticity and adhesiveness properties, moreover it is more economic than collagen. Due to its high solubility in water, a cross-linking pre-treatment with cross-linker agents such as genipin or glycidoxypropyltrimethoxysilane is required to improve gelatine conduit mechanical properties and its degradation rate (Tonda-Turo et al., 2011). Poor regeneration outcome with unmyelinated axons was observed after 8 weeks in a 10 mm sciatic nerve defect repaired using a genipin cross-lined gelatine conduit (Chen et al., 2005), but a later study performed by the same authors demonstrated that increasing the conduit porosity positively influence the final regeneration outcome (Chang et al., 2009).

#### Silk Fibroin:

Silk fibroin derives from the natural silk fibres produced by silkworms (*Bombyx mori*) or spiders (*Nephila*). This biomaterial is characterized by its unique mechanical properties demonstrating great elasticity, high tensile strength, low immunogenicity and biodegradability.

Silk fibroin has shown encouraging results in supporting neurons *in vitro* and in promoting peripheral nerve regeneration *in vivo* (Allmeling et al., 2008; Gu et al., 2011).

#### Chitosan and other natural polysaccharides:

Chitosan is the most abundant polysaccharide in nature after cellulose. It is a linear polysaccharide (copolymer of D-glucosamine and N-acetyl-D-glucosamine) derived by the full or partial N-deacetylation of chitin. Chitin is a natural constituent of crustacean shells, insect cuticles and fungi cell wall. Crustacean shells from sea food wastes are considered the main source for chitin isolation (Fornasari et al., 2020).

As a biomaterial, chitosan is characterized by its biocompatibility, biodegradability, low toxicity, and structural similarity to natural GAGs, this similarity allows interactions between chitosan and ECM molecules including laminin, fibronectin and collagen. *In vitro* studies have shown that chitosan promotes cell survival and neurite outgrowth (Simões et al., 2011). *In vivo* implantation of chitosan conduits has shown favourable results in improving peripheral nerve injury repair (Gonzalez-Perez et al., 2014; Stenberg et al., 2016). Biodegradability of chitosan conduits is affected by the degrees of deacetylation of the material (Haastert-Talini et al., 2013). The transparency of the chitosan tube eases its handling and manipulation by surgeons (Gu et al., 2011).

Nowadays two chitosan conduits are FDA approved for clinical practice with good regeneration outcome: Reaxon<sup>®</sup> Nerve and Reaxon<sup>®</sup> plus (Kerimedical, Germany). Furthermore, chitosan can be easily blended with other materials or modified on its surface to better support axonal regrowth; blended chitosan tubes proved to be efficient in bridging peripheral nerve gaps.

Alginate and Agarose purified from algae are linear polysaccharides that are proposed for peripheral nerve repair. They have good biocompatibility, biodegradability and thermo stability but possess poor mechanical resistance which made them a more suitable candidate for internal nerve guidance fillers (Shen et al., 2005).

### **5.2.2 Synthetic nerve conduits**

Synthetic materials have been extensively used to prepare nerve conduits, due to their adjustable chemical and physical properties, that renders the biodegradability and fabrication

process under control. Being of a synthetic origin, biocompatibility and induction of an adverse immune response must be carefully tested *in vitro* before *in vivo* use (Kannan et al., 2005). According to their biodegradability, synthetic materials can be divided into non-absorbable and absorbable.

Non-absorbable materials have been used in manufacturing synthetic conduit before the use of absorbable materials. Among the non-absorbable synthetic material, silicone is one of the first and most studied and used in clinical practice. Their effectiveness in repairing peripheral nerves was demonstrated. They are inert with good elastic properties and have high thermal and chemical stability (Lundborg et al., 1982). Indeed, they have been applied in clinical trials to bridge short nerve gaps with some success. Other non-reabsorbable synthetic materials that have been used in nerve conduits fabrication include plastic polymers as polyethylene, elastomer, acrylic polymers and expanded polytetrafluoroethylene, polylactic acid, polyvinyl chloride and polyethylene glycol (Muheremu & Ao, 2015).

The main drawback of non-reabsorbable conduits is that they are undegradable by host body and need a second injury to be removed, provoking a chronic inflammatory response and a possible scar tissue formation.

Absorbable materials have been used in nerve conduit fabrication to overcome the biodegradability problem of non-absorbable materials. The degradation kinetics of the conduit must be compatible with the regeneration timing of the injured nerve. A rapid degradation would impair regeneration and very slow degradation would provoke inflammation and nerve compression (Fornasari et al., 2020). Among the absorbable materials, aliphatic polyesters and co-polyesters have already been used in clinical application. Examples include poly-glycolic acid (PGA), poly-L-lactic acid (PLLA), poly-caprolactone (PCL), poly-L-lactide-coglycolide (PLGA). NeuroTube<sup>®</sup> a PGA based nerve conduit was the first FDA approved conduit for clinical practice in the human. Clinical studies on short or moderate digital nerve repair (4cm) showed positive results with motor recovery similar to autografts (Weber et al., 2000).

### **5.3 Intraluminal enrichment of nerve conduits**

The main disadvantage of the tubulization technique is its limited efficiency just in repairing relatively short peripheral nerve defects with substance loss around 3cm. To overcome this

problem and to improve the conduit efficiency, intraluminal fillers are used to enrich hollow nerve conduits (Figure 15).

### Physical structure

In an attempt to better mimic the natural architecture of nerve fascicles some modifications into the intraluminal structure of neural scaffolds are suggested. Multichannel nerve guiding conduit are fabricated by incorporating one or more intraluminal channels inside the hollow conduit structure. Multichannel conduits reduce the dispersion of regenerating axons through the conduit lumen, but they display no significant regenerating benefit over single lumen conduit NGCs (Ruiter et al., 2008).

### Internal fillers

To enhance peripheral nerve regeneration within the hollow lumen conduit, biomaterial based fillers with different physical forms (fibres, filaments, gel, or sponges) made from synthetic or natural biomaterials are inserted into the conduit lumen serving as topological cues to promote Schwann cell adhesion, proliferation, and migration, as well as axonal outgrowth. ECM proteins (laminin, fibronectin, and collagen) represent excellent candidates as lumen fillers as they promote axonal extension. Since the filler can slow down nerve regeneration physically obstructing the growth, it is necessary to finely control the distribution and the density of the gel itself (Chen et al., 2006).

### Growth factor supply:

Growth factors play an important role in all phases of nerve regeneration. Most probably the decay of growth factors released by SCs and target organs is the main reason behind regeneration failure over long distances. A controlled and prolonged release of growth factors inside the conduit lumen could enhance nerve regeneration over long distances.

Growth factor incorporation inside a hollow conduit can be done either by direct solution injection or by using a delivery system. Collagen or agarose hydrogel can be a suitable scaffold releasing growth factors in the lumen. Growth factors can be also administrated in microspheres or immobilized on nanoparticles. It has been shown that growth factor incorporation enhances the conduit efficiency in repairing nerves (Sarker et al., 2018).

Supportive cells:

Cell seeding inside a nerve conduit could be very useful since cells produce some growth factors or ECM molecules that facilitate nerve regeneration. Often the ideal cells used are Schwann cells, but other supportive cell candidates can be used as well to support the conduit lumen as embryonic stem cells, neural stem cells, bone marrow mesenchymal stem cells and adipose derived mesenchymal stem cells (Patel et al., 2018).

-Schwann cells:

In response to nerve injury, Schwann cells undergo a switch to a repairing phenotype that supports nerve regeneration by producing high levels of different growth factors and guiding the regrowing axons, forming the Büngner bands. In later stages of regeneration, they return to their myelinating phenotype and remyelinate the regenerated axons (Jessen & Mirsky, 2016). These characteristics make Schwann cells the first and most widely used supportive cells for nerve conduit enrichment. The extended time needed for *in vitro* Schwann cell isolation and purification (minimum 2 weeks) till obtaining an adequate amount to be transplanted to a patient, limits their clinical use as supportive cells (Yi et al., 2020).

To overcome this problem, undifferentiated stem cells have been thought as a suitable replacement of Schwann cells. Stem cells have fast growth rate and a wide expansion capacity in cultures, moreover their stemness allows them to differentiate into numerous specialized cell types including Schwann cells. Stem cells can be provided by different sources such as umbilical cord blood after birth, bone marrow stem cells and adipose derived stem cells. They can also be collected from an autograft to reduce the immunogenicity (Yi et al., 2020).

-Embryonic stem cells (ESCs):

ESCs are pluripotent stem cells that can differentiate to all three embryonic germ layers and form all types of cells or tissues of the body. Stem cells can survive and differentiate into myelin-forming cells up to 3 months after cell transplantation; the number of regenerated axons was improved with ESC transplantation in a rat sciatic nerve injury (Cui et al., 2008). The use of embryonic stem cells is limited as they have some tumorigenic properties and may induce the formation of teratomas. In addition, the use of embryonic stem cells poses ethical issues (Yi et al., 2020).

-Neural stem cells:

Neural stem cells, as the precursor cells in the nervous system, are an essential cell source of neurons and glial cells. They can be obtained from skin or hair follicle. Transplanted neural stem cells can differentiate into both neurons and Schwann cell-like cells; they improve angiogenesis, nerve growth and myelin formation (Wang et.al., 2017). The clinical use of neural stem cells may be limited by the difficulty in collecting them and their high rate of tumour formation when used for repair sciatic nerve defects (Johnson et al., 2008).

-Bone marrow mesenchymal stem cells (BMSCs):

Mesenchymal stem cells are multipotent adult stem cells that can be isolated from many tissues, such as bone marrow, umbilical cord blood, peripheral blood, fallopian tube and lung. BMSCs can be easily collected through the aspiration of the bone marrow in a standardized method and then expanded on a large scale for subsequent applications. Moreover, cultured BMSCs lack immune recognition, thus can be transplanted without inducing immune rejection. BMSC is one of the most widely used cell sources for nerve regeneration. They can differentiate into Schwann cell-like cells and secrete several growth factors. They are widely tested *in vivo* in repairing rat sciatic nerve injury, with successful results (improved rat walking behaviour, reduced muscle atrophy and increased regenerated axons) (Chen et al., 2007). It was found that just a little amount of implanted cells differentiate into SC-like cells, thus suggesting that BMSC activity is not dependent only on differentiation, but possibly on cell secretions in the injured environment (Kumar et al., 2016). BMSC-enriched conduits show comparable results to nerve autografts (Zheng & Cui, 2012). Unfortunately, the use of BMSCs can be invasive, ethically controversial and limited by tissue source.

-Adipose derived mesenchymal stem cells (ADMSCs)

ADMSCs have the advantage of being easily collected by a less invasive liposuction procedure, thus providing a great clinical potential. Their proliferation and differentiation capabilities are much higher than many other adult stem cells. Moreover, they can be induced to differentiate into Schwann cells, in order to secrete neurotrophic factors, stimulate neurite outgrowth and form myelin sheaths. These advantages of adipose stem cells make them a good source for transplantation strategies (Mazini et al., 2019).

Undifferentiated ADMSCs and SC differentiated ADMSC were seeded into silicone nerve conduits containing type I collagen gel to repair a rat facial nerve gap (7mm); both treatments



increased myelinated fibre number and myelin thickness and bring functional improvement of facial palsy without neuroma formation (Watanabe et al., 2014). In a study comparing the use of an autograft or fibrin conduits enriched with either ADMSCs, SCs or SC-like differentiated BMSCs, it was found that regeneration with ADMSC enriched conduits was comparable to autografts and much better than those obtained using the other cell types (Summa et al., 2011). It is worth mentioning that several factors can affect and even limit the growth properties of adipose stem cells such as donor age and harvest site/layer. Therefore, in order to obtain the maximum regenerative abilities of ADMSC, the quality of the applied cells should be strictly controlled ( Sowa et al., 2012 ; Engels et al., 2013).

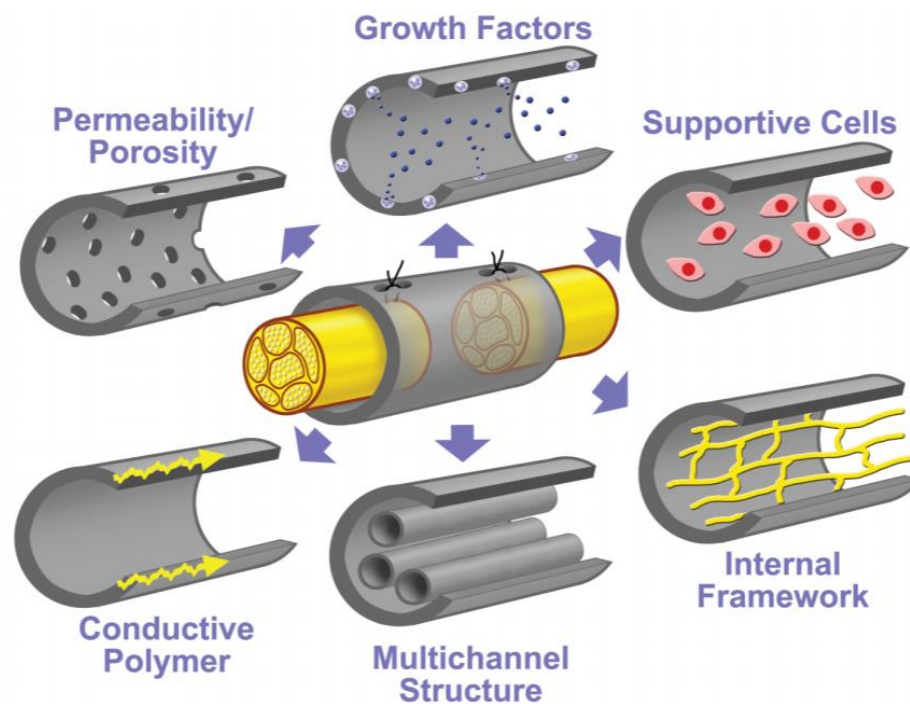


**Figure15:** Intraluminal enrichment of hollow guiding nerve conduits (De Ruiter et al., 2009).

## 6. References

- Allmeling, C., Jokuszies, A., Reimers, K., Kall, S., Choi, C. Y., & Vogt, P. M. (2008). Spider silk fibres in artificial nerve constructs promote cell proliferation. *Cell Proliferation*, 41, 408–420.
- Atanasoski, S., Scherer, S. S., Sirkowski, E., Leone, D., Garratt, A. N., Birchmeier, C., & Suter, U. (2006). ErbB2 signaling in Schwann cells is mostly dispensable for maintenance of myelinated peripheral nerves and proliferation of adult Schwann cells after injury. *Journal of Neuroscience*, 26(7), 2124–2131.
- Bao, J., Wolpowitz, D., Role, L. W., & Talmage, D. A. (2000). Back signaling by the Nrg-1 intracellular domain. *The Journal of Cell Biology*, 161, 1133–1141.
- Belanger, K., Dinis, T. M., Taourirt, S., Vidal, G., Kaplan, D. L., & Egles, C. (2016). Recent Strategies in Tissue Engineering for Guided Peripheral Nerve Regeneration. *Macromolecular Bioscience*, 472–481.
- Berti, C., Bartesaghi, L., Ghidinelli, M., Zambroni, D., Figlia, G., Chen, Z., ... Feltri, M. L. (2011). Non-redundant function of dystroglycan and  $\beta$  1 integrins in radial sorting of axons. *Development*, 138, 4025–4037.
- Binari, L. A., Lewis, G. M., & Kucenas, S. (2013). Perineurial Glia Require Notch Signaling during Motor Nerve Development but Not Regeneration. *The Journal of Neuroscience*, 33(10), 4241–4252.
- Bolívar, S., Navarro, X., & Udina, E. (2020). Schwann Cell Role in Selectivity of Nerve Regeneration. *Cells*, 9(9), 2131.
- Buckenmeyer, M. J., Meder, T. J., Prest, T. A., & Brown, B. N. (2020). Decellularization techniques and their applications for the repair and regeneration of the nervous system. *Methods*, 171(July 2019), 41–61.
- Caillaud, M., Richard, L., Vallat, J.-M., Desmoulière, A., & Billet, F. (2018). Peripheral nerve regeneration and intraneural revascularization. *Neural Regen Res*, 14(1), 24–33.
- Carriel, V., Alaminos, M., Garzón, I., Campos, A., & Cornelissen, M. (2014). Tissue engineering of the peripheral nervous system. *Expert Review of Neurotherapeutics*, 14(3), 301–318.
- Carroll, S. L. and S. H. Worley. 2016. “Wallerian Degeneration.” *The Curated Reference Collection in Neuroscience and Biobehavioral Psychology* (March 2016):485–91.
- Cattin, A. L., Burden, J. J., Van Emmenis, L., MacKenzie, F. E., Hoving, J. J. A., Garcia Calavia, N., ... Lloyd, A. C. (2015). Macrophage-Induced Blood Vessels Guide Schwann Cell-Mediated Regeneration of Peripheral Nerves. *Cell*, 162(5), 1127–1139.
- Chang, J., Ho, T., Lee, H., Lai, Y., Lu, M., Yao, C., & Chen, Y. (2009). Highly Permeable Genipin-Cross-linked Gelatin Conduits Enhance Peripheral Nerve Regeneration. *Artificial Organs*, 33(12), 1075–1085.
- Chen, C., Ou, Y., Liao, S., Chen, W., Chen, S., Wu, C., ... Hsu, S. (2007). Transplantation of bone marrow stromal cells for peripheral nerve repair. *Experimental Neurology*, 204, 443–453.
- Chen, M. B., Zhang, F., & Lineaweaver, W. C. (2006). Luminal Fillers in Nerve Conduits for Peripheral Nerve Repair. *Ann Plast Surg*, 57(4), 462–471.
- Chen, Y., Chang, J., Cheng, C., Tsai, F., Yao, C., & Liu, B. (2005). An in vivo evaluation of a biodegradable genipin-cross-linked gelatin peripheral nerve guide conduit material. *Biomaterials*, 26, 3911–3918.
- Crapo, P. M., Gilbert, T. W., & Badylak, S. F. (2011). Biomaterials An overview of tissue and whole organ decellularization processes. *Biomaterials*, 32(12), 3233–3243.
- Cui, L., Jiang, J., Wei, L., Zhou, X., Fraser, J.L., Snider, B. J., Yu, S. P. (2008). Transplantation of Embryonic Stem Cells Improves Nerve Repair and Functional Recovery After Severe Sciatic Nerve Axotomy. *Stem cells*, 26 (5), 1356–1365
- Deeken, C. R., A. K. White, S. L. Bachman, B. J. Ramshaw, D. S. Cleveland, T. S. Loy, and S. A. Grant. (2011). Method of Preparing a Decellularized Porcine Tendon Using Tributyl Phosphate. *Journal of Biomedical Materials Research - Part B Applied Biomaterials* 96 (2):199–206.
- Deumens, R., Bozkurt, A., Meek, M. F., Marcus, M. A. E., Joosten, E. A. J., Weis, J., & Brook, G. A (2010) Repairing injured peripheral nerves : Bridging the gap. *Progress in Neurobiology* Repairing injured peripheral nerves : Bridging the gap. *Progress in Neurobiology*, 92(3), 245–276
- Dreesmann, L., Mittnacht, U., Lietz, M., & Å, B. S. (2009). Nerve fibroblast impact on Schwann cell

- behavior. *European Journal of Cell Biology*, 88, 285–300.
- Durbeej, M. (2010). Laminins. *Cell Tissue Res*, 339, 259–268.
- Engels, P. E., Tremp, M., Kingham, P. J., Pietro, G., Rene, S., & Kalbermatten, D. F. (2013). Harvest site influences the growth properties of adipose derived stem cells. *Cytotechnology*, 65, 437–445.
- Falls, D. L. (2003). Neuregulins : functions , forms , and signaling strategies. *Experimental Cell Research* 284, 14–30.
- Falls, D. L., Rosen, K. M., Corfas, G., Lane, W. S., & Fischbach, G. D. (1993). ARIA, a protein that stimulates acetylcholine receptor synthesis, is a member of the neu ligand family. *Cell*, 72(5), 801–813.
- Feltri, M. L., Poitelon, Y., & Previtali, S. C. (2016). How Schwann Cells Sort Axons: New concepts. *Neuroscientist*, 22(3), 252–265.
- Fornasari, B. E., Soury, M. El, Nato, G., Fucini, A., Carta, G., ... Gambarotta, G. (2020). Fibroblasts Colonizing Nerve Conduits Express High Levels of Soluble Neuregulin1, a Factor Promoting Schwann Cell Differentiation. *Cells*, 9, 1–19.
- Fornasari, B. E., Carta, G., Gambarotta, G., Raimondo, S.(2020). Natural-Based Biomaterials for Peripheral Nerve Injury Repair. *Front. Bioeng. Biotechnol* 8(October), 1-26.
- Fricker, Florence R. and David LH Bennett. (2011). The Role of Neuregulin-1 in the Response to Nerve Injury.” *Future Neurol.* 6(6):809–822.
- Furth, M. E., Atala, A., Innovations, W. F., & Carolina, N. (2014). Tissue Engineering : Future Perspectives. In *Principles of Tissue Engineering*, Chapter 6,(Fourth Edi), 28-123.
- Gambarotta, G., Fregnan, F., & Gnani, S. (2013). Neuregulin 1 Role in Schwann Cell Regulation and Potential Applications to Promote Peripheral Nerve Regeneration. In *Tissue Engineering of the Peripheral Nerve: Chaptetr 9*, (1st ed., Vol. 108), 223-256.
- Garbay, B., Heape, A. M., Sargueil, F., & Cassagne, C. (2000). Myelin synthesis in the peripheral nervous system. *Progress in Neurobiology*, 61, 276-304.
- Geuna, S., Raimondo, S., Nicolino, S., Boux, E., Fornaro, M., Tos, P., ... Perroteau, I. (2003). Schwann-cell proliferation in muscle-vein combined conduits for bridging rat sciatic nerve defects. *Journal of Reconstructive Microsurgery*, 19(2), 119–123
- Geuna, S., Raimondo, S., Ronchi, G., Scipio, F. Di, Tos, P., Czaja, K., & Fornaro, M. (2009). Chapter 3: Histology of the peripheral nerve and changes occurring during nerve regeneration. *International Review of Neurobiology*, 1st ed., Vol. 87(9), 27-46.
- Geuna, S., Tos, P., Titolo, P., Ciclamini, D., Beningo, T., & Battiston, B. (2014). Update on nerve repair by biological tubulization. *Journal of Brachial Plexus and Peripheral Nerve Injury*, 9(1), 1–6.
- Gilbert, T. W., Sellaro, T. L., & Badylak, S. F. (2006). Decellularization of tissues and organs. *Biomaterials*, 27, 3675–3683.
- Gilpin, A., & Yang, Y. (2017). Decellularization Strategies for Regenerative Medicine: From Processing Techniques to Applications. *BioMed Research International*, 2017.
- Gonzalez-Perez, F., Cobiañchi, S., Geuna, S., Barwing, C., Freier, T., Udina, E., & Navarro, X. (2014). Tubulization with chitosan guides for the repair of long gap peripheral nerve injury in the rat. *Microsurgery*, 300–308.
- Gonzalez-Perez, F., Udina, E., & Navarro, X. (2013). Chapter 10: Extracellular Matrix Components in Peripheral Nerve Regeneration. In *Tissue Engineering of the Peripheral Nerve*, 1st ed., Vol. 108, 257-275.
- Griffin, J. W., Hogan, M. V, Chhabra, A. B., & Deal, D. N. (2013). Peripheral Nerve Repair and Reconstruction. *J Bone Joint Surg Am*, 95, 2144–2151.
- Grinsell, D., & Keating, C. P. (2014). Peripheral Nerve Reconstruction after Injury: A Review of Clinical and Experimental Therapies. *BioMed Research International*, 1-13.
- Gu, X., Ding, F., Yang, Y., & Liu, J. (2011). Progress in Neurobiology Construction of tissue engineered nerve grafts and their application in peripheral nerve regeneration. *Progress in Neurobiology*, 93(2), 204–230.
- Gupta, S. K., & Mishra, N. C. (2017). Decellularization Methods for Scaffold Fabrication. *Methods in Molecular Biology*, 34, 1-10.
- Haastert-Talini, K., Geuna, S., Dahlin, L. B., Meyer, C., Stenberg, L., Freier, T., ... Grothe, C. (2013).

- Chitosan tubes of varying degrees of acetylation for bridging peripheral nerve defects. *Biomaterials*, 34(38), 9886–9904.
- Han, G. H., Peng, J., Liu, P., Ding, X., Wei, S., Lu, S., & Wang, Y. (2019). Therapeutic strategies for peripheral nerve injury: Decellularized nerve conduits and Schwann cell transplantation. *Neural Regeneration Research*, 14(8), 1343–1351.
- Han, G., Peng, J., Liu, P., Ding, X., Wei, S., Lu, S., & Wang, Y. (2018). Therapeutic strategies for peripheral nerve injury : decellularized nerve conduits and Schwann cell transplantation. *Neural Regeneration Research*, 14 (8),1343–1351.
- Houshyar, S., Bhattacharyya, A., & Shanks, R. (2019). Peripheral Nerve Conduit: Materials and Structures. *ACS Chem. Neurosci.*, 10, 8, 3349–336.
- Hudson, T. W., Zawko, S., Deister, C., Lundy, S., Hu, C. Y., Lee, K., & Schmidt, C. E. (2004). Optimized Acellular Nerve Graft Is Immunologically Tolerated and Supports Regeneration. *Tissue engineering*, 10,(11), 1641- 1651.
- Hundepool, C. A., Nijhuis, T. H. J., Kotsougiani, D., Friedrich, P. F., Bishop, A. T., & Shin, A. Y. (2017). *Neurosurg Focus*. 42 (3), 1-7.
- Isaacs, J., & Browne, T. (2014). Overcoming short gaps in peripheral nerve repair : conduits and human acellular nerve allograft. *American Association for Hand Surgery*, 1-7
- Jabaley, M. E., & Mass, D. P. (2000). A Randomized Prospective Study of Polyglycolic Acid Conduits for Digital Nerve Reconstruction in Humans. *Plastic and Reconstructive Surgery*, 106 (5), 1036–1045.
- Jessen, K R, & Mirsky, R. (2016). The repair Schwann cell and its function in regenerating. *The Journal of Physiology*, 13(July 2015), 3521–3531.
- Jessen, Kristjan R., & Mirsky, R. (2005). The origin and development of glial cells in peripheral nerves. *Nature Reviews Neuroscience*, 6(9), 671–682.
- Jessen, Kristjan R., & Mirsky, R. (2019). Schwann cell precursors; multipotent glial cells in embryonic nerves. *Frontiers in Molecular Neuroscience*, 12(March), 1–16.
- Jessen, Kristján R., Mirsky, R., & Lloyd, A. C. (2015). Schwann cells: Development and role in nerve repair. *Cold Spring Harb Perspect Biol*, 7(7), 1-16.
- Johnson, T. S., Neill, A. C. O., Motarjem, P. M., Nazzal, J., Randolph, M., & Winograd, J. M. (2008). Tumor Formation Following Murine Neural Precursor Cell Transplantation in a Rat Peripheral Nerve Injury Model. *J Reconstr Microsurg*, 24 (8), 545–550.
- Joseph, N. M., Mukouyama, Y., Mosher, J. T., Jaegle, M., Crone, S. A., Dormand, E., ... Morrison, S. J. (2004). Neural crest stem cells undergo multilineage differentiation in developing peripheral nerves to generate endoneurial fibroblasts in addition to Schwann cells. *Development*, 131 (22) 5599–5612.
- Kannan, R. Y., Salacinski, H. J., Butler, P. E. M., & Seifalian, A. M. (2005). Artificial nerve conduits in peripheral-nerve repair. *Biotechnology and Applied Biochemistry*, 41(3), 193.
- Kaupilla, T., Jyvasjarvi, E., Huopaniemi, T., Hujanen, E., & Liesi, P. (1993). A laminin graft replaces neurorrhaphy in the restoration surgery of the rat sciatic nerve. *Experimental neurology*, 123 , 181-191.
- Kehoe, S., Zhang, X. F., & Boyd, D. (2012). FDA approved guidance conduits and wraps for peripheral nerve injury : A review of materials and efficacy. *Injury*, 43(5), 553–572.
- Kucenas, S. (2015). Perineurial Glia. *Cold Spring Harb Perspect Biol*, 7 (a020511), 1-14.
- Kucenas, S., Wang, W., Knapik, E. W., & Appel, B. (2009). A Selective Glial Barrier at Motor Axon Exit Points Prevents Oligodendrocyte Migration from the Spinal Cord. *The Journal of Neuroscience*, 29(48), 15187–15194.
- Kumar, A., Kumar, V., Rattan, V., & Jha, V. (2016). Secretome Cues Modulate the Neurogenic Potential of Bone Marrow and Dental Stem Cells. *Molecular Neurobiology*, 54(6), 4672-4682.
- Li, R., Li, D. hui, Zhang, H. yu, Wang, J., Li, X. kun, & Xiao, J. (2020). Growth factors-based therapeutic strategies and their underlying signaling mechanisms for peripheral nerve regeneration. *Acta Pharmacologica Sinica*, 41(10), 1289–1300.
- Lovati, A. B., Arrigo, D. D., Odella, S., Tos, P., Geuna, S., & Raimondo, S. (2018). Nerve Repair Using Decellularized Nerve Grafts in Rat Models . A Review of the Literature. *Front. Cell. Neurosci.* 12(November), 1–20.
- Lundborg, G. (2000). 25th Anniversary Presentation A 25-Year Perspective of Peripheral Nerve Surgery :

- Evolving Neuroscientific Concepts and. *The Journal of Hand Surgery*, 25(3), 391–414.
- Lundborg, Göran, Dahlin, L. B., Danielsen, N., Gelberman, R. H., Longo, F. M., Powell, H. C., & Varon, S. (1982) Nerve Regeneration in Silicone Chambers: Influence of Gap Length and of Distal Stump Components *Experimental Neurology*, 76(2), 361–375.
- Mackinnon SE. (1989). New Directions in Peripheral Nerve Surgery. *Annals of plastoc surgery*, 22(3), 257–273.
- Marchionni, M. A., Goodearl, A. D. J., Chen, M. S., Bermingham-McDonogh, O., Kirk, C., Hendricks, M., ... Gwynne, D. (1993). Glial growth factors are alternatively spliced erbB2 ligands expressed in the nervous system. *Nature*, 362(6418), 312–318.
- Matsuyama, T., Mackay, M., & Midha, R. (2000). Peripheral nerve repair and grafting techniques: A review. *Neurol Med Chir*, 40, 187–199.
- Mazini, L., Rochette, L., Amine, M., & Malka, G. (2019). Regenerative capacity of adipose derived stem cells (ADSCs), comparison with mesenchymal stem cells (MSCs). *International Journal of Molecular Sciences*, 20(10), 1–30.
- Mei, L., & Nave, K. A. (2014). Neuregulin-ERBB signaling in the nervous system and neuropsychiatric diseases. *Neuron*, 83(1), 27–49.
- Mei, L., & Xiong, W. (2008). Neuregulin 1 in neural development , synaptic plasticity and schizophrenia. *Nature Reviews Neuroscience*, 9(june), 437-452.
- Mendibil, U., Ruiz-hernandez, R., & Retegi-carrion, S. (2020). Tissue-Specific Decellularization Methods : Rationale and Strategies to Achieve Regenerative Compounds. *International Journal of Molecular Sciences*, 21(5447), 1–29.
- Michailov, G. V, Sereda, M. W., Brinkmann, B. G., Fischer, T. M., Haug, B., Birchmeier, C., ... Nave, K.-A. (2004). Axonal Neuregulin-1 Regulates Myelin Sheath Thickness. *SCIENCE AAAS*, 304, 700–703.
- Moran, S. L. (2009). Early Clinical Outcomes with the Use of Decellularized Nerve Allograft for Repair of Sensory Defects Within the Hand, 4, 245–249.
- Muheremu, A., & Ao, Q. (2015). Past, Present, and Future of Nerve Conduits in the Treatment of Peripheral Nerve Injury. *BioMed Res Int*, 237507, 1-7
- Nave, Klaus-Armin and Hauke B. Werner (2014). Myelination of the Nervous System: Mechanisms and Functions. *Annu. Rev. Cell Dev. Biol.* 30:503–533.
- Parrinello, S., Napoli, I., Ribeiro, S., Digby, P. W., Parkinson, D. B., Doddrell, R. D. S., ... Lloyd, A. C. (2013). Europe PMC Funders Group EphB Signaling Directs Peripheral Nerve Regeneration through Sox2-Dependent Schwann Cell Sorting. *Cell*, 143(1), 145–155.
- Patel, N. P., Lyon, K. A., & Huang, J. H. (2018, May 1). An update-tissue engineered nerve grafts for the repair of peripheral nerve injuries. *Neural Regeneration Research*, Vol. 13, pp. 764–774.
- Pfister, B. J., Gordon, T., Loverde, J. R., Kochar, A. S., Mackinnon, S. E., & Cullen, D. K. (2011). Biomedical Engineering Strategies for Peripheral Nerve Repair : Surgical Applications , State of the Art , and Future Challenges. *Critical Reviews™ in Biomedical Engineering*, 39(2), 81–124.
- Reina, M. A., Navarro, R. A., & Mateos, E. M. D. (2015). Ultrastructure of Myelinated and Unmyelinated Axons. *Atlas of Functional Anatomy for Regional Anesthesia and Pain Medicine*, 3–18.
- Ronchi, G., Haastert-talini, K., Fornasari, B. E., Perroteau, I., Geuna, S., & Gambarotta, G. (2016). The Neuregulin1 / ErbB system is selectively regulated during peripheral nerve degeneration and regeneration. *European Journal of Neuroscience*, 43(June 2015), 351–364.
- Ruiter, G. C. De, Moore, M. J., & Ph, D. (2008). Autografts, single-lumen and multichannel poly(lactic-co-glycolic acid) nerve tubes. *Neurosurgery*. 63(1), 144–155.
- Ruiter, G. C. W. de, Malessy, M. j. a., Yaszemski, M. j., Windebank, anthony j., & SPinner, robert j. (2009). Designing ideal conduits for peripheral nerve repair. *Neurosurg Focus*, 26(February), 1-9.
- Shamash, S., Reichert, F. & Rotshenker,S.(2002). The cytokine network of Wallerian degeneration: Tumor necrosis. *The journal of Neuroscience*,22(8),3052-3060.
- Sunderland, S. (1951). A classification of peripheral nerve injuries producing loss of function. *Brain*, 74(4), 491–516.
- Salzer, J. L. (2015). Schwann Cell Myelination. *Cold Spring Harb Perspect Biol.*, 7(8), 1-26.
- Sarker, M. D., Naghieh, S., McInnes, A. D., Schreyer, D. J., & Chen, X. (2018). Regeneration of peripheral

- nerves by nerve guidance conduits: Influence of design, biopolymers, cells, growth factors, and physical stimuli. *Progress in Neurobiology*, 171, 125–150.
- Seddon, H. J. (1943). Three types of nerve injury. *Brain*, 66(4), 237–288.
- Shen, F., Li, A. A., Cornelius, R. M., Cirone, P., Childs, R. F., Brash, J. L., & Chang, P. L. (2005). Biological properties of photocrosslinked alginate microcapsules. *Journal of Biomedical Materials Research - Part B Applied Biomaterials*, 75(2), 425–434.
- Siemionow, M., & Brzezicki, G. (2009). Current techniques and concepts in peripheral nerve repair. *International Review of Neurobiology*, 87 (9), 141-172..
- Simões, M. J., Gärtner, A., Shirotsaki, Y., Gil da Costa, R. M., Cortez, P. P., Gartnër, F., ... Maurício, A. C. (2011). In vitro and in vivo chitosan membranes testing for peripheral nerve reconstruction. *Acta Medica Portuguesa*, 24(1), 43–52.
- Sondell, M., Lundborg, G., & Kanje, M. (1998). Regeneration of the rat sciatic nerve into allografts made acellular through chemical extraction. *Brain Research*, 795(1–2), 44–54.
- Sowa, Y., Imura, T., Numajiri, T., Nishino, K., & Fushiki, S. (2012). Adipose-Derived Stem Cells Produce Factors Enhancing Peripheral Nerve Regeneration : *Stem Cell and Development*, 21(11), 1852–1862.
- Stassart, R. M., Fledrich, R., Velanac, V., Brinkmann, B. G., Schwab, M. H., Meijer, D., ... Nave, K. (2013). A role for Schwann cell – derived neuregulin-1 in remyelination. *Nature Neuroscience*, 16(1), 48–54.
- Summa, P. G. D. I., & Kalbermatten, D. F. (2011). Long-term in vivo regeneration of peripheral nerves through bioengineered nerve grafts. *Neuroscience*, 181, 278–291.
- Taveggia, C., Zanazzi, G., Petrylak, A., Yano, H., Rosenbluth, J., Einheber, S., ... Salzer, J. L. (2005). Neuregulin-1 type III determines the ensheathment fate of axons. *Neuron*, 47(5), 681–694.
- Thomas, P. K. (1963). The connective tissue of peripheral nerve : an electron microscope study. *J. Anat., Lond.*, 97(1), 35–44.
- Tonda-Turo, C., Gentile, P., Saracino, S., Chiono, V., Nandagiri, V. K., & Muzio, G. (2011). International Journal of Biological Macromolecules Comparative analysis of gelatin scaffolds crosslinked by genipin and silane coupling agent. *International Journal of Biological Macromolecules*, 49(4), 700–706.
- Waller A (1850). Experiments on the section of the glossopharyngeal and hypoglossal nerves of the frog, and observations of the alterations produced thereby in the structure of their primitive fibres. *Phil Transact Royal Soc London* 140:423–429.
- Wang, C., Lu, C., Peng, J., Hu, C., & Wang, Y. (2017). Roles of neural stem cells in the repair of peripheral nerve injury. *Neural Regen Res*, 12(12), 2106-2112.
- Watanabe, Y., Sasaki, R., Matsumine, H., Yamato, M., & Okano, T. (2014). Undifferentiated and differentiated adipose-derived stem cells improve nerve regeneration in a rat model of facial nerve defect. *J Tissue Eng Regen Med.*, 11(2):362-374
- Waterman, H., & Yarden, Y. (2001). Molecular mechanisms underlying endocytosis and sorting of ErbB receptor tyrosine kinases Hadassa. *Federation of European Biochemical Societies. FEBS Letters*, 490, 142–152.
- Woodhoo, A., & Sommer, L. (2008). Development of the Schwann Cell Lineage : From the Neural Crest to the Myelinated Nerve. 1490(May), 1481–1490.
- Yi, S., Zhang, Y., Gu, X., Huang, L., Zhang, K., Qian, T., & Gu, X. (2020). Application of stem cells in peripheral nerve regeneration. *Burns & Trauma*, 8, 2.
- Zheng, L., & Cui, H.-F. (2012). Enhancement of nerve regeneration along a chitosan conduit combined with bone marrow mesenchymal stem cells. *J Mater Sci: Mater Med*, 23, 2291–2302. <https://doi.org/10.1007/s10856-012-4694-3>

## *Chapter 2*

*Soluble neuregulin1 down-regulates  
myelination genes in Schwann cell*

## Soluble Neuregulin1 Down-Regulates Myelination Genes in Schwann Cells

Marwa El Soury<sup>1</sup>, Benedetta Elena Fornasari<sup>1,2</sup>, Michela Morano<sup>1,2</sup>, Elio Grazio<sup>3</sup>, Giulia Ronchi<sup>1,2</sup>, Danny Incarnato<sup>4</sup>, Mario Giacobini<sup>3</sup>, Stefano Geuna<sup>2</sup>, Paolo Provero<sup>5,6</sup>, Giovanna Gambarotta<sup>1\*</sup>

<sup>1</sup> Department of Clinical and Biological Sciences, University of Torino, Regione Gonzole 10, 10043 Orbassano (Torino), Italy

<sup>2</sup> Neuroscience Institute Cavalieri Ottolenghi (NICO), University of Torino, Regione Gonzole 10, 10043 Orbassano (Torino), Italy

<sup>3</sup> Computational Epidemiology Group and Data Analysis Unit, Department of Veterinary Sciences, University of Torino, Largo Paolo Braccini 2, 10095 Grugliasco (Torino) Italy

<sup>4</sup> Human Genetics Foundation of Torino (HUGE), Via Nizza 52, 10126 Torino, Italy

<sup>5</sup> Department of Molecular Biotechnology and Health Sciences (MBC), University of Torino, Via Nizza 52, 10126 Torino, Italy

<sup>6</sup> Center for Translational Genomics and Bioinformatics, San Raffaele Scientific Institute IRCCS, via Olgettina 60, 20132 Milano, Italy

**\* Correspondence:**

Giovanna Gambarotta

[giovanna.gambarotta@unito.it](mailto:giovanna.gambarotta@unito.it)

Published in *Frontiers in Molecular Neuroscience* 11:157.

DOI: <https://doi.org/10.3389/fnmol.2018.00157>



***Abstract***

Peripheral nerves are characterized by the ability to regenerate after injury. Schwann cell activity is fundamental for all steps of peripheral nerve regeneration: immediately after injury they de-differentiate, remove myelin debris, proliferate and repopulate the injured nerve. Soluble Neuregulin1 (NRG1) is a growth factor that is strongly up-regulated and released by Schwann cells immediately after nerve injury. To identify the genes regulated in Schwann cells by soluble NRG1, we performed deep RNA sequencing to generate a transcriptome database and identify all the genes regulated following stimulation of primary adult rat Schwann cells with soluble recombinant NRG1.

Interestingly, the gene ontology analysis of the transcriptome reveals that NRG1 regulates genes belonging to categories that are regulated in the peripheral nerve immediately after an injury. In particular, NRG1 strongly inhibits the expression of genes involved in myelination and in glial cell differentiation, suggesting that NRG1 might be involved in the de-differentiation (or “trans-differentiation”) process of Schwann cells from a myelinating to a repair phenotype. Moreover, NRG1 inhibits genes involved in the apoptotic process, and up-regulates genes positively regulating the ribosomal RNA processing, thus suggesting that NRG1 might promote cell survival and stimulate new protein expression.

This transcriptome analysis demonstrates that in Schwann cells NRG1 drives the expression of several genes which partially overlap with genes regulated *in vivo* after peripheral nerve injury, underlying the pivotal role of NRG1 in the first steps of the nerve regeneration process.

## ***Introduction***

Schwann cells represent the glial component of the peripheral nervous system. As well as supporting axonal function in a physiological status, they play a critical role during the degenerative and the regenerative processes activated after nerve injury (Namgung, 2014; Gordon, 2016; Jessen and Mirsky, 2016). A severe damage to the nerve tissue determines the loss of axon-Schwann cell contact with subsequent change in Schwann cell phenotype. Schwann cell de-differentiation occurs within 48 hours after nerve injury and is driven by changes in gene expression with the down-regulation of genes related to myelination and node organization, and the up-regulation of regeneration associated genes (RAG), such as growth factor receptors and adhesion molecules (Pereira et al., 2012; Jessen and Mirsky, 2016). Dedifferentiated Schwann cells isolate lipid droplets, composed by myelin, and participate to their degradation in the distal nerve. Few days after injury they proliferate and align to form the Büngner bands, a tubular structure that physically supports re-growing axons (Fawcett and Keynes, 1990; Ide, 1996). Moreover, Schwann cells are the source of growth factors that stimulate axon growth and create the appropriate supportive environment for axonal elongation (Hopker et al., 1999; Madl and Heilshorn, 2015). In the later phase of the regenerative process, they differentiate into myelinating and non-myelinating Schwann cells, determining the recovery of nerve morphology.

Schwann cell de-differentiation, proliferation and survival are regulated by the action of several growth factors. Among them, Neuregulin 1 (NRG1) increasingly attracted the attention for its involvement in several aspects of Schwann cell behaviour. NRG1 is a growth factor characterized by multiple isoforms thanks to alternative splicing (Mei and Xiong, 2008). Both soluble and transmembrane isoforms are present in peripheral nerves: transmembrane isoforms are expressed by neurons and are involved in myelin thickness regulation (Michailov et al., 2004; Taveggia et al., 2005), whereas soluble NRG1 isoforms are released both by Schwann cells and neurons and are thought to control Schwann cell survival, migration, de-differentiation, as well as the myelination process (Birchmeier and Nave, 2008; Fricker and Bennett, 2011; Stassart et al., 2013). NRG1 is strongly and transiently up-regulated in the distal stump immediately after nerve injury (Carroll et al., 1997; Stassart et al., 2013; Ronchi et al., 2016), suggesting a major role played by it in the response to nerve injury and in the nerve regeneration process.

Despite cellular effects induced by NRG1 stimulation, such as cell survival and migration,

---

have been widely investigated (Dong et al., 1995; Zanazzi et al., 2001; Atanasoski et al., 2006; Birchmeier and Nave, 2008; Wakatsuki et al., 2014) and single genes have been demonstrated to be regulated by NRG1 in Schwann cells (Freidin et al., 2009; Iruarrizaga-Lejarreta et al., 2012; Sonnenberg-Riethmacher et al., 2015), a deep sequencing analysis of the genes modulated by NRG1 a few hours after stimulation has not yet been performed. Here, we present a global transcriptome analysis, aimed to identify the genes regulated by soluble NRG1 stimulation in primary rat Schwann cell culture.

We chose to analyse *in vitro* the transcriptome 6 hours after NRG1 stimulation, to detect the early regulated genes and compare their expression pattern with the genes regulated *in vivo* after injury, where soluble NRG1 release and transcription are induced soon (Carroll et al., 1997; Guertin et al., 2005; Stassart et al., 2013; Ronchi et al., 2016; Yu et al., 2016) and a strong gene expression regulation is detectable between 6 and 24 hours (Yi et al., 2017).

## ***Materials and methods***

### ***Schwann cell primary culture***

To obtain Schwann cell primary cultures, sciatic nerves from adult female Wistar rats (ENVIGO, Milan, Italy) were isolated and harvested. This study was carried out in accordance with the recommendations of the Council Directive of the European Communities (2010/63/EU), the National Institutes of Health guidelines, and the Italian Law for Care and Use of Experimental Animals (DL26/14). The protocol was approved by the Italian Ministry of Health and the Bioethical Committee of the University of Torino. Conformed measures were taken into account to reduce the number of animals used and to minimize animal pain and discomfort.

Schwann cells from sciatic nerves were purified and cultured as previously described (Gnavi et al., 2015). Primary Schwann cells were routinely cultured on poly-L-lysine (PLL, Sigma)-coated plate, in complete medium consisting of DMEM (Sigma #D5671) supplemented with 10% heat-inactivated foetal bovine serum (FBS, Invitrogen), 100 units/ml penicillin, 0.1 mg/ml streptomycin, 1 mM sodium pyruvate, 2 mM L-glutamine, 8 nM recombinant soluble NRG1 $\beta$ 1 (#396-HB, R&D Systems), 10  $\mu$ M forskolin (Sigma) and incubated at 37°C in 5% CO<sub>2</sub>.

Schwann cells were cultured in the presence of 10  $\mu$ M forskolin, because Schwann cell primary cultures display dedifferentiated cell features, having lost their axonal contact (Morrissey et al., 1991), but they can be induced to reacquire the differentiated phenotype (i.e., high myelin gene expression) by exposure to agents increasing the intracellular levels of cAMP (Sobue et al., 1986).

### ***Schwann cell stimulation and RNA isolation***

Confluent Schwann cells were starved overnight in starving medium consisting of DMEM (Sigma #D5671) supplemented with 2% heat-inactivated FBS, 100 units/ml penicillin, 0.1 mg/ml streptomycin, 1 mM sodium pyruvate, 2 mM L-glutamine, and 10  $\mu$ M forskolin and then stimulated for 6 hours with 10 nM recombinant soluble NRG1 $\beta$ 1 (#396-HB, R&D Systems). Control mock samples were stimulated with the same volume of ligand resuspension buffer (PBS containing 1% bovine serum albumin/BSA, Sigma). After the stimulation, total RNA was isolated using TRIzol reagent (Invitrogen), following manufacturer's instructions. Schwann cell stimulation was performed in biological triplicate for deep sequencing analysis and in biological triplicate for gene expression validation through quantitative real time PCR analysis.

Biological triplicates were carried out using independent preparation of cells.

### ***Deep RNA sequencing***

Deep RNA sequencing was performed on three mock samples and three stimulated samples obtained in three independent experiments. RNA quality was assessed on an Agilent 2100 Bioanalyzer. All samples had RIN  $\geq$  9. For RNA-Seq library preparation, approximately 2  $\mu$ g of total RNA were subjected to poly(A) selection and libraries were prepared using the TruSeq RNA Sample Prep Kit (Illumina) following the manufacturer's instructions. Sequencing was performed on the Illumina NextSeq 500 platform.

The RNA Sequencing data have been deposited in the National Center for Biotechnology Information (NCBI) Gene Expression Omnibus (GEO), accessible through GEO Series accession number GSE104324.

### ***Analysis of RNA-seq data***

Reads were mapped to the *Rattus norvegicus* m5 reference assembly using TopHat v2.0.10 (Kim et al., 2013) and counts were generated using htseq and the refseq transcriptome. Genes with RPKM  $>$  1 in all 3 replicates were considered expressed in each condition. Differential expression was determined with DESeq2 (Love et al., 2014) with default parameters, implementing a paired design by using the biological replicate as covariate. Genes with adjusted P  $\leq$  0.01 and absolute log<sub>2</sub> fold change  $>$  1 (:fold change  $<$  0.5 and  $>$  2) were considered differentially expressed. Gene Ontology enrichment analysis was performed with

ClusterProfiler (Yu et al., 2012) with a cut off of P adjusted  $< 0.1$  (Table S2). The analysis was performed using the gene ontology annotation of the mouse orthologs of our genes, due to the better functional annotation of the mouse genome.

### ***Analysis of public gene expression datasets***

Two gene expression datasets, obtained from injured sciatic nerve samples, were downloaded from GEO as normalized expression values.

#GSE22291 series corresponds to microcrushed adult mice sciatic nerves 3 and 7 days after injury, compared with control nerves; samples were hybridized to GeneChip Mouse Genome 430 2.0 Array (Affymetrix), platform GPL1261 (Barrette et al., 2010). Genes with adjusted P  $< 0.001$  and absolute log<sub>2</sub> fold change  $> 1$  were considered differentially expressed.

#GSE33454 series corresponds to cut adult mice sciatic nerves 1 and 5 days after injury, compared with sham control sciatic nerves; samples were analysed on Illumina MouseRef-8 v2.0 expression beadchip, platform GPL6885 (Kim et al., 2012). No biological replicates are available; genes with absolute log<sub>2</sub> fold change  $> 1$  were considered differentially expressed.

Genes expressed 7 days after adult mice sciatic nerve cut, compared with contralateral uninjured nerves, were downloaded from the Supplementary Material of the paper of Arthur-Farraj and colleagues (Arthur-Farraj et al., 2017), where, to generate 100bp paired-end reads, three libraries were run on a single lane of the HiSeq 2000 platform (Illumina). All selected genes have an adjusted P value  $< 0.05$ ; those with an absolute log<sub>2</sub> fold change  $> 1$  were considered differentially expressed.

Genes expressed 0.5 hour, 1 hour, 3 hours, 6 hours, 12 hours after adult mice sciatic nerve cut, compared with sham control sciatic nerves, were downloaded from the Supplementary Material of the paper of Yi and colleagues (Yi et al., 2017); samples were hybridized to Affymetrix GeneChip Hybridization Oven 640. Genes with adjusted P  $< 0.05$  and absolute log<sub>2</sub> fold change  $> 1$  were considered differentially expressed.

### ***cDNA preparation and quantitative real-time PCR (qRT-PCR)***

To validate the deep RNA sequencing analyses, 0.5µg total RNA were retro-transcribed in a 25 µl reaction volume containing 1x RT buffer, 0.1µg/µl BSA, 7.5µM Random Hexamer Primers, 1mM deoxynucleoside triphosphate (dNTPs), 0.05% Triton X-100, 40U RIBOlock and 200U RevertAid® Reverse Transcriptase (all ingredients were purchased by Thermo

Scientific)

. The reaction was performed following the manufacturer's instructions. qRT-PCR was performed by ABI Prism 7300 (Applied Biosystems, Life Technologies Europe BV) detection system. The cDNA was diluted 10-fold in nuclease-free water, and 5µl (corresponding to 15ng starting RNA) were analysed in a 20µl reaction volume containing 1 x iTaq Universal SYBR Green Supermix (BioRad) with 300nM forward and 300nM reverse primers. Dissociation curves were routinely performed to confirm the presence of a single peak corresponding to the required amplicon. Analyses were performed in technical and biological triplicate. For each experiment the average of mock samples was used as calibrator. The threshold cycle (Ct) values were normalized to TBP (TATA Binding Protein), a general RNA polymerase II transcription factor, which has been shown to be a good housekeeping gene without retro-pseudogenes in the genome and with different exons to design forward and reverse primers separated by an intron (Vandesompele et al., 2002). Expression data were shown as  $-\Delta\Delta CT$  to compare qRT-PCR results with deep sequencing data expressed as  $\log_2(\text{fold change})$ . Primers were designed using Annhyb software (<http://www.bioinformatics.org/annhyb/>) and synthesized by BMR Genomics. Primer sequences are reported in Table 1.

**TABLE 1** | List of primers used for quantitative real time PCR (qRT-PCR) analysis to validate deep sequencing results.

Gene	Accession number	Forward primer (5'–3')	Reverse primer (5'–3')	Amplicon size
Atf3	NM_012912.2	CACCATCAACAACAGACCTCTGGAG	CCGCCGCCTCCTTTTTCTCTC	85 bp
Bmp7	NM_001191856.2	CGTCAACCTAGTGGAGCACGAC	GTCACCGCCTCTCCCTCGG	102 bp
Egr2	NM_053633.1	GACCATCTTCCCCAATGGTGAAGT	GATATGGGAGATCCAAGGGCCTCTTC	119 bp
Hmga2	NM_032070.1	CGCCACAGAAGCGAGGACG	GGGGCTCTTGTCTTGCTGCC	113 bp
Inhba	NM_017128.2	CGGAGATCATCACCTTTGCCGAG	CAGGAAGAGCCAGACTTCTGCAC	116 bp
Mag	NM_017190.4	CGCCTTCAACCTGTCTGTGGAGT	GCCACGGAGGGTTCCGG	120 bp
Mbp	NM_017026.2	GGACCCAAGATGAAAACCCAGTAGTCC	CCTTTCCTTGGGATGGAGGGGG	81 bp
Pmp22	NM_017037.1	CCTTGGGAGCCGTCCAGC	GGACGCTGAAGATGACAGACAGGATC	69 bp
Shc4	NM_001191065.1	CACCTTGGGAAAGGGAGGAGTCC	CACATCTGCAATGCCGCCTG	112 bp
Tbp	NM_001004198.1	TAAGGCTGGAAGGCCTTGTG	TCCAGGAATAATTCTGGCTCATAG	68 bp
Vegfc	NM_053653.1	CGTCGCCGCCTTGGAGTTC	GCTCATCTACACTGGACACAGACCG	122 bp

**Table 1.** List of primers used for quantitative real time PCR analysis to validate deep sequencing results.

### Statistical analysis

For qRT-PCR data, statistical analysis between two groups (mock and treated samples) was performed in GraphPad Prism 5 by the two-tailed Student's t-test. All data were expressed as mean + standard error (SEM).

## **Results**

### ***Several genes in Schwann cells are regulated by soluble NRG1 stimulation***

To identify the genes regulated early by soluble NRG1, deep sequencing analysis was applied on RNA samples obtained from Schwann cells stimulated 6 hours with 10nM recombinant soluble NRG1 $\beta$ 1 (from here on called NRG1) and mock stimulated cells, in three independent biological replicates. Preliminary assays had been previously performed to verify that treatment with 10nM NRG1 is able to stimulate ErbB3, AKT, ERK phosphorylation (data not shown).

We identified the genes expressed in the biological triplicate by mock Schwann cells (11312, 10810, 11142) and by Schwann cells following NRG1 stimulation (11239, 10811, 11197). Comparing the NRG1 stimulated cells with the mock cells, 190 genes were significantly differentially expressed: 101 up-regulated, 89 down-regulated (with a  $|\log_2\text{fold change}| > 1$ , corresponding to a fold change  $< 0.5$  and  $> 2$ , with a P adjusted  $\leq 0.01$ ). Furthermore, 93% of the differentially expressed genes have an adjusted P value  $< 0.001$ .

A heat map of the 50 most differentially regulated genes is shown in Figure 1, while the full list of differentially expressed genes is shown in Table S1.

<https://www.frontiersin.org/articles/10.3389/fnmol.2018.00157/full#supplementary-material>

to validate deep RNA sequencing data, the expression profile of 10 selected genes was analysed by quantitative real time PCR performed on RNA samples obtained from mock Schwann cells or stimulated 6 hours with 10nM NRG1. Validation was performed on three independent biological replicates different from those used for the deep sequencing.

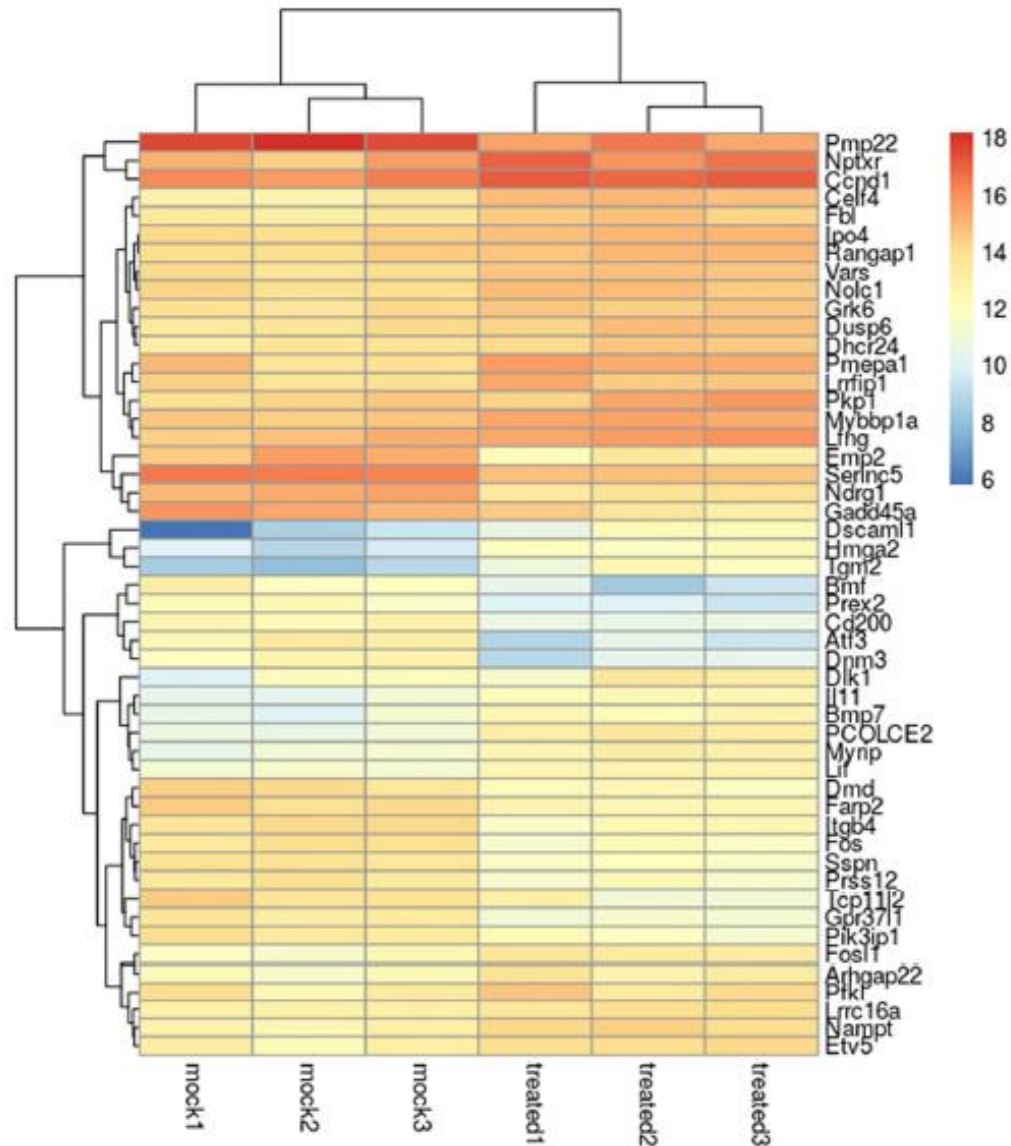


**Figure 1. Heatmap of the 50 most differentially regulated genes in Schwann cells.** The heatmap shows the biological triplicate expression of the first 50 differentially expressed genes in Schwann cells stimulated with 10nM NRG1 $\beta$ 1 based on the obtained P value. “Mock” corresponds to samples treated with the vehicle, “treated” corresponds to samples treated with NRG1 $\beta$ 1. Colour intensity reflects the expression level and represents the  $\log_2(\text{RPKM} + 1)$  of the observed gene in each sample (RPKM: Reads Per Kilo base of transcript per Million mapped reads).

5 up- and 5 down-regulated genes were chosen based on their adjusted P values or their annotated Gene Ontology categories. Among them, 8 were strongly regulated (corresponding to 4.2% of differentially regulated genes), 2 were weakly regulated; all of them were



significantly validated. *Inhba*, *Hmga2*, *Bmp7*, *Shc4*, *Vegfc* were representative for up-regulated genes, *Atf3*, *Pmp22*, *Egr2*, *Mag*, *Mbp* were representatives for down-regulated genes. As shown in Figure 2, the expression profile of these genes was consistent in both analyses.

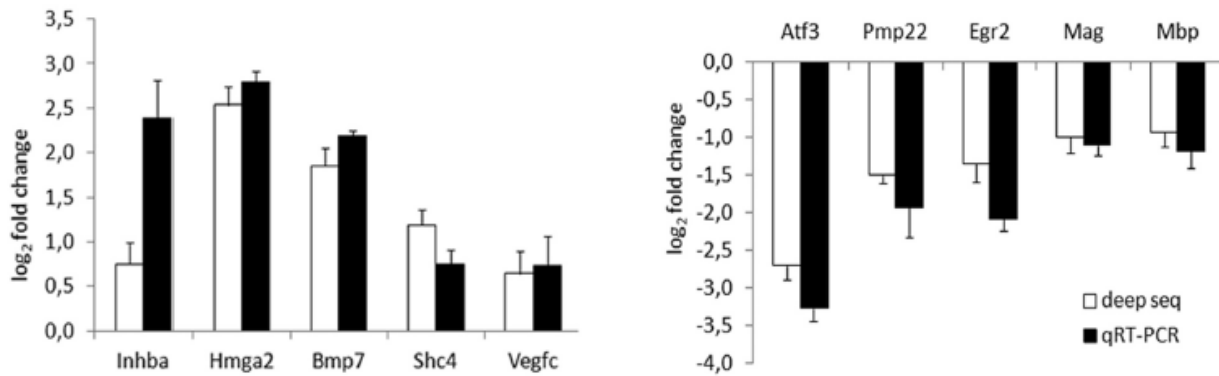


**Figure 2. Deep RNA sequencing validation through quantitative real time-PCR.** Validation of 10 representative gene transcripts was performed by qRT-PCR, showing that the behaviour of 5 up- and 5 down-regulated genes was consistent in both techniques. log<sub>2</sub> fold change (corresponding to  $-\Delta\Delta CT$  for qRT-PCR) obtained comparing samples treated with NRG1 with mock treated samples is shown, both for deep sequencing, both for qRT-PCR data.

### ***NRG1 strongly down-regulates myelination genes***

In order to assign the differentially regulated genes to their functions, Gene Ontology analysis was performed using ClusterProfiler package, focusing the attention on the biological processes.

Genes up-regulated following NRG1 stimulation were enriched in 2 annotation categories: 11 genes belong to the category of “rRNA metabolic processes”, 4 genes belong to “negative regulation of Notch signalling pathway”; the complete list of these up-regulated genes is shown in Table 2.

Due to redundancy in gene ontology annotations, here we show a selected list of up-regulated and down-regulated biological processes; the complete list of biological processes, molecular functions and cellular components is shown in Table S2.

Functional enrichment is stronger for down-regulated genes. “Myelination” is the most enriched category among down-regulated genes, with 7 genes down-regulated in response to NRG1. The following categories are “Positive regulation of ion transmembrane transport” with

6 regulated genes, “Glial cell differentiation” with 8 genes, “Regulation of membrane potential” with 9 genes, “Bleb assembly” with 3 genes, “Positive regulation of apoptotic process” with 11 genes, “Macrophage activation” with 3. The complete list of these down-regulated genes is shown in Table 2.

**TABLE 2** | Biological process (BP) enriched categories obtained by Gene Ontology analysis.

Biological process enriched category	Down-regulated genes	P adjusted	List of genes
Myelination	7	0.004263845	Pmp22, Serinc5, Ndr1, Fa2 h, Mal, Rfxrg, Egr2
Positive regulation of ion transmembrane transport	6	0.006544373	Dmd, Hspa2, Snca, P2rx7, Atp1b2, Hcn1
Glial cell differentiation	8	0.008986003	Gpr3711, Ndr1, Dmd, Epha4, Fa2 h, Egr2, Ntrk3, Lingo1
Regulation of membrane potential	9	0.010459252	Dmd, Snca, P2rx7, Grik2, Atp1b2, Kcnk5, Cldn19, Slc26a2, Hcn1
Bleb assembly	3	0.023620351	Emp2, Pmp22, P2rx7
Positive regulation of apoptotic process	11	0.080348376	Atf3, Bmf, Gadd45a, Ctsc, Snca, P2rx7, Grik2, Mal, Fbxo32, Ntrk3, Sept4
Macrophage activation	3	0.095570035	Cd200, Snca, Adgrf5
Biological process enriched category	Up-regulated genes	P adjusted	List of genes
rRNA metabolic processes	11	0.000126	Fbl, Bop1, Wdr46, Nop56, Ddx21, Nat10, Bysl, Rrp9, Nop2, Emg1, Rrp15
Negative regulation of Notch signalling pathway	4	0.02191	Bmp7, Dlk1, Lfng, Dll4

**Table 2. Biological process enriched categories obtained by Gene Ontology analysis.** Because of redundancy in gene ontology annotations, only a selected list of up-regulated and down-regulated biological processes is shown (all enriched categories of biological processes, molecular functions and cellular components are shown in Table S2).

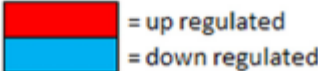
<https://www.frontiersin.org/articles/10.3389/fnmol.2018.00157/full#supplementary-material>

### **Several genes regulated by NRG1 overlap with genes regulated following nerve injury**

As expected, the genes regulated by NRG1 are annotated in categories that are related to Schwann cell response following an injury. To identify which of these genes are regulated also after a nerve injury, expression profiling data obtained from injured sciatic nerve samples were downloaded from Gene Expression Omnibus (GEO) or from Supplementary Information of published papers.

To investigate gene expression in the first hours after injury, genes regulated by NRG1 (101 up- and 89 down-regulated) were compared with genes differentially expressed 0.5 hours, 1 hour, 6 hours, 12 hours after nerve cut (Yi et al., 2017). This analysis shows that after 0.5 and 1 hour there are not differentially expressed genes in common with our data. After 6 hours 6 up-regulated genes are in common, after 12 hours 7 up-regulated and 2 down-regulated genes are in common with our data (Figure 3).

	NRG1	0.5 h	1 h	6 h	12 h
Bmf	Down				Down
Gria2	Down				Down
Epha4	Down		Up	Up	Up
Fosl1	Up			Up	Up
Il11	Up			Up	Up
Phlda1	Up			Up	Up
Slc6a17	Up			Up	Up
Ucn2	Up			Up	Up
Vgf	Up			Up	Up
Lrrfip1	Up				Up
Pth2r	Up			Down	
Osbpl6	Up				Down


  
■ = up regulated  
■ = down regulated

**Figure 3. Genes differentially regulated in vitro by NRG1 compared with 0.5-12 hour injured nerves.** Genes significantly regulated following NRG1 stimulation (101 up- and 89 down-) were compared with genes regulated 0.5h, 1h, 6h, and 12h after sciatic nerve cut (Yi et al., 2017). Among them, 7 up-regulated and 2 down-regulated show the same regulation behaviour after 12 hours.

Then, to investigate gene expression in the following phase after injury, genes regulated by NRG1 were compared with genes regulated 1 and 5 days after nerve cut (Kim et al., 2012), 3 and 7 days after nerve microcrush (Barrette et al., 2010), 7 days after nerve cut (Arthur-Farraj et al., 2017). These data show that in the first week of injury 54% of NRG1 down-regulated genes and 40% of NRG1 up-regulated genes are also regulated after nerve injury: 13 up-regulated and 9 down-regulated 1 day after nerve cut; 23 up-regulated and 40 down-regulated 3 days after nerve microcrush; 8 up-regulated and 11 down-regulated 5 days after nerve cut; 16 up-regulated and 26 down-regulated 7 days after nerve microcrush. Many genes show the same regulation at different time points. Intriguingly, few genes (9 up- and 12 down-regulated) show an opposite expression regulation, 2 genes are down-regulated 1 day after injury and after NRG1 treatment, but later their expression is up-regulated. The complete list of genes regulated both by NRG1 and by nerve injury is shown in Figure 4.

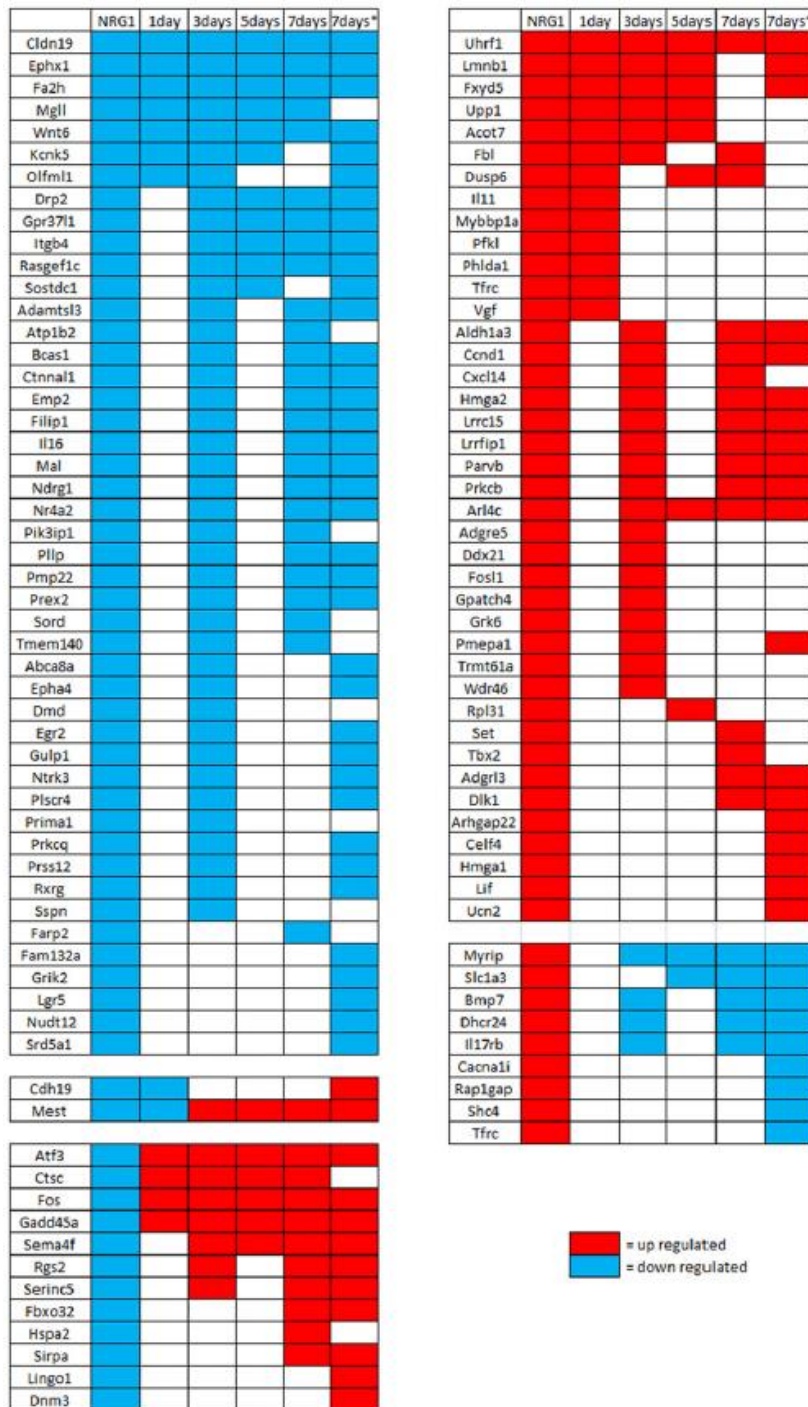


**Figure 4. Genes differentially regulated *in vitro* by NRG1 compared with 1-7 days injured nerves.**

Genes significantly regulated following NRG1 stimulation (101 up- and 89 down-) were compared with genes regulated 1 and 5 days after sciatic nerve cut (Kim et al., 2012), with genes regulated 3 and 7 days after sciatic nerve microcrush (Barrette et al., 2010) and with genes regulated 7 days (\*) after sciatic nerve cut (Arthur-Farraj et al., 2017). Among them, 40 up-regulated and 48 down-regulated show the same regulation behaviour at different time points after injury, while 9 up-regulated and 12 down-regulated show an opposite behaviour, and 2 down-regulated genes show a mixed behaviour.

Supplementary Table S1. Differential expression analysis. Sheet 1: deseq2 results for all genes; Sheets 2 and 3: up- and down-regulated genes (adjusted  $P < 0.05$  and fold-change  $> 2$  or  $< 0.5$ )

## ***Discussion***

Schwann cells, the main glial cells in the peripheral nervous system, play a key role both during development and following nerve injury, being responsible of axonal ensheathment, myelination and post-injury nerve repair (Jessen et al., 2015; Taveggia, 2016). Different factors and signalling pathways are involved in the control of these activities (Pereira et al., 2012; Boerboom et al., 2017).

It has been shown by others (Carroll et al., 1997; Stassart et al., 2013) and our research group (Ronchi et al., 2016) that different isoforms of soluble NRG1 are strongly up-regulated after injury. Moreover, in transgenic mice expressing soluble NRG1 in postnatal motoneurons and DRG neurons, but missing NRG1 in Schwann cells (Thy1.2-NRG1-I- $\beta$ 1a X Dhh-Cre X Nrg1 loxP/loxP ), nerve regeneration after crush is inefficient (Stassart et al., 2013), thus showing that soluble Nrg1 expressed by neurons does not completely compensate for the lack of NRG1 expression in Schwann cells, thus suggesting that soluble NRG1 plays a key role for their activity after injury.

Schwann cells represent 90% of the total cell number in uncut nerves, 70% in injured nerves, the majority of the rest being fibroblasts, macrophages and perineural cells (Arthur-Farraj et al., 2017). The role of the latter must not be denied, but here we focused our attention on Schwann cells, the main non-neuronal cell type in the peripheral nerve, to investigate the role of soluble NRG1 in their activity (Shin et al., 2013; Birchmeier and Bennett, 2016).

To this aim, by RNA deep sequencing, we carried out a transcriptome analysis to identify the genes regulated in vitro in Schwann cells following NRG1 stimulation.

Then, we compared this list of differentially regulated genes with the genes expressed in vivo in the injured nerve to find common regulated genes, conscious of the fact that in the injured nerve environment, besides Schwann cells, there are other different cell types, and that there are other released factors besides soluble NRG1.

A stringent analysis was performed to select genes significantly regulated in vitro by NRG1 stimulation with a 2-fold threshold and a highly significant adjusted P value ( $\leq 0.01$ ). As expected, NRG1 stimulation induces differential gene expression in Schwann cells. Applying gene ontology, the regulated genes were categorized into specific groups based on the relevant biological processes, cellular components and molecular functions. We focused our attention on the biological processes; after eliminating redundant categories, down-regulated genes were enriched in 7 categories, while up-regulated genes were enriched in 2.

Enriched gene categories are consistent with the phenotypic changes occurring in Schwann cells after injury: the portion of the nerve distal to the injury undergoes Wallerian degeneration, a complex process characterized by axonal degeneration and degradation of myelin sheath, followed by debris phagocytosis by Schwann cells and macrophages (Dubovy, 2011). Demyelination is an important step during Wallerian degeneration, starting with fragmentation of the myelin sheath into small ovoid-like structures (Ghabriel and Allt, 1979) and with the down-regulation of myelin genes (Jessen and Mirsky, 2008). Because NRG1 receptor activation is sufficient to initiate Schwann cell demyelination (Guertin et al., 2005), it has been suggested that NRG1 might play a key role in the de-differentiation process (Fricker and Bennett, 2011; Shin et al., 2013).

Both myelinating and non-myelinating (Remak) Schwann cells participate to the process of Wallerian degeneration where they trans-differentiate into a repair phenotype specialized to promote nerve regeneration (Jessen and Mirsky, 2016). Accordingly, when we consider gene expression analysis *in vivo*, both myelinating and non-myelinating Schwann cells contribute to the transcriptome, as well as *in vitro*, where primary cultures obtained from sciatic nerves contain both myelinating and non-myelinating cells.

When we analysed the enriched categories of differentially expressed genes in response to NRG1 stimulation, we found that “myelination” is the most enriched category among down-regulated genes, with several genes known to be involved in the myelination process are down-regulated (Pmp22, Serinc5, Ndr1, Fa2h, Mal, Rxrg and Krox20/Egr2), thus suggesting that myelination genes were expressed by myelinating Schwann cells undergoing trans-differentiation, while the enriched down-regulated category “glial cell differentiation” reflects gene expression of both myelinating and non-myelinating Schwann cells.

The fact that NRG1 inhibits myelination genes evokes literature data showing that the transcription factor c-Jun negatively regulates myelination (Parkinson et al., 2008), down-regulating genes essential in the myelination program, such as the zinc finger transcription factor Krox20/Egr2 (Warner et al., 1998), which in turn has been shown to inhibit c-Jun expression in a reciprocal negative feed-back loop (Parkinson et al., 2004).

We found that also soluble NRG1 inhibits Krox20/Egr2 expression, thus suggesting that NRG1 - inhibiting Krox20/Egr2 - might contribute to stimulate c-Jun expression. Accordingly, it has been shown *in vitro* that NRG1 treatment stimulates c-Jun expression (Syed et al., 2010) and phosphorylation (Parkinson et al., 2004). Further analyses *in vitro* and *in vivo* will be necessary to better investigate the crosstalk between c-Jun and NRG1.

---

Genes annotated in categories like “positive regulation of apoptotic process” and “bleb assembly” are also downregulated, suggesting that NRG1 supports Schwann cell survival following nerve injury.

NRG1 stimulation of Schwann cells showed a down-regulation of genes annotated in the enriched category “regulation of macrophage activation”, such as Cd200 and Snca. Macrophages are recruited to the nerve injured site to eliminate fragmented myelin debris and dead cells (Dubovy, 2011). Cd200 is expressed in node of Ranvier and Schmidt-Lanterman incisures and is down-regulated following nerve injury (Chang et al., 2011). It has been suggested that Cd200 down-regulation might facilitate macrophage infiltration through the node of Ranvier to eliminate degenerated axons and myelin debris (Chang et al., 2011). Also Snca (Synuclein  $\alpha$ ) is localized at nodes of Ranvier and Schmidt-Lanterman incisures, is up-regulated during myelination and down-regulated after nerve injury (D'Antonio et al., 2006) and might be involved in macrophage infiltration. Indeed, it has been shown that following sciatic nerve transection, transgenic mice over-expressing Snca show a lower number of invading macrophages (Siebert et al., 2010).

Two categories of up-regulated genes are enriched in response to NRG1 stimulation: “genes responsible for rRNA metabolic processes” and “negative regulation of Notch signalling pathway”. The up regulation of the former contributes to the synthesis and production of new proteins and molecules needed to guide Wallerian degeneration and nerve regeneration.

Notch is a transmembrane receptor that acts as a negative regulator of myelination: it is down-regulated during myelination and by Krox20, and plays an important role in demyelination in injured nerves (Mirsky et al., 2008; Woodhoo et al., 2009). For this reason, the up-regulation of negative regulators of the Notch pathway is difficult to explain, unless we hypothesize that Notch is up-regulated in a different time point or that Notch expression is regulated at protein level, or that the genes grouped in this gene ontology category actually contribute to demyelination and Schwann cell de-differentiation without inhibiting Notch pathway. Indeed, Bmp7 retards peripheral myelination by activating p38 MAPK in Schwann cells (Liu et al., 2016), while Dlk1 (delta like non-canonical Notch ligand 1) and Dll4 (Delta-like 4 Notch ligand) are both Notch ligands.

Since NRG1 is strongly up-regulated after injury and Schwann cells represent a high percentage of cells in the injured nerve, we hypothesized that their contribution to the injured nerve transcriptome is relevant. Therefore, we compared the list of genes regulated in Schwann cells in response to NRG1 stimulation with the lists of genes regulated after nerve

---

injury, with the idea to identify, among many regulated genes, the genes regulated in Schwann cells following NRG1 stimulation.

To this aim, we exploited previously published expression profiling data of injured sciatic nerves at different early time points (1, 3, 5, 7 days) following injury (Barrette et al., 2010; Kim et al., 2012). These data were obtained using microarray assay; more recently, deep sequencing data at 7 days after injury were published and made available to the scientific community (Arthur-Farraj et al., 2017). So, in Figure 3 we show two data set corresponding to 7 days after injury; they do not correspond 100%, likely because the first set derives from a microcrushed nerve, the second from a transected nerve; moreover, the first was analysed by microarray, the second was analysed by deep sequencing. Accordingly, the authors of the latter analysis compared their deep sequencing analysis with a previous microarray analysis (Arthur-Farraj et al., 2012), finding that ~20% of regulated genes were differently regulated. As expected, several genes that are regulated by NRG1 in Schwann cells overlap with genes regulated in the sciatic nerve following nerve injury. Nevertheless, some genes show a different regulation. These differences can be explained by the fact that genes expressed in injured sciatic nerves belong mainly to Schwann cells, but also to other cell types, while the gene expression profile obtained with the deep sequencing corresponds to genes expressed only by Schwann cells. Moreover, in the injured nerve environment several factors are released, not only soluble NRG1, and the nerve analysis reveals genes regulated by different factors.

Ex vivo primary cultures represent a good experimental model as they allow focusing the analysis on a single cell type (e.g. Schwann cells), while in vivo different cell types coexist in the injured nerve: Schwann cells, fibroblasts, macrophages, epineural cells, and so on. Moreover, they allow analysing a single factor stimulation (e.g. NRG1), while in vivo different factors are released after injury.

Our in vitro analysis focused on genes regulated 6 hours after stimulation with NRG1; we chose this time point because we were interested to identify genes regulated early by NRG1 in Schwann cells. Indeed, in vivo experiments showed that after nerve injury NRG1 mRNA increase is detectable between 1 and 24 hours (Yu et al., 2016) and several genes start to be differentially expressed between 6 and 24 hours (Yi et al., 2017).

By comparing the regulated genes in Schwann cells after NRG1 stimulation with genes that are regulated in peripheral nerves in response to injury, we found that many genes show the same behaviour in the two experimental models (both up- or both down-regulated) while only few genes show an opposite behaviour. As previously discussed, this opposite behaviour might

---



be explained by the fact that the expression of these genes in the peripheral nerve is not regulated in Schwann cells, but rather in other cell types belonging to the nerve tissue, or by the fact that the expression of these genes in injured Schwann cells is regulated also by other factors released in the injured environment. Among them we noticed the transcription factors Atf3, Fos (Patodia and Raivich, 2012) and Gadd45a (Lin et al., 2011), which are significantly down-regulated by NRG1 in Schwann cells in vitro and up-regulated in dorsal root ganglia (DRG) neurons and sciatic nerves (Arthur-Farraj et al., 2017) in vivo after injury.

Firstly, we compared genes differentially expressed both following Schwann cell NRG1 stimulation and early hours after nerve injury. In the early hours we found more up-regulated than down-regulated common genes. Three of them (Il11, Phlda1, Vgf) are only expressed in the first hours (6-24 h) thus suggesting that they may play a role immediately after injury.

Then, we focused our attention on up-regulated and down-regulated genes common to all time points (from day 1 until day 7) following nerve injury and following Schwann cell NRG1 stimulation.

A common up-regulated gene is Uhrf1 (Ubiquitin Like with PHD and Ring Finger Domains 1), encoding for a E3 ubiquitin ligase. This protein binds to specific DNA sequences, regulating gene expression. It has been shown that Uhrf1 plays a role in inducing basal cell proliferation following airway injury (Xiang et al., 2017), thus suggesting that it might play a similar role in stimulating proliferation of Schwann cells following a peripheral nerve injury.

Another common up-regulated gene is Lamin B1 (Lmnb1), playing an important role in the modulation of genes involved in normal myelin regulation; moreover, Lmnb1 over-expression is associated with down-regulation of proteolipid protein, a highly abundant myelin sheath component (Heng et al., 2013). Intriguingly, another gene regulated at all time points after injury and after NRG1 stimulation is Fxyd5 (FXFD domain containing ion transport regulator 5), which has been recently shown to be a regeneration-associated gene (RAG), whose over-expression increases (and knock-down decreases) neuritis length and number (Chandran et al., 2016).

The common down-regulated genes include Cldn19, Ephx1, Wnt6, Fa2h.

Cldn19 (Tight-Junction Gene Claudin 19) is the main tight junction constituent of Schwann cells and it is involved in their electrophysiological sealing function (Miyamoto et al., 2005) in the healthy nerve. Ephx1 (Microsomal epoxide hydrolase) is an evolutionarily highly conserved enzyme expressed in nearly all tissues, where it can play a role in redox homeostasis by removing reactive oxygen species (Vaclavikova et al., 2015). Abnormalities in Ephx1

---

expression are involved in neurological disorders such as Alzheimer's disease (Liu et al., 2006) and tumours. As far as we know, nothing was mentioned in literature about its role in peripheral nerves or Schwann cells.

Wnt is expressed by axons, and it has been found that Wnt signalling promotes Schwann cell lineage progression, proliferation and myelination (Grigoryan et al., 2013).

Fa2h (Fatty acid 2-hydroxylase), which is down-regulated from the first till the seventh day post injury, is found to be directly related to the process of myelin formation, where it is required for the synthesis of 2-hydroxy galactolipids in peripheral nerve myelin (Maldonado et al., 2008).

Other genes that are down-regulated by NRG1 and related to the myelination process (Mal, Ndr1, Pmp22, Egr2, Rxrg) are also down-regulated at different time points after injury, suggesting that NRG1 might be involved in the demyelination process following nerve injury. The down-regulation of genes involved in the myelination is particularly intriguing in the light of our recent data obtained from a rat model of the demyelinating neuropathy Charcot-Marie-Tooth 1A, where we demonstrated that soluble NRG1 is strongly over-expressed in the nerves (Fornasari et al., 2018). We wondered if soluble NRG1 over-expression worsens the disease or counteracts it, attenuating its symptoms and promoting nerve repair. The down-regulation of myelination genes suggests that it worsens the disease and that therapeutic approaches aimed to inhibit NRG1 activity could be more useful than therapeutic approaches involving treatment with soluble NRG1 (Fledrich et al., 2014). Accordingly, it has been shown that a high concentration of soluble NRG1 negatively affects in vitro myelination (Syed et al., 2010).

Our in vitro analysis shows that soluble NRG1 plays a key role for Schwann cell survival, differentiation and demyelination, thus suggesting that in vivo, after peripheral nerve injury, soluble NRG1 release or delivery needs to be limited to the early phases after nerve injury. Indeed, in the following phases, the remyelination will be promoted by the NRG1 transmembrane isoforms expressed by the axons (Michailov et al., 2004; Taveggia et al., 2005). This concept must be kept in mind when planning gene therapies with soluble NRG1 or recombinant factor delivery aimed to promote peripheral nerve regeneration.

---

## References

- Arthur-Farraj, P.J., Latouche, M., Wilton, D.K., Quintes, S., Chabrol, E., Banerjee, A., et al. (2012). c-Jun reprograms Schwann cells of injured nerves to generate a repair cell essential for regeneration. *Neuron* 75(4), 633-647. doi: S0896-6273(12)00583-1 [pii] 10.1016/j.neuron.2012.06.021.
- Arthur-Farraj, P.J., Morgan, C.C., Adamowicz, M., Gomez-Sanchez, J.A., Fazal, S.V., Beucher, A., et al. (2017). Changes in the Coding and Non-coding Transcriptome and DNA Methylome that Define the Schwann Cell Repair Phenotype after Nerve Injury. *Cell Rep* 20(11), 2719-2734. doi: 10.1016/j.celrep.2017.08.064.
- Atanasoski, S., Scherer, S.S., Sirkowski, E., Leone, D., Garratt, A.N., Birchmeier, C., et al. (2006). ErbB2 signaling in Schwann cells is mostly dispensable for maintenance of myelinated peripheral nerves and proliferation of adult Schwann cells after injury. *J. Neurosci.* 26(7), 2124-2131. doi: 10.1523/JNEUROSCI.4594-05.2006.
- Barrette, B., Calvo, E., Vallieres, N., and Lacroix, S. (2010). Transcriptional profiling of the injured sciatic nerve of mice carrying the Wld(S) mutant gene: identification of genes involved in neuroprotection, neuroinflammation, and nerve regeneration. *Brain Behav Immun* 24(8), 1254-1267. doi: 10.1016/j.bbi.2010.07.249.
- Birchmeier, C., and Bennett, D.L. (2016). Neuregulin/ErbB Signaling in Developmental Myelin Formation and Nerve Repair. *Curr Top Dev Biol* 116, 45-64. doi: 10.1016/bs.ctdb.2015.11.009.
- Birchmeier, C., and Nave, K.A. (2008). Neuregulin-1, a key axonal signal that drives Schwann cell growth and differentiation. *Glia* 56(14), 1491-1497. doi: 10.1002/glia.20753.
- Boerboom, A., Dion, V., Chariot, A., and Franzen, R. (2017). Molecular Mechanisms Involved in Schwann Cell Plasticity. *Front Mol Neurosci* 10, 38. doi: 10.3389/fnmol.2017.00038.
- Carroll, S.L., Miller, M.L., Frohnert, P.W., Kim, S.S., and Corbett, J.A. (1997). Expression of neuregulins and their putative receptors, ErbB2 and ErbB3, is induced during Wallerian degeneration. *J Neurosci* 17(5), 1642-1659.
- Chandran, V., Coppola, G., Nawabi, H., Omura, T., Versano, R., Huebner, E.A., et al. (2016). A Systems-Level Analysis of the Peripheral Nerve Intrinsic Axonal Growth Program. *Neuron* 89(5), 956-970. doi: 10.1016/j.neuron.2016.01.034.
- Chang, C.Y., Lee, Y.H., Jiang-Shieh, Y.F., Chien, H.F., Pai, M.H., Chen, H.M., et al. (2011). Novel distribution of cluster of differentiation 200 adhesion molecule in glial cells of the peripheral nervous system of rats and its modulation after nerve injury. *Neuroscience* 183, 32-46. doi: 10.1016/j.neuroscience.2011.03.049.
- D'Antonio, M., Michalovich, D., Paterson, M., Droggiti, A., Woodhoo, A., Mirsky, R., et al. (2006). Gene profiling and bioinformatic analysis of Schwann cell embryonic development and myelination. *Glia* 53(5), 501-515. doi: 10.1002/glia.20309.
- Dong, Z., Brennan, A., Liu, N., Yarden, Y., Lefkowitz, G., Mirsky, R., et al. (1995). Neu differentiation factor is a neuron-glia signal and regulates survival, proliferation, and maturation of rat Schwann cell precursors. *Neuron* 15(3), 585-596. doi: 10.1016/0896-6273(95)90147-7.
- Dubovy, P. (2011). Wallerian degeneration and peripheral nerve conditions for both axonal regeneration and neuropathic pain induction. *Ann Anat* 193(4), 267-275. doi: 10.1016/j.aanat.2011.02.011.
- Fawcett, J.W., and Keynes, R.J. (1990). Peripheral nerve regeneration. *Annu. Rev. Neurosci.* 13, 43-60. doi: 10.1146/annurev.ne.13.030190.000355.
- Fledrich, R., Stassart, R.M., Klink, A., Rasch, L.M., Prukop, T., Haag, L., et al. (2014). Soluble neuregulin-1 modulates disease pathogenesis in rodent models of Charcot-Marie-Tooth disease 1A. *Nat Med* 20(9), 1055-1061. doi: nm.3664 10.1038/nm.3664.
- Fornasari, B.E., Ronchi, G., Pascal, D., Visigalli, D., Capodivento, G., Nobbio, L., et al. (2018). Soluble Neuregulin1 is strongly up-regulated in the rat model of Charcot-Marie-Tooth 1A disease. *Exp Biol Med (Maywood)*, 1535370218754492. doi: 10.1177/1535370218754492.
- Freidin, M., Asche, S., Bargiello, T.A., Bennett, M.V., and Abrams, C.K. (2009). Connexin 32 increases

- the proliferative response of Schwann cells to neuregulin-1 (Nrg1). *Proc Natl Acad Sci U S A* 106(9), 3567-3572. doi: 10.1073/pnas.0813413106.
- Fricker, F.R., and Bennett, D.L. (2011). The role of neuregulin-1 in the response to nerve injury. *Future Neurol* 6(6), 809-822.
- Ghabriel, M.N., and Allt, G. (1979). The role of Schmidt-Lanterman incisures in Wallerian degeneration. I. A quantitative teased fibre study. *Acta Neuropathol* 48(2), 93-93.
- Gnavi, S., Fornasari, B.E., Tonda-Turo, C., Ciardelli, G., Zanetti, M., Geuna, S., et al. (2015). The influence of electrospun fibre size on Schwann cell behaviour and axonal outgrowth. *Mater Sci Eng C Mater Biol Appl* 48, 620-631. doi: 10.1016/j.msec.2014.12.055.
- Gordon, T. (2016). Nerve regeneration in the peripheral and central nervous systems. *J Physiol* 594(13), 3517-3520. doi: 10.1113/jp270898.
- Grigoryan, T., Stein, S., Qi, J., Wende, H., Garratt, A.N., Nave, K.A., et al. (2013). Wnt/Rspondin/beta-catenin signals control axonal sorting and lineage progression in Schwann cell development. *Proc Natl Acad Sci U S A* 110(45), 18174-18179. doi: 10.1073/pnas.1310490110.
- Guertin, A.D., Zhang, D.P., Mak, K.S., Alberta, J.A., and Kim, H.A. (2005). Microanatomy of axon/glia signaling during Wallerian degeneration. *J Neurosci* 25(13), 3478-3487. doi: 10.1523/jneurosci.3766-04.2005.
- Heng, M.Y., Lin, S.T., Verret, L., Huang, Y., Kamiya, S., Padiath, Q.S., et al. (2013). Lamin B1 mediates cell-autonomous neuropathology in a leukodystrophy mouse model. *J Clin Invest* 123(6), 2719-2729. doi: 10.1172/jci66737.
- Hopker, V.H., Shewan, D., Tessier-Lavigne, M., Poo, M., and Holt, C. (1999). Growth-cone attraction to netrin-1 is converted to repulsion by laminin-1. *Nature* 401(6748), 69-73. doi: 10.1038/43441.
- Ide, C. (1996). Peripheral nerve regeneration. *Neurosci Res* 25(2), 101-121. doi: 10.1016/0168-0102(96)01042-5.
- Iruarizaga-Lejarreta, M., Varela-Rey, M., Lozano, J.J., Fernandez-Ramos, D., Rodriguez-Ezpeleta, N., Embade, N., et al. (2012). The RNA-binding protein human antigen R controls global changes in gene expression during Schwann cell development. *J Neurosci* 32(14), 4944-4958. doi: 10.1523/jneurosci.5868-11.2012.
- Ito, Y., Yamamoto, M., Li, M., Mitsuma, N., Tanaka, F., Doyu, M., et al. (2000). Temporal expression of mRNAs for neuropoietic cytokines, interleukin-11 (IL-11), oncostatin M (OSM), cardiotrophin-1 (CT-1) and their receptors (IL-11Ralpha and OSMRbeta) in peripheral nerve injury. *Neurochem Res* 25(8), 1113-1118.
- Jessen, K.R., and Mirsky, R. (2008). Negative regulation of myelination: relevance for development, injury, and demyelinating disease. *Glia* 56(14), 1552-1565. doi: 10.1002/glia.20761.
- Jessen, K.R., and Mirsky, R. (2016). The repair Schwann cell and its function in regenerating nerves. *J Physiol*. doi: 10.1113/jp270874.
- Jessen, K.R., Mirsky, R., and Lloyd, A.C. (2015). Schwann Cells: Development and Role in Nerve Repair. *Cold Spring Harb Perspect Biol* 7(7), a020487. doi: 10.1101/cshperspect.a020487.
- Kim, D., Perteau, G., Trapnell, C., Pimentel, H., Kelley, R., and Salzberg, S.L. (2013). TopHat2: accurate alignment of transcriptomes in the presence of insertions, deletions and gene fusions. *Genome Biol* 14(4), R36. doi: 10.1186/gb-2013-14-4-r36.
- Kim, Y., Remacle, A.G., Chernov, A.V., Liu, H., Shubayev, I., Lai, C., et al. (2012). The MMP-9/TIMP-1 axis controls the status of differentiation and function of myelin-forming Schwann cells in nerve regeneration. *PLoS One* 7(3), e33664. doi: 10.1371/journal.pone.0033664.
- Lin, C.R., Yang, C.H., Huang, C.E., Wu, C.H., Chen, Y.S., Sheen-Chen, S.M., et al. (2011). GADD45A protects against cell death in dorsal root ganglion neurons following peripheral nerve injury. *J Neurosci Res* 89(5), 689-699. doi: 10.1002/jnr.22589.
- Liu, M., Sun, A., Shin, E.J., Liu, X., Kim, S.G., Runyons, C.R., et al. (2006). Expression of microsomal epoxide hydrolase is elevated in Alzheimer's hippocampus and induced by exogenous beta-amyloid and trimethyl-tin. *Eur J Neurosci* 23(8), 2027-2034. doi: 10.1111/j.1460-9568.2006.04724.x.
- Liu, X., Zhao, Y., Peng, S., Zhang, S., Wang, M., Chen, Y., et al. (2016). BMP7 retards peripheral

- myelination by activating p38 MAPK in Schwann cells. *Sci Rep* 6, 31049. doi: 10.1038/srep31049.
- Love, M.I., Huber, W., and Anders, S. (2014). Moderated estimation of fold change and dispersion for RNA-seq data with DESeq2. *Genome Biol* 15(12), 550. doi: 10.1186/s13059-014-0550-8.
- Madl, C.M., and Heilshorn, S.C. (2015). Matrix interactions modulate neurotrophin-mediated neurite outgrowth and pathfinding. *Neural Regen Res* 10(4), 514-517. doi: 10.4103/1673-5374.155426.
- Maldonado, E.N., Alderson, N.L., Monje, P.V., Wood, P.M., and Hama, H. (2008). FA2H is responsible for the formation of 2-hydroxy galactolipids in peripheral nervous system myelin. *J Lipid Res* 49(1), 153-161. doi: 10.1194/jlr.M700400-JLR200.
- Mei, L., and Xiong, W.C. (2008). Neuregulin 1 in neural development, synaptic plasticity and schizophrenia. *Nat. Rev. Neurosci.* 9(6), 437-452. doi: 10.1038/nrn2392.
- Michailov, G.V., Sereda, M.W., Brinkmann, B.G., Fischer, T.M., Haug, B., Birchmeier, C., et al. (2004). Axonal neuregulin-1 regulates myelin sheath thickness. *Science* 304(5671), 700-703. doi: 10.1126/science.1095862.
- Mirsky, R., Woodhoo, A., Parkinson, D.B., Arthur-Farraj, P., Bhaskaran, A., and Jessen, K.R. (2008). Novel signals controlling embryonic Schwann cell development, myelination and dedifferentiation. *J Peripher Nerv Syst* 13(2), 122-135. doi: 10.1111/j.1529-8027.2008.00168.x.
- Miyamoto, T., Morita, K., Takemoto, D., Takeuchi, K., Kitano, Y., Miyakawa, T., et al. (2005). Tight junctions in Schwann cells of peripheral myelinated axons: a lesson from claudin-19-deficient mice. *J Cell Biol* 169(3), 527-538. doi: 10.1083/jcb.200501154.
- Morrissey, T.K., Kleitman, N., and Bunge, R.P. (1991). Isolation and functional characterization of Schwann cells derived from adult peripheral nerve. *J Neurosci* 11(8), 2433-2442.
- Namgung, U. (2014). The role of Schwann cell-axon interaction in peripheral nerve regeneration. *Cells Tissues Organs* 200(1), 6-12. doi: 10.1159/000370324.
- Parkinson, D.B., Bhaskaran, A., Arthur-Farraj, P., Noon, L.A., Woodhoo, A., Lloyd, A.C., et al. (2008). c-Jun is a negative regulator of myelination. *J Cell Biol* 181(4), 625-637. doi: 10.1083/jcb.200803013.
- Parkinson, D.B., Bhaskaran, A., Droggiti, A., Dickinson, S., D'Antonio, M., Mirsky, R., et al. (2004). Krox-20 inhibits Jun-NH2-terminal kinase/c-Jun to control Schwann cell proliferation and death. *J Cell Biol* 164(3), 385-394. doi: 10.1083/jcb.200307132.
- Patodia, S., and Raivich, G. (2012). Role of transcription factors in peripheral nerve regeneration. *Front Mol Neurosci* 5, 8. doi: 10.3389/fnmol.2012.00008.
- Pereira, J.A., Lebrun-Julien, F., and Suter, U. (2012). Molecular mechanisms regulating myelination in the peripheral nervous system. *Trends Neurosci* 35(2), 123-134. doi: 10.1016/j.tins.2011.11.006.
- Ronchi, G., Haastert-Talini, K., Fornasari, B.E., Perroteau, I., Geuna, S., and Gambarotta, G. (2016). The Neuregulin1/ErbB system is selectively regulated during peripheral nerve degeneration and regeneration. *Eur J Neurosci* 43(3), 351-364. doi: 10.1111/ejn.12974.
- Shin, Y.K., Jang, S.Y., Park, J.Y., Park, S.Y., Lee, H.J., Suh, D.J., et al. (2013). The Neuregulin-Rac-MKK7 pathway regulates antagonistic c-jun/Krox20 expression in Schwann cell dedifferentiation. *Glia* 61(6), 892-904. doi: 10.1002/glia.22482.
- Siebert, H., Kahle, P.J., Kramer, M.L., Isik, T., Schluter, O.M., Schulz-Schaeffer, W.J., et al. (2010). Over-expression of alpha-synuclein in the nervous system enhances axonal degeneration after peripheral nerve lesion in a transgenic mouse strain. *J Neurochem* 114(4), 1007-1018. doi: 10.1111/j.1471-4159.2010.06832.x.
- Sobue, G., Shuman, S., and Pleasure, D. (1986). Schwann cell responses to cyclic AMP: proliferation, change in shape, and appearance of surface galactocerebroside. *Brain Res* 362(1), 23-32.
- Sonnenberg-Riethmacher, E., Miehle, M., and Riethmacher, D. (2015). Promotion of periostin expression contributes to the migration of Schwann cells. *J Cell Sci* 128(17), 3345-3355. doi: 10.1242/jcs.174177.
- Stassart, R.M., Fledrich, R., Velanac, V., Brinkmann, B.G., Schwab, M.H., Meijer, D., et al. (2013). A

- role for Schwann cell-derived neuregulin-1 in remyelination. *Nat Neurosci* 16(1), 48-54. doi: 10.1038/nn.3281.
- Syed, N., Reddy, K., Yang, D.P., Taveggia, C., Salzer, J.L., Maurel, P., et al. (2010). Soluble neuregulin-1 has bifunctional, concentration-dependent effects on Schwann cell myelination. *J. Neurosci.* 30(17), 6122-6131. doi: 10.1523/JNEUROSCI.1681-09.2010.
- Taveggia, C. (2016). Schwann cells-axon interaction in myelination. *Curr Opin Neurobiol* 39, 24-29. doi: 10.1016/j.conb.2016.03.006.
- Taveggia, C., Zanazzi, G., Petrylak, A., Yano, H., Rosenbluth, J., Einheber, S., et al. (2005). Neuregulin-1 type III determines the ensheathment fate of axons. *Neuron* 47(5), 681-694. doi: 10.1016/j.neuron.2005.08.017.
- Vaclavikova, R., Hughes, D.J., and Soucek, P. (2015). Microsomal epoxide hydrolase 1 (EPHX1): Gene, structure, function, and role in human disease. *Gene* 571(1), 1-8. doi: 10.1016/j.gene.2015.07.071.
- Vandesompele, J., De Preter, K., Pattyn, F., Poppe, B., Van Roy, N., De Paepe, A., et al. (2002). Accurate normalization of real-time quantitative RT-PCR data by geometric averaging of multiple internal control genes. *Genome Biol.* 3(7), RESEARCH0034.
- Wakatsuki, S., Araki, T., and Sehara-Fujisawa, A. (2014). Neuregulin-1/glia growth factor stimulates Schwann cell migration by inducing alpha5 beta1 integrin-ErbB2-focal adhesion kinase complex formation. *Genes Cells* 19(1), 66-77. doi: 10.1111/gtc.12108.
- Warner, L.E., Mancias, P., Butler, I.J., McDonald, C.M., Keppen, L., Koob, K.G., et al. (1998). Mutations in the early growth response 2 (EGR2) gene are associated with hereditary myelinopathies. *Nat Genet* 18(4), 382-384. doi: 10.1038/ng0498-382.
- Woodhoo, A., Alonso, M.B., Droggiti, A., Turmaine, M., D'Antonio, M., Parkinson, D.B., et al. (2009). Notch controls embryonic Schwann cell differentiation, postnatal myelination and adult plasticity. *Nat Neurosci* 12(7), 839-847. doi: 10.1038/nn.2323.
- Xiang, H., Yuan, L., Gao, X., Alexander, P.B., Lopez, O., Lau, C., et al. (2017). UHRF1 is required for basal stem cell proliferation in response to airway injury. *Cell Discov* 3, 17019. doi: 10.1038/celldisc.2017.19.
- Yi, S., Tang, X., Yu, J., Liu, J., Ding, F., and Gu, X. (2017). Microarray and qPCR Analyses of Wallerian Degeneration in Rat Sciatic Nerves. *Front Cell Neurosci* 11, 22. doi: 10.3389/fncel.2017.00022.
- Yu, G., Wang, L.G., Han, Y., and He, Q.Y. (2012). clusterProfiler: an R package for comparing biological themes among gene clusters. *OMICS* 16(5), 284-287. doi: 10.1089/omi.2011.0118.
- Yu, J., Gu, X., and Yi, S. (2016). Ingenuity Pathway Analysis of Gene Expression Profiles in Distal Nerve Stump following Nerve Injury: Insights into Wallerian Degeneration. *Front Cell Neurosci* 10, 274. doi: 10.3389/fncel.2016.00274.
- Zanazzi, G., Einheber, S., Westreich, R., Hannocks, M.J., Bedell-Hogan, D., Marchionni, M.A., et al. (2001). Glial growth factor/neuregulin inhibits Schwann cell myelination and induces demyelination. *J Cell Biol* 152(6), 1289-1299.

## *Chapter 3*

*Soluble neuregulin-1 (NRG1): a factor promoting peripheral nerve regeneration by affecting Schwann cell activity immediately after injury*

## **Soluble neuregulin-1 (NRG1): a factor promoting peripheral nerve regeneration by affecting Schwann cell activity immediately after injury**

**Marwa El Soury, Giovanna Gambarotta \***

Department of Clinical and Biological Sciences, University of Torino, Torino, Italy

\*Correspondence to: Giovanna Gambarotta, PhD, [giovanna.gambarotta@unito.it](mailto:giovanna.gambarotta@unito.it).

Published in Neural Regeneration research 14(8):1374-1375

DOI: doi: 10.4103/1673-5374.253516



Neuregulin-1 (NRG1) is a well-known growth factor playing contradictory roles in myelination depending on the existing isoform. Transmembrane NRG1 acts as a promyelinating factor, while the soluble isoform inhibits myelination. In this perspective, we would like to emphasize this conflicting role played by NRG1 isoforms regarding their roles in myelination, remyelination and the entire process of peripheral nerve regeneration. NRGs belong to a family of growth factors encoded by four different genes (NRG1–4); among them, NRG1 and its generated isoforms are the most well studied owing to their involvement in the developmental stages of several different systems including nervous, cardiac and muscular systems. NRG1 is a complex gene comprised of multiple promoters and several exons, consequently up to 30 different NRG1 isoforms can be produced by alternative splicing (Mei & Xiong, 2008). NRG1 mainly exists in two forms based on the N-terminal motif, either a transmembrane or a soluble form. A core epidermal growth factor like domain that is responsible for NRG1 binding to and activation of ErbB receptors is common to all isoforms. Most of the soluble NRG1 isoforms contain an additional immunoglobulin like (Ig) domain in their N-terminus, thus are called “Ig-NRG1”. These isoforms can be synthesized either as a soluble ligand released in the extracellular environment or as a single pass transmembrane anchored precursor which needs to be further processed by metalloproteases to release a soluble ligand acting in a paracrine or autocrine manner. Transmembrane NRG1 isoforms lack the Ig domain, but possess a cysteine rich domain (CRD) in their N-terminus, hence are called “CRD-NRG1”. Because CRD contains an additional transmembrane domain, precursors of these isoforms pass the cell membrane twice, thus needing a proteolytic cleavage to signal in a juxtacrine manner. NRG1 acts by binding to ErbB3 and ErbB4 receptors, which belong to the ErbB family of tyrosine kinase receptors. They are involved in many cellular processes such as proliferation, growth, migration, adhesion, differentiation and survival (Mei & Xiong, 2008). As mentioned above, in the peripheral nervous system different NRG1 isoforms play different roles (Fricker & Bennett, 2011): transmembrane NRG1 isoforms are expressed by myelinating axons, while soluble NRG1 isoforms are expressed by Schwann cells immediately after injury. These NRG1 isoforms, signalling respectively in a juxtacrine or autocrine manner, play opposite roles, giving to Schwann cells opposite messages: while axonal transmembrane NRG1 during development and after injury promotes myelination and remyelination, soluble NRG1 expressed by Schwann cells immediately after injury, inhibits myelination genes and promotes Schwann cell survival and dedifferentiation. Furthermore, it has been shown that axonal transmembrane NRG1 negatively affects the expression of soluble NRG1 in Schwann cells

---

---

(Stassart et al., 2013): when, following nerve injury, axon-Schwann cell interaction is interrupted, the interaction between axonal transmembrane NRG1 and glial ErbB receptors is lost and soluble NRG1 transcription is switched on. Myelination fate of Schwann cells is determined by the amount of the expressed transmembrane NRG1 on the axonal surface: an axon diameter  $> 1 \mu\text{m}$  expresses the adequate NRG1 threshold for stimulating myelination. It has been found that the transmembrane NRG1 knock-out mice show poor nerve ensheathment and myelination (Michailov et al., 2004; Taveggia et al., 2005), while the overexpression of transmembrane NRG1 in transgenic mice renders the typically un-myelinated sympathetic neurons myelinated (Taveggia et al., 2005). The pro-myelinating activity of transmembrane NRG1 is not exclusively dependent on its molecular level of expression, but also on the proteolytic cleavage that NRG1 precursor is subjected to, which can be mediated either by  $\beta$ -secretase 1 (BACE, promoting myelination) or tumor necrosis factor- $\alpha$ -convertase (TACE, inhibiting myelination) (Taveggia, 2016). Thus, the modulation of different protease activities could be an encouraging therapeutic strategy to promote axon remyelination following a nerve injury, as direct transmembrane NRG1 administration is not applicable, since its expression has to be axonal and would require virus transduction of sensitive neurons localized in the dorsal root ganglia and motor neurons localized in the ventral root of the spinal nerve. In the healthy nerve, myelinating Schwann cells are highly differentiated, but in response to injury they exhibit a great capacity of plasticity, and transdifferentiate into a repair phenotype (Jessen & Mirsky, 2016). Repair Schwann cells support nerve regeneration by proliferating and organizing themselves in a tubular structure called “Büngner bands”, which acts as a scaffold upon which the regenerating axon can grow and direct its path to reinnervate the target organs. Later, when the axon regeneration is successfully accomplished, Schwann cells redifferentiate into a myelinating phenotype and remyelinate regenerated peripheral axons (Figure 1). Changes in gene expression in response to nerve injury were addressed by Stassart et al. (2013) and Ronchi et al. (2016). The expression analysis of different soluble NRG1 isoforms demonstrates that it strongly increased immediately post-nerve injury, followed by an increase of NRG1 co-receptors ErbB2 and ErbB3. To further investigate the role of soluble NRG1 in Schwann cells, we analysed the regulated genes at 6 hours following soluble NRG1 stimulation in an in vitro adult Schwann cell model (El Soury et al., 2018). Our data showed that, at 6 hours post stimulation, NRG1 down-regulates several genes involved in myelination, Schwann cell differentiation and apoptotic processes. Since these are the changes required in vivo for Schwann cell transdifferentiation, it can be suggested that NRG1 plays a significant role in this

---

process in the injured nerve environment (Figure 1). Moreover, the comparison of our *in vitro* data with *in vivo* transcriptomic data on injured nerves obtained by other groups had shown that several genes are overlapping. The immediate up-regulation of soluble NRG1 could play a pivotal role in the early stage following peripheral nerve injury. Using conditional knock-out it has been shown that nerve remyelination is strongly impaired when soluble NRG1 expressed by Schwann cells is lacking (Stassart et al., 2013). We hypothesize that soluble NRG1 affects the process of remyelination only indirectly: soluble NRG1 itself is not directly implied in the remyelination process, but it is directly involved in Schwann cell transdifferentiation, a limiting step for Wallerian degeneration and subsequent nerve regeneration. The expression of soluble NRG1 in the distal nerve stump is strongly increased immediately after mild injury, such as crush or transection followed by end-to-end repair (Ronchi et al., 2016). When the nerve lesion is severe and is accompanied by substance loss, autografts are considered the gold standards in bridging the two nerve stumps. Unfortunately, there are numerous drawbacks related to this technique as secondary injuries, donor site morbidity and loss of sensitivity. Tubulization technique is considered a promising alternative to autografts. Nevertheless, while soluble NRG1 level increases immediately when using autografts to repair nerve injury, produced by the autograft Schwann cells, it takes up to 2 weeks in a hollow tube to reach the same NRG1 levels (Ronchi et al., 2018) which is likely the time required for Schwann cells to colonize the hollow tube. Several attempts have been made to improve the Tubulization technique and its outcomes. One of them is enriching the hollow tube with soluble NRG1 or other growth factors. Data obtained by different research groups and us suggest that the delivery of recombinant soluble NRG1 should be finely regulated and restricted to an early time window, to promote Schwann cell dedifferentiation and survival, while in later stages of regeneration and remyelination soluble NRG1 levels should be reduced, to avoid remyelination inhibition. The observation that soluble NRG1 promotes demyelination *in vitro* (Zanazzi et al., 2001), and that it is dramatically over-expressed *in vivo* in peripheral nerves of chronic demyelinating neuropathy rats (Fornasari et al., 2018), further suggests that soluble NRG1 could be deleterious if supplied in the inappropriate time-window. To conclude, NRG1 isoforms could be a promising therapeutic target for peripheral nerve regeneration: soluble NRG1 should be supplied immediately and transiently after injury, to promote Schwann cell survival and dedifferentiation, while transmembrane NRG1 could be activated later, acting on BACE or TACE as discussed above, to further promote remyelination. As soluble NRG1 and activators of transmembrane NRG1 might have negative side effects when supplied in the incorrect time

window, further studies will be necessary to better define doses and timing of administration.

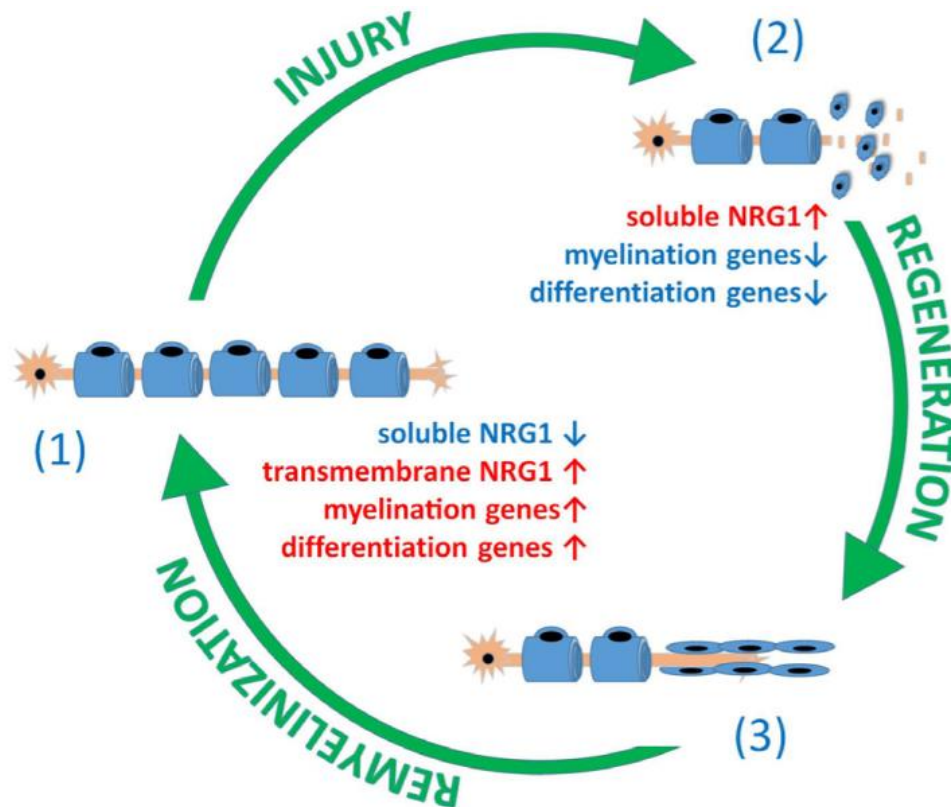


**Figure 1** Schematic representation of the hypothetical role of soluble neuregulin1 (NRG1) in Schwann cell transdifferentiation. In vitro experiment demonstrates that Schwann cell stimulation with soluble NRG1 down-regulates genes involved in myelination and differentiation. We hypothesize that in vivo, in response to nerve injury, the immediate increase of soluble NRG1 might contribute to the process of Schwann cell transdifferentiation from a myelinating Schwann cell to a repairing Schwann cell, through the down-regulation of genes involved in myelination and differentiation in the distal nerve portion. During the axonal regeneration, the interaction between Schwann cells and axonal transmembrane NRG1, and the concomitant down-regulation of soluble NRG1, might stimulate the expression of myelination and differentiation genes, thus promoting the remyelination process. In the figure, the healthy nerve (1), the injured nerve undergoing Wallerian degeneration (2), the regenerating nerve with Schwann cells organized in Büngner bands guiding axon regrowth (3) and the regenerated nerve (1) are shown. Soluble NRG1 is released by Schwann cells, transmembrane NRG1 is expressed by neurons in the axons. Up-regulated genes in the distal nerve portion are represented in red, down-regulated genes in blue.

---

**References**

- El Soury, M., Fornasari, B. E., Morano, M., Grazio, E., Ronchi, G., Incarnato, D., ... Gambarotta, G. (2018). Soluble neuregulin1 down-regulates myelination genes in schwann cells. *Frontiers in Molecular Neuroscience*, 11.
- Fornasari, B. E., Ronchi, G., Pascal, D., Visigalli, D., Capodivento, G., Nobbio, L., ... Gambarotta, G. (2018). Soluble Neuregulin1 is strongly up-regulated in the rat model of Charcot-Marie-Tooth 1A disease. *Experimental Biology and Medicine*, 243(4), 370–374.
- Fricker, F. R., & Bennett, D. L. (2011). The role of neuregulin-1 in the response to nerve injury. *Future Neurology*, 6(6), 809–822.
- Jessen, K. R., & Mirsky, R. (2016). The repair Schwann cell and its function in regenerating. *The Journal of Physiology*, 13(July 2015), 3521–3531.
- Mei, L., & Xiong, W. (2008). Neuregulin 1 in neural development , synaptic plasticity and schizophrenia. *Nature reviews neuroscience*, 9(june), 437-452.
- Michailov, G. V, Sereda, M. W., Brinkmann, B. G., Fischer, T. M., Haug, B., Birchmeier, C., ... Nave, K.-A. (2004). Axonal Neuregulin-1 Regulates Myelin Sheath Thickness. *Science* AAAs,304, 700-703.
- Ronchi, G., Fornasari, B. E., Crosio, A., Budau, C. A., Tos, P., Perroteau, I., ... Gambarotta, G. (2018). Chitosan Tubes Enriched with Fresh Skeletal Muscle Fibers for Primary Nerve Repair. *BioMed Research International*, 14(6), 1079–1084.
- Ronchi, G., Haastert-talini, K., Fornasari, B. E., Perroteau, I., Geuna, S., & Gambarotta, G. (2016). The Neuregulin1 / ErbB system is selectively regulated during peripheral nerve degeneration and regeneration. *European Journal of Neuroscience*, 43(June 2015), 351–364.
- Stassart, R. M., Fledrich, R., Velanac, V., Brinkmann, B. G., Schwab, M. H., Meijer, D., ... Nave, K. (2013). A role for Schwann cell – derived neuregulin-1 in remyelination. 16(1).
- Taveggia, C. (2016). ScienceDirect Schwann cells – axon interaction in myelination. *Current Opinion in Neurobiology*, 39, 24–29.
- Taveggia, C., Zanazzi, G., Petrylak, A., Yano, H., Rosenbluth, J., Einheber, S., ... Salzer, J. L. (2005). Neuregulin-1 type III determines the ensheathment fate of axons. *Neuron*, 47(5), 681–694.
- Zanazzi, G., Einheber, S., Westreich, R., Hannocks, M., Bedell-hogan, D., Marchionni, M. A., & Salzer, J. L. (2001). Glial Growth Factor / Neuregulin Inhibits Schwann Cell Myelination and Induces Demyelination. *The Journal of Cell Biology*, 152(6), 1289–1299.

## *Chapter 4*

*Fibroblasts colonizing nerve conduits  
express high levels of soluble  
Neuregulin1, a factor promoting  
Schwann cell dedifferentiation*

## **Fibroblasts colonizing nerve conduits express high levels of soluble Neuregulin1, a factor promoting Schwann cell dedifferentiation**

Benedetta Elena Fornasari<sup>1,2</sup>, **Marwa El Soury**<sup>1,2</sup>, Giulia Nato<sup>2,3</sup>, Alessia Fucini<sup>1</sup>, Giacomo Carta<sup>1,2</sup>, Giulia Ronchi<sup>1,2</sup>, Alessandro Crosio<sup>1,2,4</sup>, Isabelle Perroteau<sup>1</sup>, Stefano Geuna<sup>1,2</sup>, Stefania Raimondo<sup>1,2</sup>, Giovanna Gambarotta<sup>1,2\*</sup>

*1 Department of Clinical and Biological Sciences, University of Torino, Torino, Italy*

*2 Neuroscience Institute Cavalieri Ottolenghi (NICO), University of Torino, Torino, Italy*

*3 Department of Life Sciences and Systems Biology, University of Torino, Torino, Italy*

*4 Hand Surgery and Reconstructive Microsurgery, Gaetano Pini - CTO Hospital, Milano, Italy*

\* *Correspondence:* [giovanna.gambarotta@unito.it](mailto:giovanna.gambarotta@unito.it); Tel.: +39-0116705436

Published in *Cells*. 2020; 9(6):1366

DOI: doi: 10.3390/cells9061366

***Abstract***

Conduits for the repair of peripheral nerve gaps are a good alternative to autografts as they provide a protected environment and a physical guide for axonal re-growth. Conduits require colonization by cells involved in nerve regeneration (Schwann cells, fibroblasts, endothelial cells, macrophages) while in the autograft many cells are resident and just need to be activated. Since it is known that soluble Neuregulin1 (sNRG1) is released after injury and plays an important role activating Schwann cell dedifferentiation, its expression level was investigated in early regeneration steps (7, 14, 28 days) inside a 10 mm chitosan conduit used to repair median nerve gaps in Wistar rats. In vivo data show that sNRG1, mainly the isoform  $\alpha$ , is highly expressed in the conduit, together with a fibroblast marker, while Schwann cell markers, including NRG1 receptors, were not. Primary culture analysis shows that nerve fibroblasts, unlike Schwann cells, express high NRG1 $\alpha$  levels, while both express NRG1 $\beta$ . These data suggest that sNRG1 might be mainly expressed by fibroblasts colonizing nerve conduit before Schwann cells. Immunohistochemistry analysis confirmed NRG1 and fibroblast marker colocalization. These results suggest that fibroblasts, releasing sNRG1, might promote Schwann cell dedifferentiation to a “repair” phenotype, contributing to peripheral nerve regeneration. Keywords: Neuregulin 1; nerve fibroblasts; nerve regeneration; Schwann cells; nerve guide; chitosan; peripheral nerve; nerve repair; nerve injury

**Keywords:** Neuregulin 1; nerve fibroblasts; nerve regeneration; Schwann cells; nerve guide; chitosan; peripheral nerve; nerve repair; nerve injury



---

## ***Introduction***

Traumatic injury to peripheral nerve represents a relevant clinical problem that can lead to permanent disability and functional impairment; indeed, it has been estimated that ~3% of all trauma involve peripheral nerves (Modrak et al.,2020). Unlike the central nervous system, peripheral nerves regenerate spontaneously after a crush (axonotmesis) or a clear cut (neurotmesis), when proximal and distal stumps remain in close contact, facilitating the formation of a bridge and axonal re-growth (Cattin et al.,2015; Parrinello et al.,2010). Nevertheless, after a clear cut, a microsurgical intervention is always recommended to guide the re-growing axons from the proximal to the distal stump and then to their target. If it is possible to connect the two stumps without tension, a direct suture is suggested; if, following nerve tissue loss, a direct suture would cause a too high tension, it is necessary to insert a scaffold to bridge the two stumps without tension (Duffy et al.,2019). The length of the gap which needs bridging with a scaffold varies according to the characteristics of different nerves and their anatomical district (Bahm et al.,2018). Despite the progresses reached in nerve repair techniques during recent decades, peripheral nerve gap repair remains a significant clinical challenge. For severe injuries, the gold standard technique is the autograft, i.e., transplantation of an autologous nerve, but it presents some side effects, such as a secondary surgery and sensitivity loss (Deumens et al.,2010). A good alternative is the tubulization, where a tubular conduit is used to connect the gap between the nerve stumps. Different tubular conduits have been developed and several are commercially available, as recently reviewed (Belanger et al.,2016; Kornfeld et al.,2018). Conduit repair efficiency is similar to the autograft for short distance repair, while for long distances the autograft remains the most effective technique (Moore et al.,2009; Haastert-Talini et al.,2013). Indeed, autograft, being a transplanted nerve, yet contains most of the players involved in Wallerian degeneration and nerve regeneration, while conduits require colonization by Schwann cells, fibroblasts, endothelial cells, and so on. A promising biomaterial widely used for peripheral nerve regeneration and recently approved for clinical use is chitosan, a polysaccharide of natural origins (Haastert-Talini et al.,2013; Freier et al.,2005; Bāk at al.,2017). It is a highly versatile biomaterial, indeed it has been tested in several forms, such as hydrogels, films, or conduits used to repair nerve gap (Boecker et al.,2019). After a nerve cut, a bridge spontaneously forms between the proximal and the distal stumps; the analysis of the bridge showed that, during nerve regeneration, important roles are played by macrophages, endothelial cells, Schwann cells, and fibroblasts (Cattin et al.,2016).

---

Initially, the bridge, composed by inflammatory cells and extracellular matrix released by fibroblasts, is poorly vascularized and becomes hypoxic: Macrophages, sensing hypoxia, release vascular-endothelial growth factor (VEGF) which attracts endothelial cells promoting angiogenesis; blood vessels provide a track for Schwann cell migration (Cattin et al., 2016). In the degenerating distal stump, Schwann cells, releasing soluble NRG1, might promote their de-differentiation from a myelinating to a “repair” phenotype, playing a key role in myelin debris clearing, macrophage attraction, neuron survival, and axonal re-growth (Jessen & Arthur-Ferraj, 2019). Indeed, soluble NRG1 has been shown to play an important role for nerve regeneration (Fricker et al., 2011), being highly, and transiently, over-expressed immediately after injury (Ronchi et al., 2016; Stassart et al., 2013) and negatively affecting nerve regeneration when it is missing (Stassart et al., 2013). Different NRG1 isoforms obtained by alternative splicing were described (Mei & Xiong, 2008): They are mainly classified as transmembrane (expressed by axons and strongly involved in the regulation of myelination) or soluble (released by Schwann cells immediately after nerve injury), and as type  $\alpha$  or type  $\beta$ , according to the C-terminus of EGF-like domain, the domain which is involved in the interaction with NRG1 receptors, namely ErbB3 and ErbB4 (Falls, 2003; Wen et al., 1994). In Schwann cells, NRG1 signal transduction is mediated by the heterodimeric receptor ErbB2-ErbB3 (Newbern et al., 2010). While many studies have contributed to our knowledge about how peripheral nerves regenerate in case of mild injuries, such as crush (axonotmesis) or clear-cut transections (neurotmesis) followed by end-to-end repair, much less is understood about nerve regeneration after a severe injury with loss of nerve tissue. In particular, although tubulization is often and successfully used as a good alternative to autograft for short nerve gap repair (Belanger et al., 2016; Haastert-Talini et al., 2013; Bakk et al., 2017; Gonzalez-Perez et al., 2015; Meyer et al., 2016; Shapira et al., 2016; Boni et al., 2018; Subramanian et al., 2009), little is known about what happens during regeneration inside a conduit used to repair this kind of injury. A description of the different stages occurring inside a hollow conduit during nerve regeneration was carried out several years ago by means of electron microscopy analysis (Williams et al., 1983): (1) The conduit is initially filled with plasma exudate which contains extracellular matrix molecules and neurotrophic factors; (2) fibrin filaments are formed; (3) fibroblasts and dedifferentiated Schwann cells colonize the gap, proliferate and align along the conduit forming the Bands of Büngner (4) axons grow and reach their distal targets exploiting the biological cues supplied by Schwann cells; and (5) Schwann cells differentiate to a myelinating phenotype and myelinate axons (Carvalho et al., 2019). Our aim was to further

---

characterize the stages occurring inside a conduit using different techniques to identify the cells and the factors involved in the nerve regeneration, focusing our attention on the NRG1/ErbB system, with the idea that understanding what happens inside a nerve conduit might contribute to develop new strategies to further promote nerve repair.

## ***Materials and Methods***

### **Surgical Procedure**

Eighteen adult female Wistar rats (ENVIGO, Milan, Italy), weighing about 200–250 g, were used. The total number includes animals used for uninjured control nerve withdrawal. Animals were kept under standardized and controlled conditions (12 h of light and 12 h of dark and free access to water and food). Surgeries were performed under general anesthesia through intraperitoneal injection of tiletamine HCl and zolazepam HCl (Zoletil Virbac, Milan, Italy) + xilazine (Rompun, Bayer, Leverkusen, Germany) (40 mg kg<sup>-1</sup> + 5 mg kg<sup>-1</sup>). The median nerve was exposed and transected to establish a defect (8 mm of nerve was removed). Then, two experimental groups were obtained: the chitosan conduit group and the autograft group as previously described (Ronchi et al., 2018) (Figure S1). 1-for the chitosan conduit group a hollow 10 mm long chitosan tube was used to bridge the 8 mm nerve defect by inserting 1 mm of each nerve end inside the conduit (8 mm gap was chosen considering it). The nerve conduit was sutured with one 9/0 epineurial stitch (silk; Péters Surgicals, Bobigny, France) at each end. Chitosan-based conduits (Reaxon® Nerve Guide) were supplied by Medovent GmbH (Mainz, Germany). 2-for the autograft group, the transected median nerve segment was reversed (distal-proximal) and sutured to the nerve ends of the same animal with three 9/0 epineurial stitch at each end. Regenerated nerves were withdrawn 7, 14, and 28 days after the repair for biomolecular analysis (n = 3–4 for each group) and 7 days after the repair for morphological analysis; then, animals were sacrificed by anesthetic overdose (>100 mg kg<sup>-1</sup> Zoletil and 30 mg kg<sup>-1</sup> Rompun). Control nerves were healthy median nerves obtained from 4 uninjured animals.

### ***Ethics Approval and Consent to Participate***

Animal study followed the recommendations of the Council Directive of the European Communities (2010/63/EU), the Italian Law for Care and Use of Experimental Animals (DL26/14) and are in agreement with the National Institutes of Health guidelines (NIH

Publication No. 85-23, revised 1996). All animal experiments were carried out at the animal facility of Neuroscience Institute Cavalieri Ottolenghi (NICO) (Ministerial authorization DM 182 2010-A 3-11-2010). The current experimental study was reviewed and approved by the Ethic Experimental Committee of the University of Torino (Italian Ministry of Health approved project number: 864/2016/PR, 14-09-2016).

### ***Schwann Cell Primary Culture***

To obtain adult primary Schwann cell culture, 4 rat sciatic nerves were isolated for each biological replicate (n = 3). The epineurium was removed, nerves were cut into small pieces about 1 mm long, then were evenly distributed in a 3 cm diameter Petri dish and were incubated for 24 h in dissociation medium Dulbecco Modified Eagle Medium (DMEM, Gibco, Thermo Fisher Scientific, Waltham, MA, USA) containing 1 g/L glucose, 10% heat-inactivated fetal bovine serum (FBS; Invitrogen, Thermo Fisher Scientific), 100 units/mL penicillin, 0.1 mg/mL streptomycin, 10  $\mu$ M Forskolin, 63 ng/mL recombinant NRG1 $\beta$ 1 (#396-HB, R&D Systems, Minneapolis, MN, USA), 0.625 mg/mL collagenase IV, 0.5 mg/mL dispase II at 37 °C in a 5% CO<sub>2</sub> atmosphere saturated with H<sub>2</sub>O. After 24 h, mechanical dissociation was performed and the medium containing the dissociated nerves was collected in a tube, then the suspension was filtered through a cell strainer with 70  $\mu$ m pores (Sartorius Stedim Biotech GmbH, Göttingen, Germany) and transferred into a new tube. Cells were centrifuged at 100 rcf for 5 min. The pellet obtained was resuspended in DMEM D-valine medium (Cell Culture Technologies, Gravesano, Switzerland) containing D-valine, 4.5 g/L glucose, 2 mM glutamine, 10% FBS, 100 units/mL penicillin, 0.1 mg/mL streptomycin, 10  $\mu$ M Forskolin, and 63 ng/mL NRG1 $\beta$ 1. Cells were grown in a cell culture dish pre-treated with poly-L-lysine (PLL) to allow Schwann cell adhesion, at 37 °C in a 5% CO<sub>2</sub> atmosphere saturated with H<sub>2</sub>O. Medium was replaced every two days.

Cells (passage 1) were allowed to proliferate until confluence, then split and allowed to proliferate until confluence in a 6 cm diameter Petri dish (passage 2) for the subsequent extraction with TRIzol Reagent (Invitrogen, Thermo Fisher Scientific) to obtain RNA and protein, as described below. DMEM D-valine medium was used to obtain Schwann cells, as the essential amino acid D-valine in this media can be exclusively metabolized by Schwann cells and not by fibroblasts, owing to the expression of the D-amino acid oxidase (DAAO) enzyme in Schwann cells. Since fibroblasts are not able to metabolize this isoform, they die after a few days in culture, due to the lack of an essential amino acid (Kaewkhaw et al., 2012).

---

Unless specified, all reagents were purchased from Sigma-Aldrich, Merck, Darmstadt, Germany.

### ***Nerve Fibroblast Primary Culture***

To obtain adult primary nerve fibroblasts 2 rat sciatic nerves were isolated for each biological replicate (n = 3). The protocol is similar to that used for Schwann cell isolation, except for: (i) The epineurium was not removed from sciatic nerves, (ii) the culture medium DMEM (Sigma-Aldrich, Merck) contained L-valine, 4.5 g/L glucose, 10% FBS, 2 mM L-glutamine and 100 units/mL penicillin, 0.1 mg/mL streptomycin, and (iii) fibroblasts were cultured without any coating. Medium was replaced every two to three days. At least three passages were carried out to reduce the number of contaminating Schwann cells and to increase the purity of the primary culture. The purity of the culture was assessed by immunohistochemistry (data not shown). After reaching confluence, RNA and proteins were extracted for subsequent expression analysis, as described below. Sciatic nerves to obtain Schwann cell and fibroblast primary cultures were withdrawn from nine uninjured animals, four of which were the animals used for control group median nerve withdrawal.

### ***RNA Isolation, cDNA Preparation, and Quantitative Real-Time PCR***

Total RNA extraction and retrotranscription, and quantitative real-time PCR (qRT-PCR), were performed as previously described (Ronchi et al.,2016), using 0.75 µg /sample for retrotranscription. Technical and biological triplicates were performed for in vitro sample analysis, while for in vivo sample analysis, biological replicates were 4. qRT-PCR data were analysed using the “Livak  $2^{-\Delta\Delta C_t}$  method” for the relative quantification (Livak et al.,2001). Briefly, the threshold cycle (Ct) values of both the calibrator and the samples of interest were normalized to housekeeping genes to obtain  $\Delta C_t$ , then  $\Delta C_t$  were normalized to the calibrator to obtain  $\Delta\Delta C_t$  and, following, the relative quantification ( $2^{-\Delta\Delta C_t}$ ) representing the expression level of each sample relatively to the calibrator sample. As calibrator for the relative quantification the average of uninjured nerve was used. The geometric average of the two endogenous housekeeping genes ANKRD27 (Ankyrin repeat domain 27) and RICTOR (RPTOR Independent Companion Of MTOR, Complex 2) was used for data normalization (Gambarotta et al.,2014). Primer sequences for ErbB1, ErbB2, ErbB3, soluble NRG1, ANKRD27, RICTOR (Ronchi et al.,2016),( ErbB4, NRG1 $\alpha$ , NRG1 $\beta$  [30], S100, and p75 (Ronchi et al.,2017) were previously published. A new primer pair for Thy1 (accession number

#NM012673, amplicon length 127 bp) was prepared:

Thy1 forward: 5' - CTCCTGCTTTCAGTCTTGCAGATGTC-3'; Thy1reverse: 5'-CATGCTGGATGGGCAAGTTGGTG-3'.

### ***Protein Extraction and Western Blot***

After RNA extraction, total proteins were extracted by the TRIzol Reagent (Invitrogen, Thermo Fisher Scientific) according to manufacturer's instructions, then, protein pellet was dissolved in boiling Laemli buffer (2.5% sodium dodecyl sulphate, 0.125 M Tris-HCl, pH 6.8). The Bicinchoninic Acid assay kit (Sigma-Aldrich, Merck) was used to determine protein concentration and equal amounts of proteins (50 µg) were loaded into each lane. Proteins were resolved by 8% SDS-PAGE. Western blot analysis was carried out as previously described (Gambarotta et al.,2004). The list of primary and secondary antibodies is reported in Table S1. Secondary antibodies are horseradish peroxidase linked.

### ***Immunohistochemistry***

Seven days after the surgery, median nerves from each experimental group were withdrawn for the following immunohistochemistry (IHC) analysis. Before fixation chitosan conduits were removed with high precision in order to avoid loss of the tissue grown inside. Regenerated nerve specimens were fixed in 4% paraformaldehyde in PBS (phosphate buffered saline) (Sigma-Aldrich, Merck) for 2–3 h and stored in PBS at 4 °C. For the Cryo-embedding procedure, samples were cryo-protected with passages in solutions with increasing concentration of sucrose (Sigma-Aldrich, Merck, 7.5% for 1 h, 15% for 1 h, 30% overnight) in 0.1 M PBS. Next, samples were maintained in a solution of 30% sucrose and optimal cutting temperature medium (OCT, Electron Microscopy Sciences, Hatfield, PA, USA) in a ratio 1:1, for 30 min and then embedded in 100% OCT; samples were stored at –80 °C. Nine micrometre-thick cross sections of the nerve were obtained starting from the middle of the autograft or the middle of the new tissue grown inside the chitosan conduit. For IHC, samples on slices were rinsed with PBS and then permeabilized and saturated in 0.01% Triton X-100, 10% normal donkey serum (NDS, Jackson ImmunoResearch, Philadelphia, PA, USA) in PBS for 1 h at room temperature in humid chamber. Samples were incubated with primary antibodies (Table S1, double staining was performed in single step, combined as follows: CD34 + S100β, CD34 + NRG1, CD34 + RECA1) at 4 °C overnight in PBS containing 1% NDS, in humid chamber. Then, samples were rinsed three times with PBS and incubated 1h at room temperature in

---

humid chamber with secondary antibodies (Table S1). After three washes in PBS, sections were covered with a mounting solution (Fluoromount, Sigma-Aldrich, Merck) and a glass coverslip was used to cover the section before observation. After drying for at least 3 days, samples were photographed using Leica (Wetzlar, Germany) TCS SP5 confocal microscope. For specificity assessment, all these antibodies were previously checked by Western blotting, which showed a single band of staining (data not shown). These antibodies have been used for similar purposes in the literature. Anti-S100 $\beta$  was used to label Schwann cells (Zhou et al.,2015), anti-CD34 was used to specifically label nerve fibroblasts (Richard et al.,2014). even if it is known to recognize also endothelial cells. As shown below in the immunohistochemistry panel 4C, no cells co-express S100 $\beta$  and CD34, (indicating that these antibodies do not cross react). To specifically identify fibroblasts, anti-CD34 was coupled with anti-RECA1, a cell surface antigen which is expressed by endothelial cells (Van Slooten et al.,2015; Duijvestijn et al.,2012). To assess the expression of NRG1 in fibroblasts, slices were stained with anti-CD34 and anti-NGR1, a polyclonal antibody that recognizes the C-terminal of many different NRG1 isoforms (all isoforms with “type a” C terminus, which is common to many soluble isoforms) (Mei & Xiond,2008), used by several laboratories and acknowledged by the scientific community as a suitable antibody to assess NRG1 expression (Stassart et al.,2013; Fledrich et al.,2019).

### ***Statistical Methods***

For in vivo experiments a priori power analysis performed with G\*Power (v. 3.1.9.4; Heinrich-Heine-Universität Düsseldorf, Germany) (Faul et al.,2007) showed that a sample size of 12 samples (n = 4 for each group) for each time point was determined respecting an effect size of  $d = 0.6$ , with a power of 0.95 and  $\alpha$  of 0.05 defining an actual power of 0.98 to limit the number of sacrificed animals. Statistical analyses were performed with IBM SPSS Statistics 25 (IBM, Armonk, NY, USA) software. Data were expressed as mean  $\pm$  standard error of the mean (SEM). All data were tested for normal distribution in order to select the appropriate statistical test (Levene and Mauchly tests). Analysis of variance (ANOVA) for repeated measures with Bonferroni’s correction was adopted to detect the effect of time, experimental groups, and their interaction and to highlight the overall significant differences among autograft group, chitosan group and uninjured control nerves and at each time point analysed. The two-tailed Student’s t-test for normally distributed data with comparable variances was used to highlight statistical differences between the two groups (Schwann cells and fibroblasts), while for data not showing

normal distribution the nonparametric Mann–Whitney U-test was used.

The effect size of each factor was computed as partial eta-squared ( $\eta^2$ ): a small effect was considered for a value of 0.010, a medium effect for value of 0.059 and a large effect for value of 0.138 (Richardson et al., 2011).

## **Results**

### ***Soluble NRG1 is strongly expressed in the conduit after nerve repair, while ErbB2 and ErbB3 are missing***

The expression of proteins belonging to the NRG/ErbB system, which is strongly involved in peripheral nerve regeneration, was investigated in the new tissue grown inside the chitosan conduit (“chitosan “group) and compared with the grafted autologous nerve (“autograft” group), representing the surgery “gold-standard”, or with healthy median nerve, used as control group, representing the starting point and the aimed final outcome (Figure 1).

Our data show that ErbB2 and ErbB3 receptors were strongly up-regulated in the autologous nerve graft at all the time points analysed (7, 14, and 28 days after the repair), while in the chitosan conduit ErbB2 and ErbB3 were not detectable 7 days after repair; they started to be detectable one week later, and were strongly expressed 28 days after the repair.

To detect soluble NRG1, an antibody which recognizes a 75 kDa band corresponding to the C terminal fragment of NRG1 was used (Ronchi et al.,2016; Stassart et al.,2013). NRG1 is strongly expressed 7 and 14 days after the repair in both groups, with a higher expression in the chitosan group 7 days after the repair. NRG1 expression strongly decreases 28 days after the repair in both experimental groups

### ***The PI3K/AKT and ERK/MAPK pathways are activated in the autograft, not in the conduit***

AKT, ERK and cJun are strongly phosphorylated 7 and 14 days after repair with the autograft technique, while after 28 days their phosphorylation strongly decreases (AKT, ERK) or it is completely switched off (cJun). Inside the conduit, AKT phosphorylation is barely detectable 14 days after the repair, while ERK1/2 and cJun phosphorylation are not detectable; moreover, in the chitosan samples the total amount of ERK is lower than in the autograft. Myelin basic protein (MBP) is strongly expressed in the uninjured median nerve; in the autograft group it is still present 7 days after injury (during Wallerian degeneration), disappears 14 days after repair (during axon regrowth) and it is present again 28 days after the repair (during axon



remyelination). Within the chitosan conduit, where Wallerian degeneration does not occur, MBP starts to be present 28 days after the repair, during axon remyelination

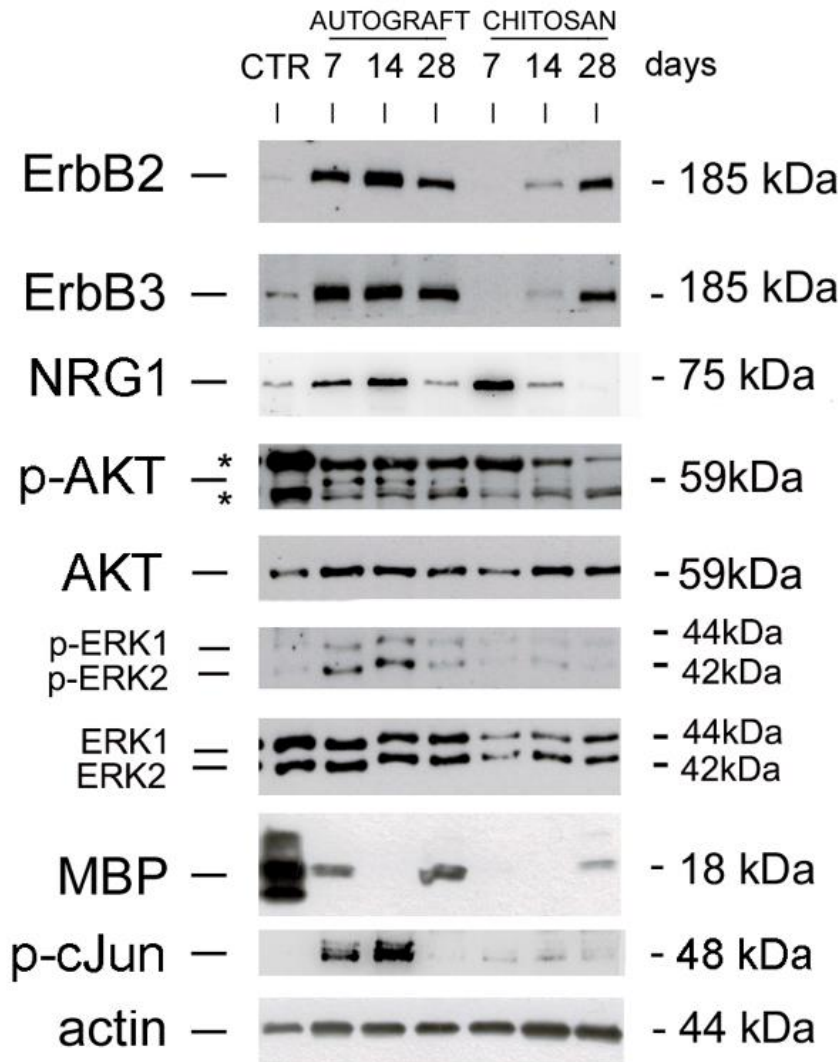


**Figure 1.** NRG1 and ErbB expression in autograft and chitosan groups. Western blot analysis of proteins extracted from healthy control nerves (CTR) and regenerating nerves belonging to autograft or chitosan groups withdrawn 7, 14, and 28 days after the repair and probed with antibodies for ErbB2, ErbB3, phospho-AKT, total-AKT, phospho-ERK, total-ERK, MBP, phospho-cJun; actin was used as a loading control. For NRG1, an antibody recognizing the C terminus fragment was used. Unspecific bands were identified with asterisks (\*). Molecular weight (kDa) are shown on the right.

#### ***Fibroblast Markers Are Highly Expressed in the Chitosan Conduit***

Western blot data analysis showed that in the chitosan conduit soluble NRG1 (usually highly expressed by Schwann cells after injury) was strongly expressed 7 days after nerve repair, while

the NRG1 co-receptors ErbB2-ErbB3 were not. To identify the cells responsible for NRG1 release, we analysed the expression of two Schwann cell (S100 $\beta$ , p75) and one fibroblast (Thy1) markers within the chitosan conduit (Figure 2 and Table 1 for statistical analysis). S100 $\beta$ , a Schwann cell marker highly expressed by differentiated Schwann cells, is significantly downregulated after injury in all samples. Our data show that at all the time points analysed S100 $\beta$  is significantly less expressed in conduit samples than in the nerve repaired through autologous graft. The effect size between all groups is significantly large for all time points analysed (see Table 1). Multiple comparison analysis for S100 $\beta$  revealed significant differences between autograft and chitosan groups ( $p = 0.0056$ , mean difference = 0.16, CI 95% = 0.06–0.26). The within subject test showed no significant effect for time ( $p = 0.065$ ) and time x group factors ( $p = 0.29$ ). p75 is a Schwann cell marker highly expressed by dedifferentiated Schwann cells, known to be strongly up-regulated after nerve injury; accordingly, when compared with uninjured nerves, p75 expression is significantly higher in all autograft samples, while in the chitosan group it is significantly more highly expressed only 28 days after the repair (see Table 1). Data show that at all the time points analysed p75 is significantly less expressed in the conduit group than in the nerve repaired through autologous graft. The effect size between experimental groups is large for all time points analysed (see Table 1). Multiple comparison analysis for p75 revealed significant differences between the autograft and the chitosan groups ( $p = 0.000016$ , mean difference = 47.15, CI 95% = 36.93–57.37) and between the autograft and the control groups ( $p = 0.000007$ , mean difference = 54.43, CI 95% = 44.21–64.65). The within subject test revealed a significant effect for time ( $p = 0.002$ ) and time x group ( $p = 0.0004$ ) factors. The nerve fibroblast marker Thy1 is significantly more highly expressed in the chitosan group, 14 and 28 days after the repair with a large effect size (see Table 1), in comparison with the autograft group and with uninjured nerves. Multiple comparison analysis for Thy1 revealed significant differences between the autograft and the chitosan groups ( $p = 0.004$ , mean difference = -6.5, CI 95% = (-10.36)–(-2.62)), between the autograft and the control groups ( $p = 0.012$ , mean difference = 5.3, CI 95% = 1.49–9.23) and between the chitosan and the control groups ( $p = 0.00017$ , mean difference = 11.86, CI 95% = 7.98–15.72). The within subject test revealed a significant effect for time x group factors ( $p = 0.01$ ), not for time alone ( $p = 0.15$ ). Soluble NRG1 is significantly higher in the chitosan group compared with the autograft group and with uninjured nerves 14 and 28 days after repair with large effect size (see Table 1). Multiple comparison analysis for soluble NRG1 revealed significant differences between chitosan and uninjured nerve groups

---

( $p = 0.0002$ , mean difference = 1.88, CI 95% = 1.18–2.58) and between chitosan and autograft groups ( $p = 0.0002$ , mean difference = 1.96, CI 95% = 1.21–2.70). The within subject test revealed a significant effect for time ( $p = 0.006$ ) and time x group ( $p = 0.000$ ) factors.

Soluble NRG1 isoforms (which are the most represented isoforms, at the mRNA level, in the peripheral nerve) include both  $\alpha$  and  $\beta$  isoforms, whose regulation and activity can be different; therefore, we analysed, separately, the expression of both isoforms. NRG1 $\alpha$  is more highly expressed in the chitosan group, in comparison with the autograft group and with uninjured nerves, 14 and 28 days after the repair with large effect size (see Table 1). Multiple comparison analysis for soluble NRG1 $\alpha$  revealed significant differences between the chitosan and the uninjured nerve groups ( $p = 0.002$ , mean difference = 20.75, CI 95% = 10.29–31.19) and between the chitosan and the autograft groups ( $p = 0.016$ , mean difference = 13.48, CI 95% = 3.03–23.93). The within subject test revealed a significant effect for time x group factors ( $p = 0.02$ ) not for time alone ( $p = 0.16$ ).

NRG1 $\beta$  is more highly expressed in the chitosan group compared with the autograft group 14 days after the repair with large effect size. NRG1 $\beta$  expression in the chitosan group is significantly lower than in uninjured nerves at 7 and 28 days, with large effect size, while for the autograft group it is significantly lower at all the time points analysed with large effect size (see Table 1). Multiple comparison analysis for soluble NRG1 $\beta$  revealed significant differences between chitosan and uninjured nerve groups ( $p = 0.034$ , mean difference =  $-0.38$ , CI 95% =  $(-0.73)$ – $(-0.03)$ ) and between autograft and uninjured nerve groups ( $p = 0.0018$ , mean difference =  $-0.70$ , CI 95% =  $(-1.04)$ – $(-0.35)$ ). The within subject test revealed a significant effect for time x group factors ( $p = 0.035$ ) not for time alone ( $p = 0.44$ ).

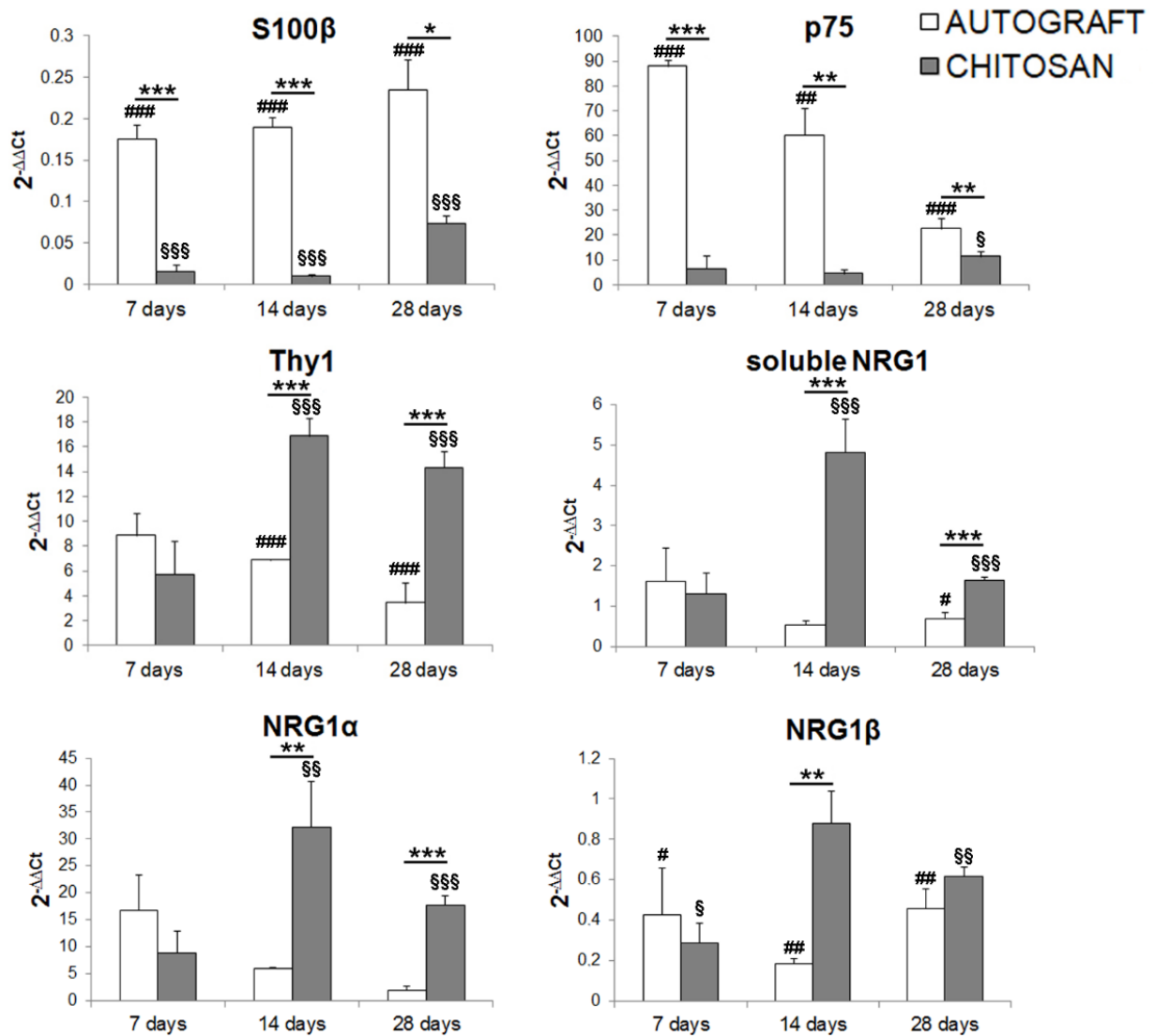


**Figure 2.** Quantitative expression analysis of Schwann cell and nerve fibroblast markers. Relative quantification ( $2^{-\Delta\Delta C_t}$ ) of S100 $\beta$  and p75 (Schwann cell markers), Thy1 (fibroblast marker), soluble NRG1, NRG1 $\alpha$ , and NRG1 $\beta$  was evaluated by qRT-PCR. The geometric average of the housekeeping genes ANKRD27 and RICTOR was used to normalize data. Values in the graphics are expressed as mean + SEM ( $n = 3-4$  for each group). ANOVA for repeated measures with Bonferroni's correction was adopted for statistical analysis; \* denotes the significant differences between autograft and chitosan groups at each time point analyzed ( $*p \leq 0.05$ ,  $**p \leq 0.01$ , and  $***p \leq 0.001$ ); # denotes the significant differences between autograft group and uninjured control nerves at each time point analyzed ( $#p \leq 0.05$ ,  $##p \leq 0.01$ , and  $###p \leq 0.001$ ); § denotes the significant differences between chitosan group and uninjured control nerves at each time point analyzed ( $\$p \leq 0.05$ ,  $$$p \leq 0.01$ , and  $$$$p \leq 0.001$ ). All data are calibrated to uninjured nerves (whose expression, not shown, is = 1).

**Table 1.** ANOVA for repeated measures with Bonferroni's correction.

	Autograft vs. Chitosan								
	7 Days			14 Days			28 Days		
	$\eta_p^2$	<i>p</i>	CI 95%	$\eta_p^2$	<i>p</i>	CI 95%	$\eta_p^2$	<i>p</i>	CI 95%
S100 $\beta$	0.85	0.001	0.1–0.24	0.87	0.001	0.11–0.25	0.63	0.02	0.35–0.26
p75	0.97	0.000	64.99–93.51	0.81	0.002	24.70–71.92	0.67	0.01	4.21–23.61
Thy1	0.05	0.59	(–5.67)–9.11	0.87	0.001	(–14.38)–(–6.27)	0.87	0.001	(–15.04)–(–6.70)
sNRG1	0.00	0.907	(–1.82)–2.02	0.93	0.000	(–6.16)–(–3.71)	0.85	0.000	(–1.43)–(–0.65)
NRG1 $\alpha$	0.11	0.42	(–10.58)–22.33	0.69	0.01	(–51.10)–(–10.24)	0.94	0.000	(–19.71)–(–11.59)
NRG1 $\beta$	0.20	0.738	(–0.46)–0.61	0.78	0.004	(–1.20)–(–0.37)	0.47	0.06	(–0.51)–0.47
	Control vs. Autograft								
	7 Days			14 Days			28 Days		
	$\eta_p^2$	<i>p</i>	CI 95%	$\eta_p^2$	<i>p</i>	CI 95%	$\eta_p^2$	<i>p</i>	CI 95%
S100 $\beta$	0.99	0.000	0.92–1.11	0.99	0.000	0.92–1.06	0.99	0.000	0.82–1.04
p75	0.97	0.000	72.65–101.16	0.83	0.002	28.37–75.59	0.87	0.001	14.70–34.11
Thy1	0.4	0.09	(–13.5)–1.28	0.94	0.000	(–20.22)–(–12.12)	0.91	0.000	(–17.46)–(–9.12)
sNRG1	0.08	0.45	(–1.18)–2.41	0.10	0.4	(–1.59)–(–0.72)	0.50	0.033	(–0.77)–(–0.05)
NRG1 $\alpha$	0.48	0.06	(–0.71)–32.21	0.06	0.57	(–15.39)–25.47	0.06	0.57	(–3.07)–5.05
NRG1 $\beta$	0.55	0.03	(–1.14)–(–0.06)	0.80	0.003	(–1.26)–(–0.42)	0.87	0.01	(–0.90)–(–0.41)
	Control vs. Chitosan								
	7 Days			14 Days			28 Days		
	$\eta_p^2$	<i>p</i>	CI 95%	$\eta_p^2$	<i>p</i>	CI 95%	$\eta_p^2$	<i>p</i>	CI 95%
S100 $\beta$	0.99	0.000	(–1.05)–(–0.91)	0.99	0.000	(–1.06)–(–0.92)	0.99	0.000	(–1.04)–(–0.82)
p75	0.22	0.237	(–21.91)–6.6	0.024	0.717	(–27.28)–19.94	0.54	0.04	(–20.21)–(–0.79)
Thy1	0.4	0.09	(–1.28)–13.5	0.94	0.000	12.12–20.22	0.91	0.000	17.46–0.91
sNRG1	0.06	0.52	(–2.31)–1.28	0.92	0.000	(–5.64)–(–3.34)	0.97	0.000	(–0.95)–(–0.27)
NRG1 $\alpha$	0.26	0.19	(–26.34)–6.57	0.75	0.005	(–56.14)–(–15.28)	0.94	0.000	(–20.71)–(–12.57)
NRG1 $\beta$	0.61	0.022	0.14–1.22	0.02	0.75	0.36–0.48	0.73	0.007	0.16–0.66

Effect of time, experimental groups, and their interaction are reported at each time point analyzed. In this table the effect size (partial eta-squared,  $\eta_p^2$ ), the significance (*p*) and the 95% confidence interval (CI) are shown. The effect of the experimental groups on the regulation of gene expression is significant and with an effect size higher than expected in most conditions.

### ***Primary Cultures of Nerve Fibroblasts Express High Levels of NRG1 Isoforms, While NRG1 Receptors Are Not Expressed***

As the expression of Schwann cell markers was very low in the chitosan conduit, while the fibroblast marker Thy1 and NRG1 were strongly expressed, we hypothesized that fibroblasts could be involved in NRG1 expression. To test this hypothesis, confluent primary cultures of fibroblasts and Schwann cells were obtained from adult rat sciatic nerves and were analysed at

both mRNA and protein level to investigate fibroblast involvement in NRG1 expression (Figure 3A, B)

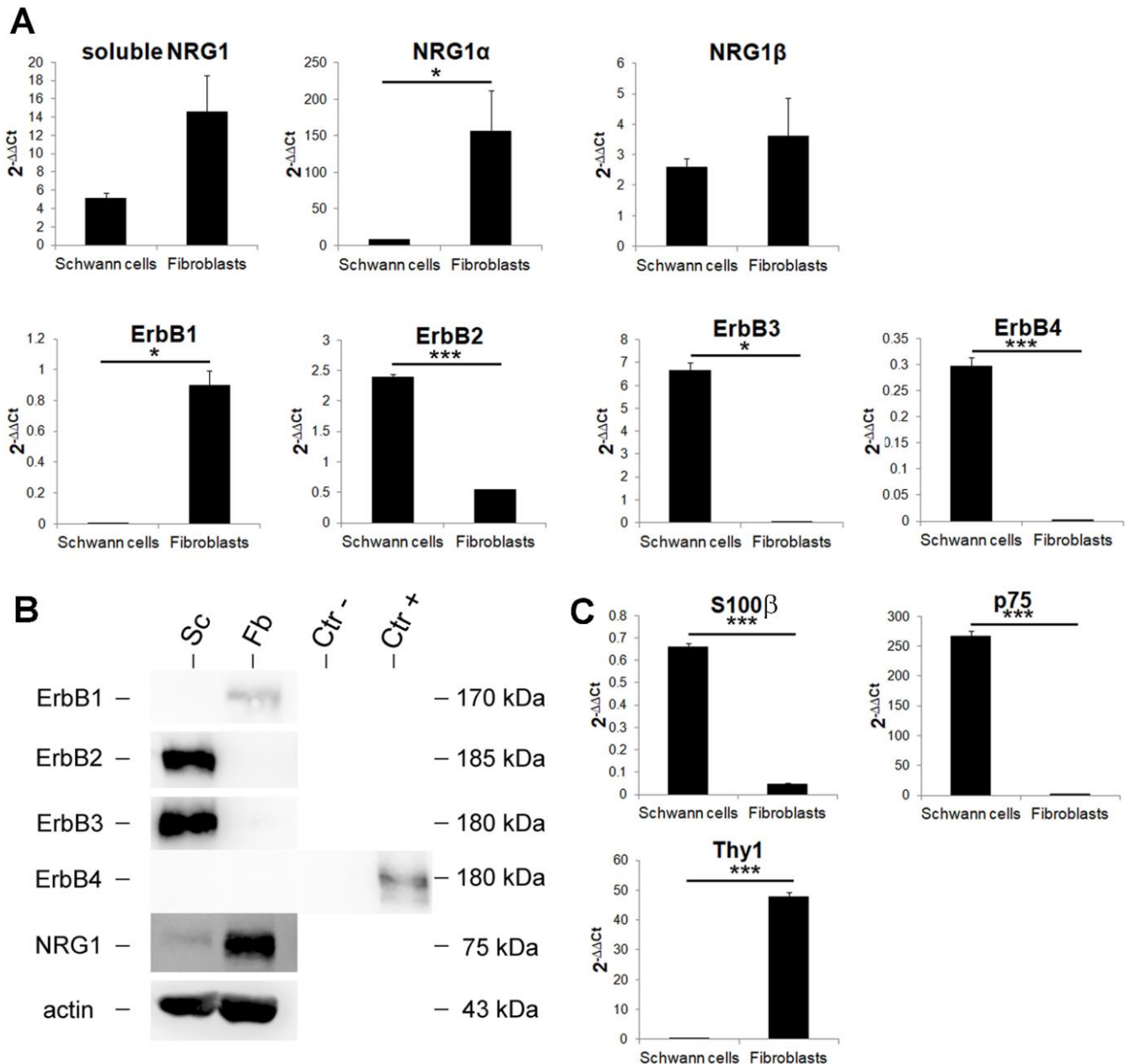


**Figure 3.** Nerve fibroblasts express high levels of soluble NRG1. **(A)** Quantitative analysis of the NRG1/ErbB system expression in primary cultures of Schwann cells and nerve fibroblasts. Relative quantification ( $2^{-\Delta\Delta C_t}$ ) of different NRG1 isoforms (soluble,  $\alpha$ ,  $\beta$ ), ErbB1, ErbB2, ErbB3, and ErbB4 was evaluated by qRT-PCR. **(B)** Western blot analysis of the NRG1/ErbB system. Proteins were extracted from primary cultures of Schwann cells (Sc) and nerve fibroblasts (Fb), separated on 8% acrylamide-bis-acrylamide gels and probed with

antibodies for ErbB1, ErbB2, ErbB3, and ErbB4; for NRG1, an antibody recognizing the C terminus fragment was used. Actin was used as a loading control. Size markers are indicated on the right. Neural progenitor cells stably expressing ErbB4 or mock cells were used respectively as positive (Ctr+) and negative (Ctr-) controls for ErbB4. (C) Quantitative expression analysis of Schwann cell and nerve fibroblast markers. Relative quantification ( $2^{-\Delta\Delta Ct}$ ) of S100 $\beta$  and p75 (Schwann cell markers) and Thy1 (fibroblast marker) was evaluated by qRT-PCR to ensure the purity of the primary cultures. For panel A and C, the geometric average of housekeeping genes ANKRD27 and RICTOR was used to normalize data. All data were calibrated to healthy median nerves, whose expression, not shown, is = 1. Values in the graphics are expressed as mean + SEM ( $n = 3$  for each group). For normally distributed data with comparable variances two-tailed Student's t-test was carried out, while for nonparametric data Mann–Whitney U-test was used; \*  $p \leq 0.05$ , \*\*\*  $p \leq 0.001$ .

The identity of both cell types was confirmed by qRT-PCR using specific biomarkers: S100 $\beta$  and p75 for Schwann cells and Thy1 for fibroblasts (Figure 3C).

At mRNA level we observed that NRG1 $\alpha$  is more highly expressed by nerve fibroblasts in comparison with Schwann cells, while soluble and  $\beta$  NRG1 isoforms are highly expressed in both cell types without significant differences (Figure 3A). At the protein level, NRG1 is more highly expressed in nerve fibroblasts than in Schwann cells (Figure 3B); NRG1 was detected with an antibody which recognizes the 75-kDa band corresponding to the C terminal fragment of NRG1 (Ronchi et al.,2016; Stassart et al.,2013). Concerning ErbB receptor mRNA expression, ErbB1 is expressed by fibroblasts only, ErbB2 is more highly expressed by Schwann cells, ErbB3 and ErbB4 (NRG1 receptors) are only expressed by Schwann cells, at high and very low level respectively. At protein level, fibroblasts express only ErbB1, Schwann cells express only ErbB2-ErbB3, ErbB4 is not detectable in both cell types; as a positive and negative controls for ErbB4 Western blot, neural progenitor cells stably expressing ErbB4 or mock cells were used (Fornasari et al.,2016).

### ***Immunohistochemistry Analysis Shows that Nerve Fibroblasts Express NRG1***

To assess in vivo the expression of NRG1 by nerve fibroblasts, immunohistochemistry analysis was carried out 7 days after nerve injury and repair, when at the protein level NRG1 is strongly expressed, while ErbB2 and ErbB3 are not detectable. The analysis was carried out in the middle of the new tissue grown inside the conduit (the chitosan conduit was removed before fixation) and in the middle of the grafted autologous nerve. In the autograft we found several cells positive for the Schwann cell marker S100 $\beta$  (Figure 4A), while the signal of the fibroblast

marker CD34 was very low; on the contrary, inside the conduit (Figure 4B), the signal of the Schwann cell marker was very low, while the signal of the fibroblast marker was highly detected. CD34 antibody was suitable for this analysis because it stains nerve fibroblasts (Richard et al.,2014), but not Schwann cells (as demonstrated in Figure 4, panels C-C'-C''). Consistent with mRNA and protein analysis, several cells were stained with NRG1 antibody in the chitosan group (Figure 4, panels E-E'), while NRG1 staining in the autograft was very low (Figure 4, panels D-D'). At higher magnification, some cells were positive for both CD34 and NRG1 (Figure 4, panels F-F'-F''-G-G'-G''). CD34 does not only recognize nerve fibroblast, but also endothelial cells (Richard et al.,2014); usually, this does not represent a problem, because vessels are not very abundant in the nerve and blood vessel cross sections can be easily recognized for their rounded shape; nevertheless, because vessels in the chitosan were found to be very abundant, to unequivocally discriminate nerve fibroblasts from endothelial cells, we analysed autograft and chitosan samples also with CD34 and RECA1 antibodies, as RECA1 antibody specifically stains endothelial cells. Data show that in the chitosan group (Figure 4, panels I-I'), unlike in the autograft (Figure 4, panels H-H'), there are several fibroblasts and several endothelial cells. At higher magnification (Figure 4, panels J-J'-K-K') it is possible to identify both cell types: endothelial cells that are positive for both CD34 and RECA1 staining (yellow signal) and nerve fibroblasts solely positive for CD34 staining (green signal).

### ***Discussion***

For short nerve gap repair in human, up to 3 cm (Kornfeld et al.,2018; Moore et al.,2009), tubulization is successfully used as a good alternative to autograft, especially in small diameter, noncritical sensory nerves (Meek et al.,2008), while short nerve gaps are successfully repaired in rat up to 1 cm (Haastert-Talini et al.,2013; Shapira et al.,2016; Stenberg et al.,2016). Because several research groups (Carvalho et al.,2019), including ours (Ronchi et al.,2018), are making efforts to functionalize and enrich tubular conduits to further promote nerve regeneration in more complex situations, such as longer nerve gap or delayed repair, we focused our attention on investigating what occurs inside a hollow conduit after nerve gap repair. Soluble NRG1 is one of the factors known to play an important role during nerve regeneration (Fricker et al.,2011); we and others previously showed (Ronchi et al.,2016; Stassart et al.,2013; Carroll et al.,1997) that soluble NRG1 transcript is strongly and transiently up-regulated in the distal



portion of the nerve 1 day after injury and that the NRG1 receptor ErbB3 is strongly down-regulated 3 days after injury and up-regulated 7, 14, and 28 days after repair, while the expression of the co-receptor ErbB2, barely detectable in the healthy nerve, is up-regulated 7, 14, and 28 days after injury (Ronchi et al.,2016).

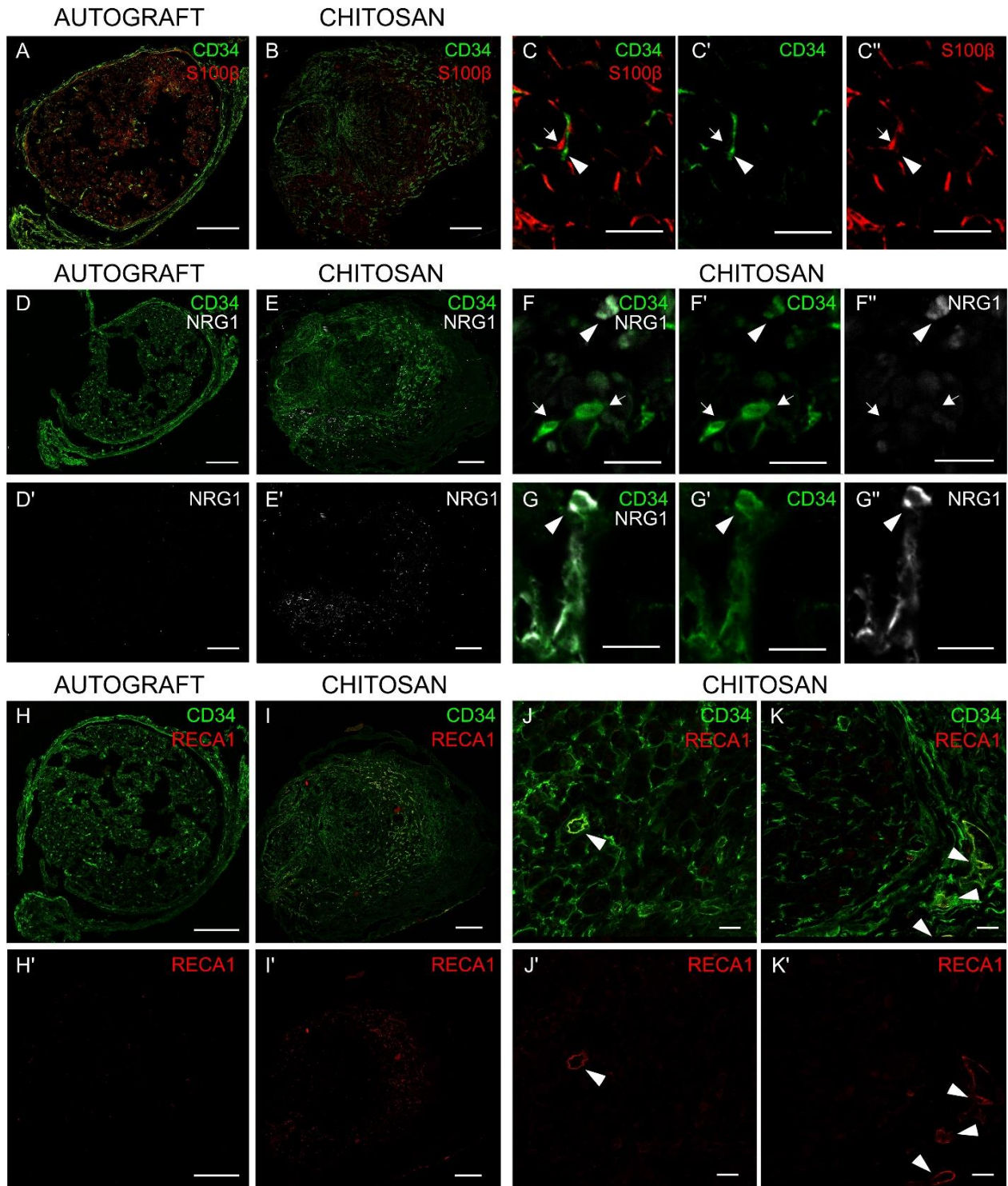


**Figure 4.** Nerve fibroblasts express NRG1 in vivo. Cross section of median nerves analyzed 7 days after repair with an autograft (A, D, D', H, H') or with a chitosan conduit (B, E, E', I, I'): (A,B) double-stained with S100 $\beta$  (Schwann cell marker, red) and CD34 (fibroblast marker, green). (C, C', C'') Images at higher magnification show the absence of colocalization between S100 $\beta$  and CD34; fibroblasts are pointed out by arrow heads, Schwann cells by arrows. (D,E) double-stained with CD34 (green) and NRG1 (white) or (D',E') single-stained with NRG1; (D') and (E') highlight different levels of NRG1 expression in the two different experimental models (higher in the chitosan group). (F, F', F'' and G, G', G'') Images at higher magnification show some CD34+ cells positive only to CD34 (arrow) and some CD34+ cells also positive to NRG1 (arrowhead). (H,I) double-stained with CD34 (fibroblast and endothelial cell marker, green) and RECA1 (endothelial cell marker, red) or (H',I') single-stained with RECA1; (H') and (I') highlight different levels of RECA1 expression in the two different experimental models (higher in the chitosan group). (J, J' and K, K') Images at higher magnification show some CD34+ cells also positive for RECA1, corresponding to endothelial cells (arrow heads), and several CD34+ cells positive only to CD34, corresponding to fibroblast cells. Scale bars: 200  $\mu$ m (A, B, D, D', E, E', H, H', I, I'); 20  $\mu$ m (J, J', K, K'); 10  $\mu$ m (C,C',C'', F, F', F'', G, G', G'')

Here, we analysed the expression of the NRG1/ErbB system inside a chitosan conduit 7, 14, and 28 days after injury and repair and we compared it with the autograft. Our data show that, while the expression of ErbB2 and ErbB3 is up-regulated in the autograft 7, 14, 28 days after injury, as occurs in the distal portion of the nerve after a crush injury or after an end-to-end repair (Ronchi et al.,2016), in the chitosan conduit ErbB2 and ErbB3 expression starts to be detectable 14 days after nerve repair and becomes high only 2 weeks later. The absence of ErbB expression one week after injury is consistent with the fact that the conduit needs time to be colonized by repair Schwann cells (Williams et al.,1983), which in the autograft play a key role either in the Wallerian degeneration, either in nerve regeneration, while in the conduit are mainly involved in nerve regeneration. Conversely, NRG1 expression is strongly detectable in both autograft and chitosan 7 days after nerve injury and repair. Moreover, it has been shown in vitro that NRG1 stimulation of Schwann cells activates ERK, AKT, and cJun phosphorylation (Monje et al.,2006; Parkinson et al.,2004; Syed et al.,2010); the lack of ERK, AKT, and cJun phosphorylation in the chitosan samples, despite the presence of high levels of NRG1, might be due to the absence (or low presence) of Schwann cells. We further confirmed this by analysis, at mRNA level, the expression of Schwann cell markers, together with a marker of nerve fibroblasts, which are supposed to colonize tubular nerve conduits earlier, as in the first stages conduits are filled with extracellular matrix and fibrin cables (Williams et al.,1983). The high expression of NRG1 and of a fibroblast marker together with the low expression of Schwann cell markers led us to speculate that nerve fibroblasts might be the main

source of soluble NRG1 detected within the conduit. As different soluble NRG1 isoforms are known to be expressed following a nerve injury (Ronchi et al.,2016), we analysed at mRNA level the relative expression of soluble NRG1 and of NRG1 $\alpha$  and NRG1 $\beta$ , two soluble NRG1 isoforms characterized by different expression pattern and activity (Fornasari et al.,2016). Intriguingly, we found that the expression pattern of all soluble NRG1 isoforms has a trend similar to the expression of the fibroblast marker Thy1, especially NRG1 $\alpha$ , whose expression is strongly upregulated in the chitosan group 14 and 28 days after repair, like the fibroblast marker Thy1. The trend is similar also for NRG1 $\beta$ , but its expression is lower. These data are highly reminiscent of our previous observation (carried out on the distal portion of different experimental rat models: Crush injury and cut followed by end-to-end repair) where we found that NRG1 $\alpha$  isoforms are more highly upregulated than NRG1 $\beta$  isoforms (Ronchi et al.,2016), thus reinforcing the idea that  $\alpha$  isoforms also might play a role in nerve regeneration (De Souza et al.,2010). Protein and mRNA data do not correspond exactly: At the protein level a stronger expression of NRG1 in the chitosan samples is observed 7 days after repair, while at the mRNA level the expression is higher 14 days after repair. This discrepancy might be explained in two ways: By the fact that mRNA and protein expression could be different because of post-transcriptional and post-translational regulation or by the fact that at the mRNA level the expression of specific isoforms (soluble,  $\alpha$ ,  $\beta$ ) is quantifiable, while no effective antibodies specific for the soluble fragment of NRG1 or for  $\alpha$  or  $\beta$  isoforms are commercially available. The antibody used for Western blot analysis, acknowledged by the scientific community as a very good antibody to detect the C terminus of the transmembrane precursor of soluble NRG1 isoforms (Stassart et al.,2013; Fledrich et al.,2019), recognizes only a subcategory of soluble NRG1 isoforms, but there are also isoforms expressed as soluble proteins without a transmembrane precursor or with a precursor with a different C terminus. To identify the different NRG1 isoforms and NRG1 receptors and co-receptors expressed by nerve fibroblasts, an accurate mRNA and protein analysis was carried out on primary cultures of nerve fibroblasts and compared with primary cultures of Schwann cells and with healthy median nerves (used as calibrator). Our results show that nerve fibroblasts express high levels of different NRG1 isoforms: Soluble, type  $\alpha$  and type  $\beta$ . Intriguingly, NRG1 $\alpha$  isoforms are significantly more highly expressed in fibroblasts than in Schwann cells and healthy nerve, while NRG1 $\beta$  expression is more similar in the two primary cultures and in the healthy nerve, thus reinforcing the idea that the soluble NRG1 we observe upregulated in the chitosan might be mainly the NRG1 $\alpha$  expressed by fibroblasts. Fibroblasts express ErbB1, while they do not express the

NRG1 receptors ErbB3 and ErbB4 and the co-receptor ErbB2, thus suggesting that nerve fibroblasts are not able to activate a signal transduction pathway after NRG1 stimulation, which is in agreement with the lack of ERK, AKT and cJun phosphorylation. Schwann cells express only ErbB2-ErbB3 co-receptors; at mRNA level, a signal for ErbB4 is detectable, but at the protein level it is not expressed, as previously shown (Pascal et al.,2014). These results are consistent with literature data obtained from in vitro study showing that primary cultures of nerve fibroblasts can release soluble Schwann cell pro-migratory factors, including NRG1 (Dreesmann et al.,2009; Van Neerven et al.,2013). However, our in vitro study demonstrated also that fibroblasts express both NRG1 $\alpha$  and NRG1 $\beta$ , while Schwann cells express mainly NRG1 $\beta$ . Our in vivo analysis, showing high levels of the fibroblast marker Thy1 and high levels of NRG1 $\alpha$ , suggests that nerve fibroblasts might be the main source of soluble NRG1 inside the conduit during nerve regeneration. To further investigate NRG1 expression in vivo, immunohistochemistry analyses were carried out 7 days after injury and repair and it was observed a high NRG1 expression in the chitosan conduit samples, while in the autograft the NRG1 signal was lower, consistently with Western blot analysis. Moreover, in the autograft samples, Schwann cells were more abundant than fibroblasts, unlike in the chitosan samples, where fibroblasts were more abundant than Schwann cells. To verify that the high amount of NRG1 observed in the conduit might be attributed to the high presence of fibroblasts, double labelling of a fibroblast marker and NRG1 was performed. Our data show that some fibroblasts were also positive for NRG1. Thy1 is a good marker for mRNA analysis, but it is not suitable for IHC or Western blot analysis because it is also expressed by neurons (Caroni et al.,1997): When we analyse RNA in the distal portion of peripheral nerves (which does not include neuron cell bodies), we are analysing RNA belonging to resident cells only (e.g., Schwann cells, fibroblasts, endothelial cells, and macrophages), while when we analyse proteins we detect proteins belonging to either the neurons, either resident cells, because neuron proteins are expressed also along the axons. According to Richard and colleagues (Richard et al.,2012), the sialylated transmembrane glycoprotein CD34 is a good marker of nerve fibroblasts for IHC analysis, since it is not expressed by Schwann cells, macrophages, and perineurial cells. Nevertheless, CD34 is expressed not only by fibroblasts, but also by endothelial cells, which usually are not very abundant in the nerves and can be easily recognized for the rounded shape of blood vessels and capillary. To unequivocally discriminate between fibroblasts and endothelial cells, a double staining was carried out for CD34 and RECA1, which specifically detects endothelial cells, showing that inside the conduit there are several fibroblasts, but also

several endothelial cells forming blood vessels. The presence of a high number of fibroblasts and blood vessels inside the chitosan conduit is consistent with the observation that fibroblasts might promote angiogenesis by secreting cytokines (Sorrell et al.,2009). Our data show that in the chitosan conduits blood vessels are highly abundant 7 days after injury and repair, while their presence is very low in the autograft samples. It has been shown by others (Cattin et al.,2016) that in the bridge formed between proximal and distal stumps, when the gap is small, blood vessels provide a track for Schwann cell migration. The high presence of blood vessels in the conduit suggests that they could play here the same role. Moreover, as vascularization is also important to supply oxygen and nutrients for nerve tissue survival, different research groups are developing new strategies to further promote vessel formation inside conduits (Muangsanit et al.,2018). Although it has been previously demonstrated that fibroblasts accumulated at the injury site secrete extracellular matrix and form scar tissue, which might impair nerve regeneration (Atkins et al.,2006), other authors demonstrated that grafted nerve fibroblasts can positively influence Schwann cell behavior during nerve repair (Wang et al.,2017). Moreover, it has been shown that in the “nerve bridge”, formed between proximal and distal stumps after nerve injury, the interaction between nerve fibroblasts and Schwann cells—mediated by ephrinB2-EphB2—plays a key role for cell sorting and for Schwann cell cord formation (Parrinello et al.,2010). Although hollow conduits are suitable for short gap repair, for long gaps they are unable to provide an adequate microenvironment for regeneration (Pabari et al.,2011); one possible reason might be that fibroblasts are not numerous enough to produce sufficient fibrin matrix, NRG1 and other factors. Indeed, it has been shown that matrix diameter is inversely proportional to the conduit length, deeply affecting the regenerative outcome after nerve transection (Zhao et al.,1993) and that soluble NRG1 plays an important role in Schwann cell dedifferentiation, proliferation, and migration ( Fricker et al.,2011; Stassart et al.,2013; El Soury et al.,2018). This study allows us to make two further methodological considerations: 1-The presence of Thy1 and NRG1 $\alpha$  also in the autograft samples, and the high levels of NRG1 $\alpha$  (together with NRG1 $\beta$ ) previously detected after crush injury or end-to-end repair (Ronchi et al.,2016) suggest that nerve fibroblasts might participate, together with Schwann cells, to NRG1 expression after nerve injury. The fact that soluble NRG1 might be produced not only by Schwann cells but also by fibroblasts, suggests that when CRE-lox technology is used to switch off NRG1 expression specifically in Schwann cells (using Schwann cell specific promoters for CRE expression), soluble NRG1 released by fibroblasts might be present in the environment and partially compensate for the absence of

Schwann cell NRG1. To completely inactivate NRG1 expression (in, e.g., Schwann cells, neurons, and fibroblasts) we suggest to use inducible knockout animals, like those developed by Fricker and colleagues, ubiquitously expressing a tamoxifen inducible CRE protein which removes floxed NRG1 in all cells after tamoxifen treatment (Fricker et al.,2013). 2-To obtain neuron specific gene expression or neuron specific CRE mediated gene inactivation, the neuron specific promoter Thy1 is often used, being expressed in motoneurons and DRG neurons (Moore et al.,2012). Nevertheless, because Thy1 is expressed also by nerve fibroblasts, the use of this promoter could give rise to unspecific effects that need to be regarded, considering that fibroblasts might be involved in the regeneration process.

### ***Conclusions***

To conclude, our results suggest that nerve fibroblasts might contribute to the high level of soluble NRG1 observed after nerve injury and repair thus promoting Schwann cell dedifferentiation. Yet, it is possible to hypothesize that nerve fibroblast grafting within conduits might be a good strategy to further promote nerve regeneration after long gap and/or delayed nerve repair.

***Author Contributions:*** Conceptualization, B.E.F. and G.G.; Methodology, G.R., A.C., and S.R.; Validation, B.E.F.; Formal Analysis, B.E.F. and G.C.; Investigation, B.E.F., M.E.S., G.N., A.C., G.R., A.C., S.R., and G.G.; Data Curation, B.E.F. and G.G.; Writing—Original Draft Preparation, B.E.F., M.E.S., and G.G.; Writing—Review and Editing, G.R., I.P., S.G., S.R., and G.G.; Validation, B.E.F., and G.G.; Visualization, B.E.F., G.G., G.N., A.F., and G.C.; Supervision, G.G.; Project Administration, B.E.F., and G.G.; Funding Acquisition, G.R., I.P., S.G., S.R., and G.G. All authors have read and agreed to the published version of the manuscript.

***Funding:*** This study was supported by Compagnia di San Paolo, No. D86D15000100005 InTheCure project to S.R. and by grants from the University of Torino to I.P., S.G., S.R., and G.G.

***Acknowledgments:*** Reaxon® Nerve Guides were supplied by Medovent GmbH (Mainz, Germany). **Conflicts of Interest:** The authors declare no conflict of interest.

### Supplementary Information

#### **Fibroblasts colonizing nerve conduits express high levels of soluble Neuregulin1, a factor promoting Schwann cell dedifferentiation**

Benedetta Elena Fornasari<sup>1,2</sup>, Marwa El Soury<sup>1,2</sup>, Giulia Nato<sup>2,3</sup>, Alessia Fucini<sup>1</sup>, Giacomo Carta<sup>1,2</sup>, Giulia Ronchi<sup>1,2</sup>, Alessandro Crosio<sup>1,2,4</sup>, Isabelle Perroteau<sup>1</sup>, Stefano Geuna<sup>1,2</sup>, Stefania Raimondo<sup>1,2</sup>, Giovanna Gambarotta<sup>1,2\*</sup>

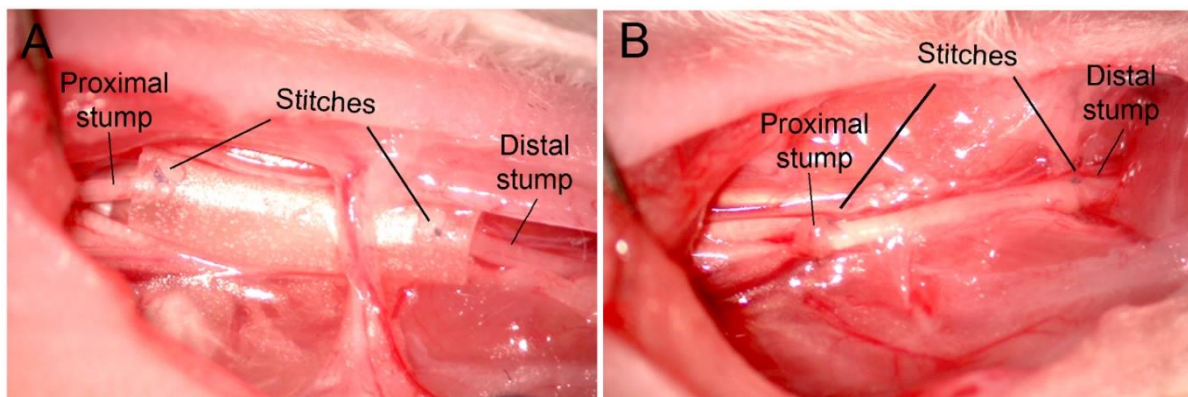


**Figure S1**

Macroscopic view of implantation sites. Rat median nerve 8 mm defect was repaired with a 10 mm long chitosan conduit (A) or with autograft technique (B).

<i>Antibodies for Western blot analysis</i>				
<i>Primary antibodies</i>				
	<b>Code</b>	<b>Dilution</b>	<b>Host</b>	<b>Source</b>
<b>AKT</b>	9272	1:1000	Rabbit	Cell Signaling Technology <sup>1</sup>
<b>phospho-AKT (Ser473)</b>	4051	1:1000	Mouse	Cell Signaling Technology <sup>1</sup>
<b>phospho-cJun (Ser63)</b>	2361	1:1000	Rabbit	Cell Signaling Technology <sup>1</sup>
<b>HER1/ErbB1</b>	sc-03	1:1000	Rabbit	Santa Cruz Biotechnology <sup>2</sup>
<b>HER2/ErbB2</b>	sc-284	1:1000	Rabbit	Santa Cruz Biotechnology <sup>2</sup>
<b>HER3/ErbB3</b>	sc-285	1:1000	Rabbit	Santa Cruz Biotechnology <sup>2</sup>
<b>HER4/ErbB4</b>	sc-283	1:1000	Rabbit	Santa Cruz Biotechnology <sup>2</sup>
<b>ERK</b>	9102	1:1000	Rabbit	Cell Signaling Technology <sup>1</sup>
<b>phospho-ERK (Thr202/Tyr204)</b>	9106	1:2000	Mouse	Cell Signaling Technology <sup>1</sup>
<b>NRG1 C terminus</b>	sc-348	1:1000	Rabbit	Santa Cruz Biotechnology <sup>2</sup>
<b>MBP</b>	SMI94 SMI99	1:4000	Mouse	Covance, BioLegend <sup>3</sup>
<b>actin</b>	A5316	1:4000	Mouse	Sigma-Aldrich, Merck <sup>4</sup>
<i>Secondary antibodies</i>				
	<b>Code</b>	<b>Dilution</b>	<b>Host</b>	<b>Source</b>
<b>HRP coniugated-anti-rabbit</b>	7074	1:15000	Goat	Cell Signaling Technology <sup>1</sup>
<b>HRP coniugated-anti-mouse</b>	7076	1:15000	Goat	Cell Signaling Technology <sup>1</sup>



<i>Antibodies for Immunohistochemistry</i>				
<i>Primary antibodies</i>				
	<b>Code</b>	<b>Dilution</b>	<b>Host</b>	<b>Source</b>
<b>CD34</b>	AF4117	1:100	Goat	R&D Systems <sup>5</sup>
<b>S100<math>\beta</math></b>	HPA015768	1:500	Rabbit	Sigma-Aldrich, Merck <sup>4</sup>
<b>NRG1 C terminus</b>	sc-348	1:200	Rabbit	Santa Cruz Biotechnology <sup>2</sup>
<b>RECA1</b>	MCA970R	1:500	Mouse	Bio-Rad (AbD Serotec) <sup>6</sup>
<i>Secondary antibodies</i>				
	<b>Code</b>	<b>Dilution</b>	<b>Host</b>	<b>Source</b>
<b>AlexaFluor 488 Anti-Goat</b>	ab150129	1:400	Donkey	Abcam <sup>7</sup>
<b>Cy3 Anti-Mouse</b>	715-165-151	1:800	Donkey	Jackson ImmunoResearch <sup>8</sup>
<b>AlexaFluor 647 Anti-Rabbit</b>	711-605-152	1:800	Donkey	Jackson ImmunoResearch <sup>8</sup>

<sup>1</sup>Cell Signalling Technology, Danvers, MA, USA; <sup>2</sup>Santa Cruz Biotechnology, Dallas, TX, USA; <sup>3</sup>Covance, BioLegend, San Diego, CA, USA; <sup>4</sup>Sigma-Aldrich, Merck, Darmstadt, Germany; <sup>5</sup>R&D Systems, Minneapolis, MN, USA; <sup>6</sup>Bio-Rad, Hercules, CA, USA; <sup>7</sup>Abcam, Cambridge, UK; <sup>8</sup>Jackson ImmunoResearch, Philadelphia, PA, USA.

**Table S1.** Antibodies used for Western blot and immunohistochemistry analysis.

## References

- Bahm, J.; Esser, T.; Sellhaus, B.; El-kazzi, W.; Schuind, F.T. Tension in peripheral nerve suture, In *Treatment of Brachial Plexus Injuries*; Vanaclocha, V., Sáiz-Sapena, N.; IntechOpen, London, UK, 2018; pp. 2–9. *tissue engineering. J. Biomed. Sci.* 2018, 25, 90.
- Bak, M.; Gutkowska, O.N.; Wagner, E.; Gosk, J. The role of chitin and chitosan in peripheral nerve reconstruction. *Polym. Med.* 2017, 47, 43–47.
- Belanger, K.; Dinis, T.M.; Taourirt, S.; Vidal, G.; Kaplan, D.L.; Egles, C. Recent Strategies in Tissue Engineering for Guided Peripheral Nerve Regeneration. *Macromol. Biosci.* 2016, 16, 472–481.
- Boecker, A.; Daeschler, S.C.; Kneser, U.; Harhaus, L. Relevance and recent developments of chitosan in peripheral nerve surgery. *Front. Cell. Neurosci.* 2019, 13, 104.
- Boni, R.; Ali, A.; Shavandi, A.; Clarkson, A.N. Current and novel polymeric biomaterials for neural Caroni, P. Overexpression of growth-associated proteins in the neurons of adult transgenic mice. *J. Neurosci. Methods* 1997, 71, 3–9. 337.
- Carroll, S.L.; Miller, M.L.; Frohnert, P.W.; Kim, S.S.; Corbett, J.A. Expression of neuregulins and their putative receptors, ErbB2 and ErbB3, is induced during Wallerian degeneration. *J. Neurosci.* 1997, 17, 1642–1659.
- Carvalho, C.R.; Oliveira, J.M.; Reis, R.L. Modern Trends for Peripheral Nerve Repair and Regeneration: Beyond the Hollow Nerve Guidance Conduit. *Front. Bioeng. Biotechnol.* 2019, 7
- Cattin, A.L.; Burden, J.J.; Van Emmenis, L.; MacKenzie, F.E.; Hoving, J.J.A.; Garcia Calavia, N.; Guo, Y.; McLaughlin, M.; Rosenberg, L.H.; Quereda, V.; et al. Macrophage-Induced Blood Vessels Guide Schwann Cell-Mediated Regeneration of Peripheral Nerves. *Cell* 2015, 162, 1127–1139.
- Cattin, A.L.; Lloyd, A.C. The multicellular complexity of peripheral nerve regeneration. *Curr. Opin. Neurobiol.* 2016, 39, 38–46.
- De Souza, F.I.; Zumiotti, A.V.; da Silva, C.F. Neuregulins 1-alpha and 1-beta on the regeneration the peripheral nerves. *Acta Ortop. Bras.* 2010, 18, 250–254.
- Deumens, R.; Bozkurt, A.; Meek, M.F.; Marcus, M.A.E.; Joosten, E.A.J.; Weis, J.; Brook, G.A. Repairing injured peripheral nerves: Bridging the gap. *Prog. Neurobiol.* 2010, 92, 245–276.
- Dreesmann, L.; Mitnacht, U.; Lietz, M.; Schlosshauer, B. Nerve fibroblast impact on Schwann cell behavior. *Eur. J. Cell Biol.* 2009, 88, 285–300.
- Duffy, P.; McMahon, S.; Wang, X.; Keaveney, S.; O’Cearbhaill, E.D.; Quintana, I.; Rodríguez, F.J.; Wang, W. Synthetic bioresorbable poly- $\alpha$ -hydroxyesters as peripheral nerve guidance conduits; a review of material properties, design strategies and their efficacy to date. *Biomater. Sci.* 2019, 7, 4912–4943.
- Duijvestijn, A.; van Goor, H.; Klatter, F.; Majoor, G.; van Bussel, E.; van Breda Vriesman, P. Antibodies Defining Rat Endothelial Cells: RECA-1, a Pan-Endothelial Cell-Specific Monoclonal Antibody. *Lab. Investig.* 2012, 66, 459–466.
- El Soury, M.; Fornasari, B.E.; Morano, M.; Grazio, E.; Ronchi, G.; Incarnato, D.; Giacobini, M.; Geuna, S.; Provero, P.; Gambarotta, G. Soluble Neuregulin1 Down-Regulates Myelination Genes in Schwann Cells. *Front. Mol. Neurosci.* 2018, 11, 157.
- Falls, D.L. Neuregulins: Functions, forms, and signaling strategies. *Exp. Cell Res.* 2003, 284, 14–30.
- Faul, F.; Erdfelder, E.; Lang, A.G.; Buchner, A. G\*Power 3: A flexible statistical power analysis program for the social, behavioral, and biomedical sciences. *Behavior Research Methods* 2007, 39, 175–191.
- Fledrich, R.; Akkermann, D.; Schütza, V.; Abdelaal, T.A.; Hermes, D.; Schäffner, E.; Soto-Bernardini,

- M.C.; Götze, T.; Klink, A.; Kusch, K.; et al. NRG1 type I dependent autocrine stimulation of Schwann cells in onion bulbs of peripheral neuropathies. *Nat. Commun.* 2019, 10, 1467.
- Fornasari, B.E.; El Soury, M.; De Marchis, S.; Perroteau, I.; Geuna, S.; Gambarotta, G. Neuregulin1 alpha activates migration of neuronal progenitors expressing ErbB4. *Mol. Cell. Neurosci.* 2016, 77, 87–94.
- Freier, T.; Montenegro, R.; Koh, H.S.; Shoichet, M.S. Chitin-based tubes for tissue engineering in the nervous system. *Biomaterials* 2005, 26, 4624–4632.
- Fricker, F.R.; Bennett, D.L. The role of neuregulin-1 in the response to nerve injury. *Future Neurol.* 2011, 6, 809–822.
- Fricker, F.R.; Antunes-Martins, A.; Galino, J.; Paramsothy, R.; La Russa, F.; Perkins, J.; Goldberg, R.; Brelstaff, J.; Zhu, N.; McMahon, S.B.; et al. Axonal neuregulin 1 is a rate limiting but not essential factor for nerve remyelination. *Brain* 2013, 136, 2279–2297.
- Gambarotta, G.; Garzotto, D.; Destro, E.; Mautino, B.; Giampietro, C.; Cutrupi, S.; Dati, C.; Cattaneo, E.; Fasolo, A.; Perroteau, I. ErbB4 expression in neural progenitor cells (ST14A) is necessary to mediate neuregulin-1beta1-induced migration. *J. Biol. Chem.* 2004, 279, 48808–48016.
- Gambarotta, G.; Ronchi, G.; Friard, O.; Galletta, P.; Perroteau, I.; Geuna, S. Identification and validation of suitable housekeeping genes for normalizing quantitative real-time PCR assays in injured peripheral nerves. *PLoS ONE* 2014, 9, e105601.
- Gonzalez-Perez, F.; Cobianchi, S.; Geuna, S.; Barwig, C.; Freier, T.; Udina, E.; Navarro, X. Tubulization with chitosan guides for the repair of long gap peripheral nerve injury in the rat. *Microsurgery* 2015, 35, 300–308.
- Haastert-Talini, K.; Geuna, S.; Dahlin, L.B.; Meyer, C.; Stenberg, L.; Freier, T.; Heimann, C.; Barwig, C.; Pinto, L.F.V.; Raimondo, S.; et al. Chitosan tubes of varying degrees of acetylation for bridging peripheral nerve defects. *Biomaterials* 2013, 34, 9886–9904.
- Jessen, K.R.; Arthur-Farraj, P. Repair Schwann cell update: Adaptive reprogramming, EMT, and stemness in regenerating nerves. *Glia* 2019, 67, 421–437.
- Kaewkhaw, R.; Scutt, A.M.; Haycock, J.W. Integrated culture and purification of rat Schwann cells from freshly isolated adult tissue. *Nat. Protoc.* 2012, 7, 1996–2004.
- Kornfeld, T.; Vogt, P.M.; Radtke, C. Nerve grafting for peripheral nerve injuries with extended defect sizes. *Wiener Medizinische Wochenschrift* 2018, 169, 240–251.
- Livak, K.J.; Schmittgen, T.D. Analysis of relative gene expression data using real-time quantitative PCR and the 2- $\Delta\Delta$ CT method. *Methods* 2001, 25, 402–408.
- Meek, M.F.; Coert, J.H. US Food and Drug Administration /Conformit Europe- approved absorbable nerve conduits for clinical repair of peripheral and cranial nerves. *Ann. Plast. Surg.* 2008, 60, 466–472.
- Mei, L.; Xiong, W.C. Neuregulin 1 in neural development, synaptic plasticity and schizophrenia. *Nat. Rev. Neurosci.* 2008, 9, 437–452.
- Meyer, C.; Stenberg, L.; Gonzalez-Perez, F.; Wrobel, S.; Ronchi, G.; Udina, E.; Sukanuma, S.; Geuna, S.; Navarro, X.; Dahlin, L.B.; et al. Chitosan-film enhanced chitosan nerve guides for long-distance regeneration of peripheral nerves. *Biomaterials* 2016, 76, 33–51.
- Modrak, M.; Talukder, M.A.H.; Gurgenshvili, K.; Noble, M.; Elfar, J.C. Peripheral nerve injury and myelination: Potential therapeutic strategies. *J. Neurosci. Res.* 2020, 98, 780–795.
- Monje, P. V.; Bartlett Bunge, M.; Wood, P.M. Cyclic AMP synergistically enhances neuregulin-dependent ERK and Akt activation and cell cycle progression in Schwann cells. *Glia* 2006, 53, 649–659.

- Moore, A.M.; Kasukurthi, R.; Magill, C.K.; Farhadi, F.H.; Borschel, G.H.; Mackinnon, S.E. Limitations of conduits in peripheral nerve repairs. *Hand* 2009, 4, 180–186.
- Moore, A.M.; Borschel, G.H.; Santosa, K.B.; Flagg, E.R.; Tong, A.Y.; Kasukurthi, R.; Newton, P.; Yan, Y.; Hunter, D.A.; Johnson, P.J.; et al. A transgenic rat expressing green fluorescent protein (GFP) in peripheral nerves provides a new hindlimb model for the study of nerve injury and regeneration. *J. Neurosci. Methods* 2012, 204, 19–27.
- Muangsanit, P.; Shipley, R.J.; Phillips, J.B. Vascularization Strategies for Peripheral Nerve Tissue Engineering. *Anat. Rec. (Hoboken)*. 2018, 301, 1657–1667.
- Newbern, J.; Birchmeier, C. Nrg1/ErbB signaling networks in Schwann cell development and myelination. *Semin. Cell Dev. Biol.* 2010, 21, 922–928.
- Pabari, A.; Yang, S.Y.; Mosahebi, A.; Seifalian, A.M. Recent advances in artificial nerve conduit design: Strategies for the delivery of luminal fillers. *J. Control. Release* 2011, 156, 2–10.
- Pascal, D.; Giovannelli, A.; Gnani, S.; Hoyng, S.A.; de Winter, F.; Morano, M.; Fregnan, F.; Dell’Albani, P.; Zaccaro, D.; Perroteau, I.; et al. Characterization of glial cell models and in vitro manipulation of the neuregulin1/ErbB system. *Biomed. Res. Int.* 2014, 2014, 310215.
- Parkinson, D.B.; Bhaskaran, A.; Droggiti, A.; Dickinson, S.; D’Antonio, M.; Mirsky, R.; Jessen, K.R. Krox-20 inhibits Jun-NH2-terminal kinase/c-Jun to control Schwann cell proliferation and death. *J. Cell Biol.* 2004, 164, 385–394.
- Parrinello, S.; Napoli, I.; Ribeiro, S.; Wingfield Digby, P.; Fedorova, M.; Parkinson, D.B.; Doddrell, R.D.S.; Nakayama, M.; Adams, R.H.; Lloyd, A.C. EphB signaling directs peripheral nerve regeneration through Sox2-dependent Schwann cell sorting. *Cell* 2010, 143, 145–155.
- Ronchi, G.; Haastert-Talini, K.; Fornasari, B.E.; Perroteau, I.; Geuna, S.; Gambarotta, G. The Neuregulin1/ErbB system is selectively regulated during peripheral nerve degeneration and regeneration. *Eur. J. Neurosci.* 2016, 43, 351–364.
- Ronchi, G.; Fornasari, B.E.; Crosio, A.; Budau, C.A.; Tos, P.; Perroteau, I.; Battiston, B.; Geuna, S.; Raimondo, S.; Gambarotta, G. Chitosan Tubes Enriched with Fresh Skeletal Muscle Fibers for Primary Nerve Repair. *Biomed. Res. Int.* 2018, 2018, 9175248.
- Ronchi, G.; Cillino, M.; Gambarotta, G.; Fornasari, B.E.; Raimondo, S.; Pugliese, P.; Tos, P.; Cordova, A.; Moschella, F.; Geuna, S. Irreversible changes occurring in long-term denervated Schwann cells affect delayed nerve repair. *J. Neurosurg.* 2017, 127, 843–856.
- Richard, L.; Védrenne, N.; Vallat, J.-M.; Funalot, B. Characterization of Endoneurial Fibroblast-like Cells from Human and Rat Peripheral Nerves. *J. Histochem. Cytochem.* 2014, 62, 424–435.
- Richard, L.; Topilko, P.; Magy, L.; Decouvelaere, A.V.; Charnay, P.; Funalot, B.; Vallat, J.M. Endoneurial fibroblast-like cells. *J. Neuropathol. Exp. Neurol.* 2012, 71, 938–947.
- Richardson, J.T.E. Eta squared and partial eta squared as measures of effect size in educational research. *Educ. Res. Rev.* 2011, 6, 135–147.
- Shapira, Y.; Tolmasov, M.; Nissan, M.; Reider, E.; Koren, A.; Biron, T.; Bitan, Y.; Livnat, M.; Ronchi, G.; Geuna, S.; et al. Comparison of results between chitosan hollow tube and autologous nerve graft in reconstruction of peripheral nerve defect: An experimental study. *Microsurgery* 2016, 36, 664–671.
- Stassart, R.M.; Fledrich, R.; Velanac, V.; Brinkmann, B.G.; Schwab, M.H.; Meijer, D.; Sereda, M.W.; Nave, K.A. A role for Schwann cell-derived neuregulin-1 in remyelination. *Nat. Neurosci.* 2013, 16, 48–54.
- Stenberg, L.; Kodama, A.; Lindwall-Blom, C.; Dahlin, L.B. Nerve regeneration in chitosan conduits and in autologous nerve grafts in healthy and in type 2 diabetic Goto-Kakizaki rats. *Eur. J. Neurosci.* 2016, 43, 463–473.

- Sorrell, J.M.; Caplan, A.I. Fibroblasts-a diverse population at the center of it all. *Int. Rev. Cell Mol. Biol.* 2009, 276, 161–214.
- Subramanian, A.; Krishnan, U.M.; Sethuraman, S. Development of biomaterial scaffold for nerve tissue engineering: Biomaterial mediated neural regeneration. *J. Biomed. Sci.* 2009, 16, 108.
- Syed, N.; Reddy, K.; Yang, D.P.; Taveggia, C.; Salzer, J.L.; Maurel, P.; Kim, H.A. Soluble neuregulin-1 has bifunctional, concentration-dependent effects on Schwann cell myelination. *J. Neurosci.* 2010, 30, 6122–6131.
- Van Neerven, S.G.A.; Pannaye, P.; Bozkurt, A.; Van Nieuwenhoven, F.; Joosten, E.; Hermans, E.; Taccola, G.; Deumens, R. Schwann cell migration and neurite outgrowth are influenced by media conditioned by epineurial fibroblasts. *Neuroscience* 2013, 252, 144–153.
- Van Slooten, A.R.; Sun, Y.; Clarkson, A.N.; Connor, B.J. L-NIO as a novel mechanism for inducing focal cerebral ischemia in the adult rat brain. *J. Neurosci. Methods* 2015, 245, 44–57.
- Wang, Y.; Li, D.; Wang, G.; Chen, L.; Chen, J.; Liu, Z.; Zhang, Z.; Shen, H.; Jin, Y.; Shen, Z. The effect of co-transplantation of nerve fibroblasts and Schwann cells on peripheral nerve repair. *Int. J. Biol. Sci.* 2017, 13, 1507–1519.
- Wen, D.; Suggs, S. V.; Karunakaran, D.; Liu, N.; Cupples, R.L.; Luo, Y.; Janssen, A.M.; Ben-Baruch, N.; Trollinger, D.B.; Jacobsen, V.L. Structural and functional aspects of the multiplicity of Neu differentiation factors. *Mol. Cell. Biol.* 1994, 14, 1909–1919.
- Williams, L.R.; Longo, F.M.; Powell, H.C.; Lundborg, G.; Varon, S. Spatial-Temporal progress of peripheral nerve regeneration within a silicone chamber: Parameters for a bioassay. *J. Comp. Neurol.* 1983, 218, 460–470.
- Zhao, Q.; Dahlin, L.B.; Kanje, M.; Lundborg, G. Repair of the transected rat sciatic nerve: Matrix formation within implanted silicone tubes. *Restor. Neurol. Neurosci.* 1993, 5, 197–204.
- Zhou, L.N.; Cui, X.J.; Su, K.X.; Wang, X.H.; Guo, J.H. Beneficial reciprocal effects of bone marrow stromal cells and Schwann cells from adult rats in a dynamic co-culture system in vitro without intercellular contact. *Mol. Med. Rep.* 2015, 12, 4931–4938.

## *Chapter 5*

*In vivo evaluation of chitosan conduits enriched with fibrin-collagen hydrogels +/- Adipose Derived Mesenchymal Stem Cells for Peripheral Nerve Repair.*

## **In vivo evaluation of chitosan conduits enriched with fibrin-collagen hydrogel +/- Adipose Derived Mesenchymal Stem Cells for Peripheral Nerve Repair.**

**El Soury M.**<sup>\*1,2</sup>, **García-García Ó.D** <sup>\*3,4</sup>, **Tarulli I** <sup>1</sup>, **Chato-Astrian J** <sup>3,4</sup>, **Perroteau I.** <sup>1</sup>, **Raimondo S.**<sup>1,2</sup>, **Carriel V** <sup>3,4</sup> #, **Gambarotta G.**<sup>1,2</sup> #

*1 Department of Clinical and Biological Sciences, University of Torino, Torino, Italy*

*2 Neuroscience Institute Cavalieri Ottolenghi (NICO), University of Torino, Torino, Italy*

*3 Tissue Engineering Group, Dept. Histology, University of Granada, Granada, Spain.*

*4 Instituto de Investigacion Biosanitaria, Ibs.Granada, Granada, Spain*

*\*These authors have contributed equally to this work and share first authorship*

*# These authors share senior authorship*

*\*\*Please note that this is the collection of the data obtained till now and the work is still in progress, the authors are the names of people who have participated in the experiments.*

*This manuscript is not definitive and still has not been read or approved by all authors.*

**ABSTRACT:**

To enhance the efficacy of hollow conduits, intraluminal fillers and mesenchymal stem cells can be used. In this study, we aimed to investigate the efficacy of combining a fibrin-collagen hybrid hydrogel with Adipose Derived Mesenchymal Stem Cells (ADMSC), as an intraluminal filler of chitosan tubes in repairing a 15 mm gap in rat sciatic nerves. Gene expression analysis at short time points shows an increased expression of genes known to be positively involved in the regeneration process, including soluble neuregulin1. Functional analysis carried out 15 weeks post injury and repair shows that ADMSC addition improved the sensitivity recovery. Morphological analysis carried out on the distal portion shows that in all experimental groups, including the hollow conduit, poor regenerative results were obtained, thus suggesting that these cannot be ascribed to the presence of the hydrogel. Rather, we hypothesized that the end time point analysed could be too early to detect regenerated nerves in the distal portion. Morphological analysis of nerve regeneration inside the conduit will help to understand if this hypothesis is correct and whether conduit enrichment promoted nerve regeneration (work in progress).

**Keywords:**

Peripheral nerve regeneration, nerve conduits, chitosan conduits, intraluminal fillers, fibrin, collagen, hydrogels, ADMSC, Nrg1 and Tissue engineering.



## ***Introduction***

Peripheral nerve injuries are a common and frequent problem, with a high occurrence incidence. Every year more than 300,000 cases are registered just in Europe (Kingham & Terenghi, 2006). Regeneration outcome in most of the severe cases is poor or even absent. Permanent irreversible motor nerve damages result in hindering the patient's activity not only leading to a poor life quality, but also adding an extra economic burden for the society (Bergmeister et al., 2020). The obtained final regeneration outcome is the summary of various factors combined together: mainly, the severity of the injury, the age of the patient, the location of the injury (near or far the innervated muscle/target), the time of delay before repairing (Modrak et al., 2019; Hoke, 2006). Peripheral nerves are capable to regenerate spontaneously with regaining full functional recovery after being subjected to mild injuries (neuropraxia or axonotmesis) when the structural continuity of the surrounding connective tissue is still maintained (Carriel et al., 2014). Severe injuries as neurotmesis resulting in nerve continuity disruption, always require surgical intervention to be repaired. Direct neurorrhaphy is the surgeon first choice as long as the two transected nerve stumps can be joined together without tension (Pfister et al., 2011). On the other hand, if the injury resulted in nerve substance loss and tensionless direct repair is impossible, a graft is needed to bridge the two nerve stumps and to substitute the lost nerve portion (Carvalho et al., 2019). Currently, autografts are the gold standard for repairing such injuries, where a sensitive nerve is sacrificed to repair a motor nerve. Despite having a complete satisfactory final regeneration outcome and a total functional recovery, other alternatives to bridge the nerve gap are needed. Unfortunately, the use of autografts is accompanied by many drawbacks as increased operation time, the limitation of available donor nerves in terms of length, dimensions and specificity, donor site morbidity and the possible formation of painful neuromas (Safa & Buncke, 2016). With the development of the field of tissue engineering and biomaterial synthesis, it was possible to synthesize tubular nerve conduits of both natural or synthetic origins to be interposed in between the transected nerve stumps (Carriel et al., 2014). Biocompatibility, biodegradability without release of toxic by-products, adequate mechanical properties and permeability are essential requirements for a successful conduit (Fornasari et al., 2020). Chitosan (copolymer of D-glucosamine and N-acetyl-glucosamine) is obtained from the N-deacetylation of chitin (naturally found in Crustacean shells); it has been used to fabricate nerve conduits and scaffolds with excellent biocompatibility properties and it has been successfully used in repairing nerve injuries (Freier

et al., 2005; Haastert-Talini et al., 2013). To further enhance the efficacy of nerve conduits, a good strategy is the use of intraluminal fillers containing extracellular matrix components (ECM) and the incorporation of viable cells, which demonstrated a superior regeneration outcome when compared to hollow conduits (Carvalho et al., 2019).

Natural polymers, such as agarose, collagen, laminin, and fibrin, are often used as luminal fillers; they can be provided in different forms as solutions, hydrogels, filaments, and porous sponges (Carriel et al., 2014; Gonzalez-Perez et al., 2013). Their characteristic softness and biocompatibility can help regenerative guidance for the reconstruction of nerve gaps. As collagen, one of the major ECM proteins, is highly conserved among species, it induces a minimal foreign body response and it has been widely used in supporting nerve regeneration (Koopmans et al., 2009). Fibrin is another matrix protein that has been shown to be a key regulator of PNS myelination and fibre regeneration following peripheral nerve injury (Alovskaya et al., 2007; Daly et al., 2012). The addition of stem cells significantly improves the regenerating outcome by supplying the regenerative environment with secreted growth factors (Seyed-forootan et al., 2019). ADMSC accessibility and purification are easy, and they retain a high ability of differentiation. Moreover, they have been successfully used in enhancing the nerve regeneration process (Carriel et al., 2013; Carriel et al., 2014; Chato-Astrain et al., 2018).

In this study, we investigated the regenerative effect of chitosan conduits enriched with a hybrid hydrogel composed of fibrin and collagen, alone or with the incorporation of ADMSC, the molecular changes were tested at 7, 14 and 28 days post injury and repair, while the final regeneration outcome was assessed following 15 weeks of repair.

## ***Materials and Methods***

### ***Adipose derived mesenchymal stem cells culture.***

ADMSC were isolated and characterized for their stemness profile as described before (Carriel et al., 2013; Chato-Astrain et al., 2018). Cells were cultured under standard conditions (at 37°C in a 5% CO<sub>2</sub> humidified environment) in DMEM supplied with 10% FBS, 100u/ml penicillin G, 100µg/ml streptomycin and 0.25µg/ml amphotericinB and were expanded until reaching the desired quantity. All reagents were purchased from Sigma-Aldrich unless otherwise specified.

***Fibrin-collagen +/- ADMSC hybrid hydrogel preparation.***

Gels were prepared under aseptic conditions. Fibrin collagen hybrid hydrogel was prepared as follows: for 10 ml, 4.125 ml collagen solution (#C4243), 3.8 ml human plasma, 1.5 ml DMEM, 75µl tranexamic acid (Amchafibrin, fides-Ecofarma, Spain), 0.5 ml 1% CaCl<sub>2</sub>). For ADMSC fibrin-collagen gel, the same recipe was followed adding 1.5 ml DMEM containing  $2 \times 10^5$  ADMSC (passage 7). 8ml of hybrid gel was poured in a 60mm petri-dish and was left to solidify in incubator under standard culture condition (2 petri dishes per each treatment). At the time of operation, the gel in each petri was carefully cut into 8 equal rectangular pieces (2cm length x 0.8cm width), then by the help of a surgical sewing thread that was fixed at one side of the gel, thread was passed inside the conduit (1.5 cm) and was gently pulled to slide the gel inside.

***Animals.***

All procedures were performed following the European Union and Spanish government guidelines (EU Directive No.63/2010, RD 53/2013) and were approved by the ethical committee of the University of Granada, Spain.

***Surgical procedure.***

48 adult male Wistar rats weighing between 200-250g (JANVIER LABS), were housed in the plastic cages with free access to food and water under a controlled light and temperature conditions (21°C and 12h light/dark) in the experimental Unit of the University Hospital Virgen de las Nieves, Granada, Spain. Before the surgical operation, animals were anesthetized by a mixture of [0.001mg/g body weight acepromazine (calmi-Neosan<sup>®</sup>) + 0.15mg/g body weight ketamine (Imalgene 1000<sup>®</sup>) + 0.05µg/g body weight atropine]. Animals were assigned randomly into 3 experimental groups (n=16), Sciatic nerve was exposed and was completely transected removing a 15 mm segment and repaired either with 1) hollow chitosan conduit (hollow tube), 2) chitosan conduit enriched with fibrin-collagen hydrogel (FCOLL tube), 3) chitosan conduit enriched with fibrin-collagen hydrogel and ADMSC (FCOLL+ADMSC). Following a timeline, animals were euthanatized by applying an anaesthetic overdose at 7, 14, 28 days post injury and 15 weeks (n=4) and sciatic nerves were harvested for the following analyses.

At 7, 14, 28 days after injury and repair the inner part of the conduit was withdrawn and immediately frozen in liquid nitrogen for RNA and protein extraction, while the proximal and distal nerve parts were fixed in 10% formalin for histological analysis. Following 15 weeks the

proximal and the inner part of the tube were fixed in 10% formalin for histological analysis and the distal nerve portion was fixed in 2.5% glutaraldehyde for morphometric and TEM analysis; healthy nerves (n=4) for each analysis were harvested from the contralateral part and used as control (Figure 1).

#### ***Pinch test.***

To assess the sensory functional recovery, the rats were subjected to pinch test, where a mild pinching stimulus was applied to the rat foot using a surgical needle. The painful stimulus was applied until the rat show a withdrawal response and on a 4 point scale, the rats were given the following score dependent of their response, 0= absence of withdrawal response, 1= withdrawal response to stimulus applied above the ankle area, 2= withdrawal response to stimulus applied at the heel/plantar area, 3= withdrawal response to stimulus applied at the foot metatarsal region, the optimum score is 3 (Chato-Astrain et al., 2018; Carriel et al., 2013).

#### ***Toe spread and Walking test.***

To assess the motor functional recovery, Toe spread test was performed where a rat was suspended by its tail and the extension and abduction reaction of the toes were examined. On a 4-point scale, rats were given different scores corresponding to their behaviour: 0 = if no toe movement was observed, 1 = if some sign of toe movement was observed, 2 = if toe abduction occurs, 3 = if toe abduction followed by extension is observed, the optimum score is 3 (Siemionow et al., 2011; Carriel et al., 2013).

For Walking test and Sciatic functional index calculation (SFI), the rat hind limbs were immersed on blue ink and left to walk in a longitudinal tract Plexiglas® device (1m length, 10cm width and 15cm height) previously lined with white paper sheet; the blue foot prints were used to calculate the SFI using the mathematical formula ( $-38.3 \times PL + 109.5 \times TS + 13.3 \times ITS - 8.8$ ), where PL: print length is the measure from the 3<sup>rd</sup> toe to the heel, TS: toe spread is the distance measured between the 1<sup>st</sup> and the 5<sup>th</sup> toe, ITS: intermediate toe spread is the distance between the 2<sup>nd</sup> and the 4<sup>th</sup>. The score ranges from 0 to 100, where 0 is the optimum regeneration result and 100 is an indicator of lacking regeneration (An et al., 2018).

#### ***Percentage of Muscle atrophy.***

To assess the degree of muscle atrophy, the whole lower leg was separated from the surrounding skin and dissected from the knee and ankle then fixed immediately in 10%

---

formalin for at least one week. The legs were weighted by means of a digital balance (Sartorius BP121 S, precision level=0.1mg, Sigma-Aldrich). The volume was measured following Archimede's principle and fluid displacement rules, where a cylinder was filled with 30 ml PBS and the leg was immersed totally in the cylinder, the volume of the immersed leg is equal to the volume of liquid displacement. For each rat the operated leg and contralateral leg were measured, and the percentage of loss was calculated as  $[100 - (\text{operated leg}/\text{contralateral leg} * 100)]$ .

### ***RNA extraction, cDNA preparation and qRT-PCR analysis***

RNA was extracted using TRIzol reagent (Life Technologies) following manufacturer's instructions, as previously described (Ronchi et al., 2016). Briefly, 500 $\mu$ l TRIzol reagent were added directly to the frozen nerve sample and was mechanically dissociated. 0.1ml chloroform was added to the homogenized samples, following centrifugation the upper aqueous phase was collected carefully and transferred into a new microtube. 5 $\mu$ g RNase free glycogen were added to facilitate RNA precipitation. RNA pellet was resuspended in sterile RNase free water and concentration was detected by NanoDrop reader. 1  $\mu$ g RNA was reverse transcribed in a 25 $\mu$ l total reaction volume containing 1mM dNTPs, 1x buffer, 0.1  $\mu$ g/ $\mu$ l BSA, 0.05% triton X-100, 7.5  $\mu$ M random primers, 200 units reverse transcriptase (RevertAid Thermo Scientific Fermentas, #EP0441), 40 units RNase inhibitor (Ribolock Thermo Scientific Fermentas #E00381). Thermocycler was set at 25 $^{\circ}$  C for 10 minutes, at 42 $^{\circ}$  C for 90 minutes, at 70 $^{\circ}$  C for 10 minutes. Quantitative Real-Time Polymerase Chain Reaction (qRT-PCR) analysis was performed using ABI prism 7300 real-time PCR system (Applied Biosystems, Thermo Fisher scientific). cDNA was diluted 1:10 in water; in each well a PCR reaction was carried out on 5  $\mu$ l diluted cDNA corresponding to 20 ng starting RNA, 1x SYBR Green PCR Master Mix (Bio-Rad) and 300nM sense and antisense primers (Invitrogen) in a reaction volume of 20  $\mu$ l. Reaction was performed as follows: an initial denaturation step for 30 seconds at 95 $^{\circ}$ C, denaturation in the subsequent 40 cycles was performed for 15 seconds at 95 $^{\circ}$ C followed by primer annealing and elongation at 60 $^{\circ}$ C for 1 minute. The RNA expression was analysed by the  $\Delta\Delta$ Ct relative quantification method (Livak & Schmittgen, 2001) normalizing the gene expression to the geometric average of two housekeeping genes that were found to be highly stable in peripheral nerves after injury, Rictor and ANKRD27 (Gambarotta et al., 2014). The data are expressed as normalized relative quantity (NRQ) calculated using the formula:  $NRQ = 2^{-(\Delta\Delta Ct)}$ . All primers were designed using AnnHyb software

(<http://www.bioinformatics.org/annhyb/>) and synthesized by Invitrogen to amplify specific isoforms of NRG1, ErbB receptors, Krox20/Egr2, ATF3, c-Jun, P75, S100, Thy and VEGF-A, Rictor and ANKRD27 (Table 1).

<i>Gene</i>	<i>Accession number</i>	<i>Primer</i>	<i>Sequence 5'-3'</i>
<b>ANKRD27</b>	NM_001271264	rAnkrd27 FW	CCAGGATCCGAGAGGTGCTGTC
		rAnkrd27 REV	CAGAGCCATATGGACTTCAGGGGG
<b>RICTOR</b>	XM_001055633	rRICTOR FW	GAGGTGGAGAGGACACAAGCCC
		rRICTOR REV	GGCCACAGAACTCGGAAACAAGG
<b>NRG1 type I/II</b>	AF194993	rNRG1 I/II FW	GGCGAAACACTTCTTCATCCAC
		rNRG1 I/II/III REV	AAGTTTTCTCCTTCTCCGCGCAC
<b>NRG1 alpha</b>	AF194439	rNRG1-alfa/beta FW	TGCGGAGAAGGAGAAAACTTTC
		mrNRG1-alfa REV	TTGCTCCAGTGAATCCAGGTTG
<b>NRG1 beta</b>	U02322 AY973245	rNRG1-alfa/beta FW	TGCGGAGAAGGAGAAAACTTTC
		mrNRG1-beta REV	AACGATCACCAGTAAACTCATTTGG
<b>ErbB2</b>	NM_017003	rErbB2 FW	TGACAAGCGCTGTCTGCCG
		rErbB2 REV	CTTGTAGTGGGCGCAGGCTG
<b>ErbB3</b>	NM_017218	mrErbB3 FW	CGAGATGGGCAACTCTCAGGC
		mrErbB3 REV	AGGTTACCCATGACCACCTCACAC
<b>Krox20/Egr2</b>	NM_053633.1	rKrox20 FW	GACCATCTTCCCAATGGTGAAGT
		rKrox20 REV	GATATGGGAGATCCAAGGGCCTCTTC
<b>ATF3</b>	NM_012912.2	rATF3 FW	CACCATCAACAACAGACCTCTGGAG
		rATF3 REV	CCGCCGCCTCCTTTTTCTCTC
<b>c-JUN</b>	NM_021835.3	rc-JUN FW	ACGACCTTCTACGACGATGCCC
		rc-JUN REV	GGGTGCGCCAGGTTCAAGG
<b>S100</b>	NM013191.1	rS100 FW	GGGTGACAAGCACAAGCTGAAGAA
		rS100 REV	TTGTCCACCACTTCTGCTCTTTG
<b>p75</b>	NM_012610	rP75 FW	AGCAGACCCATACGCAGACTG
		rP75 REV	TCTCTACCTCCTCACGCTTGG
<b>Thy1</b>	NM_012673.2	rThy1 FW	CTCCTGCTTTTCAGTCTTGAGATGTC
		rThy1 REV	CATGCTGGATGGGCAAGTTGGTG

<b>VEGF-A</b>	NM_001317043.1	rVEGF-A FW	ACCATGAACTTTCTGCTCTCTTGGG
		rVEGF-A REV	CTTCATGGGCTTTCTGCTCCCC

Table 1: Forward (FW) and reverse (REV) primers used in qRT-PCR.

### ***Protein Extraction and Western Botting***

Proteins were extracted by TRIzol following manufacturer's instructions as a subsequent step following the RNA extraction. Bicinchoninic acid (BCA) assay was performed for protein quantification following manufacturer's instructions and the optical density was measured at  $\lambda = 562$  nm (Microplate Reader, BIORAD). Western blotting was performed as previously described (Gambarotta et al., 2004); protein samples (40 $\mu$ g) were resolved by 8% SDS-PAGE and blotted on nitrocellulose membrane (HybondC Extra, Amersham). Membranes were then incubated for 1h at RT in 5% non-fat milk solution in 1x TBST (150mM NaCl, 10mM Tris-HCl pH7.4, 0.1% tween) to block unspecific binding. Membranes were incubated with primary antibodies overnight at 4°C in 5% BSA, 1x TBST, washed 4 times in TBST, then were incubated with secondary antibodies for 1 h at RT in 5% non-fat milk solution in 1x TBST (table 2). Enhanced chemiluminescence (ECL) was used for signal detection (Clarity Western ECL Substrate, Bio-Rad, #170-5061). Signal detection and image acquisition was performed by ChemiDoc Touch imaging system (Bio-Rad).

<i>Antibodies for Western blot analysis</i>				
<b><i>Primary antibodies</i></b>				
<b>NRG1 C terminus</b>	sc-348	1:1000	Rabbit	Santa Cruz Biotechnology
<b>HER2/ErbB2</b>	sc-284	1:1000	Rabbit	Santa Cruz Biotechnology
<b>HER3/ErbB3</b>	sc-285	1:1000	Rabbit	Santa Cruz Biotechnology
<b>P-AKT 308</b>	4056	1:1000	Rabbit	Cell Signalling Technology
<b>AKT</b>	9272	1:2000	Rabbit	Cell Signalling Technology
<b>P-ERK 1/2</b>	9106	1:2000	Mouse	Cell Signalling Technology
<b>ERK 1/2</b>	9102	1:2000	Rabbit	Cell Signalling Technology
<b>GAPDH</b>	AM 300	1:20,000	Mouse	Invetrogen
<b><i>Secondary antibodies</i></b>				
	<b>Code</b>	<b>Dilution</b>	<b>Host</b>	<b>Source</b>
<b>HRP coniugated-anti-rabbit</b>	7074	1:15000	Goat	Cell Signaling
<b>HRP coniugated-anti-mouse</b>	7076	1:15000	Goat	Cell Signaling

Table 2: Primary and secondary antibodies used in Western blot analysis.

### ***Resin embedding and semi-thin sections preparations***

Nerves were immediately fixed in 2.5% glutaraldehyde followed by 2h post fixation in 2% osmium tetroxide, samples were gradually dehydrated by immersion in ascending ethanol gradients (30%, 50%, 70% ,80%, 95% and 100%) followed by immersion in propylene oxide. Samples were then left overnight in a pre-infiltration solution of equal parts of propylene oxide and Glauerts resin mixture (Araldite M and Araldite Harter, HY 964 in the ratio 1:1), 0.5% dibutyl phthalate plasticizer (to reduce resin viscosity and allow better embedding medium infiltration into the specimen), the final step is to add 2% accelerator DMP-30 to promote the polymerization of the resin embedding medium, the desired nerve sample orientation is checked before final resin incubation and solidification at oven 60°C where they are left for 2-3 days. Semi-thin sections of 2.5 mm thick were prepared using an Ultracut UCT ultramicrotome (Leica Microsystems) then stained with 1% toluidine blue for high resolution light microscopy examination (DM4000B microscope equipped with a DFC320 digital camera and an IM50 image manager system, Leica Microsystems).

### ***Statistical analysis.***

Statistical analysis was performed using IBM SPSS Statistics, Version 24.0 software (Armonk, NY: IBM Corp). Statistically significant differences among experimental groups at each time point were assessed by one-way ANOVA followed by Bonferroni post hoc test; differences were considered significant at  $p < 0.05$ .

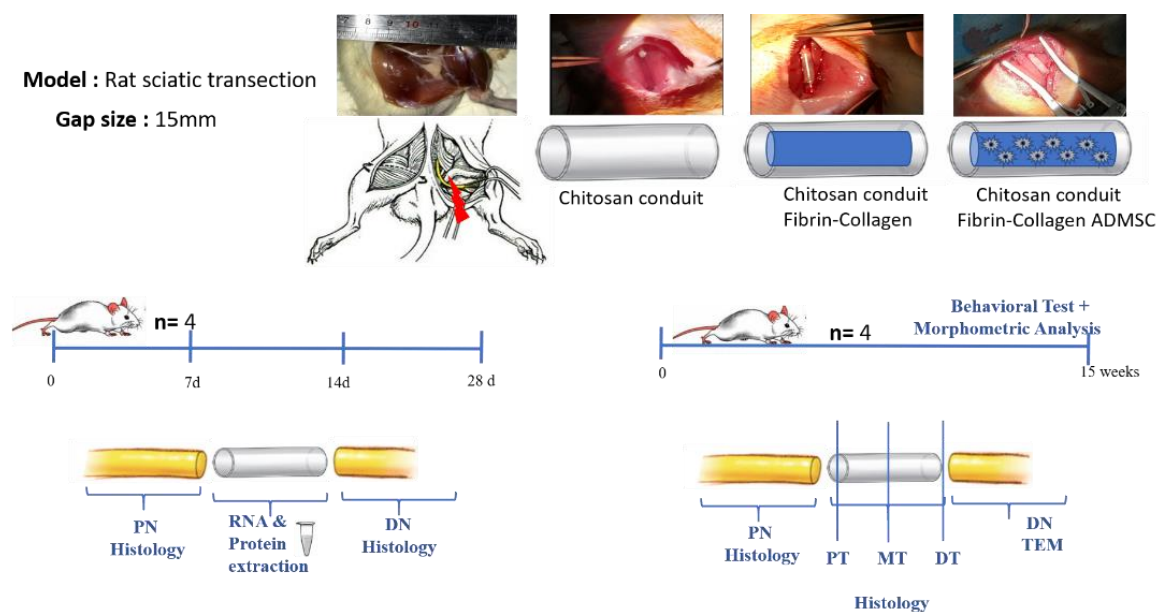




**Figure 1:** Schematic diagram showing the study plan, 15mm rat sciatic nerve gap obtained by nerve transection was repaired either by hollow chitosan conduit, or by chitosan conduit enriched with fibrin-collagen +/- ADMSC. At 7-, 14- and 28-days molecular analysis was performed on the inner part of the conduit and the proximal (PN) and distal nerve (DN) portions were harvested for histological analysis. At 15 weeks, animals were subjected to functional recovery tests, then proximal nerve portion and the inner part of the conduit were harvested for histological analysis (carried out in 3 regions: proximal tube/PT, middle tube/MT and distal tube/DT) while the distal nerve portion was withdrawn for TEM and morphometric analysis.

## Results

Three different experimental groups, corresponding to 15 mm sciatic nerve gaps repaired with 1.hollow chitosan conduits, 2.conduits enriched with fibrin-collagen (FCOLL), 3.conduits enriched with fibrin-collagen and ADMSC (FCOLL+ADMSC), were analysed at morphological and biomolecular level at early time points after injury and repair (7, 14 and 28 days) and at functional and morphological level at 15 weeks after repair (Figure 1).

As discussed in the following paragraphs, the expression of different genes involved in the regeneration process (solubleNRG1, Nrg1- $\alpha$ , Nrg1- $\beta$ , p75, Thy1, S100, Krox20/Egr2, c-Jun, Atf3, ErbB2, ErbB3 and VEGF-A) was analysed (Figure 2).

### ***soluble NRG1, both $\alpha$ and $\beta$ isoforms, are highly upregulated in FCOLL and FCOLL+ADMSC experimental groups***

Soluble NRG1 is a growth factor that is found to be highly upregulated immediately in response to nerve injury (Ronchi et al., 2016). At 7 days after repair its expression was significantly higher in both groups enriched with fibrin-collagen (FCOLL +/- ADMSC) when compared to healthy nerves (CTR group): almost 12-fold higher when compared to healthy nerve and 2-fold higher when compared to hollow conduits.

At 14 days after repair the expression level in both groups enriched with fibrin-collagen (FCOLL +/- ADMSC) was decreased, but still remaining to be statistically higher compared to CTR group only in ADMSC group. In hollow conduits the increase in soluble NRG1 expression was delayed to 14 days, but it did not reach the same level observed in fibrin-collagen +/- ADMSC groups at 7 days. At 28 days soluble NRG1 expression is decreased to CTR level in all experimental groups.

Consistent with soluble NRG1 expression, the two isoforms NRG1 $\alpha$  and NRG1 $\beta$  followed the same expression pattern: they were significantly higher at 7 days post injury both in FCOLL and FCOLL+ADMSC groups, and this upregulation was delayed to 14 days in hollow conduits.

***Fibroblast marker is highly expressed in all experimental groups***

The expression of the cellular markers p75, S100, and Thy1, corresponding respectively to immature SC, mature SC and fibroblasts, was tested to understand the infiltration and the colonization of cells in the conduits used for the different repairing strategies. At all the tested time points p75 and Thy1 was significantly upregulated in hollow chitosan conduits, while only high level of fibroblast marker was observed at 7 days in Fibrin-collagen+/- ADMSC. S100 expression was significantly lower than CTR in all experimental groups at the 3 tested time points.

***Expression analysis of transcription factors playing important roles in the myelination process***

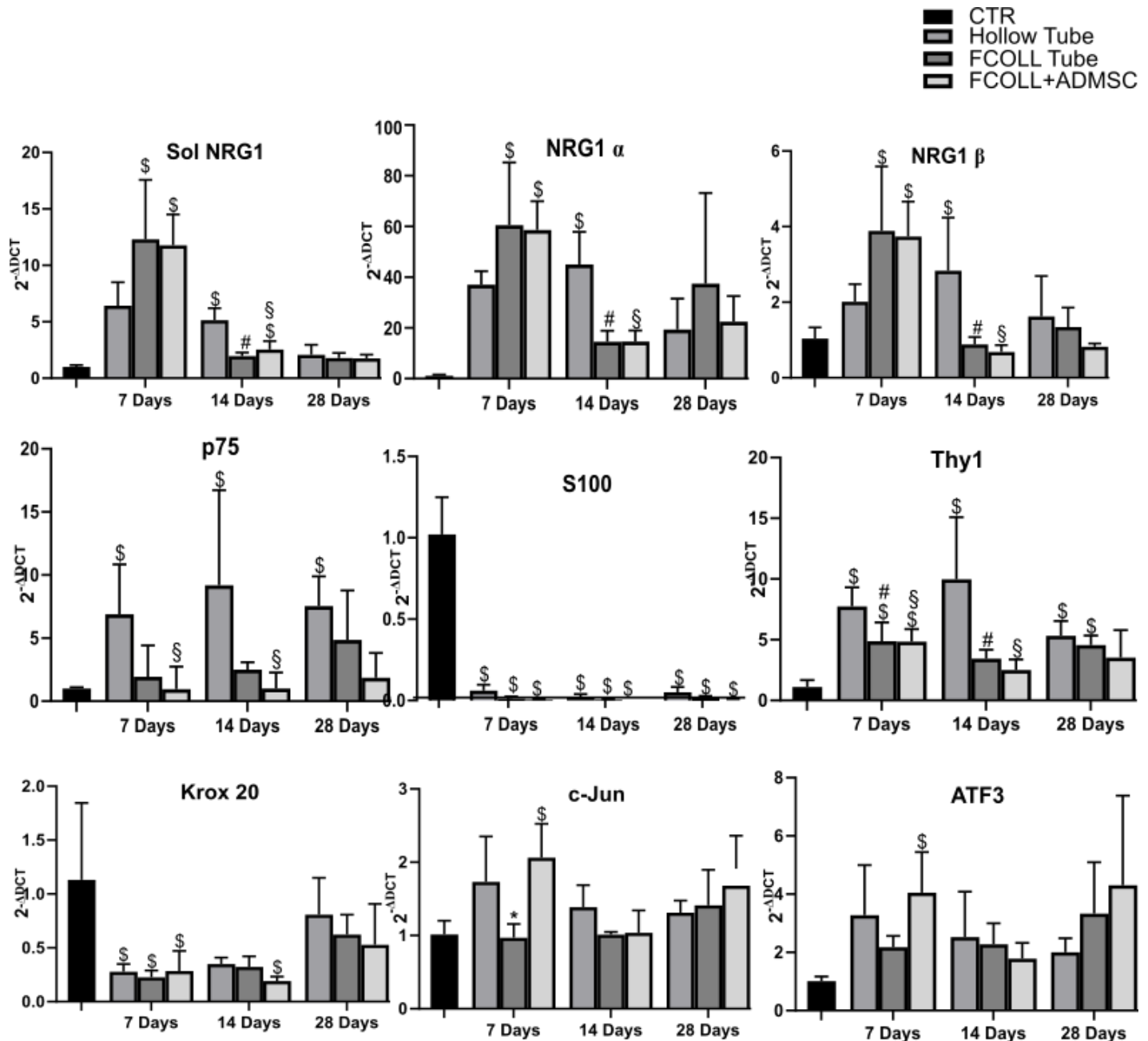
In order to support the regeneration process, adult myelinating Schwann cells need to transdifferentiate into a repair phenotype, this is achieved by downregulating genes that are directly related to myelination. Krox20, c-Jun and ATF3 are important transcription factors playing different roles in controlling myelination. At 7 days Krox20 expression was significantly lower in all the experimental groups, while c-Jun and ATF3 were significantly upregulated only in ADMSC groups. For the remaining time points the changes were not significant for the different transcription factors except for Krox20 that remain to be significantly less at 14 days only in ADMSC group.

***ADMSC upregulate ErbB2 receptor while downregulate ErbB3.***

ErbB2 and ErbB3 receptors are the main NRG1 receptors that are expressed by Schwann cells in the peripheral nervous system. We were interested to understand whether the combination of fibrin-collagen +/- ADMSC were also able to regulate NRG1 receptors. 7 days post injury ErbB2 was significantly upregulated only in ADMSC group compared to cell free fibrin-collagen group. While ErbB3 receptor has shown to be significantly downregulated in all the tested points in fibrin-collagen +/- ADMSC groups, it was only down regulated at 7 and 14 days in hollow chitosan conduits.

### ADMSC addition to fibrin-collagen upregulates VEGF-A.

Vascular endothelial growth factor is a potent angiogenic factor that is required during tissue repair. At 7 days only ADMSC group was able to dramatically upregulate the VEGF-A expression up to 25 folds when compared to CTR. Its expression was also significantly higher when compared to hollow chitosan conduit and fibrin-collagen tube. VEGF-A is significantly upregulated at 14 days in fibrin-collagen hydrogel group.



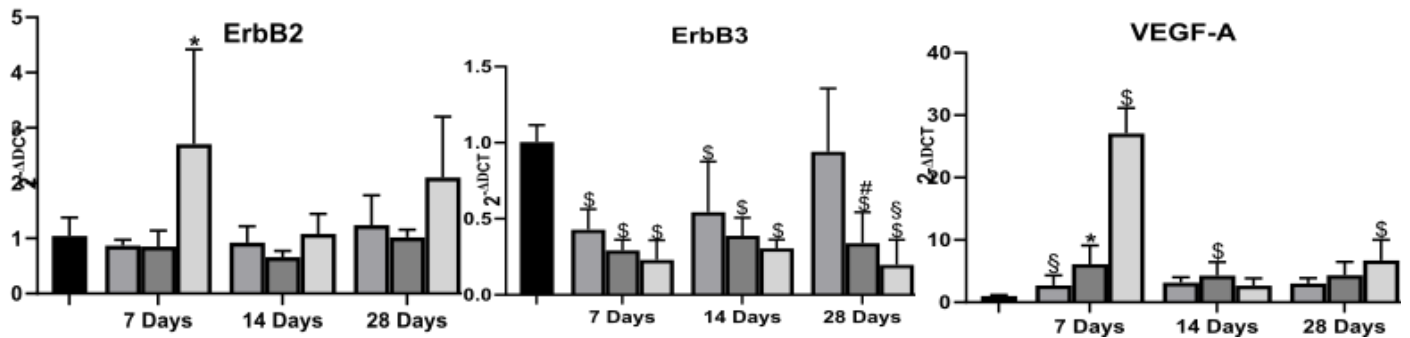


**Figure 2.** Quantitative gene expression analysis in the three experimental models: hollow conduit, FCOLL, FCOLL + ADMSC. Relative quantification ( $2^{-\Delta\Delta C_t}$ ) of NRG1 and its isoforms  $\alpha$  and  $\beta$ , their receptors (ErbB2 and ErbB3), Schwann cell markers (S100 $\beta$  and p75) and fibroblast marker (Thy1) are shown, together with transcription factors controlling myelination (Krox20, c-Jun and ATF3), and vascular endothelial growth factor (VEGF-A). The geometric average of housekeeping genes ANKRD27 and RICTOR was used to normalize data. All data were calibrated to healthy sciatic nerves, whose expression is equivalent to 1. Data were statistically analysed using one-way ANOVA followed by Bonferroni post-hoc test,  $p < 0.05$ , \$ significance between Ctr and all experimental groups, § hollow tube vs fcoll+ADMSC, \* fcoll vs fcoll+ADMSC, # hollow tube vs fcoll.

### Western blotting and Protein analysis

Protein analysis of NRG/ErbB system showed that, in consistent with the RNA expression levels, NRG 1 is expressed at 7 days post injury in all the experimental groups, being stronger in fibrin-collagen +ADMSC group, in all experimental groups NRG1 expression decreases by time. NRG1 expression in fibrin-collagen +ADMSC group is higher at 14 days compared to the other experimental groups hollow tube or Fcoll tube

A strong protein expression of NRG receptors ErbB2 and ErbB3 was shown in Fibrin-collagen +ADMSC group at 14 days, ErbB2/3 were also expressed to a lower extent in fcoll tube group, a strong expression of both receptors was delayed to 28 days in hollow tube group.

Antibodies against phosphorylated AKT and ERK1/2, two main signalling pathways that are known to be activated downstream NRG/ErbB activation, has showed that phosphor-ERK1/2

were activated at 14 days both in Fcoll and Fcoll+ADMSC groups, and was activated at 28 days in hollow tube groups, no changes were detected in AKT phosphorylation (Figure 3).

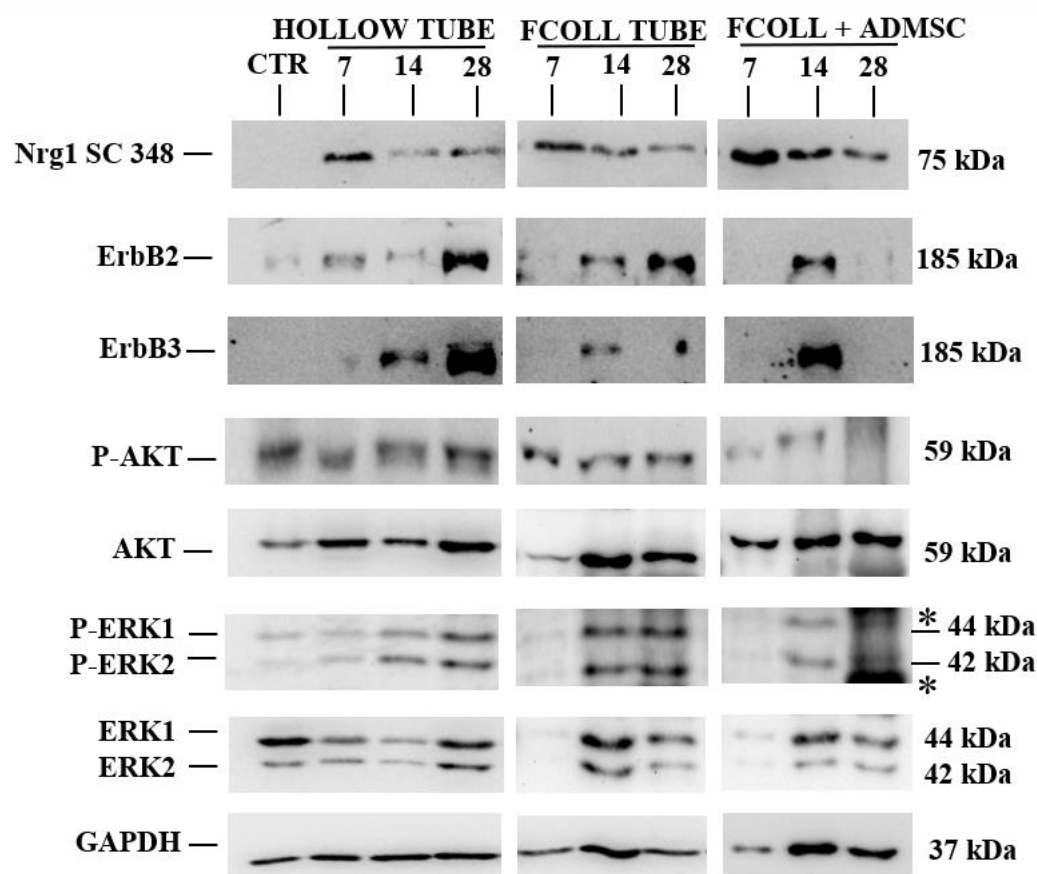


**Figure 3.** Protein expression of NRG1-ErbB system. Western blot analysis of proteins extracted from healthy control nerves (CTR) and regenerating nerves from hollow chitosan tube, fibrin collagen enriched chitosan tube (FCOLL Tube) and fibrin collagen + ADMSC enriched chitosan tube (FCOLL+ADMSC) groups withdrawn 7, 14 and 28 days after the repair and probed with antibodies for NRG1, ErbB2, ErbB3, P-AKT, AKT, P-ERK1/2, ERK1/2 and GAPDH. Molecular weight (kDa) are shown on the right.

### ***Evaluation of Sensory and Motor recovery***

Pinch test was performed to assess the sensory recovery in the three experimental groups 15 weeks post injury and repair. ADMSC Fibrin-Collagen group was found to record the highest recovery values ( $2.50 \pm 0.58$ ), followed by hollow chitosan conduit ( $1.50 \pm 1.73$ ) and Fibrin-collagen ( $1.00 \pm 1.15$ ), where ( $3.00 \pm 0.0$ ) is considered the optimal value that could be obtained in healthy rats. Walking test tract and Toe spread tests were performed for motor recovery

assessment. Inconsistent to the recovery seen at the sensory level, motor recovery was not achieved in all the tested experimental groups, Sciatic functional index (SFI) was found to be  $90.04 \pm 3.5$  in hollow conduits,  $87.75 \pm 5.50$  in fibrin-collagen enriched conduits and  $91.92 \pm 3.31$  in ADMSC-Fibrin-Collagen groups. Toe spread registered  $0.75 \pm 0.96$  for hollow conduit,  $0.00 \pm 0.00$  in Fibrin-Collagen and  $0.25 \pm 0.50$  in ADMSC-Fibrin-Collagen group

### ***Morphological assessment of the distal nerve section***

Toluidine blue semi-thin sections of the rat sciatic nerve distal portion were prepared to evaluate the general morphology of the regenerated nerves following 15 weeks post injury and repair. Consistent with the motor recovery assessment results, Fibrin-Collagen +/- ADMSC did not demonstrate nerve regeneration; moreover, the regenerating nerves did not have a uniform outer circumference. A few number of regenerating fibres with thin myelin were detected in hollow conduit group, hollow conduit regenerating nerves demonstrate uniform outer circumference (Figure 4).

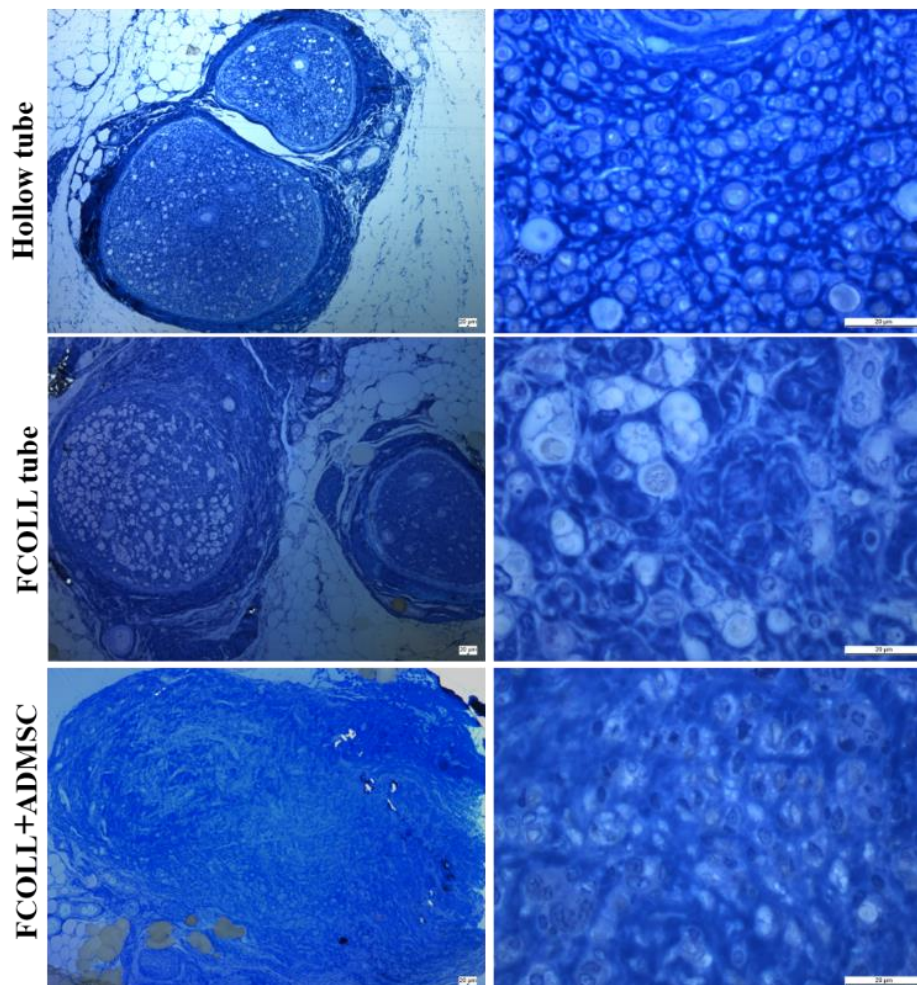


**Figure4.** Morphological analysis of the nerve distal portion 15 weeks following nerve repair. Representative high and low magnification light microscopy images of toluidine blue-stained semi-thin cross sections of nerve repaired with hollow tube, fibrin-collagen and fibrin-collagen + ADMSC (10x and 100x, scale bar =20  $\mu$ m).

### Degree of Muscular atrophy

The denervation of muscles induces their atrophy, a condition of noticeable muscle mass reduction (loss of balance between protein synthesis and protein degradation) accompanied by loss of muscle function. The degree of muscle atrophy was calculated in all the experimental groups at the different time points. As expected, there was a progressive decrease in muscle wet weight and volume with the increase of time. No significant differences were observed between the different experimental groups at the same tested time point (Figure 5).

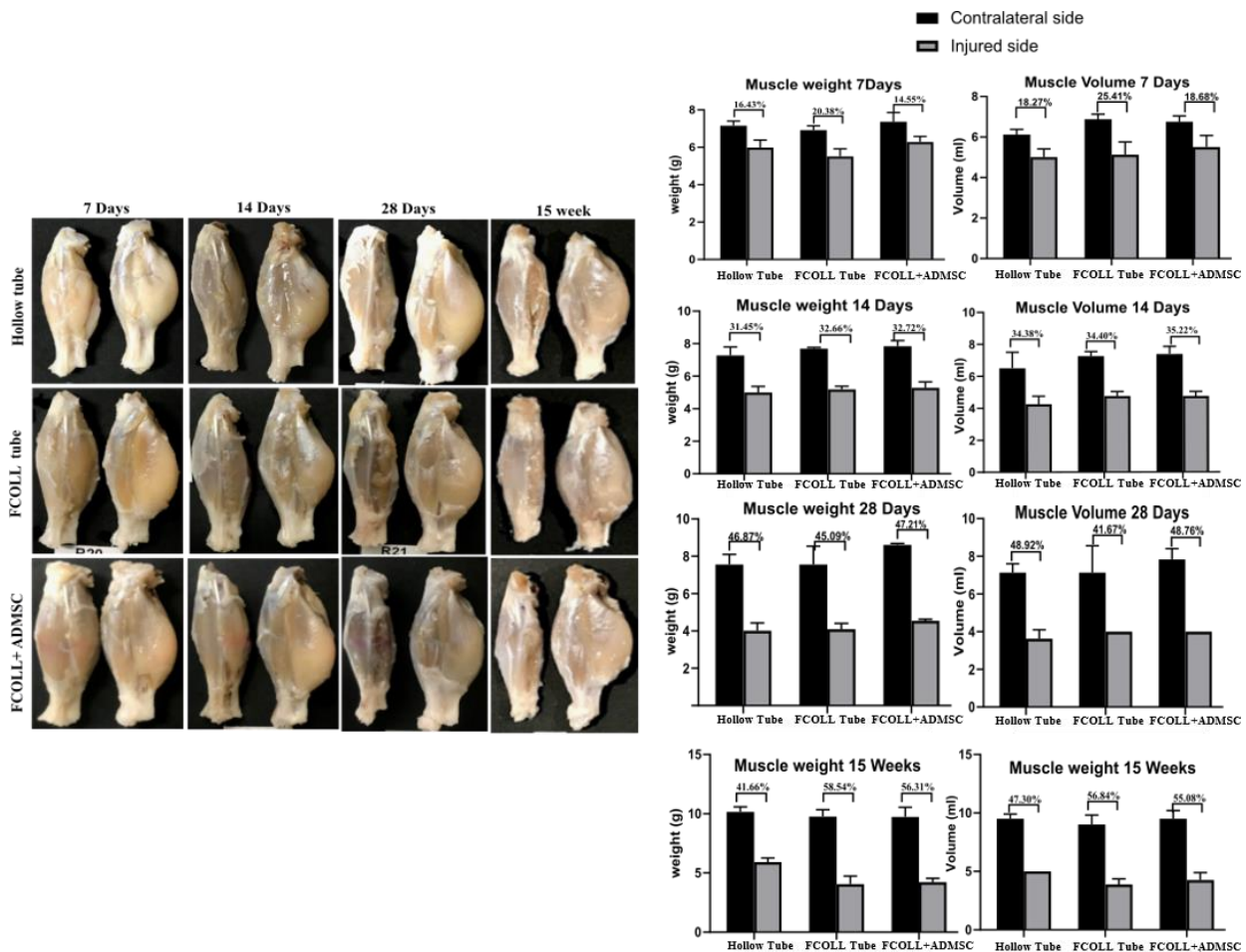


**Figure5.** Degree of muscle atrophy. Graphic representation of the weight and volume changes after peripheral nerve repair for hindlimb muscles at 7, 14, 28 days and 15 weeks. The injured limbs are shown in grey whereas the contralateral limb in black for the muscle volume and weight.

## ***Discussion***

Different strategies to repair peripheral nerve injuries have been developed with the aim to provide the injured environment with tissue engineered solutions that biomimic the nerve nature environment (Carriel et al., 2014). Hollow conduits have proved their efficiency in repairing short nerve defects with comparable results to autograft. Therefore, enriching the hollow conduit lumen with naturally derived hydrogels and cellular component was found to be a promising strategy to improve the efficacy of conduits in repairing longer nerve defects, which are more challenging (Daly et al., 2012; Dietzmeyer, 2020). In this study we investigated repairing a critical rat sciatic nerve defect (15mm) using hollow chitosan conduit, enriched with fibrin-collagen biohybrid hydrogel and its combination with ADMSC. The gene expression analysis was tested at 7, 14 and 28 days, while at 15 weeks samples were fixed for morphological analysis and regeneration assessment. We hypothesized that the combination of two ECM proteins, collagen - that is the most abundant protein constituent of all tissues - and fibrin -that is highly released in response to injury and acts as a basic transient ECM protein that later becomes substituted - could have a useful and promoting effect on regeneration (Alovskaya et al., 2007).

Our results show that while both fibrin-collagen +/- ADMSC can upregulate the expression of sNRG1, thus the main effect could be attributed to the fibrin and collagen gel combination itself and not to the ADMSC addition, ADMSC group was only able to upregulate ErbB2 receptor expression on RNA level. Thus, we can suggest that the addition of ADMSC can have a positive effect in modulating NRG1-ErbB signalling system.

Transcription to be regulated differently in each group. Krox20 expression was significantly lower in factors playing a key role in myelination as Krox20, c-Jun and ATF3 were found all tested groups compared to control. Jun and ATF3 were only significantly upregulated with ADMSC groups, highlighting the potential advantage of cell addition in having a superior modulation of transcription factors and signalling molecules in the nerve injured environment. Cellular populations of immature SC and fibroblasts were found to highly colonize the hollow chitosan conduit; this could be attributed to the ease of entrance, while the hydrogel filler presence might somehow limit their intra-conduit invasion. Fibroblasts have a higher penetration ability compared to immature SC as they were significantly present in both fibrin-collagen +/-ADMSC groups.

Recently, more attention has been focused on the direct relationship between angiogenesis and



nerve regeneration (Cattin et al., 2015), as vascular system provides the injury site with some nutritional and trophic factors that help the development of nervous tissue (Caillaud et al., 2019). VEGF-A expression was highly upregulated at 7 days in the ADMSC group, consistently with the observation that ADMSC secrete VEGF (Fraser et al., 2006). The overall increase in VEGF-A could be predictive of a better angiogenesis and better vascularization.

15 weeks post injury and repair was chosen as a late time point for evaluating the functional recovery. Pinch test was performed to evaluate the sensitive functional recovery, while Toe spread and walking tract were used to evaluate motor functional recovery. All experimental groups demonstrated sensory recovery with the FCOLL + ADMSC group registered the best sensory recovery. Nevertheless, all the experimental groups showed very poor motor recovery; this was consistent with the analysis of semi-thin section where just few regenerated nerves could be seen. This could indicate that the sensory nerves tend to regenerate better compared to motor nerves. The addition of ADMSC could promote the sensitive fibre regeneration or maybe it could promote collateral sprouting from other near nerves that recover the sensitive functionality, indeed it was found that the saphenous nerve could be an alternative source of sensory reinnervation in animals with failed sciatic regeneration (Rupp et al. 2007).

The poor motor recovery could be attributed to the fact that the presence of the hydrogels has acted as a physical barrier and did not allow regenerating axons to infiltrate inside, as was mentioned before in other studies (Dietzmeyer et al., 2020; Meyer et al., 2016), but since a poor number of regenerating fibres was also found in hollow conduits, this could indicate that the time point chosen was not enough for regenerating nerves to reach the distal stump. Nevertheless, Electromyography analysis would have been more accurate for evaluating the level of regeneration, due to the current Covid situation and extreme limitation in entering the animal facility, it was not possible to perform it.

To better understand whether 15 weeks was too early to appreciate differences in the distal portion among the different experimental groups, we are analysing the regenerated part inside the hollow tube (work in progress).

## References

- Alovskaya, a, Alekseeva, T., Phillips, J. B., King, V., & Brown, R. (2007). Fibronectin, Collagen, Fibrin-Components of Extracellular Matrix for Nerve regeneration. *Topics in Tissue Engineering*, 3, 1–27.
- An, S., Zhou, M., Li, Z., Feng, M., Cao, G., Lu, S., & Liu, L. (2018). Administration of CoCl<sub>2</sub> Improves Functional Recovery in a Rat Model of Sciatic Nerve Transection Injury. *International Journal of Medical Sciences*, 15, 1423–1432.
- Bergmeister, K. D., Große-hartlage, L., Daeschler, S. C., Cker, A. B., Beyersdorff, M., Olaf, A. K., ... Harhaus, L. (2020). Acute and long-term costs of 268 peripheral nerve injuries in the upper extremity. *PLoS ONE*, 15(4), 1–12.
- Caillaud, M., Richard, L., Vallat, J. M., Desmoulière, A., & Billet, F. (2019). Peripheral nerve regeneration and intraneural revascularization. *Neural Regeneration Research*, 14(1), 24–33.
- Carriel, V., Alaminos, M., Garzón, I., Campos, A., & Cornelissen, M. (2014). Tissue engineering of the peripheral nervous system. *Expert Review of Neurotherapeutics*, 14(3), 301–318.
- Carriel, V., Garzón, I., Campos, A., Cornelissen, M., & Alaminos, M. (2014). Differential expression of GAP-43 and neurofilament during peripheral nerve regeneration through bio- artificial conduits. *J Tissue Eng Regen Med*.
- Carvalho, C. R., Oliveira, J. M., & Reis, R. L. (2019). Modern Trends for Peripheral Nerve Repair and Regeneration : Beyond the Hollow Nerve Guidance Conduit. *Front. Bioeng. Biotechnol.* 7:337, 7(337 November), 1–30.
- Cattin, A. L., Burden, J. J., Van Emmenis, L., MacKenzie, F. E., Hoving, J. J. A., Garcia Calavia, N., ... Lloyd, A. C. (2015). Macrophage-Induced Blood Vessels Guide Schwann Cell-Mediated Regeneration of Peripheral Nerves. *Cell*, 162(5), 1127–1139.
- Chato-astrain, J., Campos, F., Roda, O., Miralles, E., Durand-herrera, D., Sáez-moreno, J. A., ... Carriel, V. (2018). In vivo Evaluation of Nanostructured Fibrin-Agarose Hydrogels With Mesenchymal Stem Cells for Peripheral Nerve Repair. *Front. Cell. Neurosci*, 12:501(December), 1–19.
- Daly, W., Yao, L., Zeugolis, D., Windebank, A., & Pandit, A. (2012). R EVIEW A biomaterials approach to peripheral nerve regeneration : bridging the peripheral nerve gap and enhancing functional recovery. *J. R. Soc. Interface*, 9, 202–221.
- Dietzmeier, N., Förthmann, M., Grothe, C., & Haastert-Talini, K. (2020). Modification of tubular chitosan-based peripheral nerve implants: Applications for simple or more complex approaches. *Neural Regeneration Research*, 15(8), 1421–1431.
- Fornasari, B. E., Carta, G., Gambarotta, G., & Raimondo, S. (2020). Natural-Based Biomaterials for Peripheral Nerve Injury Repair. *Front. Bioeng. Biotechnol*, 8:554257(October).
- Fraser, J. K., Wulur, I., Alfonso, Z., & Hedrick, M. H. (2006). Fat tissue: an underappreciated source of stem cells for biotechnology. *Trends in Biotechnology*, 24(4), 150–154.
- Freier, T., Koh, H. S., Kazazian, K., & Shoichet, M. S. (2005). Controlling cell adhesion and degradation of chitosan films by N-acetylation. *Biomaterials*, 26(29), 5872–5878.
- Gambarotta, G., Garzotto, D., Destro, E., Mautino, B., Giampietro, C., Cutrupi, S., ... Perroteau, I. (2004). ErbB4 Expression in Neural Progenitor Cells ( ST14A ) Is Necessary to Mediate Neuregulin-1  $\beta$ 1 induced Migration \*. *The journal of biological chemistry*, 279(47), 48808–48816.
- Gambarotta, G., Ronchi, G., Friard, O., Galletta, P., Perroteau, I., & Geuna, S. (2014). Identification

- and Validation of Suitable Housekeeping Genes for Normalizing Quantitative Real-Time PCR Assays in Injured Peripheral Nerves. *9*(8), 1–7.
- Gonzalez-Perez, F., Udina, E., & Navarro, X. (2013). Extracellular Matrix Components in Peripheral Nerve Regeneration. In *Tissue Engineering of the Peripheral Nerve: (1st ed., Vol. 108)*.
- Haastert-Talini, K., Geuna, S., Dahlin, L. B., Meyer, C., Stenberg, L., Freier, T., ... Grothe, C. (2013). Chitosan tubes of varying degrees of acetylation for bridging peripheral nerve defects. *Biomaterials*, *34*(38), 9886–9904.
- Höke, A. (2006). Mechanisms of Disease : what factors limit the success of peripheral nerve regeneration in humans ? *Nature clinical practice neurology* *2*(8), 448–454.
- Kingham, P. J., & Terenghi, G. (2006). Bioengineered nerve regeneration and muscle reinnervation. *Anatomical Society of Great Britain and Ireland*, *209*, 511–526.
- Koopmans, G., Hasse, B., & Sinis, N. (2009). Chapter 19 - The Role of Collagen in Peripheral Nerve Repair. In *International Review of Neurobiology (1st ed., Vol. 87)*.
- Livak, K. J., & Schmittgen, T. D. (2001). Analysis of Relative Gene Expression Data Using Real-Time Quantitative PCR and the  $2^{-\Delta\Delta CT}$  Method. *Methods*, *25*, 402–408.
- Meyer, C., Wrobel, S., Raimondo, S., Rochkind, S., Heimann, C., Shahar, A., ... Haastert-Talini, K. (2016). Peripheral nerve regeneration through hydrogel-enriched Chitosan conduits containing engineered Schwann cells for drug delivery. *Cell Transplantation*, *25*(1), 159–182.
- Modrak, M., Talukder, M. A. H., Gurgenshvili, K., Noble, M., & Elfar, J. C. (2019). Peripheral nerve injury and myelination : Potential therapeutic strategies. *J Neuro Res.* (September), 1–16.
- Pfister, B. J., Gordon, T., Loverde, J. R., Kochar, A. S., Mackinnon, S. E., & Cullen, D. K. (2011). Biomedical Engineering Strategies for Peripheral Nerve Repair : Surgical Applications , State of the Art , and Future Challenges. *Critical Reviews<sup>TM</sup> in Biomedical Engineering*, *39*(2), 81–124.
- Ronchi, G., Haastert-talini, K., Fornasari, B. E., Perroteau, I., Geuna, S., & Gambarotta, G. (2016). The Neuregulin1 / ErbB system is selectively regulated during peripheral nerve degeneration and regeneration. *European Journal of Neuroscience*, *43*(June), 351–364.
- Rupp, A., Dornseifer, U., Rodenacker, K., Fichter, A., Jütting, U., Gais, P., ... Matiassek, K. (2007). Temporal progression and extent of the return of sensation in the foot provided by the saphenous nerve after sciatic nerve transection and repair in the rat - Implications for nociceptive assessments. *Somatosensory and Motor Research*, *24*(1–2), 1–13.
- Safa, B., & Buncke, G. (2016). Autograft substitutes Conduits and processed nerve allografts. *Hand Clinics*, *32*(2), 127–140.
- Seyed-foootan, K., Karimi, H., Jafarian, A., Farzad, N. S., Ravari, K., & Karimi, A. (2019). Nerve Regeneration and Stem Cells. *Biomed J Sci & Tech Res* *18*(3)-2019., *18*(3), 13540–13545.
- Siemionow, M., Duggan, W., Brzezicki, G., Klimczak, A., Grykien, C., Gatherwright, J., & Nair, D. (2011). Peripheral Nerve Defect Repair With Epineural Tubes Supported With Bone Marrow Stromal Cells. *Annals of Plastic Surgery*, *67*(1), 73–84.
- Víctor Carriel, Juan Garrido-Gomez, P. H.-C. ´es´, Ingrid Garzon, Salome García-García, J. A. S. ´ aez-M. ´, Mar´ia del Carmen Sanchez-Quevedo, A. C., & Alaminos, and M. (2013). Combination of fibrin-agarose hydrogels and adipose-derived mesenchymal stem cells for peripheral nerve regeneration. *J. Neural Eng.*, *10*(026022), 1–14.
- Wang, C., Lu, C., Peng, J., Hu, C., & Wang, Y. (2017). Roles of neural stem cells in the repair of peripheral nerve injury. *Neural Regeneration Research*, *12*(12), 2106–2112.

## *Chapter 6*

*Comparison of decellularization protocols  
to generate peripheral nerve grafts: a  
study on rat sciatic nerves*

## Comparison of decellularization protocols to generate peripheral nerve grafts: a study on rat sciatic nerves

**Marwa El Soury**<sup>1,2,3\*</sup>, Óscar Darío García-García<sup>3,4\*</sup>, Matteo Moretti<sup>5,6</sup>, Isabelle Perroteau<sup>1</sup>, Stefania Raimondo<sup>1, 2§</sup>, Arianna Barbara Lovati<sup>5#</sup>, Víctor Carriel<sup>3,4#</sup>.

*1 Department of Clinical and Biological Sciences, University of Torino, Torino, Italy*

*2 Neuroscience Institute Cavalieri Ottolenghi (NICO), University of Torino, Torino, Italy*

*3 Department of Histology, Tissue Engineering Group, University of Granada, Granada, Spain*

*4 Instituto de Investigacion Biosanitaria, Ibs.Granada, Granada, Spain*

*5 Cell and Tissue Engineering Laboratory, IRCCS Istituto Ortopedico Galeazzi, Milan, Italy*

*6 Regenerative Medicine Technologies Lab, Ente Ospedaliero Cantonale, Lugano, Switzerland*

*\* These authors have contributed equally to this work and share first authorship*

*# These authors share senior authorship*

*§Corresponding Author: Stefania Raimondo*

Published in Journal of Molecular Sciences. 2021; 22(5):2389.

DOI: <https://doi.org/10.3390/ijms22052389>

**Abstract**

In critical nerve gap repair, decellularized nerve allografts are considered a promising tissue engineering strategy that can provide superior regeneration results compared to nerve conduits. Decellularized nerves offer a well-conserved extracellular matrix component that has proven to play an important role in supporting axonal guiding and peripheral nerve regeneration. Up to now, the known decellularized techniques are time and effort consuming. The present study, performed on rat sciatic nerves, aims at investigating a novel nerve decellularization protocol able to combine an effective decellularization in short time with a good preservation of the extracellular matrix component. To do this, a decellularization protocol proven to be efficient for tendons (DN-P1) was compared with a decellularization protocol specifically developed for nerves (DN-P2). The outcomes of both the decellularization protocols were assessed by a series of *in vitro* evaluations, including qualitative and quantitative histological and immunohistochemical analyses, DNA quantification, SEM and TEM ultrastructural analyses, mechanical testing and viability assay. The overall results showed that DN-P1 could provide promising results if tested *in vivo* as the *in vitro* characterization demonstrated that DN-P1 conserved a better ultrastructure and ECM components compared to DN-P2. Most important DN-P1 showed to be highly biocompatible, supporting a greater number of viable metabolically active cells.

**Keywords:** Peripheral nerves; decellularization; acellular; regeneration; orthopedic trauma; extracellular matrix

## ***Introduction***

Despite of the known innate capacity of peripheral nerves to regenerate injuries, in most of the cases, the desired complete functional recovery is seldomly achieved. Numerous factors govern the successfulness of nerve regeneration, of which the severity of the injury plays a key role. In 1947, Seddon classified peripheral nerve injuries into three grades of severity: Neuropraxia, Axonotmesis and Neurotmesis. While the first two types of injury can regenerate spontaneously, in neurotmesis surgical intervention is usually required (Seddon, 1943). In 1951, a more detailed and accurate nerve injury classification was made by Sunderland, where Type I corresponds to Neuropraxia, Types II, III, IV are equivalent to Axonotmesis, Types V, VI to Neurotmesis and mixed grades of nerve injury (Sunderland, 1951). In the case of Neurotmesis injuries, where the nerve continuity is completely disrupted, the repairing strategy is adopted depending whether the injury is accompanied by nerve substance loss or not.

In simple nerve transections unaccompanied by substance loss, tensionless direct surgical neurorrhaphy is the optimal choice. When tensionless epineural neurorrhaphy is impossible; nerve scaffolds must be used to join the transected nerve stumps (Siemionow & Brzezicki, 2009). In this case, autografts are considered the gold standard technique. Unfortunately, despite providing optimal results concerning nerve regeneration and subsequent functional recovery, this technique is associated with numerous drawbacks, i.e. limited availability, two-step surgery, loss of sensitivity, donor site morbidity, and neuroma formation at the donor nerve site (Carriel et al., 2014).

To overcome this problem, attention was drawn to find other alternatives to join the two distant nerve stumps. With this scope and by the aid of tissue engineering techniques, various nerve scaffolds were obtained, including nerve guidance conduits of both natural and synthetic origins. Non-nervous tissues, including tendon, vein, artery and muscular scaffolds were also used for nerve repair, as well as allografts (Grinsell & Keating, 2014). Providing nerve allograft from cadaver donors was thought to be a suitable alternative to autografts, but concurrent immunosuppressive treatments are required to prevent adverse immune reactions and subsequent graft rejection (Siemionow & Sonmez, 2007). Eliminating the cellular antigens while conserving the nerve extracellular matrix (ECM) and its structure was the main goal behind decellularization techniques.

Tissue decellularization can be achieved by combining physical factors with different chemical and biological factors. Various physical agents such as tissue exposure to thermal change, agitation and ultrasonic waves can help in the process of decellularization. Changing

temperatures through repeated cycles of freezing and thawing can effectively lyse the cells, but the membranous and cellular remains need subsequent processing for an effective removal. Hence, the combination of different chemical, biological and physical factors is commonly required (Crapo et al., 2011; Hudson et al., 2004; Sondell et al., 1998; Zilic et al., 2016).

Chemical factors include the use of acidic and basic solutions that catalyze the hydrolytic degradation of biomolecules. Hypo- and hypertonic solutions cause cell lysis by changing the cell osmotic pressure. Detergents including ionic, non-ionic, and zwitterionic ones solubilize cell membranes and remove cellular material from tissues. Organic solvents are also used, such as Tributyl phosphate (TBP) that demonstrated to be more effective in decellularizing dense tissues as tendons compared to other detergents like Triton-X100 and Sodium dodecyl sulfate (SDS) (Bottagisio et al., 2016). Biological agents mainly include enzymes (nucleases, chondroitinase ABC, trypsin, collagenase), in particular, DNase and RNase are used to complete the removal of nucleic acid remained in the tissue. However, an insufficient removal of chemical detergents from the processed tissue can result in high cytotoxicity, as also reported elsewhere (Lovati et al., 2016). Therefore, extensive washing of chemical detergents should be considered, or other solutions can be employed, such as peracetic acid. Indeed, Peracetic acid (PAA) has been commonly reported as a potent oxidizing agent used to sterilize collagen tissues (Gilbert et al., 2006), while enhancing the tissue permeability for the detergent penetration (Deeken et al., 2011; Whitlock et al., 2007; Woon et al., 2011; Woon et al., 2012; Raghavan et al., 2012; Schmitt et al., 2013). Thanks to the PAA activity, the total amount and concentration of detergents could be drastically reduced (Lovati et al., 2016), thus decreasing also the presence of remains in the tissues and therefore their potential toxicity.

Decellularized nerves also known as acellular nerve grafts provide the adequate preservation of the internal nerve structure, where endoneurial tubes, basal lamina and laminin remain intact, thus facilitating the process of axonal regeneration. Certainly, during the decellularization process some alterations of the ECM composition and some ultrastructure disruptions would be unavoidable, but a good decellularization method would minimize these undesirable effects. Up to now, three main decellularization protocols are described in the creation of a functional nerve graft: i) the one described by Sondell and colleagues (Triton X-100 and sodium deoxycholate “SDC”)(Sondell et al., 1998) , ii) the protocol described by Hudson and colleagues (Sulfobetaine \_SB-10 and SB-16) (Hudson et al., 2004) the only one patented and available in US market as Avance® Nerve Graft (AxoGen Inc. Alachua, Florida, USA), and iii) the combined Hudson protocol added with chondroitinase ABC by Krekoski and colleagues

---



(Krekoski et al., 2001). However, all these decellularization methods are very long and time-consuming, giving rise to risks of contamination and technical unsuitability (Lovati et al., 2018). A more recent strategy to perform the nerve decellularization has been proposed by Boriani and colleagues (SB-10, TritonX-100 and SDS) (Boriani et al., 2017) with the advantage of speeding up myelin and cellular debris detachment, without detrimental effects on the nerve architecture, and without breaking the aseptic chain.

The aim of the present study is to test a nerve decellularization method that could be less time consuming and require less reagents to minimize the exposure to detergents (Philips et al., 2018a). Moreover, it would be able to combine an effective decellularization in short time with a good preservation of the ECM (Philips et al., 2018a). The investigated protocol combined the use of two main reagents: TBP - to our knowledge firstly described to decellularize nerves - and PAA. TBP was hypothesized to be able to penetrate the compact nerve structure better than other detergents. With the aim to enhance the detergent penetration and to achieve the sterilization of the decellularized nerves, the use of the PAA has been planned too. Although the use of the PAA showed very promising outcomes in several tissue decellularization processes (Lovati et al., 2018), its efficacy still needs to be further analyzed for the nerve decellularization, since it has been barely described in the literature as a disinfectant agent (Cai et al., 2017; Sridharan et al., 2015). The PAA was previously tested to decellularize tendon xenografts, demonstrating a good efficacy (Bottagisio et al., 2016). Since both nerves and tendons are scarcely permeable, it was hypothesized that the use of this promising decellularization protocol for nerves could efficiently produce biocompatible and well-structured acellular nerve allografts.

To evaluate and compare the efficacy of our protocol to decellularize peripheral nerves, another previously published decellularization protocol specifically developed for this tissue (Boriani et al., 2017) has been used as control.

## ***Materials and Methods***

### ***Sciatic Nerve harvesting***

A total number of 14 adult 3-month-old female Wistar rats weighing 200-250 g (Envigo) were euthanized in carbon dioxide chambers. Rats were placed on dissecting board in dorsal recumbency to expose sciatic nerves. Briefly, a longitudinal incision was performed with a

scalpel blade from the knees to the pelvis, exposing the underneath muscles. By blunt dissection, the gluteus maximus and biceps femoris muscles were split to expose the entire length of the sciatic nerve. Muscles were further cut horizontally reaching the spinal cord and vertically upward separating the external oblique muscle from the spinal cord. The sciatic nerves were isolated from surrounding connective tissues and cut starting from the lumbosacral region to their terminal branches, thus yielding a total length ranging from 25 to 30 mm (Tao, 2013). The study was conducted according to the guidelines of the Animal Care and Use Committee (IACUC) of the University of Turin (Permit N. 864/2016-PR) approved on 14/9/2016.

### ***Decellularization Protocols***

Nerves were distributed into three main groups (n=9 each), untreated nerves serving as controls while the other groups received two different decellularization treatments: DN-P1) 1 % tri (n-butyl) phosphate (TBP) followed by 3 % peracetic acid (PAA) as described in a successful decellularization protocol developed for tendons as previously published (Bottagisio et al., 2016); DN-P2) 125mM sulfobetaine-10 (SB-10), 0.2% TritonX-100 followed by 0.25% sodium dodecyl sulfate (SDS) as a decellularization protocol specifically described for nerves (Boriani et al., 2017).

Following the decellularization treatments, nerves were cut into pieces 10 mm each and were randomly assigned for subsequent analyses (n=3 for each analysis). To assess the mechanical properties, the whole nerve was used, ranging from 25 mm to 30 mm length (n=3).

Briefly, in DN-P1, nerves were immediately dry-frozen at  $-80^{\circ}\text{C}$  until processing. Then, the specimens were thawed in Phosphate Buffer Solution without sodium and magnesium (PBS-/-) at RT for 30 min. The decellularization started immersing nerves in 1% TBP in 1 M Tris-HCl pH 7.8 solution at RT for 24 h under agitation, then rinsing twice in ddH<sub>2</sub>O for 15 min. To remove detergents, nerves were moved to PBS-/- at  $4^{\circ}\text{C}$  for 24 h, followed by a 4 h treatment with 0.0025% DNase-I at RT under agitation. After washing twice in ddH<sub>2</sub>O for 15 min and in PBS -/-, the nerves were incubated at RT in 3 % PAA under agitation for 4 h. The final step consisted in double washes in ddH<sub>2</sub>O and PBS -/- for 15 min each.

In DN-P2, nerves were immediately incubated in PBS solution containing 125 mM SB-10, 0.2% TritonX-100, 1% penicillin/streptomycin under agitation for 48 h at RT, then dry-frozen at  $-80^{\circ}\text{C}$  until processing. After thawing, nerves were washed three times in PBS for 30 min and moved to 0.25% SDS in PBS solution under agitation for 30 min followed by 5 min

sonication cycle at 40Hz. The last two steps were repeated five times, followed by three washes in PBS for 30 min.

All decellularized nerves were stored at 4°C in PBS supplemented with a ready-to-use commercially available antibiotic antimycotic solution (penicillin, streptomycin and amphotericin B) until use. All reagents were bought from Sigma-Aldrich (Sigma Aldrich, Steinheim, Germany) unless otherwise specified.

### ***Histology and immunohistochemistry***

For paraffin embedding, samples were fixed in 10% formalin solution for 48 h, and then dehydrated in ascending ethanol gradients, as standard. Briefly, the samples were treated 1 h with 70% ethanol, then three 1 h passages in 95% ethanol, and three 1 h passages in 99% ethanol, one passage in Xylene for 30 min followed by two more Xylene passages of 45 min each; finally, three passages in paraffin wax 60°C, 1 h each. Then, nerve orientation was checked before the paraffin embedding, 5 µm sections were prepared. Hematoxylin & Eosin (HE) staining was performed to assess the morphology and general structure of the nerves, proteoglycans and collagen were evaluated by Alcian Blue and Picrosirius red staining, respectively. The evaluation of myelin and collagen reorganization pattern was performed using MCOLL method following a previously described protocol (Carriel et al., 2017; Chato-Astrain et al., 2018).

For immunohistochemical analyses, sections were incubated overnight at 4°C with antibodies against basal membrane laminin (1:1000) (L8271, Sigma Aldrich, Steinheim, Germany), axonal neurofilaments (1:500) (approx.160 and 200 kDa\_ NF-M/H\_ intermediate filament) (N2912, Sigma Aldrich, Steinheim, Germany), vimentin (53kDa\_ type III intermediate filament) for fibroblasts (1:200) (V6630, Sigma Aldrich, Steinheim, Germany), and S-100 (S100B, S100A1 and S100A6) protein for Schwann cells (1:400) ( Z0311, DakoCytomation, Glostrup, Denmark ) as previously described (Philips et al.,2018a; Philips et al., 2018b). Negative controls (no primary antibody) were prepared to avoid non-specific staining. Secondary antibodies ImmPRESS IgG Rabbit (MP-7401, Vector Laboratories, Burlingame, EEUU) and Mouse (MP-7402Vector Laboratories Burlingame, EEUU,) were used. For the specific nuclear DNA detection, 4',6-diamidino-2-phenylindole (DAPI) fluorescent mounting was used and examined with a fluorescence microscope.

### ***DNA extraction and quantification***

DNA assay was performed to quantify the cellular remnants after the decellularization processes. DNA was extracted using the QIAamp® mini kit (Qiagen, Hilden, Germany) following the manufacturer's protocol. Briefly, nerve tissues were lysed by adding the provided kit ATL buffer and proteinase K at 56 °C for 3 h. Then, the second kit buffer AL was added, and samples were incubated at 70 °C for 10 min. After centrifuging, absolute ethanol was added. The whole mixture was then moved to QIAamp mini spin column, centrifuged at 6000 xg for 1 min, the flow through and the collection tubes were discarded and the QIAamp mini spin column was placed in a new collection tube, and kit buffer AW1 was added. The tube was centrifuged at 600 xg for 1 min and flow-throw and collection tube was discarded. Kit buffer AW2 was added to the column and centrifuged at full speed for 3 min. As recommended by the manufacturer, the column was centrifuged for an extra minute at full speed to eliminate any Buffer remaining. Finally, to elute DNA from the column, kit buffer AE was incubated at RT for 1 min followed by 6000 xg centrifugation for 1 min.

For each sample, DNA concentration was detected by a NanoDrop 2000 spectrophotometer (Thermo Fisher Scientific, Waltham, MA, USA), 5 measures were taken for each tested sample, the measurements were then normalized to the original dry weight of the samples before extraction.

### ***Ultrastructural Analyses***

For scanning electron microscope (SEM), samples were fixed in 2.5% glutaraldehyde 0.05M cacodylate buffer (pH 7.2) for 6 h at 4 °C, followed by 3 washes in cacodylate buffer at 4 °C, then fixed in osmium tetroxide for 1 h at 4 °C, and dehydrated in increasing acetone concentrations 30%, 50%, 70% and 90% for 15 min each at 4 °C. The last two concentrations of 96% and 100% acetone lasted 25 min each, and samples were subjected to critical point drying (CPD) where acetone present in the samples is exchanged with liquid carbon dioxide (CO<sub>2</sub>), which undergoes a phase transition to gas in a pressurized chamber. Finally, the samples were mounted on SEM specimen stubs by means of carbon based electrically conductive double-sided adhesive discs, and sputter coated with gold. Images were acquired using FEI Quanta 200 environmental scanning electron microscope (FEI Europe, Eindhoven, Netherlands) (Philips et al., 2018b).

For Transmission electron microscope (TEM), samples were embedded in resin. Specifically, samples were fixed in 2.5% glutaraldehyde followed by 2 h post fixation in 2% osmium

tetroxide; later samples were dehydrated by fully immersing in ascending ethanol gradients (30%, 50%, 70%, 80%, 95% and 100%). As ethanol is immiscible with resin and to be totally removed, samples were treated twice with a transitional solvent of propylene oxide for 7 min. Finally, samples were left 1 h in a pre-infiltration solution of equal parts of propylene oxide and Glauerts resin mixture (Araldite M and Araldite Harter, HY 964 in the ratio 1:1, 0.5% dibutyl phthalate plasticizer, plasticizer is added to reduce resin viscosity and hence allow better embedding medium infiltration into the specimen, it also improves the final block sectioning) and overnight in the Glauerts resin mixture. Then, 2% accelerator DMP-30 was used to promote the polymerization of the resin embedding medium, and samples were incubated in oven at 60 °C for 2-3 days. Later 2.5 mm semi-thin sections and 70 nm ultrathin sections were prepared using an Ultracut UCT ultramicrotome (Leica Microsystems, Wetzlar, Germany). Semi-thin sections were attached to normal glass slide and stained with 1% toluidine blue for high resolution light microscopy examination using a DM4000B microscope equipped with a DFC320 digital camera and an IM50 image manager system (Leica Microsystems, Wetzlar, Germany). Ultrathin sections were collected on a pioloform coated grid. The day after, specimens were counterstained using a solution of uranyl acetate replacement (Electron Microscopy Sciences Hatfield, PA, USA) and analyzed by means of a JEM-1010 transmission electron microscope (JEOL, Tokyo, Japan) equipped with a Megaview-III digital camera and a Soft-Imaging-System (SIS, Münster, Germany). Images were acquired for different sections at different magnifications (Ronchi et al., 2014).

### ***Biomechanical characterization***

Biomechanical response of decellularized nerves were assessed to determine the effect of the decellularization process on their elastic and tensile properties, as previously described (Carriel et al., 2017; Philips et al., 2018b). The test was performed using an electromechanical testing apparatus Instron 5943 (Instron, Needham, MA, USA) using the software Bluehill 3.62 with a 50N charge cell load. Nerves were clamped at 10 mm distance; a tensile uniaxial stress was applied to the nerves using pre-set parameters of constant strain rate 10 mm/min. Tensile strength was applied to the nerve until its failure was achieved. Young's modulus (MPa), stress of fracture (MPa), strain of fracture (%) and extension at fracture (mm) were measured.

---

### *Cell-biomaterials interactions analyses*

To evaluate the cytotoxicity of the decellularized nerves, as consequence of the decellularization procedures (residual detergents), rat adipose-derived mesenchymal stem cells (rADMSCs) were used. Cells were seeded on the inner surface of decellularized nerves and their morphology, viability and cellular metabolic activity were determined using the LIVE/DEAD™ Viability/Cytotoxicity Kit (L/D) (# L3224, Thermo-Fisher Scientific, Portland, OR, USA) (Philips et al., 2018b) and W ST-1 assay (Roche, Mannheim, Germany) respectively as previously described (Durand-Herrera et al., 2018).

For these analyses, 24 multi well plates were pre-coated with agarose type I to target the cell adherence and growth onto the decellularized nerves and prevent their possible adherence to the well bottom. A longitudinal incision was made along the whole nerve length and was opened and placed flatly on the pre-prepared agarose surface. Then,  $2 \times 10^4$  rADMSCs (passage 7) were seeded on the inner nerve surface of each decellularized nerve, then cultured in complete Dulbecco's modified Eagle's medium (DMEM, 10% FBS, 1% of commercial ready Antibiotic Antimycotic mix, all from Sigma-Aldrich # D6429, F7524, A5955 respectively (Sigma-Aldrich, Steinheim, Germany)), and incubated under normal culture conditions (37 °C, 5% CO<sub>2</sub>, 95% humidity). After 48 h of incubation, the medium was removed, and cells were rinsed once with PBS.

L/D assay was conducted according to manufacturer's instructions. In this sense, 300 µl of calcein AM and ethidium homodimer-1 mixture was added to each cell culture and incubated for 15 min. Finally, cells were observed using Nikon Eclipse Ti fluorescence equipped with a Nikon DXM 1200c Digital Camera (Nikon, Tokyo, Japan). Viable and metabolically active cells incorporated the supravital fluorochrome calcein and appeared green, while dead cells, with irreversible cell membrane damage, incorporated the ethidium fluorochrome and emitted a red nuclear fluorescence.

For WST-1 (water-soluble tetrazolium salt-1) a colorimetric biochemical assay was conducted. This method allows to quantify the activity of the mitochondrial dehydrogenase, which cleavages tetrazolium salt into formazan, demonstrating the presence of viable and metabolically active cells. The greater the number of viable cells, the greater the amount of the formazan produced. Following manufacturer instructions, seeded cells on nerves were incubated in 450 µl of WST-1 working solution for 4 h under standard culture conditions. In 96 well plate, the total incubated solution for each nerve (n=3) was distributed into 4 wells of

100 µl each (4 readings/each nerve). Absorbance was measured at 450 nm by means of ASYS UVM340 spectrophotometer using the DigiRead software (Biocrom Ltd., Cambridge, UK). In both methods  $2 \times 10^4$  rADMSCs were seeded in non-coated wells as 2D positive or negative technical controls. To generate 2D negative control, an irreversible cell-membrane and nuclei damage was induced using 2% Triton X-100. WST-1 obtained values from both tested groups DN-P1 and DN-P2 were normalized to 2 D positive control where it represents 100% viability (García-García et al., 2021).

### ***Semi-quantitative histological and immunohistochemical analysis***

Semi-quantitative analyses were performed on histochemically or immunohistochemically stained sections. In this sense, ImageJ software (National Institute of Health, Bethesda, MD, USA) was used to select the adequate color threshold. Once positive reactions were isolated, the percentage of area occupied by each histochemical or immunohistochemical reaction (or area fraction) was measured as previously described (Carriel et al., 2014). For each positive reaction, color threshold selection was chosen using the adequate Hue value and the saturation and intensity was optimized for native samples. The same parameters were then followed for the decellularized samples. The percentage of positive stained area were calculated in function of the entire nerve area at 10x. For these analyses, 3 independent nerve samples were measured per each staining for natives and decellularized nerves.

### ***Statistical analysis***

Statistical analyses were conducted using SPSS (SPSS Inc., Chicago, IL, USA). Comparison between two different independent groups were analyzed using the nonparametric Mann-Whitney U test. Analyses were performed on quantitative and semiquantitative data. In this study,  $p < 0.05$  were considered statistically significant for all two-tailed tests.

## **Results**

### ***Evaluation of nerve general structure and ECM components***

The main aim of the decellularization process is to obtain non-immunogenic nerve scaffolds of natural origin by removing cells and antigens while preserving the functional structure of the tissue. Nerves were histologically and immunohistochemically stained to determine changes in structure and cellular components compared to intact native nerves used as controls.

---

Hematoxylin & eosin staining showed a good conservation of overall nerve structure with DN-P1, in particular, the endoneurium and perineurium appeared well-conserved with visible cylindrical structures. Differently, DN-P2 resulted in a moderate disruption of the endoneurium and perineurium (Figure 1).

At higher magnifications, MCOLL histochemical method, simultaneously stained the myelin and fibrillar collagens, detected a few myelin remnants in nerves treated with DN-P2 but not in those treated with DN-P1 that showed a complete myelin removal (at light microscopy). Collagen was intensely stained in DN-P1, while this histochemical reaction was weaker in DN-P2 (Figure 1).

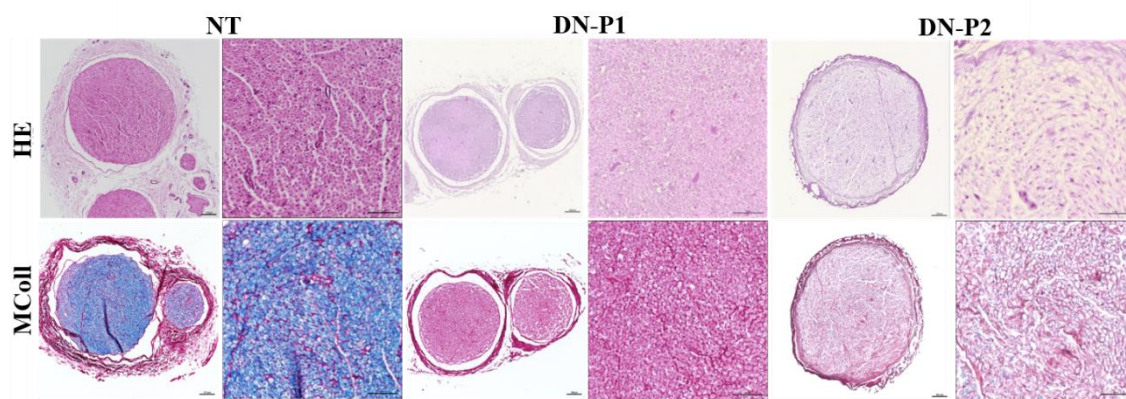


**Figure 1.** Representative panel of native and decellularized rat sciatic nerves reporting the morphological architecture. Sections stained with hematoxylin and eosin (HE) identify the overall nerve histoarchitecture. MCOLL staining shows myelin (blue) and collagen (red) simultaneously. Scale bar= 100 $\mu$ m for lower magnification images and 50 $\mu$ m for higher magnification ones.

Immunohistochemical staining of S100 (Schwann cells) and vimentin (fibroblasts) detected a greater presence of Schwann cell and fibroblast remnants in DN-P1 than in DN-P2 group. The semiquantitative analyses of S100 confirmed the removal of these elements when compared to native nerves, DN-P1 was statistically lower compared to natives and DN-P2 statistically significant compared to both natives and DN-P1 samples. Vimentin semiquantitative analysis did not show significant differences between DN-P1 and native samples, while DN-P2 samples showed a significant vimentin decrease compared to native and DN-P1 nerves.

However, immunohistochemical staining for neurofilament (axons) showed a better removal of these neuronal proteins in nerves treated with DN-P1 compared to those treated with DN-



P2 (Figure 2A). This data was confirmed also by the semiquantitative analysis where DN-P1 was significantly less compared to native and DN-P2 nerves (Figure 2B, C).

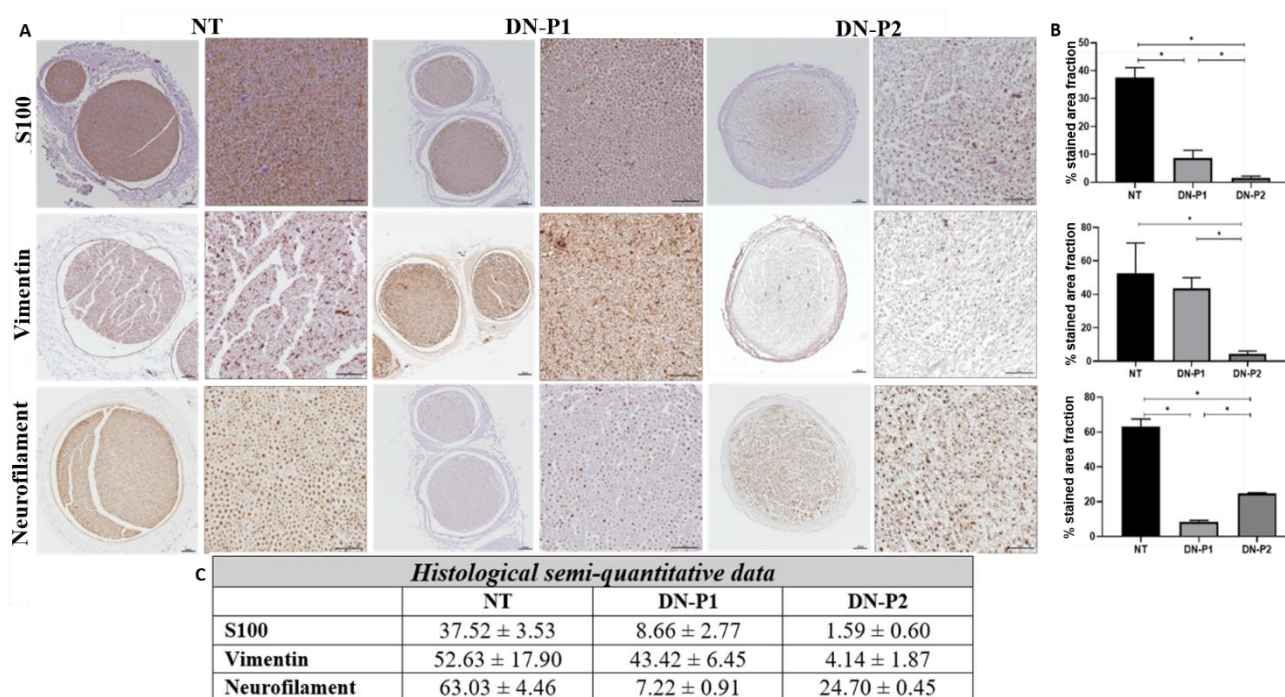


**Figure 2.** Representative immunohistochemical images and semiquantitative results of native and decellularized rat sciatic nerves reporting different cellular components. (A) The immunostaining by S100, Vimentin and Neurofilament show the Schwann cells, fibroblasts and axons, respectively. scale bar = 100 $\mu$ m for lower magnification images and 50 $\mu$ m for higher magnification images. (B) Graphs representing semiquantitative analyses of the % occupied by each immunoreaction normalized to the whole nerve area. (C) Semi-quantitative raw data. \* indicate statistically significant differences ( $p < 0.05$ ).

Conservation of the ECM in decellularized nerve is crucial as they sustain the Schwann cell migration and axonal re-growth. Nerves were histochemically stained with Picrosirius red and Alcian Blue to qualitatively evaluate the presence of collagen and acid proteoglycans, respectively (Figure 3A). The semiquantitative analyses revealed that nerves treated with both protocols resulted in a significantly reduction of the histochemical reaction against collagens as compared to native nerves ( $p < 0.05$ ). No significant differences were observed between both the experimental conditions ( $p = 0.513$ ) (Figure 3B, C). The analysis of the proteoglycans confirmed a clear removal of these non-fibrillar molecules from the epi-, peri- and

endoneurium levels with both the decellularization protocols as compared to native controls ( $p < 0.05$ ). This reduction was more evident and significant in nerves treated with DN-P2 compared to those treated with DN-P1 ( $p < 0.05$ ). Furthermore, the basal membrane glycoprotein laminin was also immunohistochemically identified due to their critical role during regeneration. These results revealed a better preservation of these molecules in nerves treated with DN-P2 compared to DN-P1 treated nerves. However, the organization pattern and distribution, obtained after decellularization, differed with respect to the well-delimited basal membranes observed in native nerves (Figure 3A). Laminin quantitative analyses confirmed the significant reduction of the molecule in nerves treated with DN-P1 than native and DN-P2 nerves ( $p < 0.05$ ). Moreover, no statistical differences were observed in nerves treated with DN-P2 compared to the native condition ( $p = 0.513$ ) (Figure 3B, C).

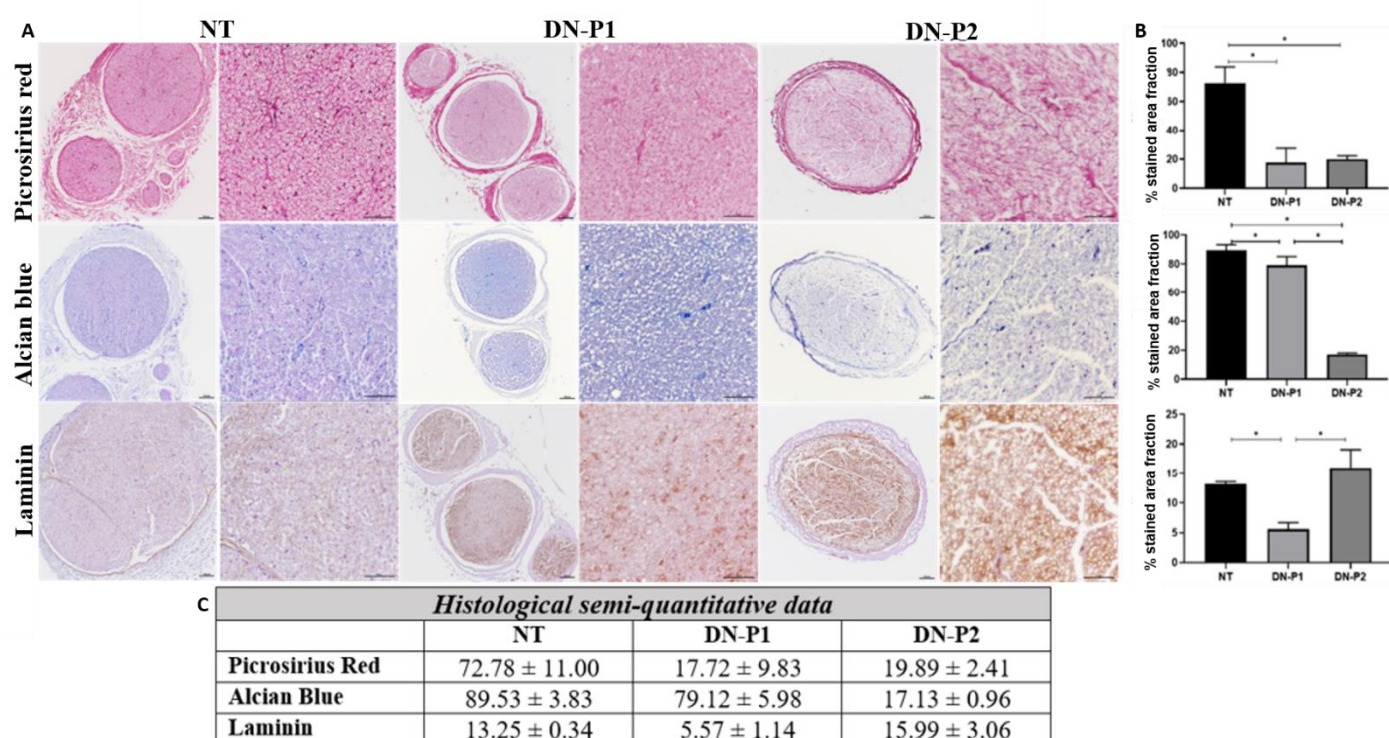


**Figure 3.** Representative histological and immunohistochemical panels and semi-quantitative analysis of native and decellularized rat sciatic nerves reporting the ECM components. (A) The three main ECM components, i.e. collagen, proteoglycans and laminin are stained with Picrosirius red, Alcian Blue and Laminin immunostaining, respectively. scale bar = 100 $\mu$ m for lower magnification images and 50 $\mu$ m for higher magnification images. (B) Graphs representing semi-quantitative analysis of the % occupied by the staining normalized to the whole nerve area. (C) Semi-quantitative raw data. \* indicate statistically significant differences ( $p < 0.05$ ).

### DNA detection

Concerning DNA testing, both fluorescent DAPI staining and DNA quantification were performed (Figure 4). Images did not show DAPI staining for DNA remnants in DN-P1 while several cell nuclei were observed in DN-P2 samples (Figure 4A). These findings were confirmed by the quantitative spectrophotometric evaluation of purified DNA. In fact, a halved DNA content was observed in nerves decellularized with DN-P1 ( $432.98 \pm 62.02$  ng DNA/mg dry weight) compared to specimens treated with DN-P2 ( $834.83 \pm 335.49$  ng DNA/mg dry weight) or native tissue ( $831.87 \pm 171.37$  ng DNA/mg dry weight) (Figure 4B).

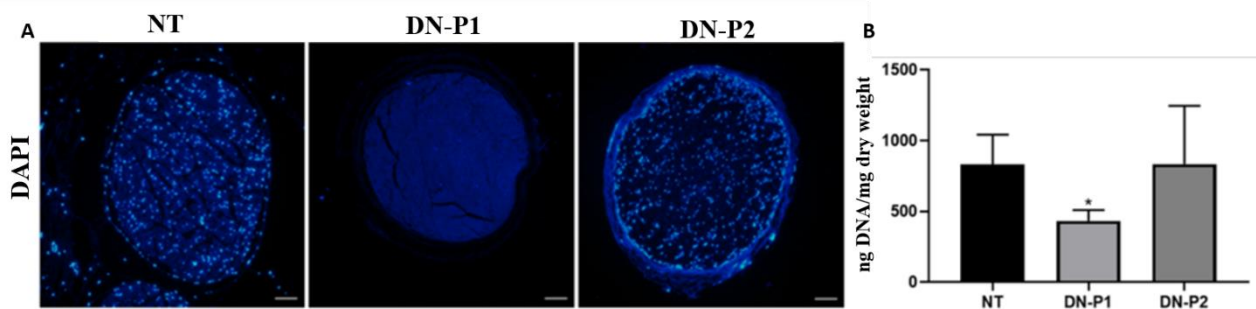


**Figure 4.** Qualitative and quantitative DNA content of native and decellularized rat sciatic nerves evaluating the effectiveness of the decellularization process to remove cell component. (A) Sections labeled with DAPI identify the cell nuclei (blue); scale bar = 100  $\mu$ m. (B) DNA quantification shows a lower DNA content in nerves decellularized with DN-P1 compared to both native tissue and nerves decellularized with DN-P2; \* indicate statistically significant differences ( $p < 0.05$ ).

### Ultrastructural changes in decellularized nerves: scanning and transmission electron microscopy

Electron microscopy of the decellularized nerves was performed to detect changes at the nerve ultrastructural level. Nerve samples were analyzed using both Scanning (SEM) and Transmission Electron Microscope (TEM) to detect the nerve surface and inner ultrastructure, respectively. SEM analysis demonstrated a very well-preserved ultrastructure of nerves treated with DN-P1 (Figure 5). Indeed, the nerves endoneurial tubes showed a well-organized net-like structure of the ECM in which a well-perforated surface can be seen. Instead, nerves treated with DN-P2 showed a less organized structure, and the net-shaped structure was not well detected. In particular, the ECM appeared severely disrupted. In native nerves, conserved nerve fascicles were easily detectable.

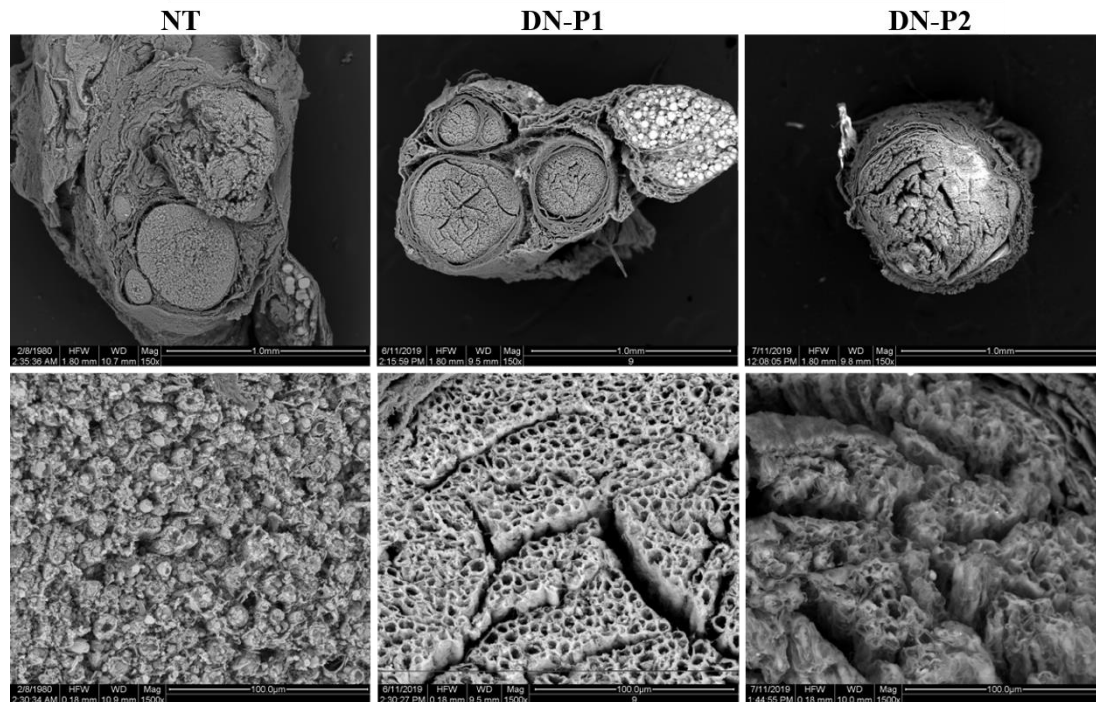


**Figure 5.** Scanning electron microscopy (SEM) representative panel. SEM detects the surface ultrastructure and the changes occurred in rat sciatic nerves following the decellularization process.

Concerning the inner ultrastructure of the decellularized nerves, TEM analysis (Figure 6) showed that unfolded myelin structures were still present in nerves treated with both the decellularization protocols. TEM analyses accurately demonstrated that a complete myelin removal was not achieved in any of the tested samples, actually multilayered cellular structures with low lipid content were identified (Figure 6). Structurally altered axonal remnants were detected in DN-P1, while in DN-P2 treated samples, some relatively intact axonal structures were still present. Collagen-rich ECM could be detected in samples treated with both protocols, even though well-conserved collagen fibers were detected only in samples treated with DN-P1. Otherwise, misfolded unintegrated collagen fibers were seen in DN-P2 specimens.

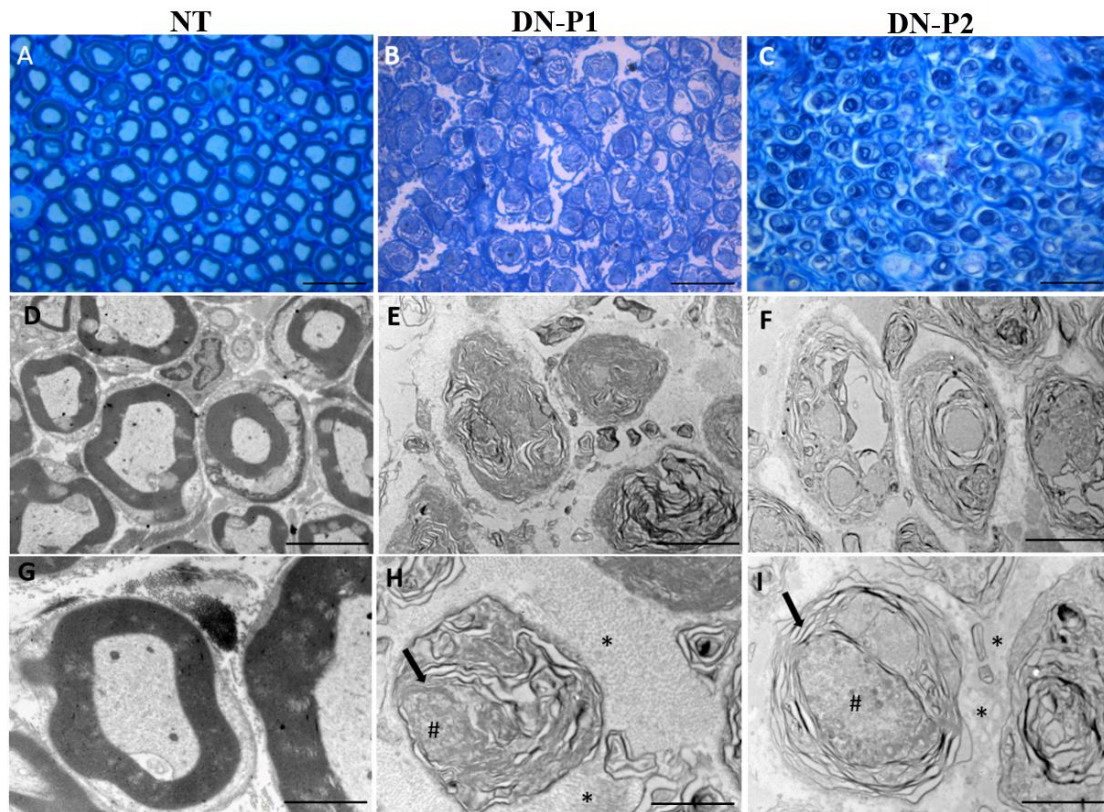


**Figure 6.** Toluidine blue staining and Transmission electron microscopy (TEM) representative panel. Toluidine blue stained sections (A-C) show the overall structure of the decellularized rat sciatic nerves. TEM (D-I) detects the changes in the inner ultrastructure of the native tissue and decellularized nerves. Myelin structures (black arrow), collagen fibers (\*), axon remnants (#). A, B, C scale bar = 20 $\mu$ m, D, E, F scale bar = 5  $\mu$ m, G, H, I scale bar = 2 $\mu$ m.

### ***Biomechanical properties***

Biomechanical properties of the samples were measured to determine potential changes induced by detergents and by the entire decellularization process. Both the decellularization protocols induced a low stiffness measured by the Young's modulus. Specifically, native nerves measured  $14.82 \pm 3.84$  MPa, while DN-P1 and 2 registered  $5.80 \pm 0.43$  and  $2.41 \pm 1$  MPa, respectively (Figure 7A). Consequently, failure stress showed a similar behavior in native nerves  $3.26 \pm 0.95$  MPa and samples treated with DN-P1 and 2 for  $1.65 \pm 0.29$  and  $0.78 \pm 0.40$  MPa, respectively (Figure 7B). Concerning the deformation occurred in nerves at the point of failure, the strain of nerves treated with DN-P1 was slightly higher than that of native nerves despite not significant, measuring  $59.32 \pm 5.19$  and  $51.50 \pm 4.66$  MPa, respectively. Nerves treated with DN-P2 had higher strain values ( $86.84 \pm 6.37$  MPa) compared to both native

controls and nerve treated with DN-P1 (Figure 7C). The strain at fracture was significantly higher in both the decellularized groups ( $7.19 \pm 0.83$  and  $9.03 \pm 1.05$  MPa for DN-P1 and 2, respectively) compared to native controls  $5.34 \pm 0.18$  MPa (Figure 7D).

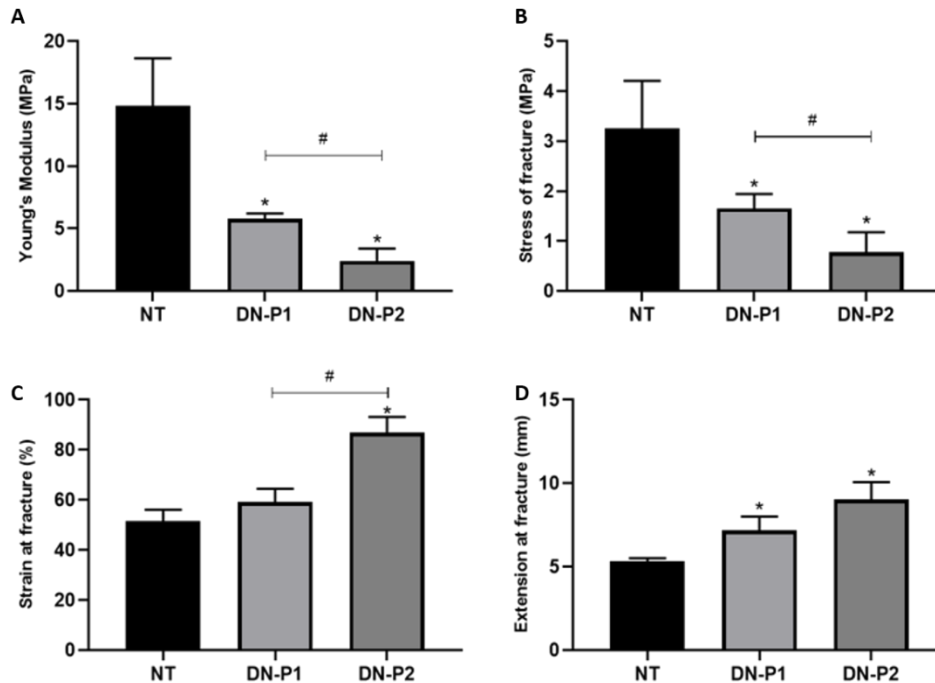


**Figure 7.** Biomechanical properties of native and decellularized rat sciatic nerves. (A) Young's modulus (MPa), (B) failure stress (MPa), (C) failure strain (%) and (D) elastic modulus (mm). \* indicate statistically significant differences ( $p < 0.05$ ) of decellularization protocols compared to natives, # indicate statistically significant differences ( $p < 0.05$ ) between the two decellularization protocols.

### *Qualitative data of cell viability*

The Live & Dead assay showed attached viable cells seeded on the inner surface of decellularized nerves following 48h of standard culture conditions. As can be seen in 2D positive and negative controls, cells are detected in green or red colors respectively. More importantly, a greater number of viable and elongated cells were detected within the nerves treated with DN-P1, while viable cells were less abundant in DN-P2 group. In relation to the presence of dead cells, they were not detected in nerves decellularized with DN-P1. However, the specimens decellularized with DN-P2 showed several dead cells on their surface (Figure 8A). These results were confirmed by WST-1 biochemical assay, where DN-P1 showed a comparable cellular metabolic activity with 2D positive controls, metabolic activity was

slightly lower compared to 2D positive controls, statistical analysis was not significant ( $p = 0.121$ ) (Figure 8B). DN-P1 showed much higher metabolic activity compared to 2D negative control ( $p = 0.0431$ ). DN-P1 showed higher WST-1 values and therefore a greater cellular metabolic activity compared to DN-P2, these differences being statistically significant ( $p = 0.046$ ). DN-P2 metabolic activity was significantly lower when compared to 2D positive controls ( $p = 0.049$ ) and DN-P1 ( $p = 0.046$ ) but was significantly higher when compared to 2D negative control ( $p = 0.046$ ) (Figure 8B). Cells seeded on DN-P1 demonstrated a mean value of 82% viability ( $81 \pm 9.38$ ), while DN-P2 demonstrated a mean value of 33% viability ( $33.39 \pm 13.63$ ). Difference between the two groups was significant ( $p = 0.046$ ).

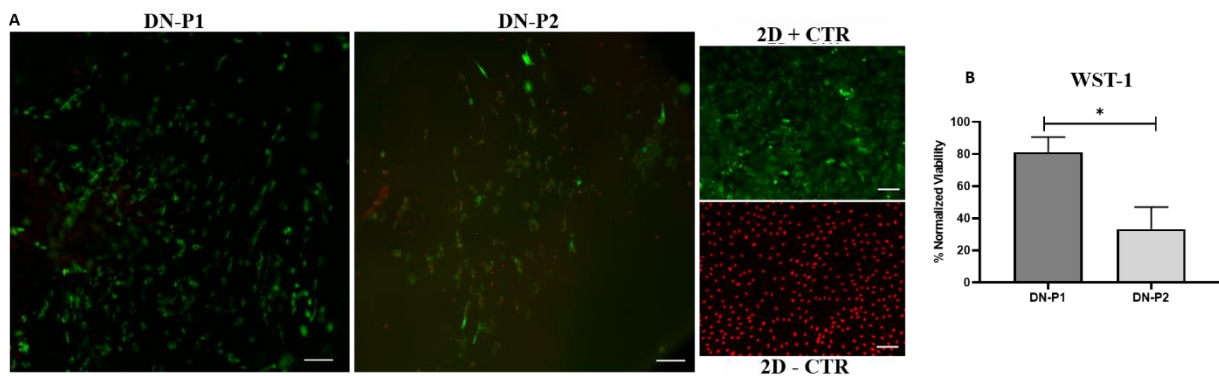


**Figure 8.** Representative qualitative and quantitative panel of Live & Dead and WST-1 assay of ADMSC-reseeded decellularized rat sciatic nerves. (A) Live&Dead (L/D) analysis. Green cells are alive while the red ones are dead. Scale bar 50 $\mu$ m. (B) WST-1 analysis, normalized viability to 2D + CTR expressed in percentage. \* indicate statistically significant differences between the two decellularization protocols. ( $p < 0.05$ ).

## Discussion

In the search of other valid alternatives to substitute the gold standard repairing technique (autograft), different tissue engineered nerve conduits have been developed. Unfortunately, nerve conduit efficiency is limited just in repairing small nerve gaps up to 3 cm (Isaacs & Browne, 2014). This phenomenon is likely to be attributed to the absence of the cellular and ECM components that have been readily supported by the autograft to the injured nerve. The enrichment of hollow conduits with cells and ECM-derived hydrogels has demonstrated to augment the regeneration, but its clinical application is limited being both time and effort consuming. Decellularized peripheral nerve allografts could be a more promising alternative in repairing critical nerve gaps when compared to hollow conduits.

Decellularized nerve allografts would provide a nerve scaffold rich in ECM components with an internal organized 3D structure formed by aligned endoneurial tubes. Furthermore, decellularized nerves offer a natural and tissue-specific mechanical support to the regenerative microenvironment. Indeed, the presence of well-distributed essential ECM, such as laminin and/or collagens, acts as guidance cues for Schwann cell migration and subsequent axon regrowth (Palispis & Gupta, 2019) decreasing or avoiding the host immunological response (Chato-Astrain et al., 2020). Therefore, the preservation of the ECM 3D organization and molecular composition results to be an important condition after the nerve decellularization (Philips et al., 2018a).

In this study, we aimed at evaluating the effectiveness of an already developed decellularization protocol for tendons (Bottagisio et al., 2016) both in terms of cellular removal, ECM structural and molecular preservation when applied on rat sciatic nerves. To demonstrate the efficacy of DN-P1, here, we compared this procedure with another detergent-based decellularization protocol specifically developed for nerves by others (Boriani et al., 2017). With this aim, *in vitro* comprehensive analyses were performed including histology (HE), histochemistry (Picrosirius red, Alcian Blue, DAPI, and MCOLL), immunohistochemistry (S100, vimentin, neurofilament, and laminin), DNA quantification, SEM and TEM analyses, and biomechanical testing. In addition, the biological properties and cytocompatibility were determined through the use cell viability and functionality assays (L/D and WST-1). In particular, the objective of the present study was to assess if detergents frequently used to decellularize dense connective tissues as tendons (TBP, PAA and DNase) could better preserve the ECM components of the treated nerves compared to Triton-X100 and SDS. The latter reagents are considered to be very aggressive decellularizing agents. Moreover, the development of a quick, efficacious protocol to decellularize nerves is strongly required to reduce the risk of contaminations during the process and to respond to clean room productions.

Overall, we demonstrated that the two applied decellularization protocols (DN-P1 and DN-P2) convey different conservation levels of the main ECM components: collagen, proteoglycans and laminin. Both protocols decreased the collagen content almost to the same extent, while DN-P1 better preserved proteoglycans and DN-P2 had a higher presence of laminin, but more disorganized. Immunohistochemically, our results showed that DN-P1 and DN-P2 had alternative points of strengths and weaknesses, for example DN-P1 had a better nerve structural preservation, while DN-P2 showed a better removal of the cellular components. These findings were not confirmed by DAPI and DNA content that demonstrated a greater cellular removal in

---



---

samples treated with DN-P1 compared to DN-P2. Therefore, these results point out the usefulness of the immunohistochemistry to accurately confirm the removal of tissue-specific cellular components after decellularization (Philips et al., 2018a). MCOLL histochemistry for myelin and collagen showed that DN-P1 induced a better myelin removal and collagen preservation than DN-P2. In addition, SEM analysis greatly confirmed these findings revealing a well-conserved ECM structure in DN-P1 rather than in DN-P2 samples. Finally, TEM ultrastructural evaluation was crucial to confirm and demonstrate the degree and efficacy of the decellularization protocols. Indeed, TEM has clearly confirmed the degree of conservation of the collagen matrix as well as the presence of axonal and cellular remnants, mainly those associated with the complex structure of the myelin sheath.

It needs to be taken into account that our study was performed on rat sciatic nerves, and this could explain the different results reached in the present study compared to the original protocol employed by Boriani and colleagues (DN-P2) that was applied on a diverse animal species, the rabbit (Boriani et al., 2017). These findings open an important and critical issue, i.e. the animal species as the source of nerve tissue. Indeed, there are substantial structural variations among nerves and among different animal species, the variations in nerve dimensions between different species can greatly affect the successfulness of the decellularization process. Unfortunately, these variations makes it difficult to compare different published studies in literature. As mentioned before (Mendibil et al., 2020) and as noticed in our results, each decellularization protocol should be adapted and optimized per each type of tissue but also the species differences should be taken into account.

In any case, the best option for clinical scenario would be the optimization of these decellularization methods to obtain human acellular nerve grafts from allogenic donors.

To our knowledge, just the studies which were published in collaboration with our group had widely compared in vitro rat sciatic decellularized nerves. The efficacy of different decellularization detergent-based protocols such as Sondell's, Hudson's and the authors' own protocol (Philips et al., 2018b) originally developed for heart valves was tested (Roosens et al., 2016). Moreover a recently published article comparing the effect of two different concentration of genipin added as a natural crosslinking agent to the previously mentioned decellularization protocols Sondell and Roosens was also tested (García-García et al., 2021) In the present study, indeed, we found more similarities with the protocols tested on rat sciatic nerves proposed in these works (García-García et al., 2021; Philips et al., 2018b) rather than with that developed by Boriani and colleagues on rabbit nerves (Boriani et al., 2017). However,

further comparative studies are needed to determine the best option. In the case of the Roosens-based acellular nerve grafts (Philips et al., 2018b) they were successfully used to repair 10-mm nerve gaps in rat obtaining promising results, which were closely comparable to the efficacy of autograft technique (Chato-Astrain et al., 2020).

It is well known that the immunogenicity of ECM of nerves is weak and almost negligible, indicating that cells are the main source of allogeneic nerve immunogenicity. The Major Histocompatibility Complex located on the surface of Schwann cells is the primary antigen material that induces an immune response against allograft transplantation. Therefore, cellular component removal is an important step in the preparation of decellularized nerve grafts (Wang et al., 2014).

A greater DNA removal was achieved using DN-P1, in which intact nuclei were completely absent, as demonstrated by DAPI staining, this was also found in the Roosens protocol alone or with the addition of genipin (García-García et al., 2021; Philips et al., 2018b). While the DNA quantification presented in Roosens protocol (Philips et al., 2018b) achieved a less DNA content, on the other hand the DNA quantification in DN-P1 and DN-P2 did not reach the limits considered optimal for decellularized tissues (50 ng/dry weight) (Crapo et al., 2011), thus indicating that both protocols were not optimal to completely eliminate DNA, albeit a halved quantity was detected in DN-P1 compared to DN-P2. The decrease noted in DN-P1 compared to DN-P2 could be the effect of the additional DNase treatment in DN-P1 differently from DN-P2 that never applied a DNase treatment.

It can be presumed that the absence of DAPI staining was due to an extreme fragmentation of the DNA that renders it undetectable through this fluorochrome. DAPI is an intercalating fluorochrome that specifically recognizes the A-T interactions, and thus the breakage of DNA directly affects the DAPI staining.

In the work presented by Bottagisio and colleagues (Bottagisio et al., 2016) using DN-P1 to decellularize tendons, adequate DNA content < 50 ng/dry weight was achieved. The differences in the DNA content could be attributed to the fact that the decellularization protocol did not have the same efficiency on different tissues and different species, and again highlighting the importance of optimizing the protocol based on these factors. To improve the DNA content removal in DN-P1, a greater concentration of DNase could be used, also integrating the use of PAA in previous passages during the decellularization protocol could be helpful to obtain a better penetration of TBP and DNase. Augmenting the incubation times or slightly increasing the detergent concentrations could also be a possible strategy.

To our knowledge the only decellularization protocol that was able to satisfy the recommended DNA content criteria is the Roosens' protocol (Philips et al., 2018b). In that article, three decellularization protocols (Sondell, Hudson and Roosens) were extensively tested *in vitro*. The DNA content revealed that Roosens demonstrated the least followed by Sondell then Hudson. Comparing our values with those presented in this article we can assess that DN-P1 and DN-P2 demonstrated higher levels compared to both Roosens and Sondell, but lower compared to Hudson. The successful removal of DNA content observed in Roosens' protocol could be attributed to a combined treatment of both DNase and RNase. While in the Sondell's protocol, there was not any DNase incubation steps but we suggest that the stronger detergents used in that protocol could result in a better DNA component removal compared to our tested protocols.

Both histological and immunohistochemical analyses showed that ECM conservation was comparable between the two decellularization techniques, with almost the same extent of collagen amount. However, only DN-P1 showed a good conservation of collagen fibers. DN-P1 showed less removal of acid proteoglycans. DN-P1 also showed some levels of laminin conservation even though to a lower extent compared to DN-P2.

SEM and TEM analysis showed that DN-P1 demonstrated superior outcomes when compared to DN-P2. SEM showed a higher preservation of the endoneurial tubes, suggesting that DN-P1 could generate a better graft concerning the structural preservation and the 3D organization of the internal basal lamina of the nerve that could act as a proper structural support for the growing nerve, resembling results obtained by Hudson and colleagues (Hudson et al., 2004).

TEM ultrastructural analysis showed that fragmented axonal debris were present in decellularized samples treated with DN-P1, while some intact axons were detected in DN-P2. These findings are very similar to data reported by previous studies using both the Hudson's or Roosens' protocols (García-García et al., 2021; Philips et al., 2018b). While Picrosirius red staining showed the collagen presence in both DN-P 1 and 2, ultrastructural TEM analysis showed that collagen fibers were present and well-conserved in the nerves decellularized with DN-P1, while in DN-P2 collagen fibers were not intact and severely disorganized. In TEM analysis, in both the employed protocols, the complete myelin elimination was not achieved, indeed, a disaggregated myelin structure was still detectable. This was in contrast with the results obtained by MCOLL histological staining that demonstrated the complete absence of myelin in DN-P1 treated nerves, as well for the Roosens' protocol (García-García et al., 2021; Philips et al., 2018b). This could be attributed to the different sensitivity and tissue processing

---

protocols of both techniques. For light microscopy tissues are fixed in formaldehyde, dehydrated in ethanol, cleared in xylol and then impregnated in warm paraffin. This aggressive process eliminates the tissue elements, such as myelin, which were altered and probably solubilized by the decellularization process. In contrast, sample preparation for TEM uses two stronger fixatives, that stabilize proteins (glutaraldehyde) and lipids (osmium tetroxide), allowing the identification of elements that have resisted the decellularization process (Philips et al., 2018a).

The differences seen in our study between the results obtained by light and electron microscopy are related to technical reasons. This demonstrates that the combination of immunohistochemistry, SEM and TEM analyses is crucial to assess the rate of decellularization of a tissue. Histochemistry and immunohistochemistry provide an overview of the structure and distribution of some general or tissue-specific elements, while the ultrastructural analyses serve to confirm these findings, but more importantly to demonstrate accurately those elements which are not detected by conventional light microscopy, such as myelin or axonal remnants. Both the decellularization protocols altered the nerve mechanical properties, in contrast with data reported by Roosens protocol (García-García et al., 2021; Philips et al., 2018b), despite in general, there is no consensus on the effects of decellularization detergents in affecting the mechanical properties of treated nerves. The Young's modulus detected a lower viscoelastic properties compared to native nerves. This means that the decellularized nerves had a low resistance to deformation when a force is applied. This finding was coherent with the stress at fracture results requiring a lower force before the decellularized nerve rupture. The deformation level in nerves decellularized with DN-P1 was not significant respect to native samples as measured by the strain at fracture, which was not the case of nerves treated with DN-P2 where a high deformation occurred at the point of fracture. These mechanical changes were expected since most of the decellularization treatments slightly affect the ECM components, mainly collagen that plays an important role in the nerve mechanical strength (Lovati et al., 2018). However, it has been shown that substitutes with biomechanical properties, not fully comparable to a native nerve, have been successfully used in experimental nerve injury repair (Wang et al., 2014; Chato-Astrain et al., 2020), suggesting that our new allograft could be tested for future in vivo preclinical studies.

To evaluate the residual cytotoxicity of detergent remains, the viability of seeded rADMSCs onto the decellularized samples was detected. ADMSCs are widely used in various tissue engineering applications for their ease purification and access, in addition to their high *in vitro*

---

---

proliferation capacity (Lovati et al.,2016; Mazini et al.,2019). Moreover, in the view of cell reseeded for nerve grafts, the use of autologous MSCs drastically reduces the invasive collection of cells from nerves as well as the patient morbidity. Finally, the immunomodulatory properties of MSCs are exploited in cell therapy-resistant graft-versus-host disease, thus better controlling the autoimmunity and inflammatory responses (Lovati et al., 2016).

DN-P1 treated nerves better support the cell viability compared to DN-P2, which decreased the cell viability and functionality. It could be related to the chemical agent used, which in the case of the DN-P2 decreased the cytocompatibility of the generated matrices. Perhaps, some chemical agents within the acellular matrices or essential ECM molecules, which support the cell adhesion and function, were irreversibly eliminated affecting the cell viability and functionality. It can be hypothesized that the use of PAA, barely employed in nerve decellularization (Cai et al., 2017; Sridharan et al., 2015), could have an impact on the nucleic acids, cellular remnants and cytoplasm removal without altering the structure of ECM, it can be easily removed from the nerve following decellularization, thus being highly biocompatible and favoring the cell viability of newly seeded cells on decellularized nerves.

The combination of different detergents used in each decellularization protocol led to different results in the tested decellularized nerves. It is difficult to assess the exact effect of each detergent used alone, as the effects can be assessed at the end of the whole protocol including the subsequent use of different detergents. One main difference between protocols could be the combination of the physical forces, agitation in addition to repeated sonification cycles in DN-P2, that to our opinion could have accounted to the extensive endoneurial damage and the disruption of the collagen fibers as detected in SEM and TEM analysis, respectively. The greater viability sustained by DN-P1 nerves could be attributed to a better removal of detergents residues as a result of the extensive washes alternating with distilled deionized water and PBS, while DN-P2 has less washes mainly in PBS. Another factor could be the harshness of the used detergents, Triton-X100 and SDS compared to TBP and PAA, so even if complete detergent removal was not achieved, the toxicity would be less using the last-mentioned reagents. A detailed study solely focused on the use of different detergents and their exact possible adverse effects on the tissue could be helpful to choose the best combination of detergents for future decellularization protocols.

The small sample size (n=3) could be considered a limitation of the present study, however, our proof of concept study was mainly focused on an overall evaluation of the outcomes of the decellularization protocol DN-P1 compared to DN-P2 already published for the nerves . Even

though the sample size was small, it was enough to guide us to detect the second limitation of this study which is the DNA content, as none of the tested protocols achieved the optimal DNA content (< 50 ng/dry weight).

The overall results of the present *in vitro* study show that DN-P1 with minor modifications could be a more promising protocol than DN-P2 to decellularize nerves. DN-P1 is a decellularization protocol that uses a novel combination of two detergents, mainly TBP and PAA, that has been already efficiently used to decellularize tendons, but whose effect has never been tested on nerves before. Both DN-P1 and DN-P2 require short preparation time compared to others such as the Sondell protocol, but DN-P1 shows a better DNA component removal, better ultrastructural organization and cell viability compared to DN-P2. In order to confirm the effectiveness of DN-P1, further *in vivo* studies are necessary to detect if the leftovers from cellular remnants could provoke an adverse immune reaction and to assess the regeneration capability of decellularized nerves treated with DN-P1.

---

**References**

- Boriani, F., Fazio, N., Fotia, C., Savarino, L., Nicoli Aldini, N., Martini, L., ... Baldini, N. (2017). A novel technique for decellularization of allogenic nerves and in vivo study of their use for peripheral nerve reconstruction. *Journal of Biomedical Materials Research Part A*, 105(8), 2228–2240. <https://doi.org/10.1002/jbm.a.36090>
- Bottagisio, M., Pellegata, A. F., Boschetti, F., Ferroni, M., Moretti, M., & Lovati, A. B. (2016). A new strategy for the decellularisation of large equine tendons as biocompatible tendon substitutes. *European Cells and Materials*, 32, 58–73. <https://doi.org/10.22203/eCM.v032a04>
- Cai, M., Huang, T., Hou, B., & Guo, Y. (2017). Role of Demyelination Efficiency within Acellular Nerve Scaffolds during Nerve Regeneration across Peripheral Defects. *BioMed Research International*, 2017. <https://doi.org/10.1155/2017/4606387>
- Carriel, V., Alaminos, M., Garzón, I., Campos, A., & Cornelissen, M. (2014, March). Tissue engineering of the peripheral nervous system. *Expert Review of Neurotherapeutics*, Vol. 14, pp. 301–318. <https://doi.org/10.1586/14737175.2014.887444>
- Carriel, V., Campos, A., Alaminos, M., Raimondo, S., & Geuna, S. (2017). Staining Methods for Normal and Regenerative Myelin in the Nervous System. *Histochemistry of Single Molecules: Methods and Protocols*, *Methods in Molecular Biology*, 1560, 207–218. <https://doi.org/10.1007/978-1-4939-6788-9>
- Carriel, V., Scionti, G., Campos, F., Roda, O., Castro, B., Cornelissen, M., ... Alaminos, M. (2017). In vitro characterization of a nanostructured fibrin agarose bio-artificial nerve substitute. *Journal of Tissue Engineering and Regenerative Medicine*, 11(5), 1412–1426. <https://doi.org/10.1002/term.2039>
- Chato-Astrain, J., Campos, F., Roda, O., Miralles, E., Durand-Herrera, D., Sáez-Moreno, J. A., ... Carriel, V. (2018). In vivo evaluation of nanostructured fibrin-agarose hydrogels with mesenchymal stem cells for peripheral nerve repair. *Frontiers in Cellular Neuroscience*, 12. <https://doi.org/10.3389/fncel.2018.00501>
- Chato-Astrain, J., Durand-Herrera, D., Alaminos, M., Philips, C., Campos, F., Roosens, A., ... Carriel, V. (2020). Detergent-based decellularized peripheral nerve allografts : An in vivo preclinical study in the rat sciatic nerve injury model. *J Tissue Eng Regen Med.*, 14(February), 789–806. <https://doi.org/10.1002/term.3043>
- Crapo, P. M., Gilbert, T. W., & Badylak, S. F. (2011). Biomaterials An overview of tissue and whole organ decellularization processes. *Biomaterials*, 32(12), 3233–3243. <https://doi.org/10.1016/j.biomaterials.2011.01.057>
- Deeken, C. R., White, A. K., Bachman, S. L., Ramshaw, B. J., Cleveland, D. S., Loy, T. S., & Grant, S. A. (2011). Method of preparing a decellularized porcine tendon using tributyl phosphate. *Journal of Biomedical Materials Research - Part B Applied Biomaterials*, 96 B(2), 199–206. <https://doi.org/10.1002/jbm.b.31753>
- Durand-Herrera, D., Campos, F., Jaimes-Parra, B. D., Sánchez-López, J. D., Fernández-Valadés, R., Alaminos, M., ... Carriel, V. (2018). Wharton’s jelly-derived mesenchymal cells as a new source for the generation of microtissues for tissue engineering applications. *Histochemistry and Cell Biology*, 150(4), 379–393. <https://doi.org/10.1007/s00418-018-1685-6>
- García-García, Ó. D., El Soury, M., González-Quevedo, D., Sánchez-Porras, D., Chato-Astrain, J., Campos, F., & Carriel, V. (2021). Histological , Biomechanical , and Biological Properties of Genipin-Crosslinked Decellularized Peripheral Nerves. *International Journal of Molecular Sciences*, 22(674), 1–21.
- Gilbert, T. W., Sellaro, T. L., & Badylak, S. F. (2006). Decellularization of tissues and organs. 27,
-

- 3675–3683. <https://doi.org/10.1016/j.biomaterials.2006.02.014>
- Grinsell, D., & Keating, C. P. (2014). Peripheral Nerve Reconstruction after Injury: A Review of Clinical and Experimental Therapies. *BioMed Research International*, 2014. <https://doi.org/10.1155/2014/698256>
- Hudson, T. W., Liu, S. Y., & Schmidt, C. E. (2004). Engineering an improved acellular nerve graft via optimized chemical processing. *Tissue Engineering*, 10(9–10), 1346–1358. <https://doi.org/10.1089/ten.2004.10.1346>
- Isaacs, J., & Browne, T. (2014). Overcoming short gaps in peripheral nerve repair : conduits and human acellular nerve allograft. <https://doi.org/10.1007/s11552-014-9601-6>
- Krekoski, C. A., Neubauer, D., Zuo, J., & Muir, D. (2001). Axonal regeneration into acellular nerve grafts is enhanced by degradation of chondroitin sulfate proteoglycan. *Journal of Neuroscience*, 21(16), 6206–6213. <https://doi.org/10.1523/jneurosci.21-16-06206.2001>
- Lovati, A. B., Arrigo, D. D., Odella, S., Tos, P., Geuna, S., & Raimondo, S. (2018). Nerve Repair Using Decellularized Nerve Grafts in Rat Models . A Review of the Literature. 12(November), 1–20. <https://doi.org/10.3389/fncel.2018.00427>
- Lovati, A. B., Bottagisio, M., & Moretti, M. (2016). Decellularized and Engineered Tendons as Biological Substitutes: A Critical Review. *Stem Cells International*, Vol. 2016. <https://doi.org/10.1155/2016/7276150>
- Mazini, L., Rochette, L., Amine, M., & Malka, G. (2019). Regenerative capacity of adipose derived stem cells (ADSCs), comparison with mesenchymal stem cells (MSCs). *International Journal of Molecular Sciences*, 20(10), 1–30. <https://doi.org/10.3390/ijms20102523>
- Mendibil, U., Ruiz-hernandez, R., & Retegi-carrion, S. (2020). Tissue-Specific Decellularization Methods : Rationale and Strategies to Achieve Regenerative Compounds. *International Journal of Molecular Sciences*, 1–29.
- Palispis, W. A., & Gupta, R. (2019). Biologic Augmentation in Peripheral Nerve Repair. In *Biologics in Orthopaedic Surgery*. <https://doi.org/10.1016/B978-0-323-55140-3.00014-X>
- Philips, C., Campos, F., Roosens, A., Sánchez-Quevedo, M. del C., Declercq, H., & Carriel, V. (2018). Qualitative and Quantitative Evaluation of a Novel Detergent-Based Method for Decellularization of Peripheral Nerves. *Annals of Biomedical Engineering*, 46(11), 1921–1937. <https://doi.org/10.1007/s10439-018-2082-y>
- Philips, C., Cornelissen, M., & Carriel, V. (2018, January 24). Evaluation methods as quality control in the generation of decellularized peripheral nerve allografts. *Journal of Neural Engineering*, Vol. 15. <https://doi.org/10.1088/1741-2552/aaa21a>
- Raghavan, S. S., Woon, C. Y. L., Kraus, A., Megerle, K., Choi, M. S. S., Pridgen, B. C., ... Chang, J. (2012). Human flexor tendon tissue engineering: Decellularization of human flexor tendons reduces immunogenicity in vivo. *Tissue Engineering - Part A*, 18(7–8), 796–805. <https://doi.org/10.1089/ten.tea.2011.0422>
- Ronchi, G., Jager, S. B., Vaegter, C. B., Raimondo, S., Giacobini-Robecchi, M. G., & Geuna, S. (2014). Discrepancies in quantitative assessment of normal and regenerated peripheral nerve fibers between light and electron microscopy. *Journal of the Peripheral Nervous System*, 19(3), 224–233. <https://doi.org/10.1111/jns.12090>
- Roosens, A. N. R., Omers, P. A. S., Omer, F. I. D. E. S., Arriel, V. I. C., & Ooten, G. U. V. A. N. N. (2016). Impact of Detergent-Based Decellularization Methods on Porcine Tissues for Heart Valve Engineering. *Annals of Biomedical Engineering*. <https://doi.org/10.1007/s10439-016-1555-0>
- Schmitt, T., Fox, P. M., Woon, C. Y., Farnebo, S. J., Bronstein, J. A., Behn, A., ... Chang, J. (2013).



- Human flexor tendon tissue engineering: In vivo effects of stem cell reseeded. *Plastic and Reconstructive Surgery*, 132(4), 567–576. <https://doi.org/10.1097/PRS.0b013e3182a033cf>
- Seddon, H. J. (1943). Three types of nerve injury. *Brain*, 66(4), 237–288. <https://doi.org/10.1093/brain/66.4.237>
- Siemionow, M., & Brzezicki, G. (2009). Chapter 8 Current techniques and concepts in Peripheral Nerve Repair. In *International Review of Neurobiology* (1st ed., Vol. 87). [https://doi.org/10.1016/S0074-7742\(09\)87008-6](https://doi.org/10.1016/S0074-7742(09)87008-6)
- Siemionow, M., & Sonmez, E. (2007). Nerve allograft transplantation: A review. *Journal of Reconstructive Microsurgery*, 23(8), 511–520. <https://doi.org/10.1055/s-2007-1022694>
- Sondell, M., Lundborg, G., & Kanje, M. (1998). Regeneration of the rat sciatic nerve into allografts made acellular through chemical extraction. *Brain Research*. [https://doi.org/10.1016/S0006-8993\(98\)00251-0](https://doi.org/10.1016/S0006-8993(98)00251-0)
- Sridharan, R., Reilly, R. B., & Buckley, C. T. (2015). Decellularized grafts with axially aligned channels for peripheral nerve regeneration. *Journal of the Mechanical Behavior of Biomedical Materials*, 41, 124–135. <https://doi.org/10.1016/j.jmbbm.2014.10.002>
- Sunderland, S. (1951). A classification of peripheral nerve injuries producing loss of function. *Brain*, 74(4), 491–516.
- Tao, Y. (2013). Chapter 9 Isolation and Culture of Schwann Cells. *Neural Development: Methods and Protocols, Methods in Molecular Biology*, 1018, 93–104. <https://doi.org/10.1007/978-1-62703-444-9>
- Wang, Q., Zhang, C., Zhang, L., Guo, W., Feng, G., Zhou, S., ... Huang, F. (2014). The preparation and comparison of decellularized nerve scaffold of tissue engineering. 4301–4308. <https://doi.org/10.1002/jbm.a.35103>
- Whitlock, P. W., Smith, T. L., Poehling, G. G., Shilt, J. S., & Van Dyke, M. (2007). A naturally derived, cytocompatible, and architecturally optimized scaffold for tendon and ligament regeneration. *Biomaterials*, 28(29), 4321–4329. <https://doi.org/10.1016/j.biomaterials.2007.05.029>
- Woon, C. Y. L., Farnebo, S., Schmitt, T., Kraus, A., Megerle, K., Pham, H., ... Chang, J. (2012). Human flexor tendon tissue engineering: Revitalization of biostatic allograft scaffolds. *Tissue Engineering - Part A*, 18(23–24), 2406–2417. <https://doi.org/10.1089/ten.tea.2012.0152>
- Woon, C. Y. L., Pridgen, B. C., Kraus, A., Bari, S., Pham, H., & Chang, J. (2011). Optimization of human tendon tissue engineering: Peracetic acid oxidation for enhanced reseeded of acellularized intrasynovial tendon. *Plastic and Reconstructive Surgery*, 127(3), 1107–1117. <https://doi.org/10.1097/PRS.0b013e318205f298>
- Zilic, L., Wilshaw, S. P., & Haycock, J. W. (2016). Decellularisation and histological characterisation of porcine peripheral nerves. *Biotechnology and Bioengineering*, 113(9), 2041–2053. <https://doi.org/10.1002/bit.25964>

## *Chapter 7*

### *Discussion*

During my PhD I have participated in different projects that collectively serve in understanding the process of peripheral nerve regeneration in a model of short gap repair and applied different tissue engineering approaches for critical nerve gap repair. Nerve regeneration is a complex process with multiple interplaying molecules, growth factors and different types of cells that synergize and cooperate in controlling the regeneration and final repair process. Despite the improved knowledge about some of these factors, their specific interactions and overlapping effects renders the process of nerve regeneration almost impossible to be fully understood. Thus, a deep understanding of these molecular bases is required and highly needed, thus offering new scopes to be applied for achieving better satisfactory nerve repair outcomes.

In the first part of my thesis I focused on studying the regeneration process in short nerve gap, first by studying *in vitro* the effect of soluble NRG1 stimulation on Schwann cell primary culture, with the aim to interpret the role behind its high expression in response to nerve injury, as observed by different research groups including ours (Carroll et al., 1997; Stassart et al., 2013; Ronchi et al., 2016) and *in vivo* studying the regeneration process inside a hollow chitosan conduit used for short median nerve gap repair.

In the second part of my thesis I applied different tissue engineering strategies for critical nerve repair, where I tested *in vivo* the possible advantage of enriching the hollow chitosan conduit with fibrin-collagen hydrogel alone or with the addition of ADMSC, and I performed an *in vitro* characterization of a novel decellularization protocol for generating acellular nerve grafts for critical nerve repair.

**solubleNRG1 plays an important role in the early response to nerve regeneration possibly by trans-differentiating Schwann cells to a repair phenotype.**

In peripheral nervous system NRG1-ErbB signalling has shown to play critical roles during developmental and adult stages, as well as during nerve regeneration. (Gambarotta et al., 2013). In the PNS, soluble NRG1 is mainly expressed by Schwann cells, while transmembrane NRG1 is mainly expressed by axons.

To investigate the possible role played by sNRG1 in response to nerve injury and the significance of its immediate upregulation, we prepared adult primary Schwann cell cultures and stimulated them with sNRG1. Deep sequence analysis shows that sNRG1 stimulation induces differential gene expression in Schwann cells; gene ontology analysis showed that regulated genes belong to functional categories that are regulated *in vivo* in response to nerve injury and might control Schwann cell response to injury. The down regulation of myelination

genes is a prerequisite for the process of Schwann cell trans-differentiation and their conformational change into a repair phenotype. Furthermore, sNRG can support Schwann cell survival following injury by down regulating genes involved in apoptosis, and it can contribute to protein synthesis by upregulating rRNA metabolic processes.

When comparing our *in vitro* data of sNRG regulated genes with *in vivo* data of regulated genes in response to injury (Barrette et al., 2010; Kim et al., 2012) we found that 40% of the upregulated genes and 54% of downregulated genes in the injured nerve environment were also regulated *in vitro* in response to sNRG1, thus suggesting that their regulation *in vivo* might be attributed also to sNRG1.

Based on these observations we hypothesize that soluble NRG1 plays a key and crucial role in the early response to nerve injury, as its upregulation helps the trans-differentiation of Schwann cells to a repair phenotype that is a limiting step for Wallerian degeneration and nerve regeneration to start. Later, soluble NRG1 returns to its normal expression levels, thus allowing the new regenerating axons to be myelinated responding to the axonal transmembrane NRG1. Thus, gene therapy with recombinant soluble NRG1 could be a good strategy, but the administration should be done in a controlled time window restricted to the first stage of nerve regeneration, as a sustained soluble NRG1 supply would inhibit further myelination of the regenerated nerves (Zanazzi et al., 2001).

#### **Future perspective:**

The transcription factor c-Jun is well known for its role in Schwann cell transdifferentiation (Arthur-Farraj et al., 2012; Jessen & Arthur-Farraj, 2019), From our data we have seen that sNRG1 play a main role in Schwann cell transdifferentiation, we have also seen that c-Jun is regulated *in vitro* in sNRG1 stimulated Schwann cells. We would like to deeply investigate and have a better understanding of the possible *in vivo* interaction between sNRG1 and c-Jun following a nerve injury.

#### **Soluble NRG1 expression in a hollow conduit is attributed to Schwann cells as well as nerve fibroblasts**

Hollow conduits have proven to be highly efficient in repairing short nerve gaps with equivalent recovery levels when compared to autografts (Palispis & Gupta, 2019).

Most of the published studies on nerve injury repair with conduits (natural or synthetic origin) focus their attention on the efficiency of the used conduit material to promote nerve

regeneration and evaluate the final recovery. In this study, we aimed to have a better understanding of the molecular and cellular events that occur inside the hollow conduit and what confers to the hollow conduit its efficiency in repairing short nerve gaps.

For this aim, short (8mm) median nerve gaps were repaired either by anautograft or a chitosan conduit. We choose chitosan conduits as previous studies have shown that they are efficient in supporting nerve repair (Haastert-Talini et al., 2013) by promoting both Schwann cell and neuronal cell survival (Freier et al., 2005; Yuan et al., 2004).

Protein analysis revealed a high NRG1 expression at 7 days post injury and repair in autograft and chitosan conduits, while ErbB2 and ErbB3 receptors, that are expressed by Schwann cells, were absent in the chitosan conduits, thus suggesting that NRG1 high expression might be devoted from other cells beside Schwann cells, most probably nerve fibroblasts. Indeed, a high expression level of a fibroblast marker (Thy1), was observed in chitosan conduits while significantly higher expression of Schwann cell markers (S100 and p75) was observed in autografts. Moreover, soluble NRG1 and NRG1 $\alpha$  and  $\beta$  expression follow the same expression pattern of the fibroblast marker expression, thus supporting our hypothesis that the NRG1 observed in western blot analysis might be expressed by nerve fibroblasts. To further assess this hypothesis, adult primary cultures of nerve fibroblasts were prepared and tested for NRG1 and ErbB receptors expression.

We found that primary cultures of nerve fibroblasts express high levels of soluble NRG1 but lack ErbB2 and ErbB3 (the main NRG1 receptors expressed in the peripheral nervous system), thus suggesting that the NRG1 released by fibroblasts might act in a paracrine manner on Schwann cells. Indeed, it has been shown before *in vitro* that fibroblasts can have an impact on Schwann cell behaviour and can increase the migratory effect of Schwann cells by releasing NRG1 as a pro-migratory factor (Dreesmann et al., 2009).

Immunohistochemical analysis was performed to investigate *in vivo* the expression of NRG1 and the presence of different cellular populations inside the conduit at 7 days post injury and repair. In autografts Schwann cells were found to be more abundant, while in the chitosan conduits fibroblasts were found to be more abundant. Double labelling of both fibroblast marker and NRG1 confirmed that fibroblasts, alongside with Schwann cells, participate in NRG1 expression.

While previously it was thought that fibroblasts hinder the nerve regeneration process by forming scar tissue that obstruct the passing of regenerating axons, lately it has been observed from another perspective. Nerve fibroblasts play an important role in peripheral nerve

---

regeneration via ephrinB/EphB2 signalling with Schwann cells that guides their sorting, proper alignment and migration to subsequently form Büngner bands (Parrinello et al., 2010). Other studies showed that fibrin cables produced by fibroblasts are the first structure formed to bridge the two transacted nerve stumps and that they serve as a guiding cue for endoneurial cells and Schwann cells to further align and form Büngner bands (Williams et al., 1983). Here, we add that they highly colonize hollow conduits in an earlier time point compared to Schwann cells and that they participate in releasing NRG1 that most probably act in a paracrine manner on Schwann cells stimulating their trans-differentiation into a repair phenotype.

**Future perspective:**

A recent study has shown that there is differential gene expression between sensory and motor fibroblasts (He et al., 2019). Studying whether these differences render different interactions with Schwann cells on a molecular level would be helpful to have a general better understanding of the regeneration process. Studying the released factors and possible activated signalling pathways in sensory and motor fibroblasts could be useful to develop new therapies to be applied in peripheral nerve regeneration and identifying other possible roles of fibroblasts in peripheral nerve regeneration.

**Enriching chitosan conduits with fibrin-collagen hydrogel and with ADMSC, highly upregulates sNRG1 expression and other molecules involved in nerve repair.**

The use of nerve conduits has proven their efficiency in repairing short nerve gaps with efficient and comparable recovery to autografts (Carriel et al., 2014). Unfortunately, conduits are not any more efficient when repairing long nerve defects. This can be related to the stability loss of the formed fibrin clots and the consequent loss of the guiding cues for Schwann cells and axonal migration, which fail to reach the target organ in the right time (Lundborg et al., 1982). Moreover, sprouting axonal growth cones are not able to sense the neurotrophic factors released by the distal stump, and the target organ undergoes atrophy as a consequence of long denervation period (Pfister et al., 2011; Deumens et al., 2010).

To overcome this limitation, many tissue engineering strategies have been adopted to modify the conduit intraluminal structure in a way that resembles as much as possible autograft natural structure. Following a nerve injury, the two transacted nerve stumps respond by secreting internal fluids containing cells, ECM structural components and various trophic factors that are essential for nerve regeneration process (Chen et al., 2006).

Many studies have tried various luminal fillers to enrich conduits and enhance their efficiency for critical gap repair by inserting ECM components as collagen, laminin and fibrin, in addition to the incorporation of cells to generate a more biomimetic nerve conduit (Dietzmeyer et al., 2020).

To study tissue engineering strategies to repair large nerve gaps, I switched to the sciatic nerve model (where longer gaps can be studied) and I spent one year in the University of Granada in the Tissue Engineering Laboratory supervised by prof. Victor Sebastian Carriel.

In this study, we enriched chitosan conduits with a combined hydrogel made of equal parts of fibrin and collagen, alone or with ADMSC incorporation for repairing a critical sciatic nerve gap (15mm). Fibrin was chosen as it is the first natural matrix scaffold that was found to be secreted in the injured nerve environment, while collagen is the most abundant ECM constituent in all tissues (Chen et al., 2006; Alovskaya et al., 2007). ADMSCs were chosen for their high proliferation and differentiation capabilities and more importantly, their availability and ease of extraction which can facilitate their translation into clinical application (Fraser et al., 2006; Masgutov et al., 2019). We investigated the molecular changes occurring in the different experimental groups in a short time course following nerve injury and repair. A final regeneration assessment was analysed at 15 weeks post injury and repair.

Interestingly, we found that just the hydrogel mixture composition is able to significantly upregulate sNRG expression and its isoforms  $\alpha$  and  $\beta$ , both at mRNA and at protein level.

ErbB2 receptor expression was just highly expressed in the ADMSC group, thus suggesting that they could have a positive effect on modulating the whole NRG1-ErbB signalling system. Fibroblasts are the most abundant cellular population infiltrating all the experimental groups, followed by immature Schwann cells. This can be either for their higher quantity in the injured nerve environment or their stronger ability to migrate and penetrate through the hydrogels compared to immature Schwann cells.

Cell markers were significantly higher in the hollow conduit group than in enriched ones; this might be explained by the ease of cell entrance in a hollow structure than in a filled one, where hydrogel might act as a physical obstacle for cell entrance.

Coherent with other studies showing that ADMSCs are capable of expressing vascular endothelial growth factor (VEGF-A) (Fraser et al., 2006) we found a significantly higher expression of VEGF-A in the experimental group in which chitosan conduits were enriched with fibrin-collagen hydrogel and ADMSCs, thus supporting the idea that this mix might promote angiogenesis. Moreover, the release of VEGF-A from ADMSCs transplanted in the

combined hydrogel emphasizes the gel biocompatibility as ADMSCs were retained viable, active and able to secrete growth factors even after one week of *in vivo* implantation.

Despite the promising results we obtained at the early time points, muscle atrophy was not recovered after 15 weeks. Consistently, no motor recovery was obtained, and regeneration was not achieved in experimental groups enriched with fibrin-collagen +/- ADMSC, while a few regenerating fibres with thin myelin were seen in hollow chitosan conduits. Similar disappointing results at repairing 15mm rat sciatic nerve using hydrogels have been reported also by other studies (Meyer et al., 2016b), but in that case it is probable that the hydrogel acted as a mechanical hindrance for axonal growth and that changes in the hydrogel concentrations may attribute to a better performance (Dietzmeyer et al., 2020).

On the contrary, sensory functional recovery was achieved in fibrin-collagen with ADMSC. As only high-resolution light microscopy examination to quantify myelinated fibres was carried out on semithin sections of the distal stump of the nerve, a more detailed electron microscopy analysis could be performed to quantify unmyelinated fibres in the different experimental groups.

#### **Future perspectives:**

Analysing the regenerated nerves inside the conduits (15 weeks following repair), we should be able to understand if regenerating axons have been blocked by the hydrogel or if more time was still needed for the regenerating axons to reach the distal stump, as very poor regeneration was also observed in hollow chitosan conduits, in which hydrogel was missing. This analysis is still in progress.

If the first hypothesis would be correct, a mixture of fibrin-collagen could be tried to be injected directly in a soluble form inside the conduit or a hydrogel of a lower concentration could be prepared. If the second hypothesis would be correct, a further analysis with a longer endpoint should be carried out, until a good motor functional recovery is obtained, at least in one of the experimental groups.

#### **New decellularization protocol for preparing acellular nerve allografts, another tissue engineering approach for critical nerve repair**

Despite all the efforts in manufacturing nerve conduits and the various different trials to enrich its lumen in a way that can biomimic nerve autografts, when it comes to repairing critical nerve gaps, the perfect combination that allows satisfactory recovery outcome is not yet achieved



(Patel et al., 2017). Autografts clearly demonstrate their superiority by offering the injured nerve a complete regenerative environment composed of cells, ready released neurotrophic factors, well organized basal lamina offered by Schwann cells and other supporting ECM components. Thus, offers a total regenerative permissive environment for peripheral nerve regeneration and optimum final regeneration outcome.

The use of a cadaver donor nerve - *allograft* - has the privilege of offering the same permissive regenerative environment as autograft, in addition to the avoidance of the need to sacrifice a functional sensory nerve and performing a second operation for nerve harvesting. Allografts also offer the possibility to perform the nerve repair with a matching nerve type; this is of great importance as it was found that miss matching nerve types, especially when using a sensory nerve in repairing a motor nerve, could have limiting regeneration outcome (Brenner et al., 2006). The disadvantage accompanied by allograft use is their ability to provoke adverse immune response when transplanted, with subsequent graft rejection; thus, allograft implantation needs to be followed by an immunosuppressant treatment that could put a patient's life into risk (Palispis & Gupta, 2019).

Nerve decellularization is considered one of the most promising tissue engineering strategies for repairing critical gaps, as it provides a non-immunogenic nerve graft of natural origin, with preserved ECM components and organized nerve ultrastructure. These characteristics offer a great support for the regenerating nerve. Various chemical, physical and biological treatments are used to generate decellularized nerve allografts. Till now the Avance® nerve graft (AxoGen® Inc., Alachua, FL,USA) is the only FDA approved acellular nerve allograft (Lovati et al., 2018). Nevertheless, the commercial selling of nerve graft is limited in several countries, including Italy, while nerve grafts offered by tissue banks are legally allowed.

In this study we tested a novel decellularization protocol using two detergents that are mainly used in tendon decellularization but were never applied before on nerves (TBP and PAA). Here, we applied a decellularization protocol that has proven to be efficient on tendon decellularization (P1) and we compared it with another decellularization protocol that was developed for nerves (P2). *In vitro* characterization was performed on decellularized rat sciatic nerves to assess cellular component removal, ECM component preservation, mechanical and ultrastructural properties and, most importantly, biocompatibility.

Morphological analyses showed a relatively well-preserved general histological structure for nerves from both decellularization protocols. Histochemical analysis did not show a positive reaction for myelin and DNA in decellularized nerves with protocol 1(DN-P1), while some

positivity for myelin and DNA was detected in decellularized nerves with protocol 2 (DN-P2). The immunohistochemical evaluation of cellular component removal in both protocols showed less cellular components compared to natives, but total cellular component removal was not achieved.

Evaluation of ECM component preservation showed a higher collagen and proteoglycan ECM preservation in DN-P1, while a higher laminin preservation was detected in DN-P2. Both decellularization protocols affected and changed the mechanical properties that can be observed in native nerves, but DN-P1 demonstrated better mechanical properties compared to DN-P2. Moreover, DN-P1, has showed superior ultrastructural organization, highly conserved endoneurial tubes and collagen fibres, which in DN-P2 were disorganized and not well conserved. DN-P1 has demonstrated to be highly biocompatible as greater number of viable and metabolically active cells were detected.

**Future perspectives:**

Some modifications in detergent concentrations or incubation time could be useful to obtain an optimal DNA removal (< 50 ng/dry weight), further these DN-P1 allografts could be used to repair critical nerve gaps *in vivo*. We would like to investigate whether the presence of ECM components would modulate the expression of NRG/ErbB system by fibroblasts or Schwann cells. Moreover, studying different conservation methods and the effect of long-time storage on decellularized nerves would be helpful to optimize decellularized graft storage.

**Conclusions:**

The full understanding of the complex process of peripheral nerve regeneration and achieving a full functional recovery in case of severe injuries are still major challenges. There is a huge need of combining efforts from different interdisciplinary fields to overcome this problem. A profound knowledge of the molecular as well as the cellular changes in nerve regeneration could serve in producing a possible gene therapy that targets specific molecules and pathways critically affecting the regeneration outcome. In addition, it can offer a better strategy for manufacturing a tailored tissue engineering strategy. The massive improvement in the field of tissue engineering and regenerative medicine in the recent years, has made it possible to offer various promising alternatives to autografts. During my PhD I studied peripheral nerve regeneration from different aspects, First, I focused my attention on the possible role played by sNRG upregulation in response to nerve injury and found that it differentially regulates different categories of genes important for the process of Schwann cell trans-differentiation. Moreover, we suggest that the presence of commonly overlapping regulated genes *in vivo* and *in vitro* could be attributed to NRG1 upregulation. Secondly, I focused my attention to better understand the efficiency of hollow chitosan conduits in repairing short gaps, and I found that high NRG1 expression was observed 7 days post injury inside the tube and this could be attributed to the release both by Schwann cells as well as by fibroblasts that were found to highly colonize hollow chitosan conduit and release NRG1 *in vivo*.

As regards long gap repair, chitosan conduit enrichment with hydrogels synthesized from ECM derived proteins as fibrin and collagen with further ADMSC incorporation have shown promising preliminary results at early time points post injury, with sensory functional recovery at 15 weeks. Nevertheless, all data analysis needs to be completed to draw conclusions. Finally, *in vitro* assessment of a new decellularization protocol provided nerves with good ultrastructural organization and biocompatibility, suggesting that this protocol could be encouraging for *in vivo* trials for repairing critical nerve gaps.

---

**References:**

- Alovskaya, a, Alekseeva, T., Phillips, J. B., King, V., & Brown, R. (2007). Fibronectin, Collagen, Fibrin-Components of Extracellular Matrix for Nerve regeneration. *Topics in Tissue Engineering*, 3, 1–27.
- Arthur-Farraj, P. J., Latouche, M., Wilton, D. K., Quintes, S., Chabrol, E., Banerjee, A., ... Jessen, K. R. (2012). Article c-Jun Reprograms Schwann Cells of Injured Nerves to Generate a Repair Cell Essential for Regeneration. *Neuron*, 75, 633–647.
- Barrette, B., Calvo, E., Vallières, N., & Lacroix, S. (2010). Brain , Behavior , and Immunity  
Transcriptional profiling of the injured sciatic nerve of mice carrying the Wld ( S ) mutant gene : Identification of genes involved in neuroprotection , neuroinflammation , and nerve regeneration. *Brain Behavior and Immunity*, 24(8), 1254–1267.
- Brenner, M. J., Hess, J. R., Myckatyn, T. M., Hayashi, A., Hunter, D. A., & Mackinnon, S. E. (2006). Repair of Motor Nerve Gaps With Sensory Nerve Inhibits Regeneration in Rats. (September), 1685–1692.
- Carriel, V., Alaminos, M., Garzón, I., Campos, A., & Cornelissen, M. (2014). Tissue engineering of the peripheral nervous system. *Expert Review of Neurotherapeutics*, 14(3), 301–318.
- Carroll, S. L., Miller, M. L., Frohnert, P. W., Kim, S. S., & Corbett, J. A. (1997). Expression of Neuregulins and their Putative Receptors , ErbB2 and ErbB3 , Is Induced during Wallerian Degeneration. *The Journal of Neuroscience* 17(5), 1642–1659.
- Chen, M. B., Zhang, F., & Lineaweaver, W. C. (2006). Luminal Fillers in Nerve Conduits for Peripheral Nerve Repair. 57(4), 462–471.
- Deumens, R., Bozkurt, A., Meek, M. F., Marcus, M. A. E., Joosten, E. A. J., Weis, J., & Brook, G. A. (2010). Progress in Neurobiology Repairing injured peripheral nerves : Bridging the gap. *Progress in Neurobiology*, 92(3), 245–276.
- Dietzmeier, N., Förthmann, M., Grothe, C., & Haastert-Talini, K. (2020). Modification of tubular chitosan-based peripheral nerve implants: Applications for simple or more complex approaches. *Neural Regeneration Research*, 15(8), 1421–1431.
- Dreesmann, L., Mittnacht, U., Lietz, M., & Å, B. S. (2009). Nerve fibroblast impact on Schwann cell behavior. *European Journal of Cell Biology* 88, 285–300.
- Fraser, J. K., Wulur, I., Alfonso, Z., & Hedrick, M. H. (2006). Fat tissue: an underappreciated source of stem cells for biotechnology. *Trends in Biotechnology*, 24(4), 150–154.
- Freier, T., Koh, H. S., Kazazian, K., & Shoichet, M. S. (2005). Controlling cell adhesion and degradation of chitosan films by N-acetylation. *Biomaterials*, 26(29), 5872–5878.
- Jessen, K. R., & Arthur-Farraj, P. (2019). Repair Schwann cell update: Adaptive reprogramming, EMT, and stemness in regenerating nerves. *Glia*, 67(3), 421–437.
- Gambarotta, G., Fregnan, F., & Gnani, S. (2013). Neuregulin 1 Role in Schwann Cell Regulation and Potential Applications to Promote Peripheral Nerve Regeneration. In *Tissue Engineering of the Peripheral Nerve: International Review of Neurobiology* (1st ed., Vol. 108, 223-256). manca qualcosa
- Haastert-talini, K., Geuna, S., Dahlin, L. B., Meyer, C., Stenberg, L., Freier, T., ... Grothe, C. (2013). Biomaterials Chitosan tubes of varying degrees of acetylation for bridging peripheral nerve defects. *Biomaterials*, 34(38), 9886–9904.
- He, Q., Shen, M., Tong, F., Cong, M., Zhang, S., Gong, Y., & Ding, F. (2019). Differential gene
-

- expression in primary cultured sensory and motor nerve fibroblasts. *Frontiers in Neuroscience*, 12(1016), 1–17.
- Kim, Y., Remacle, A. G., Chernov, A. V, Liu, H., Shubayev, I., Dolkas, J., ... Shubayev, V. I. (2012). The MMP-9 / TIMP-1 Axis Controls the Status of Differentiation and Function of Myelin-Forming Schwann Cells in Nerve Regeneration. *PLoS ONE* | 7(3), 1-15
- Lovati, A. B., Arrigo, D. D., Odella, S., Tos, P., Geuna, S., & Raimondo, S. (2018). Nerve Repair Using Decellularized Nerve Grafts in Rat Models . A Review of the Literature. *Front. Cell. Neurosci.* 12(November), 1–20.
- Lundborg, G., Dahlin, L. B., Danielsen, N., Gelberman, R. H., Longo, F. M., Powell, H. C., & Varon, S. (1982). Nerve regeneration in silicone chambers: influence of gap length and of distal stump components. *Experimental Neurology*, 76(2), 361–375.
- Masgutov, R., Masgutova, G., Mullakhmetova, A., Zhuravleva, M., Shulman, A., Rogozhin, A., ... Rizvanov, A. (2019). Adipose-derived mesenchymal stem cells applied in fibrin glue stimulate peripheral nerve regeneration. *Frontiers in Medicine*, 6(APR), 1–12.
- Mei, L., & Xiong, W. (2008). Neuregulin 1 in neural development , synaptic plasticity and schizophrenia. *Nature Reviews Neuroscience*, 9(june), 437- 452.
- Meyer, C., Wrobel, S., Raimondo, S., Rochkind, S., Heimann, C., Shahar, A., ... Haastert-Talini, K. (2016). Peripheral nerve regeneration through hydrogel-enriched Chitosan conduits containing engineered Schwann cells for drug delivery. *Cell Transplantation*, 25(1), 159–182.
- Palispis, W. A., & Gupta, R. (2019). Biologic Augmentation in Peripheral Nerve Repair. *Biologics in Orthopaedic Surgery*, Chapter 14, 141-163.
- Parrinello, S., Napoli, I., Ribeiro, S., Digby, P. W., Fedorova, M., Parkinson, D. B., ... Lloyd, A. C. (2010). EphB signaling directs peripheral nerve regeneration through Sox2-dependent Schwann cell Sorting. *Cell*, 143(1), 145–155.
- Patel, N. P., Lyon, K. A., & Huang, J. H. (2017). An update – tissue engineered nerve grafts for the repair of peripheral nerve injuries. *Neural regeneration research*, 13 (5), 764-774.
- Pfister, B. J., Gordon, T., Loverde, J. R., Kochar, A. S., Mackinnon, S. E., & Cullen, D. K. (2011). Biomedical Engineering Strategies for Peripheral Nerve Repair : Surgical Applications , State of the Art , and Future Challenges. *Critical Reviews™ in Biomedical Engineering*, 39(2), 81–124.
- Ronchi, G., Haastert-talini, K., Fornasari, B. E., Perroteau, I., Geuna, S., & Gambarotta, G. (2016). The Neuregulin1 / ErbB system is selectively regulated during peripheral nerve degeneration and regeneration. *European Journal of Neuroscience*, 43(June 2015), 351–364.
- Stassart, R. M., Fledrich, R., Velanac, V., Brinkmann, B. G., Schwab, M. H., Meijer, D., ... Nave, K. (2013). A role for Schwann cell – derived neuregulin-1 in remyelination. *Nature neuroscience*, 16(1), 48-54.
- Williams, L. R., Longo, F. M., Powell, H. C., Lundborg, G., Varon, S., W, D. B. L. R., & Pathology, F. M. L. (1983). Spatial-Temporal Progress of Peripheral Nerve Regeneration Within a Silicone Chamber : Parameters for a Bioassay. *The Journal of comparative neurology*, 218, 460-470.
- Yuan, Y., Zhang, P., Yang, Y., Wang, X., & Gu, X. (2004). The interaction of Schwann cells with chitosan membranes and fibers in vitro. *Biomaterials*, 25(18), 4273–4278.
- Zanazzi, G., Einheber, S., Westreich, R., Hannocks, M., Bedell-hogan, D., Marchionni, M. A., & Salzer, J. L. (2001). Glial Growth Factor / Neuregulin Inhibits Schwann Cell Myelination and Induces Demyelination. 152(6), 1289–1299.